

PHILIPPINE METALS

ISSN 2980 - 4957



Department of Science and Technology
METALS INDUSTRY RESEARCH AND DEVELOPMENT CENTER

MOLD TECHNOLOGY SUPPORT CENTER (MTSC)



**Your partner in addressing your
die and mold requirements.**

REGULAR TRAINING PROGRAMS

- *NX CAD Fundamental Course*
- *NX Mold Wizard Design Process*
- *Plastic Injection Mold Design*
- *Mold Assembly Using NX*
- *Plastic Injection Mold Assembly*
- *Value Analysis/Value Engineering for Die and Mold Industry*

PACKAGED TRAINING PROGRAMS

- *Plastic Injection Molding Machine Programming and Operation*
- *CNC EDM Wire-Cutting, Programming, and Operation*
- *CNC EDM Sinking, Programming, and Operation*
- *CNC Milling Programming and Operation*
- *Basic Coordinate Measuring Machine (CMM) Operation*
- *Mold Assembly*
- *Mold Processing*
- *Mold Design*

USE OF EQUIPMENT

- *CNC Milling Machines*
- *Electrical Discharge Machining (EDM)*
- *Plastic Injection Machines*
- *Surface Grinding Machines*
- *Conventional Machines*
- *Quality Control Machines*
- *Support Equipment*
- *Time Sharing - client provides their own machine operator*
- *Actual Time - MTSC provides the machine operator*

CONTACT US NOW

Mold Technology Support Center
Lot 434 Brgy. Bacao II, CEZ Gen.
Trias Cavite, Philippines
Tel. No. +63 46 501 0943
Email: mtsc@mirdc.dost.gov.ph

**DOST-Metals Industry Research
and Development Center**
MIRDC Cpd., Gen. Santos Ave.
Bicutan, Taguig City, Philippines
Tel. No. +632 8837 0431 to 38
Email: mirdc@mirdc.dost.gov.ph



PHILIPPINE METALS

PHILIPPINE METALS

ISSN 2980-4957

Copyright © 2023

Published by:

Department of Science and Technology -
Metals Industry Research and Development Center
Bicutan, Taguig City 1631
Republic of the Philippines

Telefax: (632) 8837-0479

Email: mirdctips@mirdc.dost.gov.ph

Website: <http://www.mirdc.dost.gov.ph>

All rights reserved.

This is an annual publication. No part of the book
may be reproduced in any form without the written
permission of the publisher.

About the cover:

The Mold Technology Support Center (MTSC) was established to develop the needed human resources for the local die and mold companies, encourage the advancement of the Philippine manufacturing industry's competitiveness, and contribute to the industrial cooperation between the Republic of Korea and the Republic of the Philippines. Shown is one of its facilities where the quality assurance is being conducted.

Contents

DOST-MIRDC GOVERNING COUNCIL

CHAIRMAN Renato U. Solidum, Jr.

VICE CHAIRMAN Robert O. Dizon

MEMBERS Robert O. Dizon, Jeremy T. Aguiña,
Dionosio G. Alvindia, Neil P. Catajay,
Roberto M. Cola, Ma. Corazon H. Dichosa,
Bien A. Ganapin, Augusto C. Soliman,
Danilo U. Uykieng

EDITORIAL STAFF

ADVISER Agustin M. Fudolig

MANAGING EDITOR Lina B. Afafe

TECHNICAL EDITOR Agustin M. Fudolig

ASSOCIATE EDITOR Zalda R. Gayahan

ARTIST/GRAPHICS Ronald L. Agustin,
Tracy Ann U. Tolentino

ADVERTISING MANAGER Ella Vanessa L. Lopez

PRODUCTION MANAGER Kathlyn Kai H. Negado

CIRCULATION Faith P. Macatangay
Reynaldo M. Loreto, Jr.

Materials Engineering and Additive Manufacturing.	2
Design Considerations and Fabrication of Additively Manufactured OSL Dosimeter Security Locks	2
Topology Optimization and Rapid Prototyping of Aerial Drone Attachments Fixation Devices	10
Sandpaper Leaf (<i>Ficus fiskei</i> Elmer) Extract as Green Corrosion Inhibition for Carbon Steel in Saline Environment	16
<i>Euphorbia milii</i> Extract as Natural Inhibitor for Mild Steel Corrosion in 1M Hydrochloric Acid Solution	28
Comparative Analysis of Locally Made Copper Rods and Its Imported Counterparts	34
A Comparative Analysis of Reducing Carbon Emissions from Diesel-Engine Vehicles with the use of Filnut Muffler Filter and Traditional Muffler Filter	40
Epoxy Coating Additive Filler Utilizing Bamboo Leaf Ash for Possible Metal Degradation Protection	44
Microwave-Assisted Extraction and Synthesis of Calamansi (<i>Citrofortunella macrocarpa</i>) Pectin-Mediated Silver Nanoparticles as Green Inhibitor for Carbon Steel Corrosion in Saline Environment	48
Automation, Renewable Energy, and other Engineering Applications	58
Design of Plastic Bottle Shredder Machine with Monetary Reward System . . .	58
Viability of Ammonia-pH-Temperature Model in Quantifying Ammonia Levels in Commercial Recirculating Aquaculture Systems (RAS)	62
Solar Powered Bio-Waste Recycler to Produce Fertilizer from Leftover Foods	66
Development of an Innovative Arcade Game Operated with Polyethylene Terephthalate Bottle Shredder	74
Metal and Allied Industries Processing; Machining Technologies, and Mechanical Design	82
CNC Plasma Cutter with Ink Marker for Metal Plate Marking and Cutting . . .	82
Portable Coconut Dehusker with Breaker	86
Design and Development of Coconut-Coir and Coco-Peat Extraction Device	90
Transfer of Technology Through Innovated Machine Shop Training Table for Benchwork Operation	96
A Design of Shredder Machine for Scrap Material for Meter Assembly and ECU Assembly	100
Development and Evaluation of Spring Suspension Compressor Tool for Automobile Suspension System	104
Comparative Performance of Motor-powered and Conventional Blower Furnace Using Charcoal as Fuel	110
DOST-MIRDC Initiated Researches for the Metals, Engineering, and Allied Industries	116
Development and Verification of a Laterite Ore Refining Equipment	116
Electropolishing Optimization for Additively Manufactured Aluminum Alloy .	124
Improved Patternwax Material for Investment Casting Using Fillers	132
Prototyping of the Mechanical System of a Local Oxygen Concentrator with Parts Designed Using Design for Additive Manufacturing (DfAM)	136
Design Improvement of Gear Shifting Mechanism for Riding-Type Rice Transplanter	144
Comparative Study of Sand Casting Pattern Fabrication Lead Times Using Conventional and Additive Manufacturing Processes	148
Development of Automatic Trash Rake in Malabon-Tullahan River System . .	154
Augmented Poultry Egg Hatchery	160
Improving the Workforce Skills and Enhancing the Industry's Competitiveness Through the Mold Technology Support Center	166
Modification of a 1.5kW Shredder for ASA (Acrylonitrile Styrene Acrylate) 3D Printing Wastes	172

Preface



The Department of Science and Technology-Metals Industry Research and Development Center (DOST-MIRDC) remains committed to fostering effective research and development (R&D) that thrives on collaboration and knowledge sharing. We implement programs and projects that not only advance our understanding of science, technology, and innovation concepts, but also bring tangible benefits to our esteemed partners in the industry, academe, and government. This is a manifestation of our continuous pursuit of relevance in the metals, engineering, and allied industries and within the science community.

Information exchange is one of our activities in support of the DOST's mission of providing science, technology, and innovation-based solutions to the nation's most pressing challenges. We take pride in our information exchange initiatives, especially in the 2nd National Metals and Engineering Conference (NMEC) which we held in June 2023 as part of the celebration of the Metals and Engineering Week 2023. The NMEC is a gathering of research enthusiasts from the academe, the industry, and the government where findings and new knowledge are shared.

With this, we present to you the Philippine Metals (PhilMetals) Volume 10, which contains a compilation of technical papers that were presented in the 2nd NMEC. Inside the PhilMetals, papers are grouped into three categories - 1) Automation, Renewable Energy, and other Engineering Applications, 2) Materials Engineering and Additive Manufacturing, 3) Metal and Allied Industries Processing; Machining Technologies, and Mechanical Design. This publication exemplifies the unwavering commitment of DOST-MIRDC to conduct impactful R&D, delivering substantial contributions that empower our local metals, engineering, and allied industries.



Robert O. Dizon
Executive Director

Design Considerations and Fabrication of Additively Manufactured OSL Dosimeter Security Locks

Mark Christian E. Manuel^{*1}, Jeffrey Sabariza^{*2}, Marianna Lourdes Marie L. Grande^{*3}, Ranier Jude Wendell R. Lorenzo^{*4}

Abstract

In the Philippines, ionizing radiation finds diverse applications, especially in the medical sector. To ensure safety, workers wear personal dosimeters to estimate their exposure levels. National regulations mandate the monitoring and control of radiation exposure for workers, with the Philippine Nuclear Research Institute (PNRI) offering a Personal Monitoring Service. This service employs Optically Stimulated Luminescence (OSL) Dosimeters, with the security lock component preventing tampering and being considered a consumable. Due to its recurring demand and feedback from service personnel, there is room for further improvement in the security lock's design. This paper thoroughly discusses the design considerations for utilizing additively manufactured OSL dosimeters. It highlights the advantages of additive manufacturing, such as customized production, elimination of product iteration tooling, shorter lead time, on-demand manufacturing, reduced inventory space, and sustainability with waste reduction. The design considerations are integrated into the computer-aided design process, resulting in an AM-compatible file format while also considering manufacturability and cost reduction. After which, it was printed in Crealty Halot One, a Digital Light Processing (DLP) printer, and further post-processed. Analysis shows that the nested design of the dosimeter saves up to 41% of material through manually modeling its supports. The wastage ratio dropped from 72.75% of injection molded locks to 10-20% of the 3D printed counterpart. The 3D-printed security locks have great potential for daily use and operations of the OSL Personal Monitoring Service within a year, ensuring the safety of radiation workers across the nation and increasing the economic value of laboratory supplies in the service.

Keywords: additive manufacturing, vat photopolymerization, design for AM, radiation protection

I. Introduction

Ionizing radiation is used in many applications here in the Philippines, from the medical field, to the industrial sector and also to the academic field. Of the total population of users of ionizing radiation, the medical field consists of 70%, the industrial sector takes up 29% of the users and the academic field or nuclear science education field takes about 1% of the population. It is estimated that there are 30,000 radiation workers in the Philippines[1]. Despite its benefits, radiation is generally considered a hazard and thus, it is imperative to ensure that workers are protected against the harmful effects of ionizing radiation by keeping their occupational dose exposure low. In terms of occupational radiation protection, personal dosimeters or radiation badges are used by workers worn on the chest area to best estimate the radiation dose they would receive from working with radiation.

Dosimeters are instruments used to measure ionizing radiation exposure via electromagnetic rays through a separate field in science called dosimetry and are considered an important tool for people who work in places where they are exposed to radiation[2]. To have access to these personal dosimeters, the Philippine

Nuclear Research Institute (PNRI) is one of the technical service providers here in the Philippines which provide Personal Monitoring Service. It is a support to the national regulatory requirement that radiation exposures of workers should be monitored and controlled. In the Philippines, regulations require that radiation monitoring devices be calibrated at least annually by organizations specifically authorized by PNRI [3].

Currently, PNRI provides OSL or the Optically Stimulated Luminescence Dosimeter badges, parts of which are further discussed in the next section. PNRI itself provides the calibration service which requires them to have expendable materials readily available when bulk service requests are made by institutions and companies which are using dosimeters as part of their regular duties. Among these expendable materials are OSL dosimeter security locks, which are small pin-like plastic pieces that are attached every calibration cycle to the dosimetric reading device and are removed/destroyed when authorized calibration centers are to perform the reading and recalibration procedure again. If the locks have been broken before the qualified technician performs the



^{*1} S&T Fellow II
Metals Industry Research and
Development Center
Bicutan, Taguig City
Philippines



^{*2} Science Research Specialist II
Metals Industry Research and
Development Center
Bicutan, Taguig City
Philippines



^{*3} Sr. Science Research Specialist
DOST-Philippine Nuclear
Research Institute
Commonwealth Ave. Diliman,
Quezon City, Philippines

reading or calibration, it is marked as tampered. It was established that there is a need for about 4500 pcs. per month of this small semi-expendable part, costing around Php7/pc from 3rd party supplier markets. Currently, it was already sought to fabricate via injection molding but the mold is now due for reworking and possibly some design revisions based on observations from use cases. Thus, other manufacturing methods that would meet their requirements are sought.

Additive manufacturing is one possible manufacturing method that offers advantages over traditional manufacturing methods. However, it has traditionally been used for prototypes and one-off parts, and low-volume production [4]. Given the small size of the part, it was conceptualized that using design for additive manufacturing (DfAM) processing techniques, such as nesting, could increase cost viability [5] and wastage at the same time enjoy additional benefits from adopting an AM-based manufacturing workflow. Through the AM-Cen program of the Department of Science and Technology (DOST) - Metal Industries Research and Development Center (MIRDC), available technical expertise and equipment are available for possible adopters to investigate the viability of such approaches [6][7]. This paper discusses in detail how the different advantages and design considerations have been taken into account for meeting the high quantity production of the OSL dosimeter security locks. Section II discusses in great detail the OSL dosimeter parts, which further details the security locks, its current manufacturing methods, and the need why AM was considered. Section III presents the equipment and material used, as well as the development of both the single lock and nested designs. Section IV compares the 3D-printed locks to the injection-molded ones in different areas.

II. OSL Dosimeters

The following subsections discuss the different parts of the OSL Dosimeter, its current manufacturing methods, and the identified needs or design constraints of the security pin.

A. Part Description

There are different types of dosimetry services being offered by the PNRI. Among these services is the OSL Dosimeter Personal Monitoring System (OPMS). A small LED light stimulation illuminates the OSL dots in the dosimeter and releases portions of the electron it holds. The luminescent signal is proportional to the radiation dose and is counted by a Photomultiplier thus calculating the personal dose of radiation[8].



Fig. 1. OSL Dosimeter assembly parts

Table 1. Specifications and expected operation range of OSL Dosimeter Personnel Monitoring System

Radiation Type	Energy Range	Minimum Dose Equivalent Reported
Photon(x or gamma ray)	5 keV to 20 MeV	5 mrem (50 μ SV)
Beta Particle (expressed as average energy)	150 keV to 10 MeV	10 mrem (100 μ SV)

The OSL Dosimeter (Landauer Inlight Model 2 dosimeter) is composed of several components. The main component is the Detector slide which serves as detector elements using four (4) aluminum oxide (Al₂O₃) crystals. The dosimeter detector sensor can be read out several times, as only a small and reproducible fraction of the stored energy is released during illumination[9]. The specifications are provided in Table I. It is enclosed in a case with a filter system which also contains the dosimeter serial number. The assembly badge is then inserted into a plastic badge holder and eventually attached to the badge clip, which is used for attaching the badge to the user/personnel. This assembly will be held together using the dosimeter clip and the security lock, a small pin-like plastic piece that is destroyed and attached every calibration cycle.



Fig. 2. OSL Dosimeter Lock



*4 Project Technical Specialist I
Metals Industry Research and
Development Center
Bicutan, Taguig City
Philippines

These locks provide the means for attaching the clip as well as a security mechanism against tampering within the monitoring period. During dose analysis, the device is opened by destroying the lock. If the lock is observed to be damaged prior to analysis, the security lock is marked as tampered. Tampered OSL Dosimeter before arriving in PNRI for processing may give rise to errors with dose results and possible penalties. A typical OSL security lock is shown in Figure 2. The total height is 7.85mm with the bottom part at 3.68mm in diameter. Each part is around 65mm³ and is made from high quality plastic material.

From an economic aspect, the PNRI is spending approximately Php 378,000.00 per year for these locks alone. It is deemed relatively expensive for a semi-expendable and continuously demanded piece. Thus, a more practical and economical manufacturing method via plastic injection molding was sought in 2014-2015. Through MIRDC's prototyping division, a mold for injection molding was designed and fabricated based on the dimensions of the original locks.

The mating part between the OSL security lock and the badge clip becomes worn out in time due to repeated usage and wear and tear resulting in some security lock heads not breaking when being opened for dose analysis. If the security locks can be removed without breaking, the user may have access to the dosimeter's sensing devices at any time. Thus, the primary function of the OSL dosimeter locks as a tamper-proof mechanism has failed its purpose which may cause errors and tampering. Normally, the PNRI has also stored badge clips to replace loose ones. It was observed that the size of the protruding edge on the top needs to be increased in size since the mating could be worn out. Another observation was that the OSL dosimeter lock is very sturdy, finding it difficult to insert the lock in a new badge clip and failing to break in a worn-out badge clip. Thus, PNRI sought a design revision of the locks to address this issue.

B. Current Manufacturing Methods

The supplier-provided OSL security locks are originally injection molded with high-quality plastic. Plastic injection molding is the most common modern method of manufacturing plastic parts and is ideal for producing high volumes of the same object[10]. The process is quick, has a fast production rate, and is capable of producing voluminous plastic parts in a single cycle. Plastic injection molding is a manufacturing process that allows for parts to be produced in large volumes. It involves injecting molten plastic material into a mold, where it cools and solidifies into its final form. The process is suitable for the mass production of products with complicated shapes and takes a large part in the area of plastic processing. While the mass production process is quite straightforward, several challenges in mold design, processing parameters, and new material tuning to name a few to increase quality and reduce defects[11]. In terms of processing parameters, several can be adjusted to optimize the process[12], including mold temperature, melt temperature, packing time, cooling

Table 2. Material properties of possible plastics used for OSL dosimeter parts

Material	Ave. density, g/cc	Ave. Ultimate Tensile Strength, MPa	Ave. Yield Tensile Strength, MPa	Ave. Flexural Yield Stress, MPa	Ave. Modulus of Elasticity, GPa
Polycarbonate (PC), molded	1.2	64.2	62.4	90.9	2.39
Polyvinyl chloride (PVC), molded	1.29	16.6	43.2	74.4	2.16
Acrylonitrile Butadiene Styrene (ABS), molded	1.07	40.7	44.8	70.6	2.35
High Impact Polystyrene (HIPS)	1.04	21.6	-	44.13	2.157



Fig. 3. Core and Cavity molds designed, fabricated, and used for local production of dosimeter security locks

time, injection time, packing pressure, etc. Material choice and processing parameters are known to heavily affect the physical properties of the final injection molded part[13].

While the exact material cannot be found in the available literature, it is mentioned that the dosimeter is designed in France and manufactured to their specifications[14]. Common materials used in dosimeter clips or housings include plastics such as polycarbonate (PC) or polyvinyl chloride (PVC). Plastic components are often used for the housing of the dosimeter clip due to their durability and ease of manufacturing. Some physical characteristics of molded plastics are given in Table 2.

Due to the cost constraints of an imported security lock and to improve the sustainability of the service, a locally designed and produced mold (Figure 3) was fabricated at MIRDC and used to create mass-produced dosimeter security locks using HIPS pellets which are locally available and are commonly processed in the facility. The produced locks have been functionally tested and are used for more than 3 years with service requests for manufacturing done annually with around 25 kgs. of material serving the majority of their requirements. Due to repeated use, the mold patterns have worn out and need to be refurbished.

Plastic injection molding serves as a more practical and economical option for manufacturing OSL security locks as compared to purchasing commercial security locks. Apart from lowering the cost, this method enabled PNRI to conduct a revision in the design of the security lock.

C. Needs Identification

Design revisions are desired by the end users since they have observed room for improvement in the long-term use of the dosimeter model. This section defines some of the functional needs identified for this work.

Reworking of the mold to keep the existing design was quoted at P16,570.00. While the design was initially revised, the PNRI finds that the design of the lock could be further improved. However, for a simple iteration in the design, the fabrication of a new mold would cost around P250,000 – P350,000.00. It is expected that there should be at least 2-3 possible revision items which could be costly if individual molds are to be fabricated.

To determine the approximate functional force requirement, pull tests were performed by PNRI on an old security lock design, a new security lock design, and the locally fabricated security lock. Tests were performed on both a new mating clip holder and a relatively worn-out clip holder. 20 trials were conducted and the average is reported in Table 3. While there has been an observed drop in force handled by the lock with the locally made security locks, the cost and functionality still made it a viable option. It was also known that the supplier locks had undergone revisions that had lower force requirements.

It is also worth noting that the delivery lead time of the locks increased from 4-5 months and to 7-8 months, which includes documentary processing requirements from both PNRI and the locally available locks. Also, the locks are delivered with the sprue and runners still intact, consuming more storage space and time removing the locks piece by piece. Relatively, more material is consumed by the mold stem as compared to the security locks. By computing the ratio of the usable part and the total weight, it was found that 72% of the materials are discarded. It is highly desirable to reduce this amount of wastage that goes unutilized to improve environmental friendliness and sustainability.

Based on these considerations, the PNRI are exploring other manufacturing methods that would meet their requirements. Additive Manufacturing (AM) is one possible manufacturing method.

Table 3. Force requirement to pull dosimeter clips

Dosimeter lock design	New Clip Force requirement, lbf	Old Clip Force requirement, lbf
Old design, commercial	8.18	9.31
New design, commercial	4.10	4.20
Locally fabricated	3.25	2.76

III. Design Considerations for OSL Dosimeter Locks

After the needs have been properly identified, the security locks had to be redesigned for AM, and the following sections elaborate factors that have been considered.

A. Material and Equipment Selection

A consumer-class resin 3D printer was used to print the security locks. Creality Halot One [15], a Digital Light Processing (DLP) 3D printer with a build volume of 127mmL x 80mmW x 160mmH projects the image of the part's cross-section to polymerize the resin in a vat. The machine (Figure 4a) can print up to 10µm-200µm layer thickness. Locks were printed using off-the-shelf commercial resin, blue eSun Hard Tough photopolymer resin [16] with machine parameter settings obtained through an optimization strategy which is outside the scope of this paper. Optimized parameters are shown in Table 4. The 3D model STL files were sliced using Prusa slicer [17], for generating supports and Halot box, for changing the print settings. After printing, the parts are washed in a bath of isopropyl alcohol (IPA) for ten (10) minutes in the Formlabs Washing module (Figure 4b) and further cured using Formlabs Form Cure (Figure 4c) module for sixty (60) minutes.

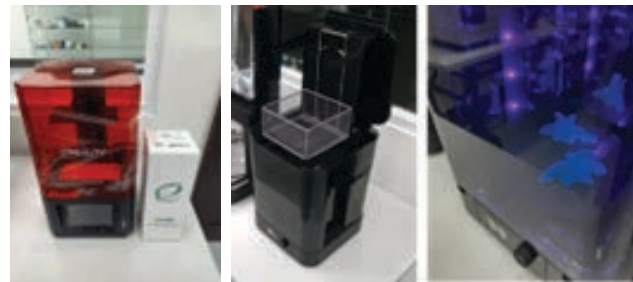


Fig. 4. a) Creality Halot One b) Formlabs Formwash c) Formlabs Formcure

Table 4. Print settings used in halotbox slicer

Parameter	Value
Initial Exposure	40s
Exposure Time	4s
Layer Height	0.05mm
Rising Height	7mm
Turn-off Delay	2s

B. Component Design Iteration

The geometry of the commercially available lock was replicated using a CAD modeling software, Solidworks. Table 5 shows the four design iterations of the single dosimeter lock. Test prints have been conducted to test their performance and adjusted accordingly.

To further optimize the number of manufactured pieces, different approaches for nested design were investigated.

Table 5. Lock design iterations






Revisions	Design changes	Issues encountered
 Original	Original design from the manufacturer	Locks not breaking upon removal.
 Revision 1	Increased cone base diameter to 2.9mm, added break-at-neck feature.	difficult to insert, premature breaking, difficulty in post-processing due to unintentional fusion of resin between layers of locks
 Revision 2	Added 0.3mm slit at the head to secure insertion to the clip, added tapered hole at the bottom to prevent fusion of dosimeter locks during nested printing	Premature breaking of locks during insertion
 Revision 3	Reduced cone base diameter to 2.6mm. Removed break-at-neck feature	Premature breaking of locks during insertion
 Revision 4	Added 0.3mm fillet at the tip. Added DOST Logo on the base of the lock.	Final design approved by the PNRI

Table 6. Nested designs comparison

Support configuration	Print time	Resin consumption
Auto-generated support/ default setting 100%	2h 16min	3.24mL
Auto-generated support/ default setting 50%	2h 16min	2.53mL
Manual support placement	2h 4min	1.91mL

Initially, a nested print consisting of 26 pcs of locks was printed using an auto-generated support structure with default support settings from the PrusaSlicer software. Support structures were optimized by changing support density to 50% but increased the risk of print failure. Manual placement of supports using CAD was also conducted. Table 6 shows the comparison of the materials consumed by the three approaches of a nested design.

Figure 5a shows a conservative support strategy that ensures a high rate of success during printing. However, support removal of this is laborious and the touch points are detrimental to the surface and the overall geometry of the print. Furthermore, the support structure constrains the inner locks preventing them to be thoroughly washed and cured resulting in the curing of unnecessary resins.

Table 7. Various nested prints comparison

Nested Design	Quantity	Weight per nested print	Utilized Volume	Approx. Wastage Ratio	Print Time	Remarks
	8 pcs	2.1g	54.43mmL x 33.45mmW x 63.58mmH	72.75%	17s (cycle time)	Injection molded locks
(a) 	26 pcs	3g	23.31mmL x 23.31mmW x 22.8mmH	13.33%	~2hrs	Low risk, quick print
(b) 	476pcs x 4 = 1904 pcs	55g x 4 = 220g	120mmL x 78mmW x 61mmH	13.45%	~5.5hrs	Moderate risk Can fit 8 hr shift
(c) 	590 pcs	72 g	118mmL x 69mmW x 22.8mmH	18%	~2hrs	Quick print, high risk, uneven curing of locks
(d) 	1156pcs x 4 = 4624 pcs	116g x 4 = 464g	124mmL x 78mmW x 136.4mmH	10.31%	~12.5hrs	Build volume is utilized, Moderate risk, Lowest wastage ratio

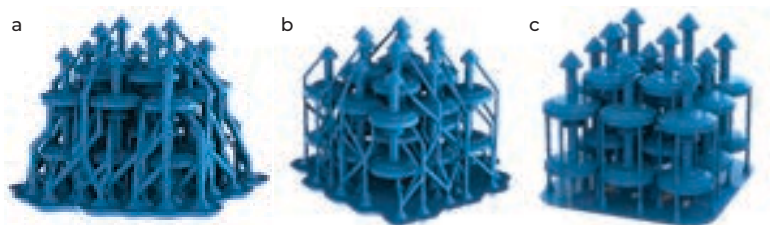


Fig. 5. Nesting prints with a) Auto-Generated Supports @ 100% Density b) Auto-Generated Supports @ 50% Density c) Manually-modeled supports

The support structure also consumes more resin thus, more wasted feedstock materials as thermoset resins are not reusable and recyclable. Figure 5b consumes lesser resin however, touchpoints increased. Figure 5c reveals promising results as it consumes the least resin and reduced print time. The supports were manually modeled in Solidworks as part of the locks. Supports were only touching the back and outer part of the lock, thus, leading to more dimensionally accurate geometry. Trial prints proved that supports at the head of the lock are not necessary; it also may prematurely break when removed from the nested part. The nested design supports were also as small as possible, 0.3mm-0.5mm to reduce the touchpoint size, thus, making it easier to remove.

With the establishment of the most economical and minimal wastage approach in support generation, different nested designs with varying quantities have been printed to assess the effectiveness of the manually modeled support approach. The wastage ratio, utilized volume, and print assessment are shown in Table 7.

IV. Analysis and Comparison

The main goal of this study is to determine and establish design considerations to fabricate additively manufactured OSL dosimeter locks, however, it is worth mentioning that Additively Manufactured dosimeter locks have significant benefits and cost savings in comparison with the current plastic injection manufacturing method.

Figure 6 summarizes the usable part and wastage of the 4 nested prints and the injection molded locks. The graph shows that nested design (d) has the least wastage percentage of 10.31% in comparison to the injection molded locks with 72.75% wastage. It can be mentioned that wastage was further reduced by the manual placement of supports as explained in section III.b. This is also evident in Table VII where a significant reduction in resin consumption from 3.24 mL to 1.91 mL was observed.

A. Manufacturing time

In terms of manufacturing time, Table VII shows that nested design (d) can be printed in approx. 12.5 hours. Curing and washing of the prints could take up to around

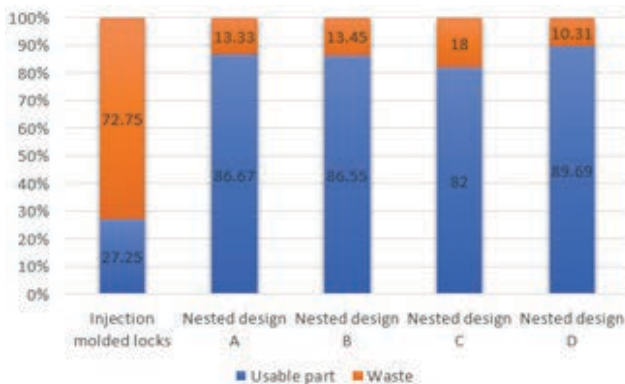


Fig. 6. Usable part to wastage of the different nested prints

1 hour. In total, it would take around 14 hours to produce 4624 functional 3D-printed dosimeter locks. On the other hand, although it only took 17s cycle time for producing eight (8) injection molded dosimeter locks, the overall process for this manufacturing method can take 7-8 months. This includes purchasing pellets, processing job orders, and locks delivery.

As mentioned previously, 25 kgs of HIPS pellets are used by PNRI for their annual supply of dosimeter locks. Table VII states that eight (8) dosimeter locks with the sprue and runners still intact weigh 2.1g. Based on these data, it can be assumed that the PNRI is stocking around 95,588 pcs of locks. For comparison, using the data in Table VII, the nested design (d) would take 21 batches of prints to produce 95,588 pcs of locks for 290 hrs. Since 3D printers can operate 24 hours, it can be assumed that the same number of locks can be 3D printed for approx. 13 days.

B. Inventory and Logistics

One advantage of AM is it has the ability to manufacture parts on demand reducing the need for storage space and eliminating associated costs. Currently, the injection molded locks are delivered in 940mm x 1016mm - XXL black bags (Figure 7).

As stated by the PNRI, 25 kgs of HIPS pellets could produce four (4) full XXL bags containing the dosimeter locks with the sprue and runners still intact. Nested print (d) has a dimension of 63.5mmL x 40mmW x 125.23mmH. A similar number of locks produced by 25kg HIPS pellets would take around 84 nested prints. For comparison, four XXL bags stacked would occupy 1880mmL x 1880mmW x 2032mmH whereas the 84 nested prints could be stacked in a 20L storage bin with a dimension of 450mmL x 320mmW x 204mmH (Figure 8). Based on this, it can be noted that the 3D printed locks are more compact than locks produced by injection molding in terms of storage.



Fig. 7. Injection molded locks storage



Fig. 8. Storage Space for 3D Printed Locks

The cost of printing the locks was also estimated. Typical cost assumptions for AM-based scenarios were applied that are adapted from Hopkinson et al. [18]. The machine was assumed to operate 75-90% of the time, utilize the build volume, and produce a single type of part for one year. This uptime is reasonable for both injection molding and 3D printing. The range was considered since the Advanced Manufacturing Center (AMGen) is a new facility. Figure 9 shows the three main cost drivers, machine depreciation and maintenance, materials used, and labor.

It can be noted that AM-based manufacturing is cheaper than the retail price of the original product.

3D-PRINTED LOCKS

Number of Locks, pcs		4624
Print time, h		12.5
Production Rate/hr, pcs		369.92
Production Rate/yr, pcs		559319.04
Machine Cost	P	13,500.00
Resin Cost/L	P	2,899.00

Machine Cost per Part

Equipment Depreciation	P	1,687.50	P	1,687.50
Maintenance Cost	P	1,350.00	P	1,350.00
			P	0.005

Material Cost

Volume	305.64	P 2,899	886.05036
			P 0.19

Labor Cost

Set Up	0.25	100.46	P 25.12
Printing	12.5	100.46	P 1,255.75
Post Processing	1.17	100.46	P 117.54
Total Cost per Build			P 1,398.40
Labor Cost per Part			P 0.30

TOTAL COST/part P 0.50

Fig. 9. Estimated Cost of 3D Printed Locks

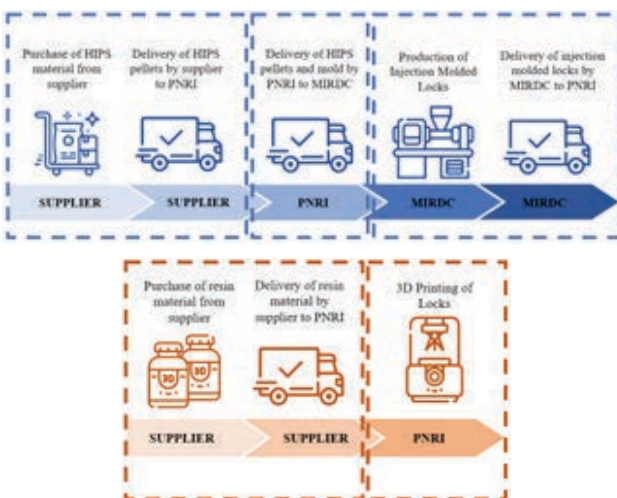


Fig. 10. Supply chain comparison a) Injection Mold manufacturing b) Additive Manufacturing

V. Others Aspects for Consideration

A. Sustainability

Apart from the aforementioned benefits, Additive Manufacturing (AM) offers sustainability advantages by reducing material waste. The dosimeter lock's small size and simple geometry require a smaller support structure, unlike injection molding, which generates significant waste and high material costs. Moreover, AM's on-demand manufacturing shortens the supply chain by empowering consumers with direct manufacturing, resulting in reduced environmental impacts, transportation costs, and operational expenses. This shift also decreases vulnerability to disasters and disruptions, exemplified by the disruptions caused by the Covid-19 pandemic in 2020. AM's resilience lies in the ability of the PNRI to manufacture its own OSL Dosimeter locks, mitigating the supply chain vulnerabilities associated with traditional manufacturing methods, Figure 10.

B. Security features

AM enables the ability to design and create in novel ways but poses problems in terms of intellectual property, and unauthorized copying leading to potential liability issues. By incorporating tamper-proof elements in the dosimeter locks such as unique codes, material-specific parameters, and colors, even if CAD models are stolen, the resulting products will be flawed if produced with the same equipment and printer settings [19].

VI. Conclusions and Recommendations

Plastic injection molding is proven to be a more practical and cost-effective choice for producing OSL security locks compared to purchasing ready-made commercial locks. However, Additive Manufacturing introduces a novel manufacturing approach. With the ability to rapidly generate four design iterations without the need for expensive and time-consuming tooling, it offers significant advantages. Additionally, by manually designing supports instead of relying on slicer-generated ones, waste material has been greatly reduced by 41%. The on-demand manufacturing capability of 3D printing also minimizes the need for inventory space. Rather than relying on multiple suppliers and third-party manufacturers, end users have complete control over the production process through 3D printing. Lastly, the cost of each lock has been reduced by an impressive 90%. While plastic injection molding is currently a favorable option when it comes to high-volume production, Additive Manufacturing presents exciting possibilities for efficient and customizable production.

VII. Acknowledgment

This work is partially funded by the Department of Science and Technology with Project No. 10970/11632, a research project of the Advanced Manufacturing Center (AMCen). The authors would like to thank the Metals Industry Research and Development Center (MIRDC), Philippine Nuclear Research Institute (PNRI), and Philippine Council for Industry, Energy, and Emerging Technology Research and Development (PCIEERD). The authors would also like to thank Mr. Jhon Ray L. Amparado of PNRI for his invaluable inputs in this study.

References

- [1] M. L. Grande, et al., "Viability of 3d printing dosimeter security locks for the osl personnel monitoring service," presented at the 3rd Philippine Nuclear Research and Development Conference (PNRDC) 2022, Dec. 2022, p. 22. [Online]. Available: <https://aew.pnri.dost.gov.ph/aew/2022/pnrdc.php>
- [2] A. H. M. Abaza. New trend in radiation dosimeters. *American Journal of Modern Physics*. Vol. 7, No. 1, 2018, pp. 21-30
- [3] K. Romallosa, et. al. (2019). Development of the Philippine national dose registry as a tool for the tracking and assessment of occupational radiation exposures and risks in the Philippines. *Philippine Journal of Science*. 149. 10.56899/149.S1.09.
- [4] J. P. Rogelio et al., "Modal analysis, computational fluid dynamics and harmonic response analysis of a 3d printed x-ray film handler for assistant robotic system using finite element method," 2020 IEEE 12th International Conference on Humanoid, Nanotechnology, Information Technology, Communication and Control, Environment, and Management (HNICEM), 2020, pp. 1-6, doi: 10.1109/HNICEM51456.2020.9400014.
- [5] Sculpteo(2014). A sculpteo guide to cost efficiency through short series manufacturing. Retrieved from <https://www.sculpteo.com/en/ebooks/3d-printing-vs-injection-molding/>.
- [6] R. G. D. Libre Jr., and A. B. Culaba. "Assessing 3d printing as new normal for manufacturing: review on trends and applications." *Innovative Technology and Management Journal* 3 (2020): 1-5.
- [7] M. B. De Leon et. al. "3d-printing for cube satellites (cubesats): Philippines 'perspectives." In *Engineering Innovations*, vol. 1, pp. 13-27. Trans Tech Publications Ltd, 2022.
- [8] "Inlight-Infofiche-EN.pdf." Accessed: May 31, 2023. [Online]. Available: <https://www.sckcen.be/sites/default/files/uploads/Services/Dosimetrie/Inlight-Infofiche-EN.pdf>
- [9] "OSL Dosimeters | InLight Systems | Nagase Landauer, Ltd." <https://www.nagase-landauer.co.jp/english/inlight/dosimeters.html> (accessed May 31, 2023).
- [10] D. V. Rosato and M. G. Rosato. *Injection molding handbook*. Springer Science & Business Media, 2012.
- [11] N. Y. Zhao, J. Y. Lian, P. F. Wang, and Z. B. Xu. Recent progress in minimizing the warpage and shrinkage deformations by the optimization of process parameters in plastic injection molding: a review. *Int J Adv Manuf Technol*. 2022;120(1-2):85-101. doi:10.1007/s00170-022-08859-0
- [12] H. Radhwan, et. al. "Optimization parameters to reduce the warpage defect of plastic injection molding process for a thin-shell part using design of experiment." *IOP Conference Series: Materials Science and Engineering* 551 (2019): n. Pag.
- [13] Z. Chen, and L.-S. Turng. "A review of current developments in process and quality control for injection molding." *Advances in Polymer Technology: Journal of the Polymer Processing Institute* 24, no. 3 (2005): 165-182.
- [14] "FT-NEU-006-RevE_Neutrak_jan22_EN.pdf." Accessed: May 31, 2023. [Online]. Available: https://www.landauer-fr.com/voy_content/uploads/2022/02/FT-NEU-006-RevE_Neutrak_jan22_EN.pdf
- [15] "HALOT-ONE Resin 3D Printer". Shenzhen Creality 3D Technology Co., Ltd. <https://www.creality.com/products/creality-halot-one-resin-3d-printer> (accessed June 6, 2023)
- [16] "Esun Hard Tough Resin". Shenzhen Esun Industrial Co., Ltd. <https://www.esun3d.com/hard-tough-resin-product/> (accessed June 6, 2023)
- [17] "Prusa Slicer". Prusa Research by Joseph Prusa https://www.prusa3d.com/page/prusaslicer_424/ (accessed June 03, 2023)
- [18] N. Hopkinson, and P. Dickens. 2003. "Analysis of rapid manufacturing—using layer manufacturing processes for production." *Proceedings of the Institution of Mechanical Engineers, Part C: Journal of Mechanical Engineering Science* 217 (1): 31–39.
- [19] F. Chen, G. Mac, N. Gupta. Security features embedded in computer aided design (CAD) solid models for additive manufacturing. *Materials & Design*, Volume 128, 2017, Pages 182-194, ISSN 0264-1275, <https://doi.org/10.1016/j.matdes.2017.04.078>.

Topology Optimization and Rapid Prototyping of Aerial Drone Attachments Fixation Devices

Ramcis Allen A. Chan*¹, Ulysses B. Ante*², Earl John T. Geraldo*³, Jozal B. Carrido*⁴, Mark Christian E. Manuel*⁵, Marc Adrian O. Yu*⁶

Abstract

Due to low-cost sensors and cameras, processing units, and a wide range of payload for various applications, drones have become more useful and versatile in recent years. Vibration, interference, and component collisions can occur with off-the-shelf enclosures and fixation which affects battery life and limit maneuverability under sudden loads. A project by the Rizal Technological University developed a Light Pollution Luminance Device (POLLUX) that can be attached to commercially available drones. This paper focuses on the use of topology optimization software in automatically generating lightweight structural designs for the drone attachment of mounting POLLUX to a DJI Agras MG-1P drone of Pasig City LGU. which is above the 7kg weight class. The LGU of Pasig City acquired various drones and Rizal Technological University has collaborated with them to mount the POLLUX sensors and processing unit that can gather elevated, real-time, spatiotemporal data measurement of environmental pollution parameters. The initial design for POLLUX is capable of housing the sensors; however, it can be improved to mount the sensors more securely and reduce the overall weight in relation to its carrying capacity by redesigning it to be used for data gathering. Using MSC Apex, topology optimization was performed, resulting in an overall weight reduction of 15%. Attachments were manufactured using additive manufacturing techniques, specifically Fused Filament Fabrication (FFF) technology. Rapid iterative prototypes were successfully adapted to evolving hardware conditions. The final FFF-deployed prototype underwent successful test flights and was deemed adequate for its intended application, and serves as a benchmark for future production and commercialization.

Keywords: light pollution, drone, fused filament fabrication, fused deposition modeling, additive manufacturing, topology optimization, finite element analysis

I. Introduction

Artificial nighttime lighting, also known as "light pollution," is an increasing yet frequently disregarded anthropogenic stressor on the environment. Despite not traditionally receiving as much attention as other types of pollution, research over the past few decades has shown that light pollution has a detrimental impact on people, animals, and ecosystems. Understanding light pollution's impacts on circadian physiology, organismal fitness, life history features, and tradeoffs, population trends, and social interactions is urgently needed as light pollution's regional, spectral, and temporal reach continues to increase.¹ In this regard, it's critical to evaluate the light pollution situation right now and create optimum management strategies to lessen its effects.²

The Center for Astronomy Research and Development (CARD), Rizal Technological University (RTU) initiated the study of light pollution in the Philippines by surveying the night sky of the City of Pasig and the City of Mandaluyong. The RTU created a device that measures light and air pollution and other elements. The RTU-CARD approached the DOST Advanced Manufacturing Center (DOST-AMCen)

for collaboration on printing the casing/housing of the sensors and brackets to attach them to the drone to be used on the aerial survey.

The RTU-CARD collaborated with the DOST-AMCen for the printing of the POLLUX enclosures and fixations design. The researchers proposed light weighting of the print and the reduction of the materials to be used in order to prolong the flight time of the drone.

II. Materials and Methods

With the selected model of the drone from the LGU of Pasig City, the researchers were able to obtain the profile using a 3D scanner then importing it in Solidworks, a CAD modeling software. Using the imported scanned model as a graphic, the solid body of the drone 3D model was patterned after it. This enabled the researchers to determine the dimensions of the fixation parts necessary to attach the POLLUX on to the drone (Fig.1 and 2).



*1 Project Technical Assistant IV
Metals Industry Research and
Development Center
Bicutan, Taguig City
Philippines



*2 Sr. Science Research Specialist
Metals Industry Research and
Development Center
Bicutan, Taguig City
Philippines



*3 Project Technical Specialist I
Metals Industry Research and
Development Center
Bicutan, Taguig City
Philippines

Among the components of the drone attachment enclosures and fixations, the researchers focused on the fixation parts for the lightweighting study, specifically the Drone Clamp and Connecting Link. Conducting topology optimization³ simulation using MSC Apex software enabled lightweighting of the parts while retaining its structural integrity and functionality. Parameters for the simulation are shown in Table 1.

In order to verify and compare the structural performance of the fixation parts, the researchers used ANSYS

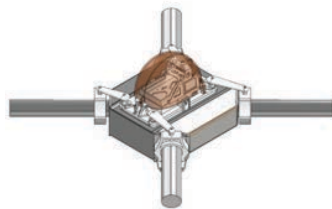


Fig. 1. POLLUX drone attachments assembly

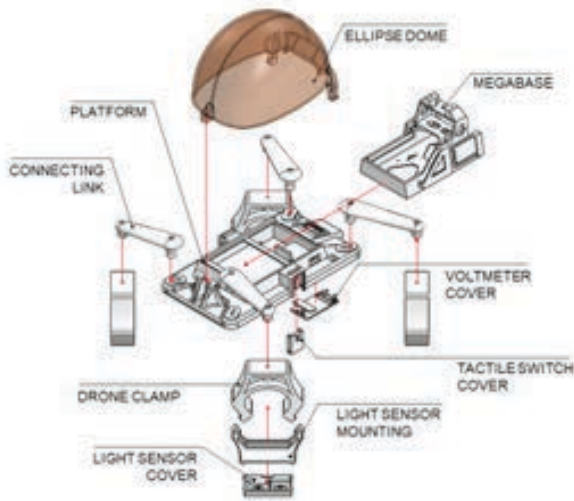


Fig. 2. Drone attachments components

Table 1. Topology optimization simulation parameters

Parameter	Value
Material	ABS
Density	1.10E-006 kg/mm ³
Safety Factor	2
Complexity	50
Strut Density	Sparse

software to conduct Finite Element Analysis (FEA) study⁴. Conducting a simulation on an assembly required a fastener (bolt and nut) modeled in Solidworks to be able to imitate how the parts will perform when assembled. Material parameters for the FEA Simulation are shown in Table 2 and 3.

Loads and constraints for the FEA simulation are almost similar to the Topology Optimization study with a few minor changes. The models were imported on ANSYS as an assembly with contacts mostly Frictionless except for

Table 2. Loading of 3D parts for topology optimization

Image	Reference	Direction	Value	Rationale
	Clamp Force Moment 1	Fy	+6.0 N	Weight of the drone attachment assembly exerting an upward force on the clamp upon landing
	Clamp Force Moment 2	Fy	-75.0 N	Weight of the drone itself exerting a downward force on the clamp upon landing
	Clamp Force Moment 3	Fy	-75.0 N	Weight of the drone itself exerting a downward force on the clamp upon landing
	Link Force Moment 1	Fy	+20.0 N	Weight of the drone attachment assembly exerting an upward force on the link upon landing
	Link Force Moment 2	Fy	-150.0 N	Weight of the drone itself exerting a downward force on the link upon landing

Table 3. F.E.A. material parameters

Part	Material	Density	Yield Strength	Ultimate Strength
Drone Clamp	Plastic, ABS (high-impact)	1030 kg/m ³	27.44 MPa	36.26 MPa
Connecting Link	Plastic, ABS (high-impact)	1030 kg/m ³	27.44 MPa	36.26 MPa
Bolt	Stainless Steel	7750 kg/m ³	207 MPa	586 MPa
Nut	Stainless Steel	7750 kg/m ³	207 MPa	586 MPa



*4 Project Technical Specialist I
Metals Industry Research and Development Center
Bicutan, Taguig City
Philippines



*5 S&T Fellow II
Metals Industry Research and Development Center
Bicutan, Taguig City
Philippines



*6 Project Technical Specialist I
Metals Industry Research and Development Center
Bicutan, Taguig City
Philippines

the Bolt and Nut which were defined as Bonded contact. Parameters for the static structural are shown in Table 4 and Figure 3.

Once the optimized models are structurally validated, prototyping the design was the next step. For this, the researchers opted to use FFF technology to fabricate the prototype. Using Ultimaker Cura software, the model to be printed was sliced based on the following parameters (Table 5 and Figure 4):

Table 4. F.E.A. static structural parameters

Reference	Type	Direction	Value
Condition	Standard Earth Gravity	-Y	-9806.6 mm/s ²
Load	Force	+Y	20 N
Constraint	Fixed Support	-	-



Fig. 3. FEA Simulation Load, Condition and Constraint

Table 5. Printing parameters

Parameters	Inputs
Printer	Ultimaker S5
Material	Generic ABS
Profile	Normal - 0.15 mm
Wall Line Count	3
Infill Density	20%
Infill Pattern	Cubic

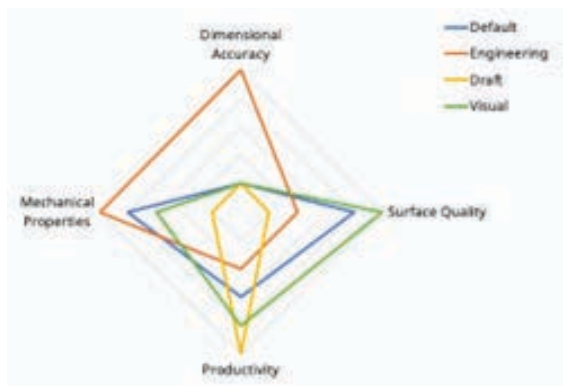


Fig. 4. Visual configuration of Ultimaker Cura printing profiles [6]

III. Results

3D models from MSC Apex of the fixation parts, while optimized, require further polishing and finalization; and can be only saved as an Standard Tessellation Language (.STL) file preventing it from being utilized in simulation software such as ANSYS for verification.⁵ Because of this, the researchers imported the optimized 3D models back to Solidworks for design finalization and adjustments. The models are then saved as Standard for the Exchange of Product Data (.STEP) file for ANSYS simulation.

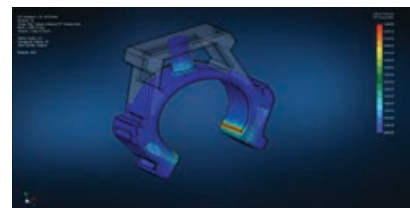


Fig. 5. Drone Clamp Topology Optimization



Fig. 6. Connecting Link Topology Optimization



Fig. 7. Model from MSC Apex (left) and finalized model from Solidworks (right) of the drone clamp



Fig. 8. Model from MSC Apex (left) and finalized model from Solidworks (right) of the connecting link

Figure 9 shows the von-Mises stress and the total deformation of the part between the unoptimized drone clamp and connecting link. Maximum stress on the study occurred through compression in the contact between the connecting link and drone clamp while the maximum deformation was observed at the opposite end of the connecting link in reference to the drone clamp. Deformation as seen on the connecting link was minor and was considered elastic. Furthermore, there were no failures reported on the part assembly.

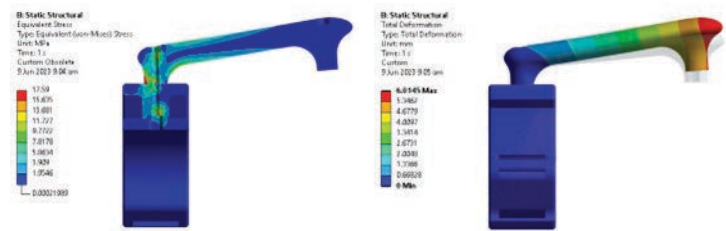


Fig. 9. von-Mises Stress (L) and Total Deformation (R) of the Unoptimized Assembly

Figure 10 shows the von-Mises stress and total deformation of the part between the optimized drone clamp and connecting link. Maximum stress on the study occurred through compression in the contact between the connecting link and drone clamp while the maximum deformation was observed at the opposite end of the connecting link in reference to the drone clamp. Deformation as seen on the connecting link was greater than the unoptimized assembly and was considered plastic. Nevertheless, even though the stress generated was greater than the unoptimized assembly, there were still no failures reported on the part assembly.

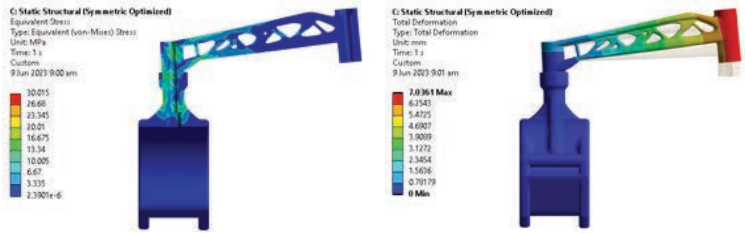


Fig. 10. von-Mises Stress (L) and Total Deformation (R) of Optimized Assembly

Comparison between the 3D-printed designs were made by determining the weight of each fixation part. Figure 11 and Figure 12 shows that the optimized design was 33.33% and 26.92% lighter in terms of weight of the connecting link and drone clamp respectively.



Fig. 11. Weight comparison between unoptimized (L) and optimized (R) connecting link

Furthermore, a test flight was conducted to determine the functionality of the POLLUX device along with the additively manufactured attachments, especially the fixation parts as shown in Figure 13 and Figure 14. The test was done in the evening to be able to gather data not only for air but light pollution as well, which was obtainable at that time of the day. Flight time was recorded to be 42.5 minutes in total with the attachment not affecting the flight time of the drone significantly.



Fig. 12. Weight comparison between unoptimized (L) and optimized (R) drone clamp



Fig. 13. POLLUX attachments installed in the AGRAS MG-1P drone



Fig. 14. Drones fully operational during the test

IV. Conclusions and Future Work

The study was able to produce weight optimized fixation parts for the drone attachments without compromising its structural integrity. This resulted in lighter fixation parts with structural performance on par with the unoptimized design. Though there were differences on the maximum stresses experienced on the design iterations due to the compression of the parts, this can be resolved by adding fillet features on the edges. Furthermore, there were only minor discrepancies in terms of the amount of deformation on both designs.

Exploring other material options can also provide better weight reduction and strength in the future in comparison with ABS (Acrylonitrile Butadiene Styrene). In addition, using Stereolithography technology for fabricating the optimized parts can provide a better surface finish and material bond over the result increasing its marketability and aerodynamic properties in flight.

In the flight test, it was observed that the optimized fixation parts did not have a significant impact on the flight time and maneuverability of the drone despite the presence of stress and deformation.

V. Acknowledgment

This work is/was partially funded by the Department of Science and Technology (DOST), Metal Industry Research and Development Center (MIRDC), Technological Readiness and Innovation through Advanced Manufacturing in the Philippines (TRIAMPH) with Project No. 19-007-01-08-96, 2023. The researchers would like to acknowledge the following institutions: Rizal Technological University - Center of Astronomy Research and Development (RTU-CARD) for their initial design given to the researchers and inputs for the finalization of this design. Pasig City DRRMO - Drone Team for leading their time and resources to testing the 3D printed parts. The researchers would like to acknowledge the following individuals for letting their time, knowledge, and resources for the project: Fred Liza, Jose Bernardo Padaca III, Hannah Ramos, Ranier Jude Wendell Lorenzo, Pedrito Domingo, Jr.

References

- [1] Gaston KJ, Duffy JP, Bennie J. Quantifying the erosion of natural darkness in the global protected area system. *Conserv Biol*. 2015 Aug;29(4):1132-1141. doi: 10.1111/cobi.12462. Epub 2015 Feb 17. PMID: 25693660.
- [2] Mayer-Pinto M, Jones TM, Swearer SE, Robert KA, Bolton D, Aulsebrook AE, Dafforn KA, Dickerson AL, Dimovski AM, Hubbard N, McLay LK, Pendoley K, Poore AGB, Thums M, Willmott NJ, Yokochi K, Fobert EK. Light pollution: a landscape-scale issue requiring cross-realm consideration. *UCL Open Environ*. 2022 Jun 29;4:e036. doi: 10.14324/111.444/ucloe.000036. PMID: 37228454; PMCID: PMC10171420.
- [3] Sbrugnera Sotomayor, Nicolas Alberto, Fabrizia Caiazzo, and Vittorio Alfieri. "Enhancing design for additive manufacturing workflow: optimization, design and simulation tools." *Applied Sciences* 11.14 (2021): 6628.
- [4] Thompson, Mary Kathryn, and John Martin Thompson. *ANSYS mechanical APDL for finite element analysis*. Butterworth-Heinemann, 2017.
- [5] Wang WB, Chang SM. Three-dimensional morphological study of type B lateral malleolar fractures with special reference to the end-tip location of proximal apices. *Front Bioeng Biotechnol*. 2023 May 4;11:1152775. doi: 10.3389/fbioe.2023.1152775. PMID: 37214301; PMCID: PMC10192872.
- [6] "Support Community," support.makerbot.com, Jun. 09, 2023. <https://support.makerbot.com/s/article/1667411132905> (accessed Jun. 09, 2023).



Accutech Steel & Service Center Inc.

Steel Coil Service Centre for Sheetmetal raw materials supply
Housing Components: Micropiles, Light Gauge Steel System, Bathroom Pods

Arturo Drive corner Alicia Drive, Tanyag, Bagumbayan, Taguig City, Metro Manila, Philippines 1500
Telephone: +63 2 8838-9192 to 95 Telefax: + 63 2 8838-9196 Cellphone: +63 922 839 9192
Email: accutechsteel@pldtdsl.net Website: www.accutechsteel.com



Micropiles



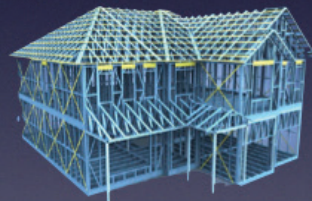
**Deep
Pile**




MSH
MyStrongHome



Cold Form Steel / Light Gauge Steel



Residential
concrete slab



**Dovetail
Metal Deck**



CFS/LGS Joist

Mid Rise Bldg.
Prefab House




Supply of Cut to Size:

(Sheet, Plates, Coils & Strips)

1. Plain & Coated Cold Rolled Steel
2. Hot Rolled Steel



Sandpaper Leaf (*Ficus fiskei* Elmer) Extract as Green Corrosion Inhibition for Carbon Steel in Saline Environment

Ainne Marie A. Mercado*¹, Tiffany Mae C. Nuelan*², Harley Ned S. Aquino*³, Jannah P. Regencia*⁴, Dr. Sicily B. Tiu*⁵



Abstract

Green corrosion inhibitors are one of the existing solutions that address the growing problem of different industries with corrosion. This study explored the use of Sandpaper leaf, commonly known as "As-is" as a green corrosion inhibitor for carbon steel in saline environment, as its phytochemical and FTIR analysis revealed that ethanolic extracts of Sandpaper leaf plant contains natural corrosion inhibitive compounds such as flavonoid, tannin, saponin, and phenol. Moreover, the effects of temperature and powder-to-solvent (PS) ratio on the antioxidation (AO) activity of Sandpaper leaf extracts (SPLE) was also investigated. The result revealed that the highest AO activity obtained was 91%, from the sample that was extracted at 25°C temperature and 1:15 PS ratio. Furthermore, the effect of parameters such as viscosity and number of coating application was also assessed using weight loss method wherein highest corrosion inhibition efficiency (IE) was recorded at 92.31%, the coating condition that has 4.59×10^{-2} Pa-s viscosity and three layers of coating. In addition, the performance of coating mixture of paint and SPLE that gave the highest IE was further evaluated using SEM EDX, water absorption, Water Contact Angle (WCA), and electrochemical analysis. SEM EDX, water absorption, and WCA analyses gave favorable results toward the coating with SPLE when compared to the uncoated CS and CS coated with paint only. Additionally, electrochemical measurements of the coating with SPLE exhibited higher open circuit potential and higher phase angle than the uncoated CS and CS coated with paint only, denoting its better corrosion IE performance.

Keywords: corrosion, Sandpaper leaf Extract, Carbon Steel, Saline Environment Antioxidation Activity, Corrosion Inhibition Efficiency

I. Introduction

Corrosion degrades material qualities as the result of its interaction with its environment. It is a one-way process and occurs when electrons are transferred between a solid electrode and an electrolyte, thus degrading the material or substrate. It is a common problem in industry as most of the materials used in industrial processes utilize metal such as carbon steels. [1]

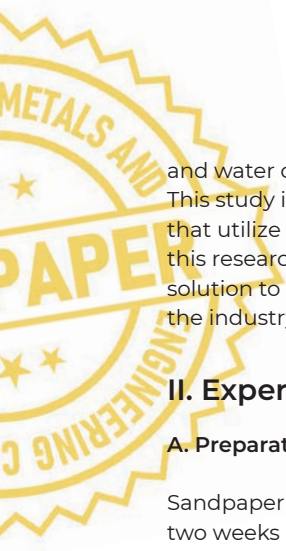
Carbon steel is an iron-based alloy that contains carbon and at least three other alloying elements in trace amounts, it is well known for its mechanical properties, however, it is less resistant to corrosion because its composition requires little to no chromium content and a higher percentage of iron. [2] Inhibitors are the most widely used form of corrosion prevention because they are the most comprehensive in terms of cost-effectiveness and efficiency [3]. Due to the expensive and toxic effects of some chemical inhibitors, plant-based inhibitors also termed as green inhibitors are gaining popularity over the years due to their equal benefits.

Sandpaper leaf plant (*Ficus fiskei* Elmer), also known as "Is-is" or "As-is" is a member of *Ficus* genus, which is rich in phytochemical compounds and has numerous health

advantages due to its high phenolic compound concentration that is commonly employed in the production of antibacterial medications. These species has shown promising results as a potential therapeutic agent for several ailments [4]. The sandpaper plant has been shown to have beneficial effects against inflammation, free radicals, and germs. Alkaloids, saponins, flavonoids, tannins, and phenolics are some of the phytochemicals that are present in sandpaper leaf extract. These compounds made sandpaper leaf a promising candidate for studies on corrosion inhibition [5]. This study explored the use of Sandpaper leaf extract as a possible green corrosion inhibitor for carbon steel in saline environments. Specifically, this study aimed to determine the corrosion inhibitive compound present in Sandpaper leaf extracts (SPLE). Also, it sought to investigate the antioxidant ability of SPLE upon varying the extraction temperature and powder to solvent ratio, and to test its efficiency to act as corrosion inhibitors upon using different coating conditions (varying viscosity and number of coatings) through weight loss analysis and potentiostatic polarization method. Moreover, the formulated coating was analyzed through methods such as scanning electron microscopy (SEM), water absorption,



*1, 2, 3, 4
Student
BS Chemical Engineering
Batangas State University - TNEU
Alangilan, Batangas City, Philippines



and water contact angle to characterize its properties. This study is significant to the community and industries that utilize carbon steel because the general objective of this research was to develop an environmentally friendly solution to steel corrosion that is an inherent problem in the industry itself.

II. Experimental Procedure

A. Preparation of Sandpaper Leaf Extracts (SPLE)

Sandpaper leaves were collected, washed, and air-dried for two weeks before pulverizing them using a food grinder. After that, the 15g Sandpaper leaf plant powder was mixed with varying amounts of solvent (ethanol) to attain the desired powder-to-solvent ratio of 1:5, 1:10, and 1:15 (%w/v). After being adequately homogenized for 1–2 minutes, the mixture was extracted at different temperatures for four (4) hours while being stirred continuously in a water bath shaker. Then, the samples were collected from the water bath and were prepared for the separation of powder and plant extracts. After filtering the mixture via filter paper, the filtrate has been heated in a rotary evaporator to 87°C to remove the excess ethanol, the extract was then placed in a clean container [6].

B. Phytochemical Analysis of SPLE

The ethanolic SPLE were tested for the presence of phytochemicals such as alkaloids, tannins, saponins, and flavonoids. The results were presented in terms of signs such as (+) to denote the presence, while (-) to express the absence of these phytochemicals.

For Saponins. 0.5mL of plant extract was added to 10mL water. The solution was shaken vigorously for 15 minutes. The formation of bubbles indicates the presence of saponins.

For Alkaloids. Wagner's reagent was used to determine the presence of the alkaloids in the extracts, 1 mL of plant extracts was added with 1 mL of Wagner's Reagent, the formation of reddish-brown precipitate indicates the presence of alkaloid.

For Tannin. 2.5 mL of plant extracts was placed in a test tube and was added with 1mL of 5% FeCl₃. The formation of greenish black precipitate implies that there is a tannin present in the extract.

For Flavonoid. One (1) mL of SPLE was added with a few drops of dilute NaOH solution. The change in color of the solution indicates the presence of flavonoid.

Estimation of Total Phenolics. The total phenolic content was assessed using the Folin-Ciocalteu method. The phenolic concentration of the extracts was determined using the gallic acid calibration curve. The calibration curve was prepared using five (5) different concentrations (0, 6.25, 12.5, 25, and 50 mg/L) and was added with 2.5 mL Folin Ciocalteu (diluted to ten-fold) and 2.5 mL (75 g/L) sodium carbonate. After 30 minutes of incubation, the absorbance was read at 765 nm..

C. FTIR Analysis of SPLE

The functional groups present in the chemical constituents found in SPLE were identified using Fourier-Transform Infrared (FTIR) spectroscopy. Characterization of the plant extracts was necessary to confirm the presence of compounds that are responsible for the corrosion inhibition property of the plant. FTIR is usually used to identify the chemical bonds or the functional groups within the molecule by generating an infrared absorption spectrum [7].

D. Determination of antioxidant activity of SPLE Using DPPH Radical Scavenging Assay

The free radical scavenging ability of the plant extracts, and ascorbic acid, the standard used, was measured using the method utilized on other researches [8] with slight modifications. The DPPH needed was four (4) milligrams that were dissolved in 100 mL of ethanol, the same solvent used for the extraction, for all the samples to be tested. Ascorbic acid was prepared at different concentrations (0, 5, 10, 15, and 20 mg/L), which was then added to the 3 mL freshly prepared DPPH solution, to prepare the calibration curve. The same procedure was conducted for the plant extracts. The DPPH with samples were left in a dark room to incubate for 15 minutes. After 15 minutes, the absorbance of the samples was measured and used in the calculation of the Radical Scavenging Activity (RSA) given in the formula:

$$RSA (\%) = \frac{A_{control} - A_{sample}}{A_{control}}$$

where, $A_{control}$ is the absorbance of the control and A_{sample} is the absorbance of the sample.

E. Measuring the Viscosity of SPLE

The viscosity (μ) of the corrosion inhibitor was determined using the falling-sphere method. The setup consisted of a sphere with known density, the fluid that needed to be tested, and the tube as the container of the fluid. In this method, the sphere was dropped in the tube filled with the fluid, then the time the ball reaches a certain distance



*5
Associate Professor V
Department of Chemical Engineering
Batangas State University - TNEU
Alangilan, Batangas City, Philippines

was recorded. For Reynolds number ($Re < 1$), the viscosity of the fluid can be computed by the equation given below:

$$\mu = \frac{2(\rho_b - \rho_f)gR^2}{9v}$$

where μ is the viscosity, ρ_b is the density of the ball, ρ_f is the density of the fluid, R is the radius of the sphere, g is the acceleration due to gravity, and v is the constant velocity.

F. Coating Application

The prepared SPLE was mixed with water-based paint (WBP) at 15% volume ratio. The mixture was manually stirred for 20 minutes to 45 minutes until they were well combined. The cleaned and prepared CS samples were coated with WBP and the coating with SPLE. The method of application of the inhibitor was through dip coating at a controlled rate [9].

G. Weight Loss Measurement

The effects of the number of coatings and the varying viscosity of the SPLE were tested using the weight loss method. The CS samples were weighed and immersed in the saline solution having 3.5% (w/w %) NaCl solution. The saline solution was prepared by mixing 3.5g NaCl to 96.5 g distilled water. After 3 days of immersion, the metal samples were retrieved, then reweighed after being rinsed and dried [10]. The corrosion rate and inhibition efficiency were determined using the equation provided below:

$$E\% = \frac{w_0 - w_c}{w_0} \times 100\%$$

where $E\%$ is the anti-corrosion efficiency, w_0 is the weight loss without coating, and w_c is the weight loss with coating [9].

H. Surface Morphology

The CS sample exhibited the best corrosion inhibitory effect when exposed in 3.5 wt.% NaCl environment was characterized using SEM. The magnified surface images of the samples were assessed to determine the extent of corrosion damage by comparing the surface micrographs of the sample without inhibitor and the sample with inhibitor. Also, the elemental analysis was also conducted to determine the effect of coating on the oxygen level of the sample.

I. Water Contact Angle

Water contact angle analysis was used to determine the wettability of the CS surfaces with and without SPLE coating. Using an optical tensiometer, a single droplet of water was used to evaluate the contact angle of the water droplet to the surface of the sample that was fixed on stage of the equipment. An image recorder captured a close-up photograph of the water droplet, and the image

was analyzed for the contact angle with the governing equation of Young-Laplace equation. Using this analysis, the surface of the samples with and without coating was verified to be hydrophobic or hydrophilic depending on the angle of contact.

J. Water Absorption

The ability of the uncoated CS sample, the CS coated with WBP, and the CS coated with 15% SPLE with varying viscosity to absorb water was determined using water absorption analysis. The mass of the uncoated CS sample, the CS coated with WBP only, and the CS coated with WBP and 15% SPLE with varying viscosity were measured using analytical balance before and after immersion to distilled water for 10 days. The excess amount of water had been removed from the samples using a fabric before the measurements to be taken. The amount of water absorbed was determined using the equation provided below:

$$WA = \frac{w_2 - w_1}{w_2} \times 100$$

where W_A is the water absorption capacity, w_2 is the mass of the sample after immersion and w_1 is the mass of the sample before immersion.

K. Electrochemical Analysis

The electrochemical analysis was carried out using a standard three-electrode cell connected in a potentiostat. The prepared samples, uncoated CS, CS coated with WBP only, and CS coated with WBP and 15% SPLE were exposed to 3.5% NaCl solution while being subjected to open-circuit potential (OCP) measurement. The OCP was used to evaluate the potential that the working electrode (WBP with 15%SPLE) and the saline solution manifested in relation to the reference electrode, which can determine the behavior and mechanism of inhibition of the SPLE. The electrochemical impedance spectroscopy (EIS) was also utilized to generate 50 different frequencies data which will be measured from 100kHz to 10mHz at 10mV amplitude voltage[9].

III. Results And Discussion

The analyzation, and interpretation of the results of the experimental study conducted by the researchers including the phytochemical screening, FTIR analysis, antioxidant testing, weight loss measurement, SEM, water contact angle, water absorption, and electrochemical analysis were discussed in this section.

A. Determination of Phytochemicals in SPLE

The determination of the phytochemicals present in SPLE was essential to confirm the presence of the compounds that can act as corrosion inhibitors which was investigated using phytochemical and FTIR analysis.

1. Phytochemical Screening of Sandpaper Leaf Plant Extracts

Phytochemical analysis was conducted to analyze the chemical constituents present in the ethanolic SPLE and results were presented below in Table 1.

Table 1. Phytochemical Screening of SPLE

Phytochemical	Result
Alkaloids	-
Flavonoids	+
Saponins	+
Tannins	+

From Table 1, it was shown that SPLE has the presence of constituents such as flavonoids, saponin and tannin but alkaloids were not detected in the extract. These constituents contain antioxidants (AO) and AO are structures that have multiple polar atoms and electron rich bonds or hetero atoms that facilitate their electron donating ability, ability that are proven to manifest effective corrosion activity [11]. The existence of AO on the phytochemicals of SPLE makes it a suitable material for paint formulation.

Table 2. Total Phenolic Content of SPLE

Analysis	Result
Total Phenol Content	562.1538 mg GAE/g

The total phenolic content found in SPLE was quantified to be 1562.1538 mg GAE/g. High phenolic content indicates the high AO and anticorrosion property of the extracts. Polyphenols are compounds with a wide range of chemical structures and properties because of the various phenolic functions they contain. Polyphenolic compounds and other hydroxy aromatic compounds make up the bulk of the oxygen found in the extracts. Several hydroxyl (OH) groups are believed to lure the molecule into forming strong hydrogen bonds and metal complexes.

2. FTIR Analysis of the SPLE

FTIR is a valuable analytical tool for determining the structure of functional groups and determining the nature of their covalent bonds.

Figure 1 displayed the FTIR spectrum of SPLE. Absorption bands were detected at 3278.2, 2980, 2903.6, 1638.2, 1455.5, 1418.3, 1386.6, 1325.1, 1274.7, 1084.7, 1043.7, and 877.8 cm⁻¹.

FTIR Spectrum showed the presence of N-H, C-H, O-H, C=C, and C-O functional groups. The existence of these functional groups confirms the presence of corrosion

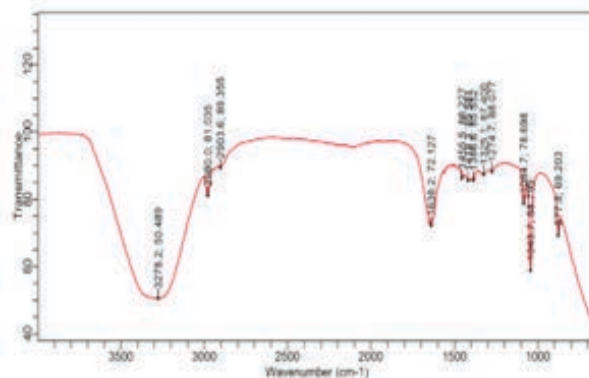


Fig. 1. FTIR Analysis of SPLE

inhibitive compounds in SPLE as shown by their characteristic absorption frequencies.

In a related study, it has been proven that the phenolic chemicals quercetin, kaempferol, mercitin, and isorhamnetin contain amine functional groups as well as OH, C=O, C=N, and C-C groups, which are the primary compounds responsible for the Ficus plant's antioxidation ability [23].

B. AO Activity of SPLE at Varying Extraction Conditions

The determination of the radical scavenging activity (RSA) of the SPLE samples was done using ultraviolet visible spectroscopy or UV-VIS where in a calibration curve of standard antioxidant (AO) was prepared using Ascorbic acid, a naturally occurring effective AO [8].

Table 3 presents the antioxidant (AO) activity of the SPLE prepared at different extraction conditions in terms of their radical scavenging activity (RSA). The extraction conditions used in this study were the extraction temperature and powder to solvent ratio. From the results, the sample that was extracted at 25°C, the lowest extraction temperature, and 1:15 solid to solvent ratio, the highest ratio used, exhibits the best radical scavenging activity of 91%. This result demonstrates the effect of temperature and powder to solvent ratio on the RSA of

Table 3. AO Activity of Sandpaper leaf Extracts Prepared at Different Extraction Conditions

Extraction Temperature (°C)	Powder to Solvent Ratio	Radical Scavenging Activity (%)
25	1:5	89.01
25	1:10	89.95176
25	1:15	91.36678
45	1:5	84.10397
45	1:10	86.41974
45	1:15	89.68043
65	1:5	82.71577
65	1:10	85.29656
65	1:15	87.17536

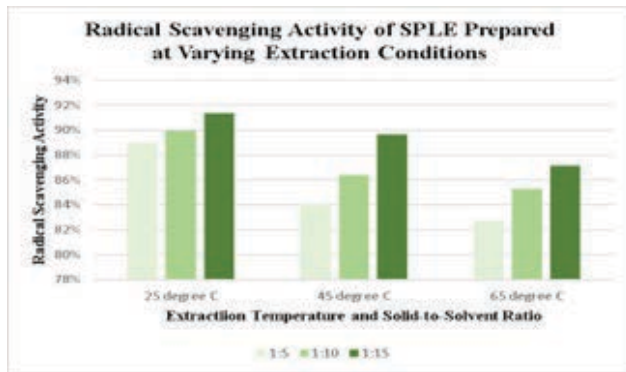


Fig. 2. AO Activity of SPLE Prepared at Different Extraction Conditions

the SPLE as higher temperature may have disrupted the structural stability of the AOs, especially phenolics since studies shown that these compounds were sensitive to high temperatures. Further discussion of the effect of temperature and powder to solvent ratio were presented in Figure 2 which illustrates the radical scavenging activity of SPLE. It was observed that at 25°C temperature, the radical scavenging activity was higher when compared to the samples prepared at 45°C and 65°C. This indicates the heat sensitivity of phenolic compounds, because samples with higher temperature gave a lesser value of AO activity, hence at higher temperatures, the preservation of compounds may not be observed [12].

Moreover, the solid-to-solvent ratio that exhibits the best AO activity was 1:15, which was the set up with least amount of Sandpaper leaf powder, and although the number of phenolic compounds usually increases when the number of solids present in the extraction solvent was greater, the increase in the AO activity of the sample may not be proportional [13]. Also, the increase in solid-to-solvent ratio increases the AO capacity of the extracts, until it reaches the optimum levels [14]. Thus, the 1:15 ratio implies that it is the optimum ratio that would give the highest AO activity.

Table 4 showed that there was a significant difference in the AO activity of SPLE when they are grouped according to temperature with $F(9,2)=27.234$; $p=.005$ and grouped with powder to solvent ratio with $F(9,2)=17.598$; $p=.01$. In both parameters, the calculated values of the p-value from the analysis were less than that of the alpha, which is why the null hypothesis was rejected. This confirms that both parameters have significant

Table 4. Double-factor ANOVA on AO activity of SPLE with varying extraction temperature and powder to solvent ratio based on Radical Scavenging Assay

Groups	Mean	SD	F-value	p-value	Decision on H_0	Interpretation
25°C	90.110	1.186	27.234	.005	Reject H_0	Significant
45°C	86.735	2.802				
65°C	85.063	2.239				
1:5	85.277	3.307	17.598	.01	Reject H_0	Significant
1:10	87.222	2.429				
1:15	89.408	2.109				

Table 5. Sample identification of each CS set-up

Sample	Extract Viscosity (Pa/s)	Number of Coating
Set-up A1	4.59×10^{-2}	1
Set-up A2	4.59×10^{-2}	2
Set-up A3	4.59×10^{-2}	3
Set-up B1	7.66×10^{-1}	1
Set-up B2	7.66×10^{-1}	2
Set-up B3	7.66×10^{-1}	3
Set-up C1	8.42×10^{-1}	1
Set-up C2	8.42×10^{-1}	2
Set-up C3	8.42×10^{-1}	3
Set-up W1	N/A	1
Set-up W2	N/A	2
Set-up W3	N/A	3
Uncoated CS	N/A	0

Table 6. Corrosion IE of CS samples

Sample	Average Weight Loss	Corrosion IE
Set-up A1	0.0277	77.72%
Set-up A2	0.0197	80.90%
Set-up A3	0.0107	91.51%
Set-up B1	0.028	77.98%
Set-up B2	0.024	84.35%
Set-up B3	0.0097	92.31%
Set-up C1	0.0257	79.58%
Set-up C2	0.0253	79.84%
Set-up C3	0.011	91.25%
Set-up W1	0.0813	35.28%
Set-up W2	0.074	41.11%
Set-up W3	0.0607	51.72%
Uncoated CS	0.024	0%

effect on the AO activity of the SPLE based on the scavenging activity.

C. Corrosion IE of SPLE on CS Samples

Corrosion inhibition testing were done to measure the ability of the plant extract to act as green corrosion inhibitor. The identification of each sample that was used in this study can be seen in Table 5.

From the table, Set-up A1, A2, and A3 were all coated with the same exact viscosity (4.59×10^{-2} Pa-s) that rotary evaporated for 2 hours. The following group Set-ups B1, B2, and B3 were coated with a 4-hour rotary evaporated extract that resulted in viscosity of 7.66×10^{-1} Pa-s. The ones coated with 6 hours rotary evaporated extract having a viscosity of 8.42×10^{-1} were the group of Set-ups C1, C2, and C3. On the other hand, the Set-ups A1, B1, and C1 were coated with the extracts only once, Set-ups A2, B2, and C2 twice, and finally Set-ups A3, B3, and C3 thrice.



Fig. 3. Corrosion IE of SPLE on CS samples

The results of the weight loss measurement were used in the calculation of the corrosion inhibition efficiency of the tested CS samples prepared at different coating conditions. Table 6 shows the corrosion inhibition efficiency (IE) of each set-up.

From the resulting calculations, it was revealed that Set-up A1, A2, and A3 had the lowest corrosion IE with an average of 83.38% across the three samples. These are the samples coated with extract that rotary evaporated for two hours. Set-ups B1, B2, and B3 possessed the most efficient corrosion inhibitor activity with an average of 84.88%. These are the samples that were coated with 4 hours rotary evaporated extract. Finally, the last group, Set-ups C1, C2, and C3 were in the middle of the two at 83.55% corrosion IE and the extract used for them was the one that was rotary evaporated for 6 hours.

In terms of the groupings according to the number of coatings, set-ups A3, B3, and C3 showed the best results with an average of 91.69% while set-ups A1, B1, and C1 showed the worst results with an average of 78.43%. The former was coated thrice while the latter was coated once. Set-ups A2, B2, and C2 group, coated twice sit in the middle of the two groups with 81.70% corrosion IE.

From the results of Figure 3, it can be inferred that the conditions used for set-up B3 were the best among all the parameters. First, the viscosity of the plant extract after four hours of rotary evaporation was the best choice because of the concentration of the inhibitive compounds after the extraction. The concentration of the extract increases, the more viscous the extract will become and as the viscosity increases, it is said that the inhibitor's ability to inhibit will be more effective [15]. However, the viscosity of the extract may also negatively affect the corrosion inhibition. Lower viscosity values were better [16,17]. This may be the reason why the most viscous extract did not produce the best corrosion IE because during the duration of the rotary evaporation process, the inhibitive compounds needed may be included in the removal of the ethanol content in the SPLE.

As for the number of coatings, Set-up B3 was coated thrice and gave the best result. The protective effectiveness of a coating improves with increasing coating thickness [18]. This is why the best results came from the greatest number of coatings which in the range of parameters for this study is three times coating.

Table 7. Single-factor ANOVA on corrosion inhibition efficiency of samples with varying viscosity

Groups	Mean	SD	F-value	p-value	Decision on H_0	Interpretation
(0.0459 Pa-s)	83.378	7.222				
(0.7658 Pa-s)	84.881	7.177	.041	.960	Failed to reject H_0	Not Significant
(0.8424 Pa-s)	83.554	6.663				

Table 8. Single-factor ANOVA on weight loss efficiency of samples with varying number of coatings

Groups	Mean	SD	F-value	p-value	Decision on H_0	Interpretation
1 coating	78.426	1.004				
2 coatings	81.698	2.358	62.522	<.001	Reject H_0	Significant
3 coatings	91.689	.552				

Table 7 shows the difference in the corrosion inhibition of SPLE when they are grouped according to viscosity. It can be gleaned from the above table that there is no significant difference on the corrosion inhibition with $F(9,6)=.041$; $p=.960$. The value of the p-value being higher than the alpha, which is equal to .05, means that the data did not meet the requirement to reject the null hypothesis. This means that viscosity has no significant effect on the corrosion inhibition efficiency of the samples.

Similarly, to verify the significance of the number of coatings on the corrosion IE, single factor ANOVA was used to determine the significance of a single parameter in each three or more sets of data.

Table 8 displays the difference in the corrosion inhibition of SPLE when they are grouped according to number of coatings. It can be inferred from the above table that there is significant difference on the corrosion inhibition with $F(9,6)=62.522$; $p < .001$. The value of the p-value being lower than the alpha, which is equal to .05, that means that the null hypothesis will be rejected. This means that the number of coatings has a significant effect on the corrosion IE of the samples.

The comparison of the corrosion IE of set-up B3, the sample that exhibited the highest AO activity, and W3, the sample coated with Water-based paint (WBP) only, the result showed that Set-up B3 was 40.58% higher than the reference set-up coated three times using paint with no SPLE. This proves that the formulated coating with SPLE

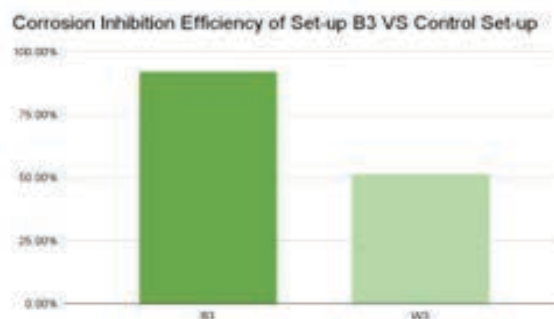


Fig. 4. Comparison of the corrosion IE of Set-up B3 VS Control Set-up

performed better than that of WBP-only. The infusion of green inhibitors generated better results because of the added corrosion inhibitory effect of the plant extract [19]. This is true for the case of this study as well because the previous result was calculated among the samples.

D. Performance Evaluation of Uncoated CS and CS-SPLE

The performance of the coating infused with SPLE was further analyzed using SEM, water contact angle, and water absorption.

1. Scanning Electron Microscopy (SEM)

After immersion in 3.5% NaCl for 72 hours at room temperature, morphological analyses of the surfaces of the uncoated CS samples were studied by SEM.

After immersion in 3.5% NaCl for 72 hours at room temperature, morphological analyses of the surfaces of the uncoated CS samples were studied by SEM. Figure 5 displays SEM images of the uncoated CS sample at different magnification levels. It can be observed that only small black spots can be seen on the 500x and 1000x magnification. However, on the 5000x magnification, pores on the surface of the sample were noticeable. The pores formed means that formation of iron oxide occurred on the uncoated CS sample upon the immersion to a corrosive media.

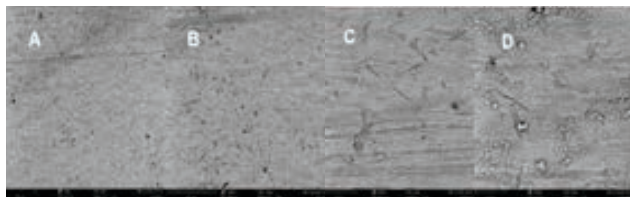


Fig. 5. SEM Analysis of uncoated CS in different magnification level (a) 500x (b) 1000 x (c) 3000 x (d) 5000

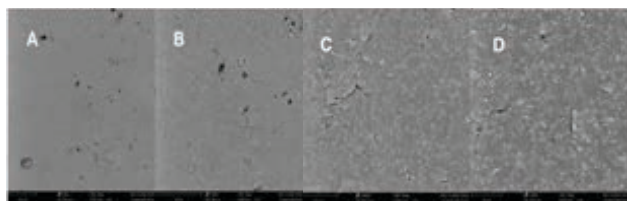


Fig. 6. SEM Analysis of CS-WBP in different magnification level a) 500x (b) 1000 x (c) 3000 x (d) 5000

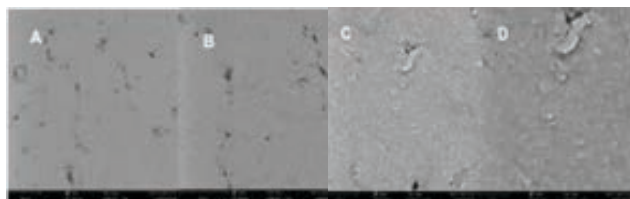


Fig. 7. SEM Analysis of CS-SPLE in different magnification level (a) 500x;(b)1000 x;(c) 3000 x;(d) 5000 x

Figure 6 showed the SEM images of the CS-WBP. It was evident that only a few black spots were seen on the surface of the sample. In comparison to the uncoated CS sample, there were less pores that occurred on the sample coated with WBP. This means that the WBP prevents corrosion from occurring on the surface of the CS. The addition of SPLE to the WBP as a protective coating on the CS surface prevents further corrosion.

The formation of a protective layer on the surface of a steel surface prevents corrosion [19]. Also, the rate of corrosion is being reduced and preserves a smooth surface when an inhibitor is present due to the formation of a protective layer on the mild steel surface.

The SEM micrographs of the CS-SPLE were presented in Figure 7. It was observed that the CS-SPLE was less corroded compared to the uncoated CS sample and the CS-WBP.

The specimen composition was determined, and the elements were analyzed using the EDX analytical method. The result of the three samples showed a high

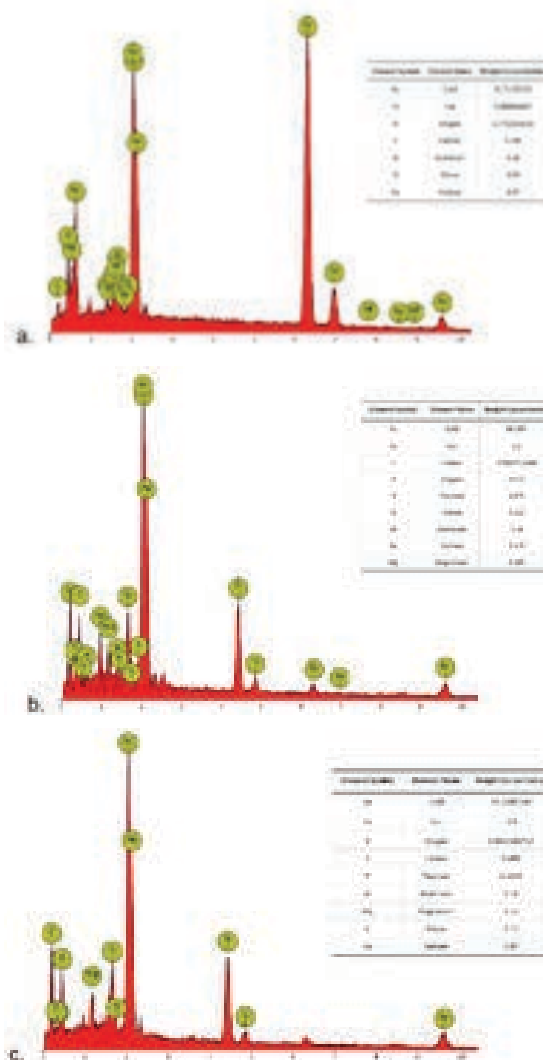


Fig. 8. EDX Spectrum for (a) uncoated CS sample, (b) CS-WBP, (c) CS-SPLE

concentration of gold on the surface of the metals. This is due to the gold sputtering that was done to the samples prior to testing.

Comparing the three samples of this study, the uncoated CS that had high amounts of iron and had the highest oxygen peak indicated that there was iron oxide formation, or it generated corrosion products. In the CS-WBP, the sample's oxygen concentration is lower compared to the oxygen concentration of the uncoated CS sample. However, in the CS-SPLE, it had the lowest concentration of oxygen. It can be deduced that the addition of SPLE to the WBP had reduced the corrosion product in the CS. Also, the presence of titanium and magnesium helped combat the detrimental effects of corrosion to the CS sample.

2. Water Contact Angle (WCA)

This analysis was conducted to determine the surface wettability of the surface of the coated and uncoated CS samples. Using this water contact angle analysis, the surface of the samples may be determined to have hydrophobic or hydrophilic properties. The table below presents the tabulated data collected from the analysis.

Table 9. Water contact angle of coated and uncoated CS samples

	Uncoated CS	CS-WBP	CS-SPLE
Trial 1	42.3°	49.80°	56.82°
Trial 2	72.59°	52.84°	50.9°
Trial 3	82.89°	44.32°	52.73°
Average	65.93°	48.99°	53.48°

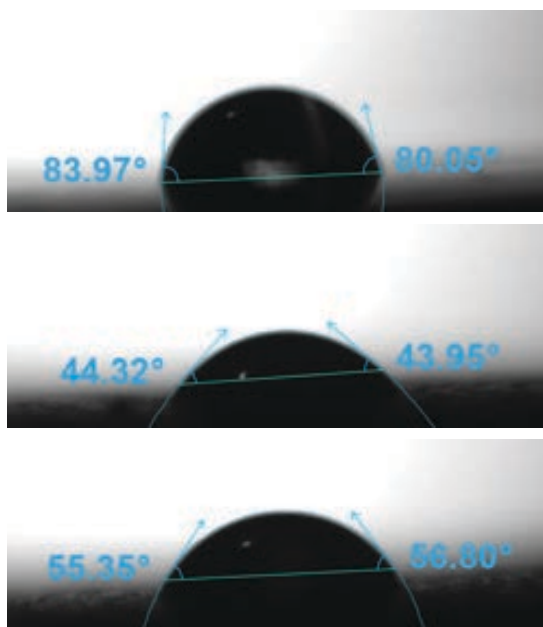


Fig. 9. WCA of (a) uncoated CS, (b) CS-WBP, and (c) CS-SPLE

Reflected on **Table 9** is the WCA of the coated and uncoated CS samples. The average contact angle for the uncoated CS was 65.93°, for CS-WBP was 48.99°, and lastly for CS-SPLE was 53.73°, all of which are less than 90°. This correlates to good wettability and can therefore be concluded that all the samples have hydrophilic properties. Furthermore, it can be observed that the value of the water contact angle increased when the SPLE was added to the coating solution which means that the plant extract made the surface of the CS sample more hydrophobic and it therefore an indicator of good corrosion inhibition property of the SPLE.

Shown in **Figure 9** are the water contact angle results for uncoated CS, CS coated with WBP only, and CS coated with 15% SPLE samples. Based on the test, the WCA of uncoated CS has the highest contact angle followed by CS-SPLE, the CS-WBP. It can be deduced from the information that all the samples are hydrophilic as they are less than 90°.

The WCA of steel is between 40°-70° depending on the surface roughness of the sample itself. With this data established, it can be inferred that the hydrophobicity of the CS sample decreased from an average of 65.93° to 48.99° when it was CS-WBP. The contact angle tells that the samples became even more hydrophilic. Moreover, as reflected on the photos taken from the WCA test, the values of the contact angle increased from the CS coated WBP only to CS coated with 15%SPLE with the average of 48.99° to 53.48°. This may be because of the addition of SPLE on the WBP. Since the extract was determined to have phytochemical constituents that include phenols, flavonoids, saponins, and tannins [20].

Furthermore, the addition of SPLE on the WBP suggests that the SPLE made the formulated coating exhibit higher WCA denoting that the wettability value of the CS-SPLE sample was gearing towards hydrophobicity, thus supports the corrosion inhibitory effect of the plant extract [21].

Table 10. Paired t-test on water contact angle of coated with SPLE and uncoated CS samples

	Mean	SD	t-value	p-value	Decision on H_0	Interpretation
Coated	53.48	3.03	2.92	.230	Failed to reject H_0	Not significant
Uncoated	65.93	21.10				

It can be gleaned from **Table 10** the difference in the water contact angle of the uncoated CS and the CS-SPLE. The results showed the water contact angle of the CS-SPLE (M=53.48; SD=3.03) and uncoated CS (M=65.93; SD=21.10). This is proven by the calculated $t(3,2)=2.92$; $p=.230$. The computed values failed to reject the null hypothesis

concluding that there is no significant difference between the two samples.

3. Water Absorption

The amount of water that can be absorbed by the coatings prepared at different viscosity of SPLE mixed with WBP was determined using the water absorption test. This method is an efficient way for evaluating the liquid absorptiveness or resilience of the coated and uncoated CS samples.

Figure 10 displays the graph of the percentage of the water absorption of the SPLE at different viscosities with three (3) layers of coatings on CS samples. The coating that has the viscosity of 7.65×10^{-1} Pa·s had an average maximum water uptake of 1.44% while the coating that has the viscosity of 8.42×10^{-1} Pa·s and 4.59×10^{-2} Pa·s had an average maximum water uptake of 1.32% and 1.26%, respectively. It showed that the coating that has the viscosity of 7.65×10^{-1} Pa·s had the highest water absorption, while the coating that has the viscosity of 4.59×10^{-2} Pa·s had the lowest water absorption. This was because an increase in the hydrophobicity of a coating led to reducing its water absorption, and less water absorption improves the corrosion resistance of the coating. This means that the lower the value of the water uptake of the coating, the better its anti-corrosion properties. Comparing the results of the water uptake of the SPLE coatings at different viscosities, the coating that has the viscosity of 4.59×10^{-2} Pa·s which has the lowest water uptake is more anti-corrosive.

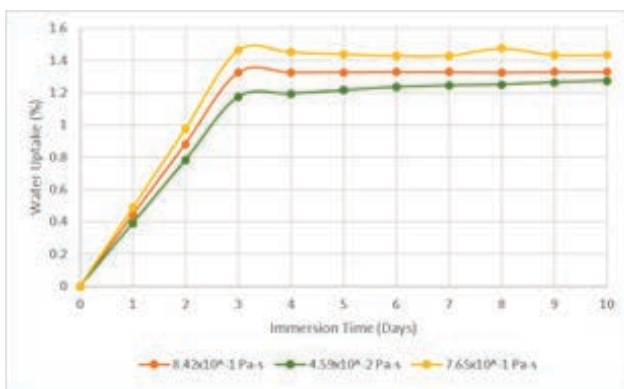


Fig. 10. Time dependence of the percentage of water absorption of the SPLE coatings at different viscosities

To compare the results of the water uptake capacity of the CS-SPLE, the CS-WBP, and the uncoated CS, the CS-WBP sample and the uncoated CS were also tested for water absorption. Figure 11 displays the graph of the percentage of the water absorption of CS-SPLE, the CS-WBP, and the uncoated CS immersed in water for 10 days.

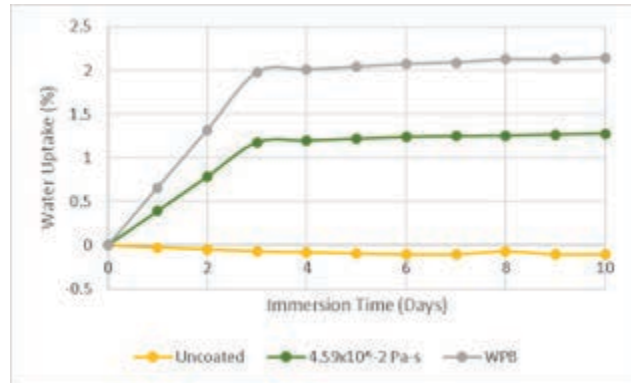


Fig. 11. Time dependence of the percentage of water absorption of the CS-SPLE, the CS- WBP, and uncoated CS

As shown in the graph, the values of the water absorption of the uncoated CS had negative values due to the loss of weight as it corrodes in water. It indicates that the uncoated CS sample degrades with contact to water rather than absorbing water. On the other hand, the water absorption of the WBP coating had an average maximum water uptake of 2.13%, while for the 15% SPLE, the coating that has the lowest water uptake on the first water absorption test was used which is the extract that has the viscosity of 4.59×10^{-2} Pa·s.

Comparing the results to the coated samples, it can be inferred that the coating was the reason for the higher water absorption percentage, whereas for the uncoated CS, corrosion is much more likely to occur than water absorption, which leads to a negative percentage of water absorption. Thus, this implies that the CS coated with 15% SPLE that has the viscosity of 4.59×10^{-2} Pa·s was the best coating that would give a better anti-corrosive ability.

Table 11 shows the difference in the weight loss of the CS samples with and without SPLE. The results showed that there is a significant difference in the weight loss of the CS-SPLE ($M=.015$; $SD=.008$) and uncoated CS ($M=.126$; $SD=.002$). This is proven by the computed $t(3,2)=2.92$; $p < .001$.

Table 11. Paired t-test on weight loss of coated and uncoated CS samples

	Mean	SD	t-value	p-value	Decision on H_0	Interpretation
Coated	.015	.008	2.92	< .001	Reject H_0	Significant
Uncoated	.126	.002				

E. Electrochemical Analysis of Uncoated CS and CS-SPLE

The electrochemical analysis of the samples was conducted through Open Circuit Potential (OCP) and Electrochemical Impedance Spectroscopy (EIS).

1. Open-Circuit Potential

Open circuit measurement analyzes the corrosion inhibition properties of the coating through the determination of the potential difference between the surface of the CS sample, also known as the working electrode, and the reference electrode or Ag/AgCl without the application of a potential or a current.

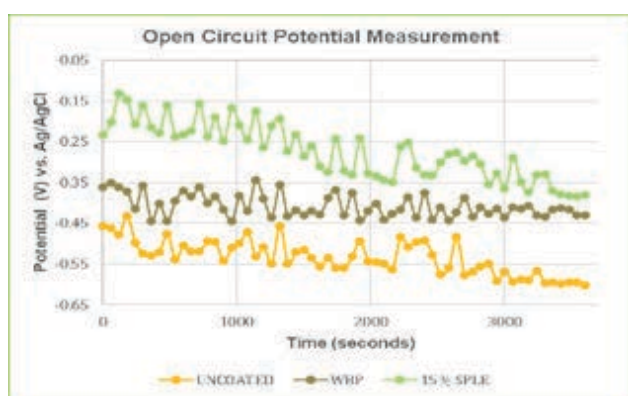


Fig. 12. Open Circuit Potential Measurement of Uncoated, Coated with WBP, and 15% SPLE Extract CS Samples at 3.5% NaCl Solution

From the figure, it was shown that the incorporation of the 15% SPLE to the WBP gave the most noble initial potential of -0.23 V which can be attributed to the initial formation of passive layer and/or corrosion products on the surface of the metallic substrate.

The results in the Open Circuit Potential (EOCP) measurement of the three (3) samples illustrated in Figure 12, were supported by a study that also utilized OCP to determine the corrosion inhibition behavior of their formulated inhibitor. The result of their study revealed that the decrease in EOCP values was the result of the spontaneous oxidation and dissolution of the metal substrate due to the exposure to saline media. Additionally, the increase in the EOCP values signifies the formation of corrosion products and/or passive film, which can decrease the corrosion rate [9].

Furthermore, the downward trend that was exhibited by the graph of the CS-SPLE, demonstrated its mechanism of inhibition when exposed to 3.5% NaCl solution. This downward trend graph signifies the shift of corrosion potential to a more negative direction, denoting that SPLE in this case acted as a cathodic inhibitor. Cathodic

inhibitors prevent corrosion through slowing down the reduction reaction rate and shifting the corrosion potential to the anodic direction, so that cations can move toward the cathode surfaces where they form cathodic precipitates or protective layers that acts as the barriers on the metal surface [22].

2. Electrochemical Impedance Spectroscopy

Figure 13 presents the result of the EIS of the uncoated CS, CS-WBP, and CS-SPLE measured at a frequency of 100kHz to 10mHz, immersed at 3.5% NaCl solution.

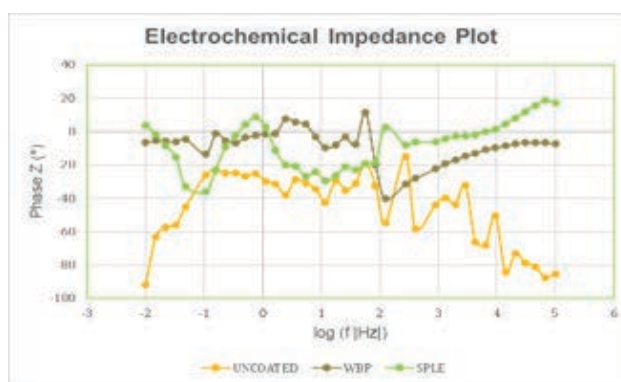


Fig. 13. Electrochemical Impedance Plot of Uncoated, Coated with WBP, and 15% SPLE Extract CS Sample at 3.5% NaCl Solution

Figure 13 reveals that the graph of the uncoated CS recorded its lowest and highest phase angle at -91° and -14° , respectively. Meanwhile, CS-WBP generated a different graph compared to the uncoated sample as it obtained higher phase angle at 11° , and after reaching its peak, it was observed that the graph of the CS-WBP gradually decreases as the frequency increases and gave its lowest phase angle of -40° after the peak. Lastly, the CS-SPLE presented the highest phase angle among the three (3) samples tested, with phase angle value of 17° at its highest peak, and -46° on its lowest. However, unlike the other two plots, the highest phase angle value of the CS-SPLE was recorded near the highest value of the x-axis, and after it reached its maximum peak, the phase angle value started to decrease. The increase in the phase angle values in electrochemical plots implies that there was formation of protective film layer on the surface of the sample, thus attributing to the improvement of the surface coverage and inhibition efficiency of the inhibitors.

The increase in phase angle indicates the development of a passive layer in the surface of the sample steel that protects it from oxidation thus preventing corrosion [23].

IV. Conclusion

Corrosion inhibition of Sandpaper leaf extracts (SPLE) on carbon steel in saline environment was obtained in this study. The corrosion inhibitive property of SPLE was primary due to the phytochemicals it contains. FTIR and phytochemical analysis revealed that most of the phytochemicals present in SPLE such as flavonoids, tannins and saponins, possess corrosion inhibitive properties. Also, SPLE has high phenolic content which indicates its high antioxidizing and anti-corrosion property. Moreover, the presence of functional groups that contain N, O, and pi- bonds contributes to the corrosion inhibitive property of the SPLE.

In addition, the parameters in developing the AO potential of the SPLE such as extraction temperature and amount ratio of Sandpaper leaf plant powder to ethanol have significant effects on giving the highest antioxidant activity of the SPLE. In terms of the corrosion inhibition activity of the CS samples in saline environments, weight loss method was used, and it was determined to have a significant difference in terms of varying the number of coatings. On the other hand, the results showed that there is no significant difference on the corrosion inhibition activity when it comes to varying viscosities of the SPLE. Also, the samples that were prepared using CS coated with 15%SPLE presented significant differences when compared to the uncoated CS sample.

At the best coating condition, CS coated with 15% SPLE exhibited a significant difference in comparison with uncoated CS in terms of water absorption. However, in terms of water contact angle there was no significant difference concluded and since there was no quantitative data gathered using surface morphology analysis, the comparison was based on the SEM images that showed the difference on the surface morphology of the samples as well as the elemental composition found using EDX. Furthermore, the electrochemical analysis confirms the formation of the protective layer on the surface of CS sample coated with 15% SPLE when exposed in 3.5% NaCl solution. Furthermore, it was determined that the formulated SPLE coating acts as a cathodic inhibitor when exposed to saline environment.

V. Acknowledgment

The researchers would like to extend their deepest and sincerest gratitude towards their thesis adviser, Dr. Sicily B. Tiu for her support and guidance, to the Department of Science and Technology – Science Education Institute (DOST-SEI) for the thesis allowance grant that they have given, and to the DLSU Phenom Laboratory for their assistance on providing the results of the analyses conducted in this study.

References

- [1] B. E. A. Rani and B. B. J. Basu, "Green Inhibitors for Corrosion Protection of Metals and Alloys: An Overview," *International Journal of Corrosion*, vol. 2012, pp. 1–15, 2012, doi: <https://doi.org/10.1155/2012/380217>.
- [2] A. Berradja, *Electrochemical Techniques for Corrosion and Tribocorrosion Monitoring: Fundamentals of Electrolytic Corrosion*. IntechOpen, 2019. Available: <https://www.intechopen.com/chapters/67077>
- [3] T. Islam and H. Rashed, "Classification and Application of Plain Carbon Steels," *Reference Module in Materials Science and Materials Engineering*, 2019. <https://www.semanticscholar.org/paper/Classification-and-Application-of-Plain-Carbon-Islam-Rashed/7737f07100c91be2a369399353708d2ad66d11b5> (accessed May 19, 2023).
- [4] L. Helen, A. Rahim, B. Saad, M. Saleh, and P. Bothi Raja, "ELECTROCHEMICAL SCIENCE Aquilaria Crassna Leaves Extracts -a Green Corrosion Inhibitor for Mild Steel in 1 M HCl Medium," *Int. J. Electrochem. Sci*, vol. 9, pp. 830–846, 2014, Accessed: May 19, 2023. [Online]. Available: <http://www.electrochemsci.org/papers/vol9/90200830.pdf>
- [5] S. K. Sharma, A. Peter, and I. B. Obot, "Potential of Azadirachta indica as a green corrosion inhibitor against mild steel, aluminum, and tin: a review," *Journal of Analytical Science and Technology*, vol. 6, no. 1, Oct. 2015, doi: <https://doi.org/10.1186/s40543-015-0067-0>.
- [6] Đ. Bui et al., "ANTIOXIDANT AND ANTITYROSINASE ACTIVITIES OF FLAVONOID FROM BLUMEA BALSAMIFERA (L.) DC. LEAVES EXTRACT," *European Journal of Research in Medical Sciences*, vol. 5, no. 1, 2017, Available: <https://www.idpublications.org/wp-content/uploads/2016/12/Full-Paper-ANTIOXIDANT-AND-ANTITYROSINASE-ACTIVITIES-OF-FLAVONOID-FROM-BLUMEA-BALSAMIFERA.pdf>.
- [7] A. Santiago and B. Balido, "Prooxidant and Antioxidant Polar Phytoconstituents from Endemic Philippines Ficus fiskei Elm. (Moraceae)," *Balido. Prooxidant and Antioxidant Polar Phytoconstituents from Endemic Philippines Ficus fiskei Elm. (Moraceae)*. IJPTP, vol. 6, no. 2, pp. 2127–2135, 2015, Available: <https://www.iomcworld.org/articles/prooxidant-and-antioxidant-polar-phytoconstituents-from-endemic-philippines-ficus-fiskei-elm-moraceae.pdf>.
- [8] M. khatoun et al., "Estimation of total phenol and in vitro antioxidant activity of Albizia procera leaves," *BMC Research Notes*, vol. 6, no. 1, p. 121, 2013, doi: <https://doi.org/10.1186/1756-0500-6-121Y>
- [9] B. D. B. Tiu and R. C. Advincula, "Polymeric corrosion inhibitors for the oil and gas industry: Design principles and mechanism," *Reactive and Functional Polymers*, vol. 95, pp. 25–45, Oct. 2015, doi: <https://doi.org/10.1016/j.reactfunctpolym.2015.08.006>.

- [10] Đ. Bui et al., "ANTIOXIDANT AND ANTITYROSINASE ACTIVITIES OF FLAVONOID FROM BLUMEA BALSAMIFERA (L.) DC. LEAVES EXTRACT," *European Journal of Research in Medical Sciences*, vol. 5, no. 1, 2017, Available: <https://www.idpublications.org/wp-content/uploads/2016/12/Full-Paper-ANTIOXIDANT-AND-ANTITYROSINASE-ACTIVITIES-OF-FLAVONOID-FROM-BLUMEA-BALSAMIFERA.pdf>
- [11] G. S. Vasyliiev, V. I. Vorobyova, and O. V. Linyucheva, "Evaluation of Reducing Ability and Antioxidant Activity of Fruit Pomace Extracts by Spectrophotometric and Electrochemical Methods," *Journal of Analytical Methods in Chemistry*, vol. 2020, pp. 1–16, Dec. 2020, doi: <https://doi.org/10.1155/2020/8869436>.
- [12] G. A. Akowuah, Z. Ismail, I. Norhayati, and A. Sadikun, "The effects of different extraction solvents of varying polarities on polyphenols of Orthosiphon stamineus and evaluation of the free radical-scavenging activity," *Food Chemistry*, vol. 93, no. 2, pp. 311–317, Nov. 2005, doi: <https://doi.org/10.1016/j.foodchem.2004.09.028>.
- [13] L. T.-H. Tan et al., "Streptomyces sp. MUM212 as a Source of Antioxidants with Radical Scavenging and Metal Chelating Properties," *Frontiers in Pharmacology*, vol. 8, May 2017, doi: <https://doi.org/10.3389/fphar.2017.00276>.
- [14] Wong, C. Tan, and Ho, "Effect of solid-to-solvent ratio on phenolic content and antioxidant capacities of 'Dukung Anak' (*Phyllanthus niruri*)," *International Food Research Journal*, vol. 20, no. 1, pp. 325–330, 2013, Available: [http://www.ifrj.upm.edu.my/20%20\(01\)%202013/44%20IFRJ%2020%20\(01\)%202013%20Ho%20\(346\).pdf](http://www.ifrj.upm.edu.my/20%20(01)%202013/44%20IFRJ%2020%20(01)%202013%20Ho%20(346).pdf)
- [15] R. Guo, Q. Zhang, Z. Wang, M. Tayebi, and B. Hamawandi, "The Effect of Eco-Friendly Inhibitors on the Corrosion Properties of Concrete Reinforcement in Harsh Environments," *Materials*, vol. 15, no. 14, p. 4746, Jul. 2022, doi: <https://doi.org/10.3390/ma15144746>.
- [16] S.-C. Shi and C.-C. Su, "Corrosion Inhibition of High Speed Steel by Biopolymer HPMC Derivatives," *Materials*, vol. 9, no. 8, p. 612, Jul. 2016, doi: <https://doi.org/10.3390/ma9080612>.
- [17] S. Pourhashem, M. R. Vaezi, A. Rashidi, and M. R. Bagherzadeh, "Exploring corrosion protection properties of solvent based epoxy-graphene oxide nanocomposite coatings on mild steel," *Corrosion Science*, vol. 115, pp. 78–92, Feb. 2017, doi: <https://doi.org/10.1016/j.corsci.2016.11.008>.
- [18] A. MUBARAK, P. AKHTER, E. HAMZAH, M. R. HJ. MOHD TOFF, and I. A. QAZI, "EFFECT OF COATING THICKNESS ON THE PROPERTIES OF TIN COATINGS DEPOSITED ON TOOL STEELS USING CATHODIC ARC PVD TECHNIQUE," *Surface Review and Letters*, vol. 15, no. 04, pp. 401–410, Aug. 2008, doi: <https://doi.org/10.1142/s0218625x08011524>.
- [19] F. E. Awe, S. O. Idris, M. Abdulwahab, and E. E. Oguzie, "Theoretical and experimental inhibitive properties of mild steel in HCl by ethanolic extract of *Boscia senegalensis*," vol. 1, no. 1, pp. 1112676–1112676, Nov. 2015, doi: <https://doi.org/10.1080/23312009.2015.1112676>.
- [20] A. Abadon., "Hydrophilic Functional Groups - Biology As Poetry," 2016 www.biologyaspoetry.com. http://www.biologyaspoetry.com/terms/hydrophilic_functional_groups.html
- [21] G. Palanisamy, *Corrosion Inhibitors*. IntechOpen, 2019. Available: <https://www.intechopen.com/chapters/64392>
- [22] Z. Golshani, F. Arjmand, M. Amiri, S. M. A. Hosseini, and S. J. Fatemi, "Investigation of *Dracocephalum* extract based on bulk and nanometer size as green corrosion inhibitor for mild steel in different corrosive media," *Scientific Reports*, vol. 13, no. 1, p. 913, Jan. 2023, doi: <https://doi.org/10.1038/s41598-023-27891-y>.
- [23] J. P. Flores-De los Ríos, M. Sánchez-Carrillo, C. G. Nava-Dino, J. G. Chacón-Nava, J. G. González-Rodríguez, E. Huape-Padilla, M. A. Neri-Flores, A. Martínez-Villafañe, "Opuntia ficus-indica Extract as Green Corrosion Inhibitor for Carbon Steel in 1M HCl Solution", *Journal of Spectroscopy*, vol. 2015, Article ID 714692, 9 pages, 2015. <https://doi.org/10.1155/2015/714692>

Euphorbia milii Extract as Natural Inhibitor for Mild Steel Corrosion in 1M Hydrochloric Acid Solution

Grace N. Batarina*¹, Emmanuel L. Ferrer*², Mark Joseph B. Enojas*³

Abstract

In the industrial environment, it is important to know the different corrosion attacks on mild steel. Some of the solutions to prevent or slow down the rate of these attacks in metals are through the use of nitric acids, sulfuric acids, and hydrochloric acids for various industrial processes including acid pickling, chemical cleaning, and oil well acidification. In this study, the inhibiting effect of ethanolic extract of Euphorbia milii plant on the corrosion of mild steel in 1M HCl solution has been investigated by different techniques such as fourier-transform infrared spectroscopy, UV-Vis, and weight loss for two different concentrations of plant extract from 0.1g/L and 0.5g/L. The results indicated that the corrosion inhibition efficiency increased on increasing plant extract concentration of 0.5g/L. Surface analysis was also carried out to find out the surface morphology of the mild steel in the presence and in the absence of the inhibitor to find out its efficiency. The obtained results show that the Euphorbia milii extract acts as a good inhibitor for the corrosion of mild steel in 1 M HCl solution. A formulation of corrosion inhibitors with mainly surfactants, solvents, and intensifiers are recommended to improve the effectiveness of the individual compounds at elevated temperatures.

Keywords: corrosion inhibition, mild steel, euphorbia milii, hydrochloric acid, spectrophotometry

I. Introduction

Corrosion weakens the properties of metals due to its relations to the environment. It develops fast after the interference of the protective barrier and goes along with several reactions that change the composition and properties of both the metal surface and the local environment [1]. It can cause severe damage to metal and alloy structures resulting in a financial deficiency in terms of renovation, replacement, product losses, safety, and environmental pollution [2].

The first structures made of mild steel were fabricated by bolting in the same way as wrought iron. Mild steel has 0.05%–0.29% carbon, making it malleable and ductile, and has a relatively low tensile strength [3]. However, the challenge is that it has low corrosion resistance, especially in acidic environments. In the industrial environment, mild steel is affected by different corrosion attacks through the usage of acids such as nitric, sulfuric, and hydrochloric acid for various industrial processes including acid pickling, chemical cleaning, and oil wells acidification to control the corrosion outbreak in metallic materials [4].

In the industrial setup, there are general and localized corrosion occurrences. Hydrochloric acid, which is widely used for cleaning, descaling, and etching of metals, on the other hand also contributes to the corrosion of metal surfaces. While there are effective anti-corrosion materials and techniques being employed by industries today, many

of these materials contain highly toxic substances such as hexavalent chromium from chromate-based inhibitors. Consequently, several researchers have proposed the use of environmentally friendly materials in a corrosive medium. These compounds are natural products of plant origin; seeds, latex, bark, flowers, roots and leaf extracts, and organic compounds, which have been classified as environmental-friendly materials. To investigate the inhibition efficiency of these eco-friendly inhibitors in various acid media, there are several experimental methodologies that have been employed including weight loss measurements, potentiodynamic polarization technique, surface analysis (SEM), electrochemical impedance spectroscopy, hydrogen evaluation method, and energy dispersive spectroscopy.

In this work, Euphorbia milii (EM) extract is used as a natural inhibitor for mild steel corrosion in one molar (1 M) of hydrochloric acid solution. Different extract concentrations were tested and observed to analyze their effects in corrosion inhibition. The next sections are discussed as follows: Section II discusses the preparations of the Euphorbia milii and the experiments that were conducted, Section III presents the results of the tests, and Section IV presents the conclusion and future work.



*¹ Student
Bachelor of Engineering and
Allied Department
Technological University of the
Philippines Taguig



*² Associate Professor
Civil Engineering and
Allied Department
Technological University
of the Philippines Taguig



*³ Assistant Professor
Electrical Engineering and
Allied Department
Technological University of the
Philippines Taguig

II. Methodology

A. Materials

There are two main materials used in this study; Euphorbia plant and mild steel. Specifically, the species of EM was used which were known to be abundant in the provinces of Rizal, Bulacan and Batangas in the Philippines. Figure 1a shows the EM, while Figure 1b shows some samples of the mild steel as test subjects for the experiments.

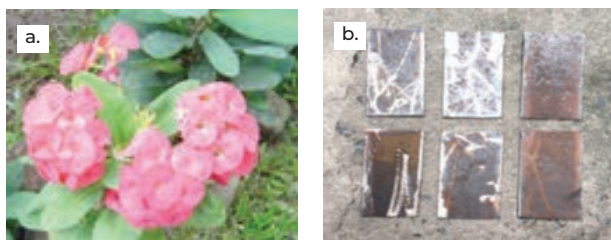


Fig. 1. Materials for the experiment (a) the Euphorbia milli (also known as crown of thorns) (b) mild steel samples

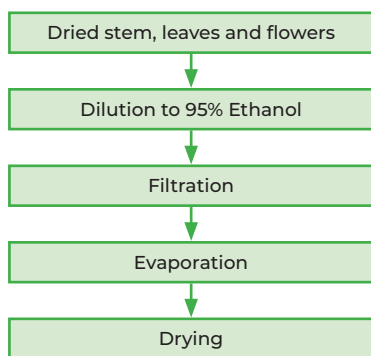


Fig. 2. Extraction Process

B. Extraction and Drying

As shown in Figure 2, the dried stem, leaves and flowers of EM were soaked in 95% ethanol solution. The extract was filtered to separate the plant materials and the solvent was removed from the extract via evaporation until a powdered product was recovered. The powder extract was then dried in an oven at 110°C.

C. Specimen and Corrosive Solution Preparation

Corrosion tests were performed on a mild steel with the following percentage composition: C = 0.14%; Si = 0.20%; Mn = 0.59%; P = 0.014%; S = 0.004%; Cu = 0.01%; Ni = 0.01%; Cr = 0.02%; Mo = 0.005% and the remaining as Fe. Sample coupons were cut into 10 cm x 3.5 cm x 0.6 cm dimensions and were polished successively with fine grade carbide papers (100, 200, 300, 400, 600, and 1000) prior to weight loss measurements. The specimens were then washed thoroughly with distilled water and finally degreased with methanol and dried at room temperature.

1 M HCl solution was prepared by diluting 37% HCl with distilled water. The concentration ranges of EM extract employed varies from 100 ppm (0.1 g/L) to 500 ppm (0.5 g/L). This concentration range was chosen based upon the maximum solubility of EM extract. The powder extract was first dissolved in 1% (v/v) ethanol before it was diluted with 1 M HCl solution. All chemicals and reagents were of AR grade. The concentration (1 M HCl) was prepared by using distilled water and AR grade hydrochloric acid.

D. Weight loss measurement

The cut mild steel specimens were immersed individually in 250 mL solution containing different concentrations of EM extracts at 0.1g/L and 0.5 g/L at ambient temperature (303K) with a control solution without EM extract using 1 M HCl (blank) solution. The weight loss of mild steel specimens were determined after 72 hours of immersion. After immersion, the surface of the specimen was cleaned by double distilled water followed by rinsing with methanol. The samples were weighed again to calculate the inhibition efficiency ($\eta\%$) shown in equation (1) and the corrosion rate (CR) as presented in equation (2).

The inhibition efficiency of the Euphorbia extract can be calculated using the equation below:

$$\eta\% = \frac{CR(\text{uninhibited}) - CR(\text{inhibited})}{CR(\text{uninhibited})} * 100\% \quad (1)$$

while the Corrosion Rate is expressed as:

$$CR = \frac{W_L * K}{D_A * A_E * T_E} \quad (2)$$

where:

CR – corrosion rate

W_L – weight loss due to corrosion and is determined by subtracting the weight after cleaning from the initial weight

D_A – alloy density

A_E – surface area of the coupon that is exposed to the corroding process

T_E – period in days between installation and removal of the specimen

K – K-factor (constant)

E. Characterization of EM on mild steel

The surfaces of the exposed mild steel samples were analyzed using Fourier Transform Infrared Spectrophotometer (Shimadzu IRAffinity-1S) after 72h immersion. The presence of the protective film formed on the selected mild steel sample was evaluated using IR spectra recorded together with the EM extract for comparison. UV-Visible (Optizen 3220UV) absorption spectrophotometric method was also carried out on the solutions used after immersion in 1 M HCl with and without the EM extract. The surface morphology of mild steel specimens immersed in 1 M HCl in the absence and presence of 0.5g/L of Euphorbia extract at room temperature for 72 hours was studied using JEOL JSM 5310 scanning electron microscope (SEM).

III. Results and Discussion

A. Weight loss, corrosion rates, and inhibition concentration

The rate of corrosion can be defined as the ratio of the loss in weight of the sample (ΔW) to its area (A) and the time length over which the test was undertaken. A major advantage of this method is its relative simplicity and availability. In addition, the method uses a direct parameter for the quantitative evaluation of corrosion, i.e., the loss in mass of the metal. The data obtained from the weight loss measurements of mild steel in 1 M HCl solution containing different EM extract concentrations and the calculated inhibition efficiency and corrosion rate are presented in Tables 1 and 2, respectively.

Table 1. Weight of mild steel before and after immersion in 1 M HCL

Inhibitor concentration (g/L)	Initial weight before immersion (g)	Weight after 72 hours of immersion (g)	Weight loss (g)
Blank (HCL)	175.11	169.4374	5.6753
0.1 g/L	174.69	170.8341	3.8559
0.5 g/L	174.32	171.7432	2.5768

Table 2. Inhibition efficiencies and corrosion rate of various concentrations of inhibitors for the corrosion of mild steel in 1 M HCL obtained by weight loss measurements at room temperature.

Inhibitor	Inhibitor concentration (g/L)	Weight loss (g)	Inhibition Efficiency (%)	Corrosion Rate (mm/year)
Blank (HCL)	-	5.6752	-	10.20
Euphorbia milii extract	0.1	3.8559	32.06	6.93
	0.5	2.5768	54.61	4.63

The corrosion-inhibiting effect of plant extracts of EM can be attributed to phytochemical constituents including cardiac glycosides, steroids/ phytosterols, anthocyanin, proteins, terpenoids, flavonoids and tannins. The different constituents may react with freshly generated Fe²⁺ ions on a corroding metal surface forming organometallic [Fe-Inh] complexes. The inhibiting effect of such complexes then depends on their stability and solubility in an aqueous solution, which from our result is a function of the extract's exact concentration. Corrosion inhibition process is complex in nature. This complexity is increased by several orders of magnitude when one considers plant extracts with their complicated chemical compositions. This makes it difficult to assign the inhibitive effect to adsorption of any constituent, since some of these constituents, including tannins, organic and amino acids, alkaloids, proteins and flavonoids are known to exhibit inhibiting action.

The corrosion rate profile and inhibition efficiency in the absence and presence of different extract concentrations

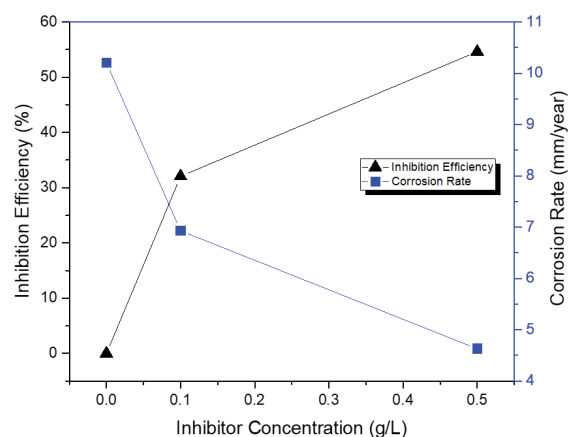


Fig. 3. Inhibition Efficiency and Corrosion Rate at different inhibitor concentrations from EM extract.

are shown in Figure 3. Results show that the extracts act as good corrosion inhibitors for mild steel in 1 M HCl solution as seen in the corrosion rates being reduced in the presence of the extracts compared to the blank solution. In addition, it was observed that the inhibition efficiency increases with increasing extract concentration which supports the results obtained from the calculated corrosion rate. The highest inhibition efficiency was achieved at 54.61% using 0.5 g/L EM concentration equivalent to a corrosion rate of 4.63 mm/year. This indicates that a protective film may have formed on the surface of the mild steel samples which slows down the rate of corrosion. This corrosion protection can be attributed to the presence of tannins in the extract which are known to be natural corrosion inhibitors. Further tests are needed if a higher EM concentration may lead to better corrosion protection and know the optimum concentration to achieve the best result.

B. FT-IR analysis

It is well-established that the FTIR spectrophotometer is an effective tool that can be used to identify the type of bonding particularly functional group(s) present in organic compounds. Since extracts contain organic compounds with polar functional groups, they can be adsorbed on the metal surface protecting the substrate against corrosion. Thus, FTIR analyses of the metal surface can be a useful tool for identifying whether organic inhibitors are adsorbed or not on the metal surface. In the present study, FTIR spectra were used to support that the corrosion inhibition of mild steel in an acid medium can be attributed to the adsorption of inhibitor molecules on the mild steel surface and to provide new bonding information on the steel surface after immersion.

Figure 4 shows the FTIR spectrum of the protective film formed on the surface of the metal after immersion in the solution containing the spectra of Tannin or reference, 0.5 g/L plant extract, and blank aqueous solution.

The bands at 1600 cm⁻¹ are attributed to C-C in the ring (for aromatic). The absorption bands in the range above 2000

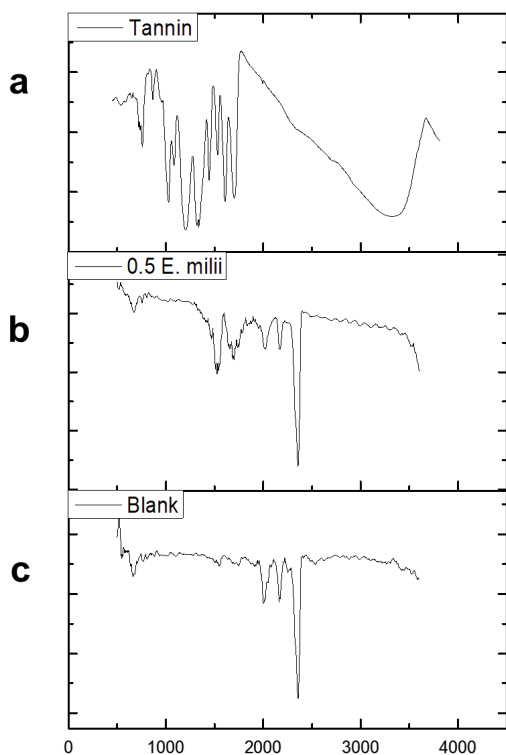
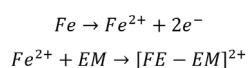


Fig. 4. FTIR Spectra of (a) Tannin reference from *Euphorbia milii* extract and surface of mild steel samples immersed for 72 hours with (b) 0.5 g/L EM extract and (c) without EM extract in 1 M HCl solution.

cm⁻¹ are assigned to the -C≡C-H:C-H bending vibration. This shows that these plant extracts contain mixtures of compounds, i.e., alkaloids, flavonoids, and organic acids.

The inhibitive action of EM leaves and stem extracts towards the acid corrosion of steel can be attributed to the adsorption of the active functional groups from the compounds in the extract. FTIR results also show that the extracts of EM contain oxygen and nitrogen atoms in functional groups (C-H, N-H, C-N, and C-O) and aromatic rings, which meet the general consideration of typical corrosion inhibitors. In aqueous acidic solutions, the components of the plant parts extracts exist either as neutral molecules or in the form of cations. In general, two modes of adsorption could be considered. The neutral species may adsorb on a metal surface via the chemisorption mechanism, involving the displacement of water molecules from the metal surface or the sharing of electrons between the N and O atoms and Fe. The EM extracts components can also adsorb on the surface of the metal-based on donor-acceptor connections between p-electrons of the aromatic ring and unoccupied d-orbitals of Fe. A large number of different chemical compounds for plant extracts of EM may react with the iron, which is first dissolved from the metal surface, forming organo-metallic complex such as Fe-plant extract [Fe-EM] according to the following mechanism [6]:



These complexes might be adsorbed onto the steel surface by van der Waals force forming a protective film to isolate mild steel from corrosion. This hypothesis could be further confirmed by the FTIR results.

C. UV-VIS analysis

To confirm the possibility of the formation of EM plant extract, UV-Visible absorption spectra obtained from 1 M HCl solution containing 0.1 g/L and 0.5 g/L extracts of EM after 72h of mild steel immersions are shown in Figure 5. Figure 5a shows the UV-VIS spectra at 1g/L solution while Figure 5b shows its results after immersion in 72 hours.

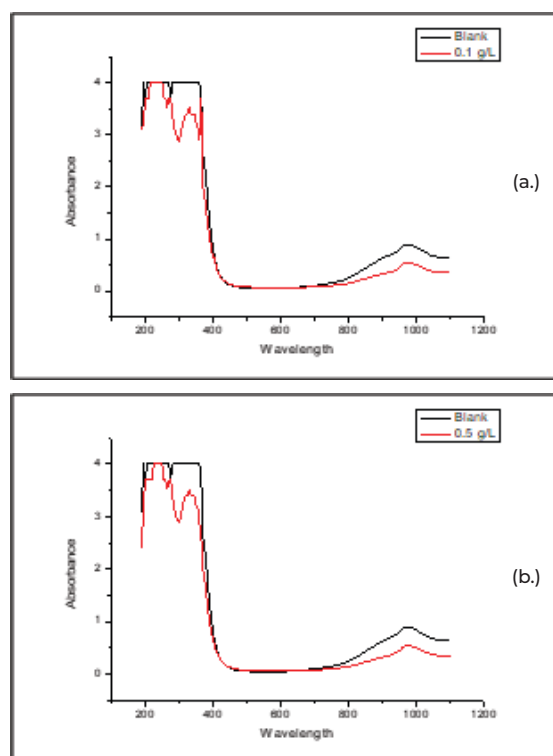


Fig. 5. UV-Visible spectra of the 1 M HCl Solution containing (a) 0.1 g/L and (b) 0.5 g/L *Euphorbia milii* after 72 hours of mild steel immersion.

From these figures, there are two distinct peaks observed at around 250nm and 350nm in both solutions with different EM extract concentrations after mild steel immersion. This suggests that there is a possible formation of the complex between the Fe²⁺ and the phytoconstituents of the plant extract. The formation of this complex may be responsible for the observed deviation in the absorbance and its intensity value and can be associated with the anti-corrosion activity of the natural inhibitor.

D. Surface analysis

The surface analysis was carried out using Scanning Electron Microscopy (SEM) for the mild steel surface immersed in 1 M HCl solution for 72h in the absence and presence of the EM extract. The SEM images of the

exposed mild steel with and without the inhibitor are shown in Figures 6 and 7, respectively.

Based on the morphological features of the SEM images, the surface of the exposed area of the mild steel sample was protected with the addition of the inhibitor as exhibited by a smoother surface indicating resistance to corrosion (Fig. 6) when compared to an unprotected sample (Fig. 7) [7]. This result further supports that the Euphorbia extract can inhibit corrosion of mild steel in 1 M HCl solution.

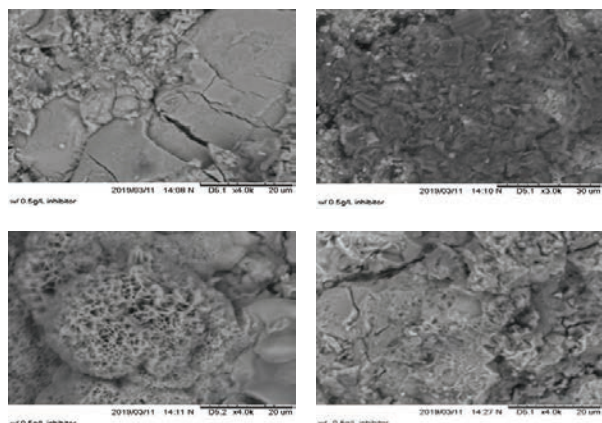


Fig. 6. Mild steel with inhibitor

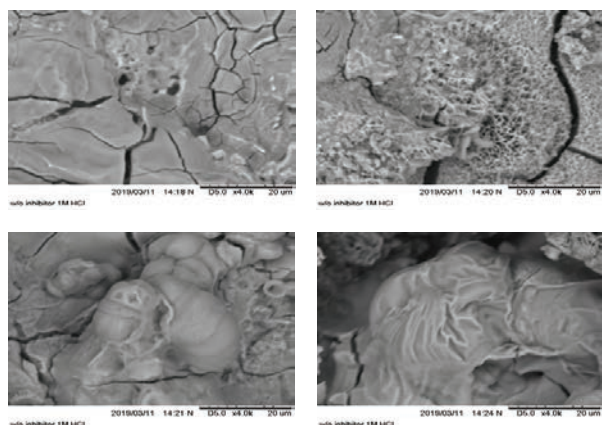


Fig. 7. Mild steel without inhibitor

IV. Conclusion and Future Work

The prevention of metal corrosion is a crucial strategy for guaranteeing longer serviceability of metallic structures and equipment as well as ensuring human safety, which ultimately lead to greater economic gains. In this study, an organic corrosion inhibitor was extracted from *Euphorbia milii* and its effect in the prevention of corrosion in mild steel under acidic conditions was investigated. It was observed that the maximum inhibition efficiency of 54.61% was reached when the inhibitor concentration was also maximum at 0.5 g/L. Furthermore, corrosion rate was reported to be maximum for samples without the natural corrosion inhibitor (blank). These findings demonstrate

that mild steel provides more corrosion protection under acidic conditions when the inhibitor concentration is higher. However, further tests are needed to obtain the optimal conditions in achieving the best protection for the substrate. In addition, FTIR and UV-Vis analyses revealed that the corrosion inhibiting properties of the EM extract can be attributed to the presence of certain active organic compounds. These results were further supported by SEM micrographs showing a smoother surface of exposed metal substrates immersed in the EM extract. The smoother surface may be due to the formation of a protective Fe-EM film complex preventing conditions that promote corrosion. In conclusion, the results show the potential of EM extract as a natural corrosion inhibitor for mild steel samples in an acidic environment.

In the future, a formulation design or mixtures of corrosion inhibitors with surfactants, solvents, and intensifiers can be investigated to improve the effectiveness of the individual compounds at elevated temperatures. This can be useful for diverse industrial fields, primarily for the well acidizing procedures, and secondly for other applications where corrosion inhibitors for steel materials are needed.

V. Acknowledgment

The authors would like to acknowledge the support from the Technological University of the Philippines Taguig Research and Extension Office and the Office of the Vice President for Research and Extension.

References

- [1] B. E. A. Rani and B. B. J. Basu, "Green inhibitors for corrosion protection of metals and alloys: An overview," *Int. J. Corros.*, vol. 2012, no. 1, 2012.
- [2] A. Peter, I. B. Obot, and S. K. Sharma, "Use of natural gums as green corrosion inhibitors: an overview," *Int. J. Ind. Chem.*, vol. 6, no. 3, pp. 153–164, 2015.
- [3] K. Kreislova, D. Knotkova, and H. Geiplova, "Atmospheric corrosion of historical industrial structures," in *Corrosion and Conservation of Cultural Heritage Metallic Artefacts*, 2013, pp. 311–343.
- [4] D. K. Verma and F. Khan, "Green approach to corrosion inhibition of mild steel in hydrochloric acid medium using extract of *spirogyra* algae," *Green Chem. Lett. Rev.*, vol. 9, no. 1, pp. 52–60, 2016.
- [5] X. Zhang, "WHO guidelines on good agricultural and collection practices (GACP) for medicinal plants," *World Health Organization Geneva*. p. 80, 2003.
- [6] S. A. Umoren, U. M. Eduok, M. M. Solomon, and A. P. Udoh, "Corrosion inhibition by leaves and stem extracts of *Sida acuta* for mild steel in 1 M H₂SO₄ solutions investigated by chemical and spectroscopic techniques," *Arab. J. Chem.*, vol. 9, pp. S209–S224, 2016.
- [7] P. Arockiasamy, X. Q. R. Sheela, G. Thenmozhi, M. Franco, J. W. Sahayaraj, and R. J. Santhi, "Evaluation of Corrosion Inhibition of Mild Steel in 1 M Hydrochloric Acid Solution by *Mollugo cerviana*," *Int. J. Corros.*, vol. 2014, 2014.

GYS

CENTER

INDUSTRIAL SUPPLY CORPORATION

WELDING AND CUTTING SOLUTIONS

Center Industrial Supply Corporation is a leading welding and cutting products distributor in the Philippines. Representing global brands who are leaders in process development and advanced technology, we pride ourselves with being not only a supplier but primarily a solutions provider to Philippine industries for over six decades now.

Our product range includes welding and cutting equipment, consumables and accessories for practically all welding and cutting processes. Equipment in our line range from simple yet high-performance manual equipment, to the more advanced digital-based machines, to fully-automated systems and robotics.

STANDARD PRODUCTS



Multi-process Welder



TIG Welder



MIG Welder



Welding Generator

ROBOTICS & ADVANCED SYSTEMS



Welding Robot



CNC Plasma



CNC Laser

CONSUMABLES AND ACCESSORIES



HEAD OFFICE

10 South AA Street, Quezon City, Metro Manila
Phone: +63 (2) 8373-9651, 3416-8688, 3415-6097
Email: info@centerindustrial.com

TECHNOLOGY CENTER

Lot 2 Blk 2, Filinvest Technology Park, Calamba, Laguna
Phone: +63 (49) 572-2719, 572-2720, 572-2643
Email: techcenter@centerindustrial.com

CEBU OFFICE

Units 2 & 3 CTK Commercial Bldg., Tabok, Mandaue City, Cebu
Phone: +63 (32) 268-7512, 268-5866
Email: cebuofc@centerindustrial.com

DAVAO OFFICE

KM 1 J.P. Laurel Avenue, Acacia, Davao City
Phone: +63 (82) 224-6032
Email: dvoofc@centerindustrial.com



Scan to check out
our website!

Comparative Analysis of Locally Made Copper Rods and Its Imported Counterparts

Edwin Roven T. Cañezal^{*1}, Michael Angelo O. Verdijo^{*2}, John Ivan Gonzales^{*3}

Abstract

The study conducted tests to examine the elemental composition, microstructure, and microhardness of four copper rod samples – three imported and one locally made. The results were used to confirm the quality of the locally made copper rod and identify the treatment needed to improve its microstructure and microhardness like its imported counterparts. An X-ray fluorescence spectrometer was utilized to determine the elemental impurities present in the copper rod samples. The grain size number for each photomicrograph of etched copper surfaces was also calculated using the Planimetric method. A Vickers hardness tester was used to determine the microhardness of copper rod specimens. Results of elemental analysis suggested that there were elemental impurities that may have contributed to higher microhardness values for some copper rod samples. Microhardness testing and metallographic analysis, both in the longitudinal and cross-sectional directions, confirmed that local copper rod was significantly different to its imported counterparts. A copper rod sample with high hardness such as the locally made copper rod could be detrimental to a copper wire production line where low breakability is needed. Thus, annealing parameters for the local copper rod were investigated that would provide the optimum microstructural and microhardness changes that would result to less occurrence of breakage and less interruption in the copper wire drawing process.

Keywords: copper rod, microstructure, microhardness

I. Introduction

The Philippines has copper mines (e.g. Carmen Copper Corporation, Philex Mining Corporation), a copper smelter (i.e. Philippine Associated Smelting and Refining Corporation (PASAR) and wire drawers. Currently, the industries are not linked (i.e. the output of one is not the input of the other) [1].

The copper mine's concentrate is 100% exported, instead of being processed locally by the local smelter. The country's copper smelter (PASAR) acquires 100 % of its concentrates (input) from abroad. Their output (copper cathodes) is largely (95-100%) exported. For the downstream copper industries, the wire and cable manufacturers acquire 95-100% of its copper rods (input) from abroad [1,2].

In the current setting, hardly any local casting facility is around. If there is, the copper rod produced is of small quantity sufficient only for own use. Only a few wire manufacturers use locally produced rods, most of them import copper rods to produce wires. This is due to the observation that imported copper rods have better quality (i.e., lower breakage tendency) compared to the locally produced copper rods. High breakage tendency is a hassle to wire manufacturers because it may entail delays on schedule and additional costs to the production. As a result, local wire manufacturers would opt to just import

copper rods from other countries like Australia, Indonesia, and Korea for their wire drawing [1, 2].

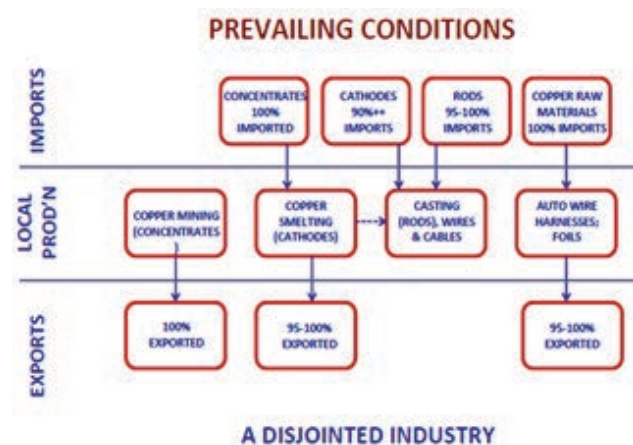


Fig. 1. The copper industry condition in the Philippines at the present [1]

In 2012, the industry roadmap for copper was completed by the Department of Trade and Industry's Board of Investments. Among the roadmap's findings is that the Philippine copper industry is disjointed. The country has significant deposits of copper, a world-class smelting



^{*1} University Researcher
Department of Mining,
Metallurgical and Materials
Engineering University of the
Philippines, Diliman, Quezon
City



^{*2} Researcher
Department of Mining,
Metallurgical and Materials
Engineering University of the
Philippines, Diliman, Quezon
City



^{*3} Assistant Professor
Department of Mining,
Metallurgical and Materials
Engineering University of the
Philippines, Diliman, Quezon
City

facility, a thriving wire and cable manufacturing industry, a globally competitive automotive wire harness and copper foil industries, but there are no domestic linkages among them. The establishment of a copper rod industry was identified as the missing link between copper refining (smelting) and wire cable manufacturing [2].

Research and development for the downstream copper manufacturing industry is one of the important steps in promoting local copper rod manufacturing. This endeavor could pave the way in further boosting the local copper industry which could aid in meeting the projected growth in copper demands in various industries like construction, automotive and electronics.

II. Experimental Procedure

A. Rod Procurement

One-foot 8.0mm diameter imported rod samples were requested and acquired from Philflex and London Metals Industries (LMI). While, one-foot 7.0mm diameter local rod samples is obtained from LMI.

B. Metallographic Inspection

Samples were mounted using PVC pipe as mold and Bakelite polymer plus hardener. This was done for convenient specimen handling. Grinding was then conducted using progressively finer silicon carbide papers. After which, the specimens were held against a polishing wheel saturated with alumina powder dissolved in water [3].

Alcoholic FeCl₃ etchant was prepared using 48mL ethanol, 1 g anhydrous FeCl₃ and 1mL concentrated HCl. Etching was conducted by soaking polished samples for around 60 seconds and drying with ethanol. The surface of samples was then observed under the microscope. Photomicrograph of each sample was taken using a camera. The preceding steps can be repeated until the desired photomicrograph is achieved [3].

The photomicrograph obtained was then used for quantitative metallography. The ASTM grain size number was to be determined using the Jeffries' (Planimetric) method [4]. Using the following equation, the ASTM grains size number, was determined.

$$N_A = f \left(N_{inside} + \frac{N_{intercepted}}{2} \right) \quad (1)$$

Where f is the Jeffries multiplier found in ASTM E-112, N_{inside} is the number of grains completely inside the shape with known area and $N_{intercepted}$ is the number of grains intercepted by the shape with known area [4].

C. Hardness Testing

Vickers micro hardness testing is utilized to ensure accuracy of hardness values. The samples' hardness was

measured by analyzing surface indentations made by a 25gf load. The indentations for the samples are spaced at regular intervals. Using an optical microscope, the diagonal length of the indentations was then measured at 50x magnification with the aid of a micrometer slide. The hardness of the samples was calculated using the following equation.

$$HV = 1854.4 \frac{L}{d^2} \quad (2)$$

Where load L is in grams-force (gf) and the average diagonal d is in micrometers [5].

D. Elemental Analysis

X-ray Fluorescence (XRF) was chosen to characterize constituent elements of rod samples. For this study, elemental analysis of samples were provided by the Metal Industries Research and Development Center (MIRDC). The elemental impurities contained in the copper rod have been determined and then quantified as percentages.

E. Annealing

An annealing treatment (i.e. heating the copper metal to a given temperature for a given time) was suggested since the Philippine copper rods were proven to have higher hardness values compared to its imported counterparts. For this purpose, nine 5mm length local copper rod were prepared. The treatments summarized in Table 1 were applied.

The annealing temperatures were chosen because copper would normally be annealed at the temperature range of 350-650°C depending on its impurities [6]. The annealing time and the interval between them were chosen to make sure that significant changes in the microstructure, if any, will be captured. Similar metallographic inspection and hardness testing procedures were performed focusing on the longitudinal direction (L) of the copper rod samples.

Table 1. Design of experiment

Time (min)	Temperature (°C)		
	400	500	600
10	1L	4L	7L
20	2L	5L	8L
30	3L	6L	9L

III. Results and Discussions

The suitability of copper rods in the subsequent copper wire manufacturing can be affected by the elemental composition, microstructure, and hardness.

A. Microhardness

Local rod samples are harder than imported samples based on the obtained data summarized in Table 2. In rod drawing or extrusion processes, the stress is only

concentrated in the longitudinal direction [7]. This study thus focused on hardness testing on the mentioned direction.

Table 2. Microhardness readings for the longitudinal section of the copper rod samples

Sample Rod	Imported 1	Imported 2	Imported 3	Local
Hardness	49.22	55.01	64.13	94.41

With a Vickers' hardness value of 94.4, local samples are almost twice as hard as its imported counterparts. It is important to note that because of the different microstructure exhibited by the local sample, its grain size number was not determined and included in the following figure.

When the grain size number increases, the size of the grains decreases (i.e. a higher grain size number corresponds to a smaller grain). As the grain size number increases, the hardness of the sample also increases. Smaller grains would entail more grain boundaries which impede the movement of dislocations.

B. Elemental Analysis

Composition of each copper rod samples including elemental impurities is tabulated in Table 3. It is observed that the copper content of locally fabricated rod at 99.29% is lower than any of the imported rods. It may suggest that the type of copper the company is using is recycled ones, or at least a portion of it. This means they might have added a certain amount of scrap copper to their copper rod production line.

Table 3. Elemental analysis of the copper rod samples

Elements	Percentage			
	Imported 1	Imported 2	Imported 3	Local
<i>Cu</i>	99.51	99.66	99.64	99.29
<i>Fe</i>	0.014	0.052	-	0.155
<i>Mn</i>	0.015	-	-	0.035
<i>Mo</i>	0.002	-	0.067	-
<i>Ni</i>	-	0.014	-	0.049
<i>Ti</i>	0.067	0.022	-	0.038
<i>V</i>	0.108	-	0.218	0.059
<i>Co</i>	0.010	-	0.208	-
<i>Pb</i>	0.006	-	-	-
<i>Sn</i>	0.005	-	0.237	-
<i>Zn</i>	0.049	0.067	-	0.246
<i>Sb</i>	0.016	0.003	0.453	-
<i>Ag</i>	0.166	0.150	0.657	0.038
<i>Pd</i>	0.006	0.011	-	0.005
<i>Nb</i>	0.001	0.001	0.035	-
<i>Zr</i>	0.022	0.014	0.054	0.064
<i>Bi</i>	-	-	-	0.009
<i>Se</i>	-	-	-	0.008

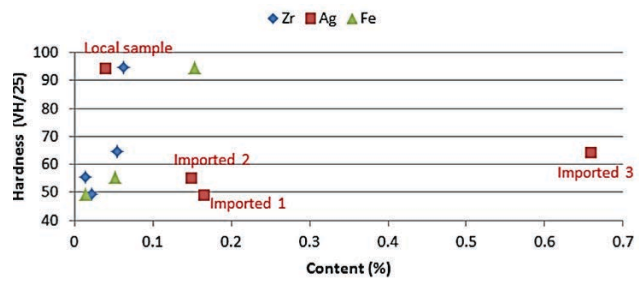


Fig. 2. Graph of the microhardness vs. the Zr, Fe and Ag content of the copper rod

Zirconium, iron, and silver are only some of the metallic impurities found in the samples in the preceding table. The researchers then decided to have a closer look at these elements and how they may affect the properties of copper rod products.

Zirconium and iron are common inoculants in copper. Inoculation or grain refinement is applied to control the grain size of the metal. This results to an increase in strength of the grain boundaries of the metal [8]. From Figure 2, the local rod sample with higher hardness values also has relatively higher amounts of the mentioned elements.

On the other hand, Ag increases the temperature at which the annealing is done [9]. That for the same degree of annealing, the one with the higher silver content must have the treatment done at a higher temperature. Notably, for the Imported 3 sample (0.657%, 64.13 VH/25), the silver content is much higher than the other three samples. On the other hand, the local rod sample has lower Ag content. This might imply that annealing for this sample may be performed at lower temperatures compared to other samples.

C. Microstructure

The three imported copper rods have similar microstructure in contrast with the local rod as shown in Figure 3. Coarser grain size was revealed by the photomicrographs in a, b and c. The opposite is true for the local rod. That is, layering or fibrous microstructure can be observed in the longitudinal direction.

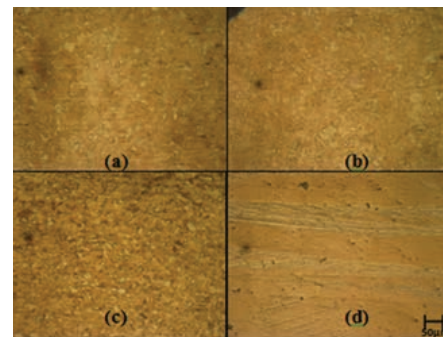


Fig. 3. Microstructures of (a) Imported 1, (b) Imported 2, (c) Imported 3 and (d) Local copper rods in the longitudinal direction at 10x magnification

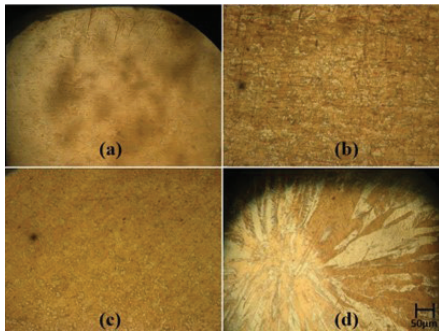


Fig. 4. Microstructures of (a) Imported 1, (b) Imported 2, (c) Imported 3 and (d) Local copper rods in the cross sectional direction at 10x magnification

The same observations can be made by looking at the cross-sectional direction as shown in Figure 4. A coring or branching out microstructure is observed for the cross-sectional section of the local rod. This is indicative that the manufacturing process for the imported copper rod samples is different compared to the locally produced copper rod.

The grain size for both directions was then calculated to give a quantitative analysis to the microstructure. Results are tabulated in Table 4.

Table 4. Grain size measurements using planimetric method

Sample Rod	Longitudinal	Cross section
Imported 1	6.34	6.48
Imported 2	6.43	6.51
Imported 3	6.74	6.78
Local	-	-

The three imported samples have similar grain size measurements as summarized. This is expected since similar microstructures were observed in their respective photomicrographs. For the local rod sample, no grain size is assigned as shown Table 4. This is because the grains are too fine that it is impractical to do counting of individual grains as required by the Jeffries Planimetric method.

D. Annealing of Local Copper Rod Sample

Results of initial inspection of the copper rod samples confirmed that the local copper rod sample is significantly different in terms of elemental composition, hardness and microstructure when compared to its imported counterparts.

In terms of hardness, the local copper rod sample has higher values when compared to the three imported copper rods. For copper, the acceptable Vickers' hardness is 40-50, it is 100 for cold worked copper [10]. The local rod

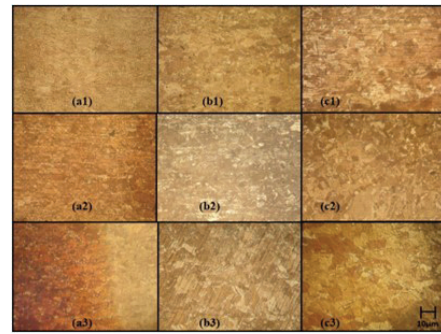


Fig. 5. Comparison of the microstructures of the local copper rod which undergone annealing at different temperatures and time (a) 400 C, (b) 500 C and (c) 600 C at (1) 10 minutes, (2) 20 minutes and (3) 30 minutes at 30x magnifications

Table 5. Microhardness readings and grain size number for the annealed local copper rod

Annealing Parameters		Grain Size Number	Micro hardness (VH/25)
400 °C	10 min	7.28	78.753
	20 min	6.92	71.894
	30 min	6.63	63.201
500 °C	10 min	6.57	60.114
	20 min	6.45	53.314
	30 min	6.09	45.160
600 °C	10 min	6.22	48.724
	20 min	5.98	37.441
	30 min	5.76	30.488

has a 94.41 VH/25 which is almost twice the hardness of sample labelled as Imported 1. The annealing parameters summarized in Table 5 was used.

From Figure 5, it is evident that the grain size increases as the annealing temperature and/or annealing time increases.

As expected, both the grain size number and the microhardness decreased as annealing time and/or annealing temperature is increased. For the locally copper rod tested on this study, the manufacturer may choose the time-temperature combination from the table above that would yield around 40-60 VH which is close to the actual hardness values (i.e., 45-65 VH) obtained for the imported copper rod samples.

IV. Conclusion

Testing results confirmed that the locally made copper rod sample is significantly different in terms of elemental composition, hardness and microstructure when compared to its imported counterparts.

A copper rod sample with high hardness such as the locally made copper rod could be detrimental to a copper wire production line where low breakability is needed. Thus, annealing parameters for the local copper rod were investigated that would provide the optimum microstructural and hardness changes that would result to less occurrence of breakage and less interruption in the copper wire drawing process.

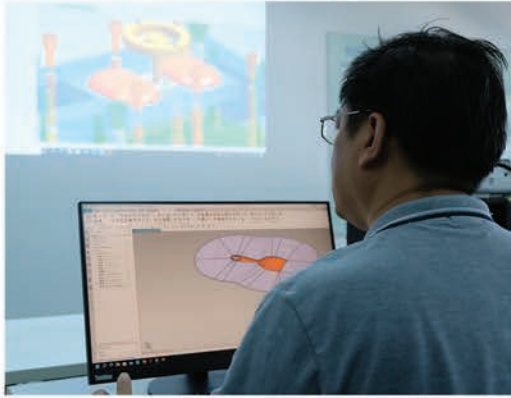
The recommended annealing parameters may be used by the local copper rod manufacturer (i.e., LMI) to improve the quality of their copper rods. Also, results of this study may provide some preliminary data needed in realizing the strategic vision for the copper industry wherein imports of high-value copper rods will be replaced by domestic copper rod production.

V. Acknowledgment

The researchers would like to thank Philflex and London Metals Industries (LMI) for providing samples of their copper rods. Furthermore, the researchers would like to thank their colleagues at the UP Department of Mining, Metallurgical and Materials Engineering, DMMME staff and faculty members especially Sir John Ivan Gonzales (adviser) and Sir Brian Buenaventura for their guidance and support which were essential to the successful implementation of this study.

References

- [1] Icamina, B. N. A PowerPoint Presentation entitled Philippines: Industry Roadmap for Copper Board of Investments - Philippines, 2012
- [2] Board of Investments (2013). Pre-feasibility study on copper wire rod casting plant in the Philippines. Department of Trade and Industry, 1-32.
- [3] ASTM International. "Standard Guide for Preparation of Metallographic Specimens (E 3)" ASTM International, 2011
- [4] ASTM International. "Standard Test Methods for Determining Average Grain Size (E 112)" ASTM International, 2004
- [5] ASTM International. "Standard Test Method for Knoop and Vickers Hardness of Materials (E 384)" ASTM International, 2012
- [6] Brandes, E.A., Brook, G.B. "Smithells Metals Reference Book, Seventh Edition" Reed Educational and Professional Publishing Ltd, 1992
- [7] Cho, J., et al. "Investigation of Recrystallization and Grain Growth of Copper and Gold Bonding Wires" Metallurgical and Materials Transactions A (Volume 37), 2006
- [8] Stefanescu, D. M. "Science and Engineering of Casting Solidification" Springer, 2002
- [9] Davis, J.R. "Copper and Copper Alloys" ASM International, 2001
- [10] Scott, D. A. "Metallography and Microstructure of Ancient and Historic Metals" Getty Conservation Institute, 1991
- [11] Banganayi, C., Nyembwe, K. & Mageza K. (2020). Annealer curve characteristics of electrolytically refined tough pitch copper (Cu-ETP) and oxygen free up-cast copper (Cu-OF) for electrical cable wires. Results in Materials 8, 100146



A Comparative Analysis of Reducing Carbon Emissions from Diesel-Engine Vehicles with the use of Filnut Muffler Filter and Traditional Muffler Filter

Camile D. Dumaquit*¹, Wilma Ungod*²

Abstract

This study presents a comparative analysis of the efficacy in reducing carbon emissions from diesel-engine vehicles using the Filnut muffler filter and the traditional muffler filter. Carbon emissions from these vehicles are a significant contributor to global warming and climate change, necessitating effective strategies to mitigate their impact on the environment. Carbon emission tests were conducted to gather data for the study, with both the Filnut muffler filter and the traditional muffler filter being evaluated. The tests focused on diesel-engine vehicles and were carried out under varying conditions in order to ensure data reliability. Multiple trials were conducted for each type of muffler filter, providing a comprehensive assessment of their effectiveness. The results of the carbon emission tests revealed that the Filnut muffler filter outperformed the traditional muffler filter in reducing carbon emissions from diesel-engine vehicles. On average, the Filnut muffler filter demonstrated a significant reduction in emissions, with carbon emission levels measuring at X g/km, while the traditional muffler filter yielded an average of Y g/km. The superior performance of the Filnut muffler filter can be attributed to its unique design utilizing granulatedpuly peanut shells as a filter material, which contains a high concentration of lignin. Lignin has been proven to effectively neutralize harmful pollutants emitted by internal combustion engines. The findings of this study emphasize the significant potential of the Filnut muffler filter in reducing carbon emissions from diesel-engine vehicles, surpassing the performance of traditional muffler filters. The utilization of Filnut muffler filters presents a promising strategy for mitigating the environmental impact of diesel-engine vehicles and improving overall air quality. Further research and development in this area could lead to the widespread adoption of Filnut muffler filters as an effective solution for reducing carbon emissions and promoting sustainable transportation practices.

Keywords: copper rod, microstructure, microhardness

I. Introduction

This study investigates the use of reusable exhaust filtration primarily utilizing peanut shells as the agent's absorption and absorption of vapor contaminants. The research from the department of environment technology needs the microorganism grow naturally on peanut shell, which can be used to clean the air. (Biotech, Raul Pineda Olmedo 2016) it is designed to be ecofriendly by using peanut shell wastes, and at the same time, it is advantageous in reduction of carbon emission. The peanut shell is special for these applications because it is naturally hollow and has an area of contact with air, which favors the development of micro-organisms," says Pineda Olmedo.

This organic material, which is widely available and considered as waste, can also be applied as biological filters similar to those used in motorcycles, but instead

of stopping dust ingress, it degrades the contaminants instead.

Additionally, the peanut shell's hollow structure maximizes their surface area allowing for more contact with the air. Like other filtration materials, they do also trap airborne particles such as those that up dust and smoke (Investigation Y Desarrollo, 2016). Industry description in 2020 alone, 136.06 million tons have been recorded as the Philippines' annual CO₂ emission. (Ritchie, Roser and Rosado 2020) local air pollution problem and as well as the impacts of the climate change will continuously affect and deteriorate the Philippines unless a new engineering for land-use and transportation planning is implemented. Majority of vehicles being used today highly contribute to climate change as it also warmed of its harmful effects. (Unido 2016) highway vehicles release greenhouse gasses



*^{1, 2}
Student
BS in Industrial Engineering, Taguig City
University

(GHGS) into the atmosphere each year-mostly on that of carbon dioxide (co2) contributions global climate change.

II. Research Method Used

The Filnut Muffler Filter is a type of muffler filter designed to reduce carbon emissions from diesel-engine vehicles. It is made from a unique material called granulated peanut shells, which contain a high concentration of lignin. Lignin is a natural polymer that has been shown to have the ability to neutralize harmful pollutants emitted by internal combustion engines.

The filter is installed in the muffler of a diesel-engine vehicle, where it works to capture and neutralize carbon emissions produced by the engine. As exhaust gases flow through the filter, the lignin in the granulated peanut shells binds to harmful pollutants, such as particulate matter and nitrogen oxides, and converts them into harmless substances.

The filtered exhaust gases then exit the muffler and are released into the environment.

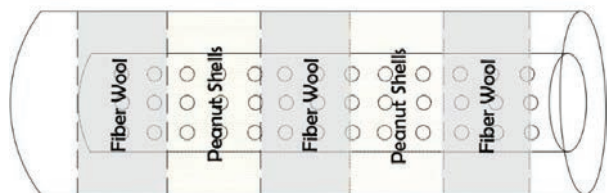


Fig. 1. Components of Filnut Muffler Filter

The Filnut muffler filter is made from a combination of granulated peanut shells and fiber wool. Each layer of the filter contains of:

- 150 grams of granulated peanut shells
- 250 grams of fiber wool.

The granulated peanut shells provide a surface area for the adsorption of harmful pollutants, while the fiber wool helps to trap and filter particulate matter. As exhaust gases flow through the filter, they first pass through the layer of granulated peanut shells.

The high concentration of lignin in the peanut shells binds to harmful pollutants, such as nitrogen oxides and sulfur dioxide, and converts them into harmless substances. The filtered gases then pass through the layer of fiber wool, which helps to trap and filter out particulate matter, such as soot and ash. The combination of granulated peanut shells and fiber wool in the Filnut muffler filter provides an effective way to reduce carbon emissions from diesel-

engine vehicles. The peanut shells provide a natural and renewable source of lignin, which is known to have air-cleaning properties, while the fiber wool helps to ensure that the filtered gases are clean and free from harmful pollutants.

The weight of a Filnut muffler can vary widely depending on the make and model of the diesel-powered engine vehicle as proposed that is it can be customized. As a rough estimate, a Filnut muffler can weigh anywhere from 2 to 10 pounds (0.9 to 4.5 kilograms), depending on factors such as its size, shape, and construction. However, the filnut muffler filter may weigh even less or more than this range.

The granulated peanut shells used inside the filnut muffler must have a required diameter of 2mm in order to effectively prevent burning. This specific diameter is essential for optimal performance and safety. When the peanut shell particles are of this size, they create a tightly packed barrier within the muffler that restricts the flow of air and gases, reducing the risk of combustion. The 2mm diameter ensures that the shells are small enough to create a dense layer that limits the amount of oxygen available for combustion while allowing the exhaust gases to pass through. This controlled environment inside the muffler helps to prevent the peanut shells from igniting and burning, maintaining the integrity of the muffler and ensuring the safe operation of the equipment. It is important to adhere to the recommended diameter to ensure the desired fire prevention properties and maintain the overall efficiency and longevity of the filnut muffler.

The Filnut muffler is designed to be used for a maximum duration of three months, providing efficient noise reduction and exhaust gas management during that time. This timeframe ensures optimal performance and reliability, as the muffler's materials and components are specifically engineered to withstand the rigors of regular use within this timeframe. Additionally, the Filnut muffler is washable, allowing for easy maintenance and cleaning. It can be washed up to three times a week when in use. Regular washing helps remove accumulated debris, dirt, and pollutants that may hinder its functionality or impede the flow of exhaust gases. By maintaining a clean and well-maintained muffler, the Filnut muffler can continue to perform optimally, ensuring proper noise control and efficient exhaust gas dispersion. However, it's important to adhere to the manufacturer's guidelines and recommendations when washing to ensure the longevity and effectiveness of the Filnut muffler.

III. Summary of Findings

The study aimed to investigate the efficacy of the Filnut muffler filter as compared to the traditional muffler filter in reducing carbon emissions from vehicles. Carbon emissions are a major contributor to global warming and climate change, and reducing these emissions is crucial for mitigating their impact on the environment.

To gather data for the study, carbon emission tests were conducted using both the Filnut muffler filter and the traditional muffler filter. The tests were carried out using a diesel-powered engine vehicle of Barangay Upper Bicutan. To ensure the reliability of the data, three separate trials were conducted for each type of muffler filter. This allowed the researchers to gather a larger sample of data and to test the efficacy of each filter under a range of different conditions.

The results of the carbon emission tests conducted in the study showed that the Filnut muffler filter was significantly more effective in reducing carbon emissions from vehicles than the traditional muffler filter. Specifically, the Filnut muffler filter produced an average of 4.42 g/km of carbon emissions, while the traditional muffler filter produced an average of 13.17 g/km. This difference in emissions can be attributed to the unique material used in the Filnut muffler filter. The filter is made from granulated peanut shell, which contain a high concentration of lignin. Lignin is a natural polymer that has been shown to have the ability to neutralize harmful pollutants emitted by internal combustion engines.

IV. Conclusion

The researchers concluded based on the carbon emission tests conducted that the Filnut muffler filter is significantly more effective than the traditional muffler filter in reducing carbon emissions from diesel-engine vehicles. The use of granulated peanut shells as a filter material in the Filnut muffler filter seems to have contributed to its effectiveness, as the high concentration of lignin in the shells can neutralize harmful pollutants emitted by internal combustion engines. The Filnut Muffler Filter has been shown to be significantly more effective in reducing carbon emissions from diesel-engine vehicles than traditional muffler filters. Its use can be a promising strategy for reducing the environmental impact of diesel-engine vehicles and improving air quality. These findings suggest that the use of Filnut muffler filters can be a promising strategy for reducing carbon emissions from diesel-engine vehicles, which can have a significant positive impact on the environment.

V. Recommendation

Based on the findings of this study, it is highly recommended that the Filnut muffler filter be considered as a highly effective tool for reducing carbon emissions from vehicles, especially diesel-powered engines. The unique combination of granulated peanut shell and fiber wool used in the filter has shown to be highly effective in neutralizing harmful pollutants and significantly reducing carbon emissions.

To promote the use of the Filnut muffler filter, it is recommended that automotive manufacturers explore the possibility of incorporating it into their vehicles as a standard feature. This could involve partnering with Filnut or other companies that specialize in producing eco-friendly muffler filters. Additionally, governments and regulatory bodies can provide incentives to manufacturers that incorporate such eco-friendly technologies into their vehicles.

Further research can also be conducted to improve the design and effectiveness of Filnut muffler filters. For example, researchers can explore the possibility of using different ratios of granulated peanut shell and fiber wool, or investigate the impact of other materials that can enhance the filter's effectiveness. By continuing to invest in research and development, we can continue to improve the effectiveness of Filnut muffler filters and other eco-friendly technologies, leading to a more sustainable and environmentally-friendly future.

VI. Acknowledgment

The completion of this thesis paper entitled "A Comparative Analysis of Reducing Carbon Emissions from Diesel – Engine Vehicles with the use of Filnut Muffler Filter and Traditional Muffler Filter" could not have been possible without the participation and assistance of so many people whose names may not all be enumerated. Their contributions are sincerely appreciated and gratefully acknowledge. However, the researchers would like to express their deep appreciation and indebtedness particularly to the following:

First and foremost, the authors would like to thank our Almighty God for giving the strength to finish this study. The authors immensely grateful to Dean, Dr. Esterlina B. Pepito for her invaluable guidance and expertise as thesis adviser. Her profound knowledge in the field and her unwavering commitment to academic excellence have been instrumental in shaping the direction and quality of this research.

The authors would also like to acknowledge Barangay Upper Bicutan for their kind assistance in providing a vehicle for the testing of the Filnut muffler filter. Their generosity and support have been crucial in conducting

the necessary experiments, and the authors deeply grateful for their contribution.

The authors would like to extend sincere appreciation to the esteemed panelists: Prof. Mary Ann Basilio, Engr. Maria Joy Reyes, and Engr. Carmen Asor. Their expertise, insightful feedback, and constructive criticism have significantly enriched this research and contributed to its overall excellence.

Lastly, authors would like to express heartfelt gratitude to Engr. Dennis B. Abesamis for his outstanding leadership and guidance as the chairman of the panels. His expertise and organizational skills ensured a smooth and productive defense.

The authors acknowledge that this research study would not have been possible without the collective effort and support of all these individuals and organizations.

References

- [1] A. M. Balisacan and B. R. Fuertes, "Diesel or Electric Jeepney? A Case Study of Transport Investment in the Philippines Using the Real Options Approach," in *Journal of Open Innovation: Technology, Market, and Complexity*, 3(3), 51, 2017. [Online]. Available: <https://doi.org/10.3390/joitmc3030051>.
- [2] E. S. Fabian, "CO2 Emissions from the Land Transport Sector in the Philippines: Estimates and Policy Implications," in *Transport Science and Society*, 3(1), 32-46, 2009. [Online]. Available: <https://ncts.upd.edu.ph/tssp/wp-content/uploads/2018/08/Fabian09.pdf>.
- [3] H. Hao, Y. Wu, Z. Wang, and Y. Xie, "Diesel Emissions and Their Control," in *Clean Technologies and Environmental Policy*, 16(1), 1-19, 2014. [Online]. Available: <https://doi.org/10.1007/s10098-014-0793-9>.
- [4] R. McGill and C. Yang, "Diesel Exhaust Emissions Reduction by Diesel Oxidation Catalysts and Fuel-Borne Catalysts: A Review," in *SAE Technical Paper*, 1999-01-0108, 1999. [Online]. Available: <https://doi.org/10.4271/1999-01-0108>.
- [5] The National Academies of Sciences, Engineering, and Medicine, "Reducing Transportation Fuel Consumption and Greenhouse Gas Emissions: Utilizing Intelligent Transportation Systems Strategies," 2018. [Online]. Available: <https://trid.trb.org/view/1309590>.
- [6] United States Environmental Protection Agency, "Learn about Impacts from Diesel Exhaust and the Diesel Emissions Reduction Act (DERA)." [Online]. Available: <https://www.epa.gov/dera/learn-about-impacts-diesel-exhaust-and-diesel-emissions-reduction-act-dera>.
- [7] World Bank Group, "Cleaning Up Diesel Exhaust Improves Health, Climate," April 29, 2014. [Online]. Available: <https://www.worldbank.org/en/news/feature/2014/04/29/cleaning-up-diesel-exhaust-improves-health-climate>
- [8] World Bank Group, "The Cost of Air Pollution: Strengthening the Economic Case for Action," 2014. [Online]. Available: <https://openknowledge.worldbank.org/bitstream/handle/10986/17785/864850WP00PUBL010report002April2014.pdf>

Epoxy Coating Additive Filler Utilizing Bamboo Leaf Ash for Possible Metal Degradation Protection

Benhamin I. Mamalo*¹, Katherine J. Cabañas*²

Abstract

Epoxy has been widely used in various engineering and industrial applications. But due to its drawbacks, epoxy limits its performance as high durability coating. In this regard, bamboo leaf ash (BLA) was used as an innovative filler for epoxy coatings. The production of BLA was done by calcination process using a muffle furnace heated at 650°C for two hours. BLA-Epoxy mixture was formulated with different mixing ratios of 90% Epoxy and 10% BLA, 80% Epoxy and 20% BLA, 70% Epoxy and 30% BLA. The adhesion test was performed according to ASTM D3359 Method A standard while the thermal behavior of the coating was carried out using a differential scanning calorimeter analysis. SEM-EDX Analysis and XRD analysis was also conducted to characterize the ash in terms of its morphology, microscopic and crystallographic structure. Findings show that bamboo leaf ash was an amorphous material with Silicon and Oxygen as the major elements present. Also, the ash particles have a rough surface and vary in size. Results for the adhesion test revealed that the addition of BLA filler improves the adhesion strength of the coating when applied to the mild steel substrate, where 20% BLA filler has the highest adhesion strength among the other Epoxy-BLA mixtures. On the other hand, the DSC curve shows the occurrence of an endothermic event which indicates the presence of moisture in the sample. Glass transition temperatures were also observed wherein the cured coating with 70% Epoxy and 30% BLA filler has a higher T_g value among the other mixtures.

Keywords: adhesion, bamboo leaf ash, epoxy, filler, thermal behavior

I. Introduction

Epoxy has been widely used in various engineering and industrial applications. This type of material has wide variety of properties that make them suitable as lightweight construction materials, insulation materials, potting, adhesives, automobiles, surface coatings, as well as other advanced composites on a global scale. However, the usage of epoxy limits its performance as high durability coating s due to its brittleness [1], fracture toughness, delamination [2], and inferior wear resistance [3]. These limitations can be overcome by adding additives, fiber, and nano-fillers with improved thermal and dynamic properties along with mechanical, electrical, and morphological properties [1]. Several researchers have also investigated the possibilities of modifying the behavior of epoxy resin by adding different types of fillers.

Fillers are categorized into oxides, silicates, silicas, carbonates, sulfates, and organic fillers, and they can be natural or synthetic [4]. Natural fillers are advantageous over synthetic ones in many aspects, including being low-cost, their accessibility, biodegradability, safe, and environmentally friendly. Moreover, plants provide a natural filler source mainly derived from seeds, roots, and leaves [5]. In previous studies, bio-silica from rice husk ash was utilized as a reinforced material for epoxy coating, which enhances elongation, scratch resistance, and wear resistance, and increases paint plasticity [6]. Similarly, the

bamboo leaf is also one of the sources of bio-silica with about 75.90–82.86%, according to [7], which is suitable for use as an additive filler to epoxy coating. Bamboo is one of the highest-yielding natural resources and construction materials that can be found in any locality. A huge amount of bamboo is processed in some countries, such as the Philippines, resulting in a large number of residues, such as bamboo leaves, which becomes waste that is often burned and harms the environment. As a result, bamboo leaf ash (BLA) will be utilized as a reinforcement material for the epoxy coating.

In this study, SEM-EDX Analysis and XRD Analysis were carried out to characterize bamboo leaf ash in terms of its surface morphology, and microscopic and crystallographic structure. Also, epoxy and bamboo leaf ash (Epoxy-BLA) mixture was formulated with different mixing ratios and evaluated their adhesion strength in mild steel substrate as per ASTM D3359 Method A standard. Thermal transitions and coating behavior were also investigated using Differential Scanning Calorimeter.



*1 Faculty
Department of Agricultural and
Biosystems Engineering,
University of Southern Mindanao-
Kabacan Campus



*2 Student
BS Agricultural and
Biosystems Engineering
University of Southern
Mindanao-Kabacan Campus

II. Materials and Methods

A. Materials

The Bamboo leaf used in this study belongs to the *Bambusa spinosa* species, which is locally known as Bayog. Other materials include epoxy resin and hardener, mild steel plate, distilled water, sandpaper, acetone, crucibles, tape, and a cutter.

B. Production of Bamboo Leaf Ash

The bamboo leaves were washed with distilled water to get rid of any dirt and completely dried in the open air. Then, the dried bamboo leaves were initially burned until it was all charred. A muffle furnace was used for the calcination of the samples and heated at 650°C for 2 hrs. to produce Bamboo Leaf Ash and was cooled down at room temperature [8]. Lastly, the Bamboo Leaf Ash was sieved to obtain ashes with a mesh size under 50 µm.

C. Characterization of Bamboo Leaf Ash

The bamboo leaves were washed with distilled water to get rid of any dirt and completely dried in the open air. Then, the dried bamboo leaves were initially burned until it was all charred. A muffle furnace was used for the calcination of the samples and heated at 650°C for 2 hrs. to produce Bamboo Leaf Ash and was cooled down at room temperature [8]. Lastly, the Bamboo Leaf Ash was sieved to obtain ashes with a mesh size under 50 µm.

D. Determination of Adhesive Strength of the Coating

Epoxy-BLA coating was formulated with different mixing ratios of 90% Epoxy and 10 % BLA, 80% Epoxy and 20% BLA, and 70% Epoxy and 30% BLA. An adhesion test was carried out to examine the effect of different coating mixtures on mild steel substrate as per ASTM 3359 Method A standard. Epoxy-BLA mixture was applied to the substrate in one layer with less than 0.5 mm thickness. Before applying the coating to the mild steel substrate, the surface was polished and washed with acetone to improve adhesion. Then, the paint coating was dried completely for 72 hours at ambient temperature to completely cured.

ASTM D3359 Method A was done by creating two incisions (an "X") that intersect near their middle with a smaller angle of 40°. Each cut is about 40 mm long. A 75-mm-long piece of tape is attached at the intersection of the cuts, running parallel to the smaller angles. The tape was removed within 90 seconds of application by grabbing the free end and rapidly (not jerked) bringing it back upon itself at as nearly as 180° angle as possible. The X-cut area was examined for the removal of the coating from the substrate and the adhesive strength was rated.

E. Thermal Analysis of the Coating

A Differential Scanning Calorimeter Analysis was carried out to determine the thermal transitions following

changes in the coating when it heated. About 3 mg to 5 mg of sample was put in the instrument with a temperature range of 0°C to 250°C at a heating rate of 10°C/min.

III. Results and Discussions

A. Characterization of Bamboo Leaf Ash

A detailed observation of the ash by Scanning Electron Microscope Analysis in Figure 1 shows that BLA particles have a rough surface and have traces of elements present, which can be seen in EDX Analysis. Also, Bamboo leaf ash has a variety of sizes, as can be seen at 50,000x magnification, where BLA particles have a smaller size of 1 µm. Furthermore, the SEM image shows that there is a cell-like structure present in the BLA.

The elemental composition of Bamboo Leaf Ash was determined by Energy Dispersive X-ray (EDX) Analysis. Based on Table 1, the bamboo leaf ash was determined to have a composition of 52.35 wt.% silicon, 38.49 wt.% oxygen, 4.54 wt.% calcium, 3.81 wt.% carbon, and 0.82 wt.% potassium. It can be observed that silicon and oxygen are the main elements present, confirming the siliceous nature of the ash. One of the main fillers is often based on silicon dioxide, which can improve the hardness, abrasion resistance, viscosity, thermal stability, and dirt and water-repellent properties of the coating. On the other hand, the presence of calcium and potassium in the ash can improve the rheological and mechanical characteristics of the coating. Lastly, the presence of carbon indicates incomplete combustion during the calcination process in the furnace at 650°C for 2 hours.

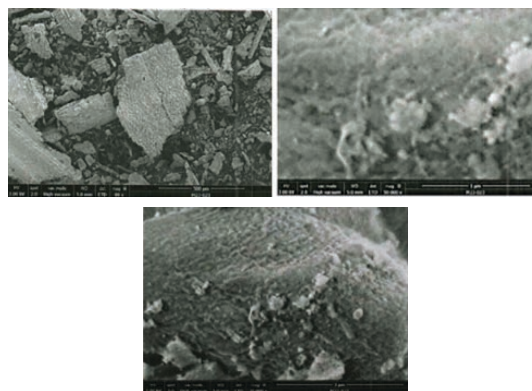


Fig. 1. SEM image of Bamboo Leaf Ash

Table 1. Quantitative results of elemental composition of BLA

Elemental Composition	%Weight
Silicon	52.35
Oxygen	38.49
Calcium	4.54
Carbon	3.81
Potassium	0.82

The XRD analysis allows the qualitative determination of the BLA mineralogy, which means that it is possible to verify if the ash presents crystalline phases, represented by characteristic peaks in the diffractogram, and if it possesses amorphousness, characterized by a deviation of the baseline between $2\theta=15$ and $2\theta=35$ [9]. **Figure 2** illustrates the XRD pattern corresponding to the bamboo leaf ash analyzed. Based on the graph, BLA was found to be an amorphous material containing amorphous silica, which corresponds with the broad band localized between 17.06° to 29.08° 2θ .

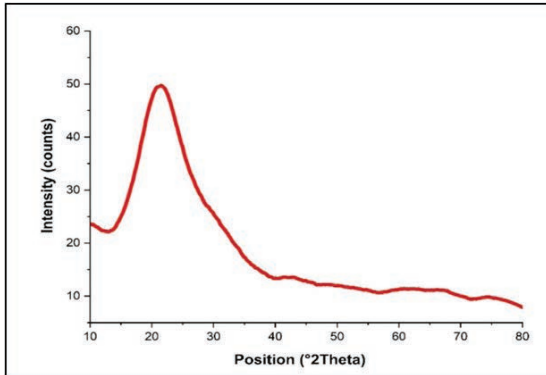


Fig. 2. XRD pattern of Bamboo Leaf Ash

B. Adhesion Strength of the Coating

Figure 3 shows the results of the adhesion test as per ASTM 3359-Method A. A mixture of 20% BLA and 80% Epoxy has the highest adhesion strength among the other mixtures, having a rate of 5A, which indicates that there is no removal or peeling on the X-area. While the 10% and 30% BLA fillers have the same rate of 4A, which shows that there is a removal or peeling along incisions or at their intersection. On the other hand, the 0% BLA filler has a rate of 1A, which indicates that most of the area of the X under the tape has been removed. Based on the results, the addition of fillers shows a significant improvement in the adhesion strength of the epoxy coating when applied to steel substrates. The presence of silica improved the adhesion strength of the coatings. Furthermore, the adhesion strength of a coating offers a

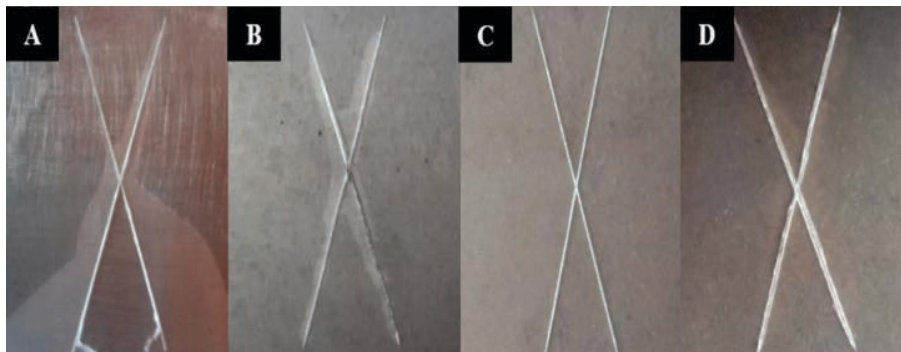


Fig. 3. Adhesion Test Result. A) 0% BLA; B) 10% BLA; C) 20% BLA; D) 30% BLA

significant indicator of the long-term effectiveness of a coating system. Thus, it improves the corrosion protection properties of the substrate by providing a passive barrier layer between the substrate and the corrosive environment [10].

C. Thermal Analysis of the Coating

DSC thermogram of Epoxy-BLA coatings cured at ambient temperature is shown in **Figure 4**. Initially, the cured Epoxy-BLA mixtures underwent an endothermic reaction. The endothermic events of the coating with 10% BLA, 20% BLA, and 30% BLA filler ranged between 47°C to 61°C , 40°C to 60°C and 35°C to 55°C , respectively. The presence of moisture in the coating causes an endothermic event to occur in which the composites absorb heat from the source. On the other hand, glass transition temperature (T_g) was also observed in which the T_g of the coatings with 10% BLA, 20% BLA, and 30% BLA are at $\sim 103^\circ\text{C}$, $\sim 108^\circ\text{C}$, and $\sim 114^\circ\text{C}$, respectively. Based on the results, Epoxy-BLA coating with 30% BLA filler had the highest glass transition temperature among the other mixtures. T_g is also related to chemical and heat resistance for cured polymers; the greater the T_g value, the more resistant the material [11].

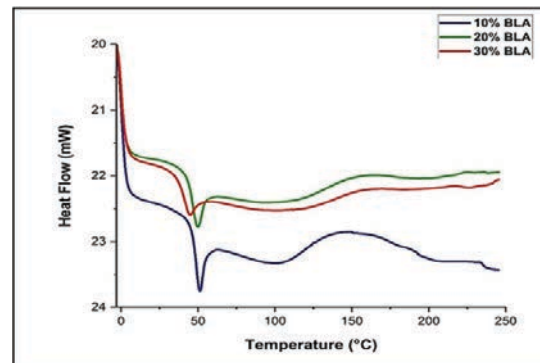


Fig. 4. DSC thermogram of cured Epoxy-BLA mixtures

IV. Conclusion

Bamboo Leaf Ash was used as reinforcement material for epoxy coating. SEM analysis shows that BLA particles have a rough surface and in a variety of sizes, where it plays an important role in enhancing the adhesion capacity through the mechanical interlocking mechanism of the coating to the steel substrate. Also, based on EDX analysis, silicon, and oxygen are the major element present which confirms the siliceous nature of the ash. Furthermore, the adhesion test result shows that the addition of filler has a significant impact on the adhesion strength of the coating wherein 20% of BLA filler has the highest adhesion strength among the other mixtures. Moreover, thermal analysis of the cured Epoxy-BLA mixtures shows that the glass transition temperature increased when there is increasing in the amount of filler added. The highest amount of BLA filler in the mixture attains the highest value of glass transition temperature, hence, the more resistant the material to heat. Thus, bamboo leaf ash can be used as filler material for epoxy coating and can be an alternative replacement for commercialized fillers such as silica.

V. Acknowledgment

The authors would like to acknowledge the USMARDC- Central Laboratory for providing the necessary equipment during the conduct of the study.

References

- [1] Y. Yang, G. Yang, K. Hou, H. Wang, N. Wang, S. Yang, and J. Wang, "Environmentally-Adaptive Epoxy Lubricating Coating Using Self-Assembled PMXene@Polytetrafluoroethylene Core-Shell Hybrid as Novel Additive." *Carbon*, vol. 184, Oct. 2021, pp. 12–23.
- [2] D. Li, R. Prevost, D. Ayre, A. Yoosefinejad, S. Lotfian, F. Brennan, & H.Y. Nezhad, 'Development of Damage Tolerant Composite Laminates Using Ultra-Thin Interlaminar Electrospun Thermoplastic Nanofibres'. 18th European Conference on Composite Materials (ECCM), 2020, pp. 1–10.
- [3] K. Song, D. Chen, R. Polak, M.F. Rubner, R.E. Cohen, and K.A. Askar, "Enhanced Wear Resistance of Transparent Epoxy Composite Coatings with Vertically Aligned Halloysite Nanotubes". *ACS Applied Materials & Interfaces*, vol. 8, no. 51, Dec. 2016, pp. 35552–35564.
- [4] D. Gysau. *Fillers for paints*, 3rd ed. Hannover Germany: Vincentz Network, 2017.
- [5] R.A. Ibrahim, "Effect of Date Palm Seeds on the Tribological Behaviour of Polyester Composites under Different Testing Conditions". *Journal of Material Science & Engineering*, vol. 04, no. 06, OMICS Publishing Group, 2015.
- [6] M. Azadi, M.E. Bahrololoom, and F. Heidari, "Enhancing the Mechanical Properties of an Epoxy Coating with Rice Husk Ash, a Green Product." *Journal of Coatings Technology and Research*, vol. 8, no. 1, July 2010, pp. 117–23.
- [7] S. Mohapatra, R. Sakthivel, G. Roy, S. Varma, S. Singh, and D. Mishra, *Materials and Manufacturing Processes*, vol.26, 2011, pp. 120-124.
- [8] K. Kow, R. Yusoff, A.RA. Aziz, and E.C. Abdullah, "From bamboo leaf to aerogel: Preparation of water glass as a precursor. *Journal of Non Crystalline Solids*, vol. 386, Elsevier BV, Feb. 2014, pp. 76–84
- [9] M.J.B. Moraes, J.C.B. Moraes, M.M. Tashima, J.L. Akasaki, L. Soriano, M.V. Borrachero, and J. Payá, "Production of Bamboo Leaf Ash by Auto-Combustion for Pozzolanitic and Sustainable Use in Cementitious Matrices". *Construction and Building Materials*, vol. 208, Elsevier BV, May 2019, pp. 369–380.
- [10] N. Parhizkar, B. Ramezanzadeh, and T. Shahrabi, "Corrosion Protection and Adhesion Properties of the Epoxy Coating Applied on the Steel Substrate Pre-Treated by a Sol-Gel Based Silane Coating Filled with Amino and Isocyanate Silane Functionalized Graphene Oxide Nanosheets". *Applied Surface Science*, vol. 439, Elsevier BV, May 2018, pp. 45–59.
- [11] I.J. Fernandes, R.V. Santos, E.C.A. Santos, T.L.A.C. Rocha, N.S. Domingues Junior, C.A.M. Moraes, "Replacement of Commercial Silica by Rice Husk Ash in Epoxy Composites: A Comparative Analysis". *Materials Research*, vol. 21, no. 3, FapUNIFESP (SciELO), Apr. 2018.

Microwave-Assisted Extraction and Synthesis of Calamansi (*Citrofortunella macrocarpa*) Pectin-Mediated Silver Nanoparticles as Green Inhibitor for Carbon Steel Corrosion in Saline Environment

Dr. Sicily B. Tiu^{*1}, Ray Anthony U. Escoton^{*2}, Christene Joy P. Managaysay^{*3}, Melizza D. Maala^{*4}, Mary Rose D. Villete^{*5}

Abstract

The rapidly increasing amount of fruit waste is directly attributable to the rise in fruit consumption and the subsequent processing of their edible components. In this study, silver nanoparticles were synthesized using pectin from calamansi (*Citrofortunella macrocarpa*) rind for corrosion inhibition of carbon steel in saline environments using microwave-assisted extraction and synthesis methods. Factors such as microwave power, irradiation time, and volume of AgNO₃ solution have substantial impacts on their responses to pectin yield, methoxyl content, and yield of crude-AgNPs. It was discovered that the responses of the variables increased as the parameters were increased. The FTIR spectra of extracted calamansi pectin revealed the presence of polygalacturonic acid, ester, and carboxyl groups, whereas the FTIR spectra of AgNPs revealed the presence of ester and carboxyl groups. The SEM analysis revealed that the synthesized pectin-mediated silver nanoparticles have a quasi-spherical shape with an average particle size of 61.25 nm. The EDX spectrum showed a strong silver signal at 3.0 keV and a silver peak (9.2%). The TGA has confirmed that the AgNPs are thermally stable until 492 °C. The formulation with 20% AgNP showed greater open-circuit potentials as inhibitor concentration rose, showing that the water-based primer with inhibitors had better anticorrosion capabilities than primers without inhibitors. Organic corrosion inhibitors' anticorrosive abilities were validated using electrochemical impedance spectroscopy. The EIS revealed the Nyquist plot diameter and absolute impedance values rising with inhibitor concentration. The inhibitor at 20% AgNP gives maximal corrosion protection, according to an analogous circuit model with two-time constants. The water-based primer coating's anticorrosive capabilities increased best with AgNP at 20%.

Keywords: pectin, methoxyl content, crude-AgNPs, open-circuit potential, electrochemical impedance spectroscopy, Nyquist

I. Introduction

Metal corrosion is a significant and well-studied industrial problem that has found fruitful ground in green chemistry research. Corrosion is metal degradation caused by chemical reactions in its environment, which is a recurring and ongoing problem that is frequently difficult to eliminate. Corrosion destroys barrier protection and causes a chain of reactions that modify the structure and composition of the surface of a metal as well as the surrounding environment [1]. In the oil and gas industry, carbon steel is frequently utilized in the construction of pipeline systems. However, carbon steel is vulnerable to corrosion. It has been demonstrated that the vast majority of corrosion problems experienced in the oil and gas sectors are related to pipes and that the conditions of carbon steel exposed in the environment are what

determine the selection of the most appropriate type of carbon steel. With this, several organic and inorganic inhibitors, such as passive protective coatings, have been developed to protect the steel [2]. As a result, corrosion inhibitors could be added to the solution to counteract the corrosive effects of corroding media such as sodium chloride (NaCl).

In the Philippines, calamondin fruits, commonly called "kalamansi," are abundantly grown and were utilized in most of the Filipino classic meals as a flavoring. In a calamansi, the juice is commonly extracted, while the rind is sent straight to the bins as waste. Additionally, calamansi was considered to have a substantial amount of pectin, which can be used for a variety of purposes.



^{*1}
Associate Professor
Chemical Engineering Department
Batangas State University – TNEU
Alangilan, Batangas City



^{*2, 3, 4, 5}
Student
BS Chemical Engineering
Batangas State University – TNEU
Alangilan, Batangas City

Pectin is a polysaccharide found naturally in the main cell walls of higher plants and can act as a promising corrosion inhibitor under certain circumstances (Morte & Acero, 2016). Recent research has revealed that combining plant extracts with additives can increase the effectiveness of plant extracts by utilizing synergistic effects that are beneficial to both the extract and the additive. It is possible that the reaction of some active chemicals contained in plant extracts when combined with metal salts will result in the formation of metal ion compounds and nanoparticles if the concentration of the extracts, pH, and temperature are optimized (Ituen, 2021). In addition, it has also been reported that the addition of nanoparticles can enhance the effectiveness of various inhibitors.

The development of environmentally friendly alternative chemical processes based on the biological compounds taken from plants has sparked a lot of attention since it presents a possibility to reduce harmful by-product development. In line with this, the researchers have found a technique that uses microwave irradiation for extraction and synthesis applications as a result of their search for a more efficient and environmentally friendly method. Even though various plant extracts have been shown to effectively reduce corrosion, little emphasis has been paid to the evaluation of plant extract-mediated nanoparticles as corrosion inhibitors. In this regard, the current study focused on the use of synthesized silver nanoparticles made from microwave-assisted pectin extracts of calamansi rind, which is readily available in the Philippines, as a green corrosion inhibitor. The effectiveness of synthesized silver nanoparticles in inhibiting carbon steel corrosion in NaCl medium was investigated in this study.

II. Experimental Procedure

A. Materials and Reagents

Calamansi rinds were collected from Batangas City Market. Hydrochloric acid (HCl), ethanol, acetone, sodium chloride (NaCl), sodium hydroxide (NaOH), phenolphthalein, silver nitrate and deionized water were purchased from Belman Laboratories. All chemicals used were of commercially available analytical grade.

B. Microwave-Assisted Synthesis of Calamansi Pectins

To extract pectin from calamansi rinds, microwave equipment (Whirlpool MWX 203 BL) was used at an operating power consumption of 700 W with adjustable irradiation time and microwave power. For this process, in a 1 L beaker, 10 g of calamansi rind powder and 5 mL of hydrochloric acid were added to 295 mL distilled water. Then, it was placed in the center of the microwave oven over a rotating dish and subjected to sets of microwave power such as 560, 630, and 700 watts and irradiation times such as 60, 120, and 180 seconds, respectively. The solution in the beaker was already allowed to cool until it reached room temperature before being filtered using a cheese cloth and centrifuged at 4000 rpm for about 15 minutes. Also, with an equal volume concentration of 97%

ethanol, the supernatant was precipitated. To eliminate the mono- and disaccharides, the coagulated pectin mass was rinsed three times with 97% ethanol, then air-dried to remove the remaining ethanol.

a) Analysis of Extracted Calamansi Pectin in terms of Pectin Yield

The yield of pectin was calculated using the weight ratio of calamansi pectin to the dried calamansi rind. The formula that was used for calculating the pectin yield was adapted from the study of [5].

$$\text{Pectin Yield} = \frac{\text{weight of calamansi pectin (g)}}{\text{weight of calamansi rind (g)}} \times 100\%$$

b) Analysis of Extracted Calamansi Pectin in terms of Methoxyl Content

The method for determining the methoxyl content that was used is acknowledged by Wongkaew et al. (2020) with slight modifications. To determine the methoxyl content of the pectin, the equivalent weight was first determined. On an analytical balance, 0.01 g of pectin powder was weighed. The powder was mixed with 20 mL of distilled water and 1 mL of ethanol. Then, the solution was stirred using a hot magnetic stirrer for about 1 hour with moderate heating. A total of 0.2 g of NaCl was added right after stirring. Then, the stirred solution was filtered using cheesecloth. The solution was transferred to an Erlenmeyer flask. Then, 3 drops of phenolphthalein were added to the filtered solution. Each sample was titrated, and the amount of NaOH was determined.

For the methoxyl content, 10 ml of 0.2 N NaOH solution was added to the titrated sample. The sample was then allowed to settle for 30 minutes to allow the reaction to settle. After 30 minutes, the solution went to titration again for the second time. When the solution turned pink, 10 ml of a 0.1 N HCl solution was added to the titrated sample and the pH of the solution was checked again.

$$\text{Methoxyl Content} = \frac{(\text{Volume of NaOH})(E)(N \text{ NaOH})(100)}{(S)}$$

C. Microwave-Assisted Synthesis of Calamansi Pectin

For the green synthesis of silver nanoparticles, microwave-extracted calamansi pectin was used. Silver nitrate was weighed precisely and mixed in distilled water. The method for the green synthesis using the extracted pectin was based on the method of Dong-lin Su et al. (2019) with minor modifications. The 0.8 mmol silver nitrate solution was prepared using a 0.135 g silver nitrate powder and mixed to 1 L distilled water. Meanwhile, for the preparation of pectin solution, 0.1 g of pectin powder were added to a 50-mL beaker containing 20 mL of 1 g/L NaOH aqueous solution. The prepared solution was agitated using a magnetic stirrer until the pectin powder was fully dissolved. Then, varying amounts of 0.8 mmol of AgNO₃ solution (15, 20, and 25 mL) were added to the pectin solutions.

The latter solution was exposed to microwave radiation with varying irradiation times (30, 60, and 90 seconds) heated at 700 W, cooled down at a room temperature in a dark chamber and allow the reaction to further takes place. After the reaction, a definite color change occurred from pale yellow to dark brown, indicating a complete bio-reduction and nanoparticle production. Additionally, the presence of pectin-mediated silver nanoparticles was confirmed and monitored using a UV-Vis spectrophotometer.

The pectin-mediated silver nanoparticle solution was centrifuged to separate the supernatant. The precipitates were dried using a freeze dryer. The synthesized silver nanoparticle powder was stored in an amber glass and kept in a cool, dry place for further characterization.

D. Performance Evaluation of Pectin-Mediated Silver Nanoparticles as Green Corrosion Inhibitor

a) Preparation of Carbon Steel Specimen

300 pieces of carbon steel plate 1045 were cut to dimensions of 3 mm by 15 mm by 20 mm. These specimens were acquired from Visayan Marine Industrial Services, which is located at Purok 5 Sta. Rita Karsada, in the municipality of Batangas City. These specimens of carbon steel were initially polished using emery paper with grits including 120, 180, 240, and 600, then further refined using sandpaper with grits ranging from 120, 240, and 1000. Afterward, the samples were thoroughly cleaned with acetone and placed in plastic Ziplock bags for future use.

b) Coating of Carbon Steel Samples

3 samples were prepared for the evaluation of crude-AgNP solution: uncoated carbon steel, coated with primer, and coated primer and 20% (w/w) crude-AgNPs.

c) Corrosion Testing through potentiostatic polarization

The carbon steel sample will be placed in a typical three-electrode cell with a 3.5% aqueous NaCl solution. The reference and counter electrodes will be an aqueous Ag/AgCl electrode and platinum wire, respectively. The General-Purpose Electrochemical System and Frequency Response Analyzer applications will control a potentiostat that is connected to the setup.

The open-circuit potential of the samples will be measured after they are subjected to a 3.5% aqueous NaCl solution. After an hour, electrochemical impedance spectroscopy data will be measured as an AC voltage signal with an amplitude voltage of 10 mV at initial frequency of 100kHz and final frequency of 10mH, respectively. The Powell method will be used to match the impedance spectra to equivalent circuit models using the EIS Spectrum Analyzer program (ABCChemistry.org).

III. Results and Discussion

A. Characterization of Calamansi Pectin

a) Analysis of total pectin yield and methoxyl content of calamansi peel

The extent of microwave-assisted extraction of calamansi pectin was quantified using the weighted mass of dried precipitated pectin. Meanwhile, the total methoxyl content was quantified using titrimetric analysis. The highest yield of pectin with a value of 0.6925 g pectin sample was obtained at an extraction having 180 s irradiation time and 700 W microwave power. Likewise, the highest amount of methoxyl with a value of 1.8939 mg pectin sample was obtained at an extraction having 180 s irradiation time and 700 W microwave power.

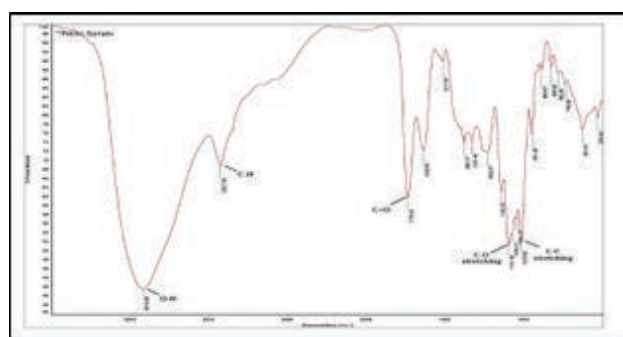


Fig. 1. FTIR Spectrum of Calamansi Pectin

b) Surface Functional Groups of Calamansi Pectin

Figure 1 presents the characteristic peaks of calamansi pectin's functional groups that has similarity to the characteristics of orange pectin from the study of (Duwee et al., 2022). A peak could be observed between 3000 and 3600 cm^{-1} based on the FTIR spectrum. The presence of OH functional groups in the molecular structure of pectin contributed to the detection of a medium-broad peak at 3419.08 cm^{-1} . This region indicated the presence of intermolecular and intramolecular hydrogen bonds in the galacturonic acid structure of pectin (Hundie, 2020). Meanwhile, the recorded strong absorption at 1739.62 cm^{-1} was ascribed to C=O bonding that corresponds to the characteristic of esterified pectin, which arises from the ester carbonyl-stretching band. Moreover, peaks at 1600–1640 cm^{-1} and 1500–1550 cm^{-1} are attributable to the antisymmetric and symmetric stretching frequencies of the ionic carboxyl groups, respectively. The region with a frequency range between 950 and 1200 cm^{-1} is referred to as the "fingerprint" for carbs, more specifically sugar content. Intense peaks associated with the properties of pectin polysaccharides (polygalacturonic acid) were measured at 951, 1018, 1051, 1101, and 1233 cm^{-1} , and have been attributed to C–O bending, C–C stretching, C–O stretching, and C–H stretching, respectively (Rodsamran P., 2019).

B. Characterization of Crude AgNPs

a) Analysis of the total yield of crude AgNP

The extent of microwave-assisted synthesis of silver nanoparticles was quantified using the weighted mass of dried crude AgNPs. The highest yield with a value of 14.8114 mg of lyophilized crude AgNP sample was obtained at synthesis having 90s irradiation time and a volume of 25 mL AgNO₃. Furthermore, the lowest yield with a value of 8.5406 mg of lyophilized crude AgNP sample was obtained at synthesis having 30s irradiation time and a volume of 15 mL AgNO₃.

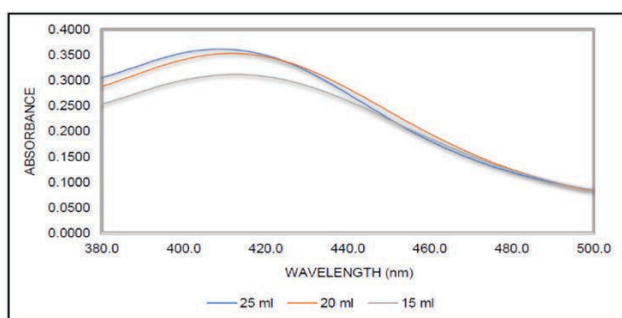


Fig. 2. UV-Vis Spectra of Formation of Pectin-AgNPs

b) UV-Visible Spectrophotometer

Figure 2 shows that the value of absorbance was found to be significantly higher in the 25 mL volume of the AgNO₃ solution when compared to the 15 mL and 20 mL volumes of the solution. However, at the longer wavelength, the absorbance of the 25-milliliter solution drops below that of the 15 mL and 20 mL solutions. When the volume of the AgNO₃ solution is increased from 15 mL to 25 mL, the absorbance of the solution likewise increases. This shows that the solution is becoming more concentrated, which results in a greater amount of light being absorbed. On the other hand, the ability of the 25 mL solution to absorb light of longer wavelengths significantly decreases, which indicates that it is less effective at absorbing light at those longer wavelengths. The relationship between volume and absorbance depends on the substance's concentration and the solution's path length (Ilyas et al., 2017). The results show that increasing the volume of AgNO₃ solution increases its absorbance, but this effect is not uniform across all wavelengths. The observed value indicates that the volume of the AgNO₃ solution can affect its absorbance properties and that these properties can vary depending on the wavelength of the light used to measure it.

c) Surface Functional Groups Analysis

From Figure 3, it was observed that the majority of the peaks appear at almost the same wavelength as those detected for pure calamansi pectin. A medium sharp peak was determined at 3425.65 cm⁻¹ and 2925.40 cm⁻¹ from the wavenumber of the FTIR spectrum. This particular region indicated the presence of O-H bonds in the galacturonic acid structure of calamansi pectin. Furthermore, the shift from of wavenumber from 3419.08

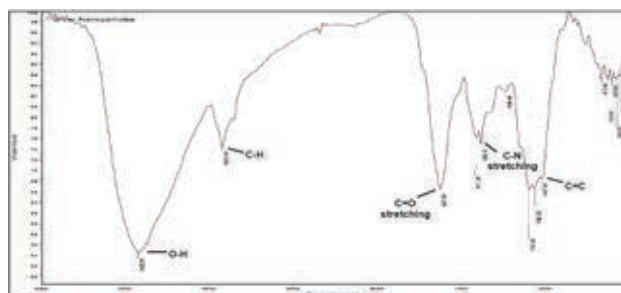


Fig. 3. FTIR Spectra of Crude AgNPs

cm⁻¹ to a higher wavenumber peak at 3425.65 cm⁻¹ would be responsible for the reduction of silver.

Moreover, the peak at 1027.50 cm⁻¹ can be ascribed to the pectin C=O or C=C group. The absorption band at 1739.62 cm⁻¹ in the FTIR spectrum of calamansi pectin is adjusted to 1627 cm⁻¹ which corresponds to the vibration of amines from plant proteins which also indicates the silver nanoparticle formation (Barros et al., 2018). Furthermore, an intense peak at 1384.51 also determines C-N stretch vibrations of the amide I band in the pectin. Meanwhile, the FTIR peaks that are comparable to the functional groups of calamansi pectin were found and identified in AgNPs indicating the presence of pectin molecules on the surface of the particles (Balachandran et al., 2013).

d) Surface morphology

The shape and size of the synthesized pectin-mediated silver nanoparticles were determined using Scanning Electron Microscopy (SEM). Only the optimal condition of pectin-AgNPs (0.8 mmol AgNO₃ at 90 seconds and 700 Watts) was analyzed for this study. Figures (4a) and (4b) display the SEM images at magnifications of 4,000x and 10,000x, respectively, while Figure 5 depicts the particle size distribution of pectin-AgNPs.

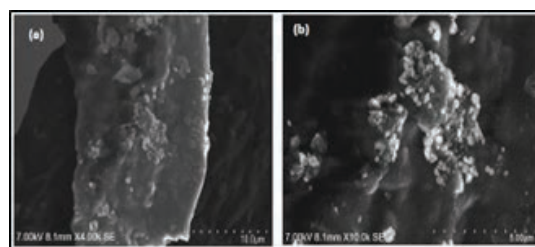


Fig. 4. SEM Images of Pectin-AgNPs

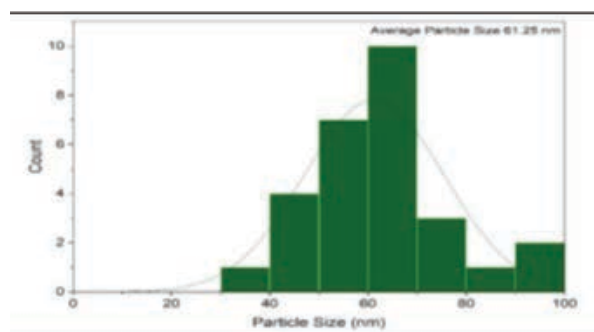


Fig. 5. Particle Size Distribution of Pectin-AgNPs based on SEM Image

The analysis reveals that the synthesized pectin-mediated silver nanoparticles have a quasi-spherical shape with a particle size that predominantly falls between 60 and 70 nm, with an average particle size of 61.25 nm, which is significantly larger than the desired particle sizes of 6 to 30 nm. This is due to the fact that as the concentration of AgNO₃ increases, the synthesized nanoparticles tend to collapse and begin to aggregate into bigger particles. In addition, by increasing the temperature, the produced spherical AgNPs exhibited higher kinetics and tend to aggregate into larger clusters (Zahran, et al., 2014).

e) Elemental Analysis

An Energy Dispersive X-ray (EDX) analysis was carried out in order to determine the elements that were present in the sample by utilizing a concentration of 8 mmol with an amount of 25 mL AgNO₃ solution at 700 W for 90 seconds. Figure 6 shows the results of the analysis, which showed a strong signal of carbon (48.4%), together with a weaker oxygen (27.7%), and a silver peak (9.2%). Similar results were found in this analysis, which was comparable with those found by Gong et al. (2020). These results could have existed from silver particles with biological molecules bonded to their surface. Carbon from the pectin in the calamansi peel may have been the source of the highest peak in the EDX.

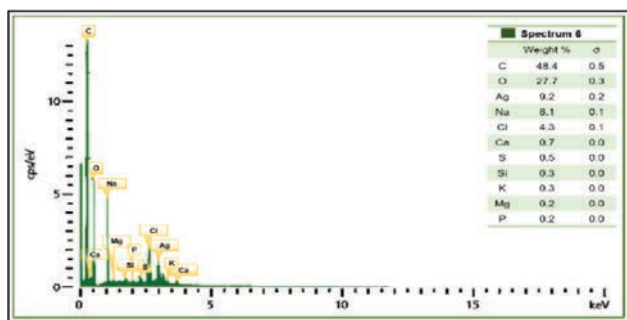


Fig. 6. EDX Analysis of Crude - pectin-mediated Silver Nanoparticles

Citrus fruit peels contain pectin at concentrations between 0.5% and 3.5% of their dry weight, as reported by Mudgul (2017). The signals of C (48.4%), O (27.7%), and Cl (4.3%) can also be attributed to the organic capping layer, similar to the elements present in the EDX spectra presented by Saha et al. (2021). The signals of N (8.1%), Ca (4.3%), S (0.5%), Si (0.3%), K (0.3%), Mg (0.2%), and P (0.2%) have also originated from the plant extract. When silver nanoparticles were synthesized using the pectin extract of calamansi peel, the presence of these components in small amounts showed that phytochemical groups of the calamansi peel were involved in the process of reducing and capping the formed silver nanoparticles.

f) Thermal Stability

The thermal stability of the pectin-mediated silver nanoparticles was examined by thermogravimetric analysis (TGA). In this analysis, the sample is subjected to a nitrogen atmosphere at 100 ml/min at a heating rate of 10 C/min using a Simultaneous Thermal Analyzer – (TGA-DSC). Figure 7 shows the results of the thermogravimetric

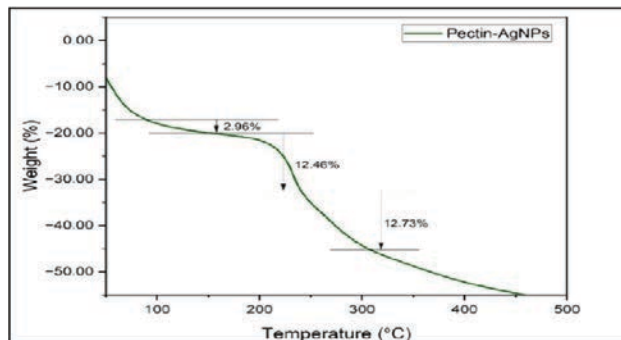


Fig. 7. TGA Curve of Crude Pectin-AgNPs

analysis (TGA) of crude pectin-mediated silver nanoparticles (Pectin-AgNPs).

The thermal mass loss profile of the pectin-mediated silver nanoparticles was evaluated at temperatures ranging from 29 to 492 °C. The initial step of the decomposition process, which occurred between 50 and 100 °C, is attributed to the evaporation of water molecules from AgNPs, with a recorded mass loss of 7.39%. A further degradation, with an associated weight loss of 5.89%, was observed between 100 and 200 °C as a result of the desorption of the bioorganic molecules present on the surface of the pectin-AgNPs. This weight loss may be due to the breakdown of phenolic acids, flavonoids, and carbohydrates originally derived from the fruit extract and responsible for the stabilization of silver nanoparticles (David et al., 2020).

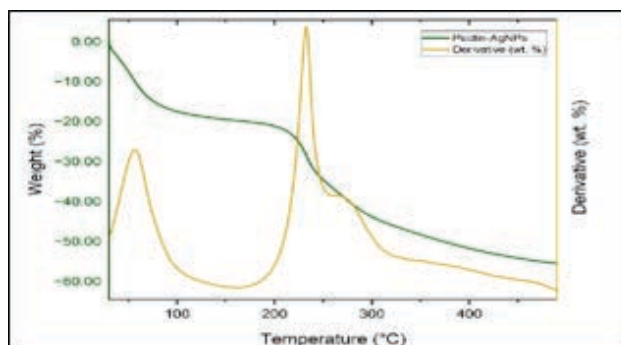


Fig. 8. TGA vs. DTG Curve of Crude Pectin-AgNPs

Peaks at the DTG plot are noted. The first trough point found at approximately 55 °C indicated the degradation of pectin as stated earlier. Finally, the thermal decomposition of pectin-AgNPs was identified at 231 °C as Figure 8 suggests.

The results obtained were also comparable to those reported by Shankar (2016), who reported the TGA and DTGA curves of pectin-AgNPs. In a similar manner, there were also 3 distinct stages of thermal degradation that occurred: moisture evaporation at around 50 °C, degradation of biopolymer pectin and glycerol between 170 and 240 °C, and polymer and extract oxidation at around 320 to 350 °C.

The signals of C (48.4%), O (27.7%), and Cl (4.3%) can also be attributed to the organic capping layer, similar to the elements present in the EDX spectra presented by Saha et al. (2021). The signals of N (8.1%), Ca (4.3%), S (0.5%), Si (0.3%), K (0.3%), Mg (0.2%), and P (0.2%) have also originated from the plant extract. When silver nanoparticles were synthesized using the pectin extract of calamansi peel, the presence of these components in small amounts showed that phytochemical groups of the calamansi peel were involved in the process of reducing and capping the formed silver nanoparticles.

C. Performance Evaluation of Pectin-AgNPs through Potentiostatic Polarization

a) Open-Circuit Measurements

Figure 9 shows that the treatment under 20% AgNP coating has the highest measurement, followed by waterborne paint (WBP) coating and the one with no coating. During the first 10 minutes of observation, the open circuit potential of carbon steel was significantly high under 20% AgNP compared to the uncoated and WBP coated. The OCP measured was not constant to the preceding time of observation in all treatments.

In general, a high OCP measurement indicates that the metal is more noble or resistant to corrosion. This means that the metal is less likely to corrode or react with its environment (Bixenman, n.d.). Since silver is known to be resistant to corrosion, as it does not oxidize easily, when Silver is exposed to air, a layer of silver sulfide is formed on the surface (Edward, 2015).

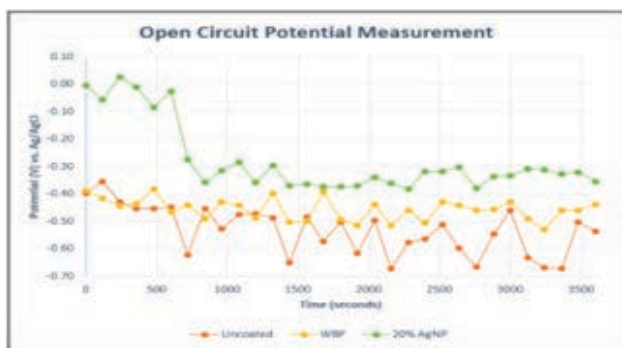


Fig. 9. Open Circuit Potential Measurement

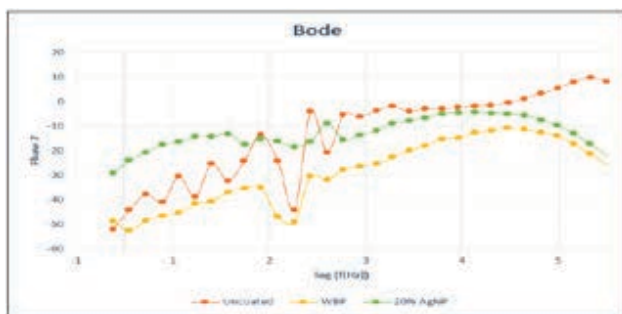


Fig. 10. Electrochemical Impedance Plot

b) Electrochemical Impedance Plot

Figure 10 shows that uncoated carbon steel would show a steep drop in impedance at lower frequencies, indicating that it is more susceptible to corrosion at lower frequencies. Uncoated carbon steel typically has a high rate of corrosion due to its chemical composition and lack of protective coating. As shown in the figure, the Bode plot for waterborne paint-coated carbon steel shows a less steep drop in impedance at lower frequencies, indicating that it is less susceptible to corrosion at lower frequencies compared to uncoated carbon steel.

Meanwhile, 20% silver nanoparticle-coated carbon steel has a protective coating that is even more effective at reducing the rate of corrosion. The Bode plot for 20% silver nanoparticle-coated carbon steel shows a gradual drop in impedance at lower frequencies, indicating that it is highly resistant to corrosion even at lower frequencies.

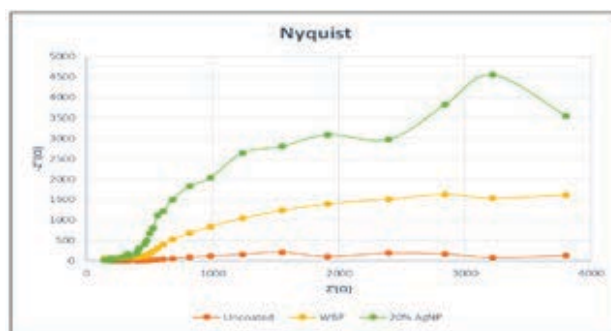


Fig. 11. Nyquist Plot

The 20% AgNP coating shows a significant increase in negative impedance, which indicates increasing voltage opposition. It is followed by WBP coating and uncoated carbon steel. Electrical conductivity is a measure of how easily electrical current can flow through a material. It is defined as the inverse of resistivity, which is the resistance of a material per unit length and cross-sectional area. The higher the electrical conductivity of a material, the lower its resistivity, and the easier it is for electrical current to flow through it [11].

IV. Conclusion

From the findings of the study, the following conclusions were drawn:

1. There were significant effects on the pectin yield and methoxyl content using microwave-assisted extraction methods at varying microwave irradiation time and power.
2. There were significant effects on the yield of crude-AgNPs using the microwave-assisted synthesis method at varying microwave irradiation time and volume of AgNO₃ solution. The yield of crude-AgNPs from the calamansi rind increased as the volume of AgNO₃ solution and irradiation time increased.

3. The synthesized pectin-mediated silver nanoparticles from calamansi rind conformed to the physicochemical properties of silver nanoparticles. FTIR revealed the presence of polygalacturonic acid, ester group, and carbonyl group in calamansi pectin. The EDX analysis showed a strong signal at 3 keV which revealed the presence of silver nanoparticles and it showed elements such as Ag (9.2%), C (48.4%) and O (27.7%). The TGA revealed that the pectin-AgNPs are thermally stable.
4. The water-based primer with 20% AgNP had better anti-corrosion properties than primers without inhibitors as inhibitor concentration increased. Electrochemical impedance spectroscopy showed organic corrosion inhibitors' anticorrosive capabilities. Inhibitor concentration increased Nyquist plot width and absolute impedance in EIS. 20% AgNP reduced corrosion best in a two-time constant circuit model. SEM showed these inhibitors decreased blister diameters.
5. The study revealed 20% AgNP corrosion inhibitors stabilized water-based primer coatings. AgNP at 20% made the water-based primer layer most anti-corrosive.

V. Recommendation

The use of different pectin-rich materials was recommended for the extraction of pectin using various methods of extraction. Addition of parameters for pectin extraction such as temperature and pH while in the synthesis of silver nanoparticles, silver nitrate concentration, pH, temperature and reaction time might be considered in the extraction and synthesis techniques. Further characterization techniques such as SEM and Zeta potential can be used to determine the particle size of each sample and the surface charge of silver nanoparticles, respectively. Other, potential green inhibitors may be investigated for corrosion inhibition in carbon steel.

VI. Acknowledgment

The proponents send their deepest gratitude to their adviser, Dr. Sicily B. Tiu for her guidance in the completion of this study, to their parents for their financial and moral support, and to Sir Mike Ajero and the DLSU-Manila Chemistry Instrumentation Laboratory for their service on the sample material characterization of the study.

References

- [1] B. E. A. Rani and B. B. J. Basu, "Green inhibitors for corrosion protection of metals and alloys: An overview," *Int. J. Corros.*, vol. 2012, 2012, doi: 10.1155/2012/380217.
- [2] D. Dwivedi, K. Lepková, and T. Becker, "Carbon steel corrosion: a review of key surface properties and characterization methods," *RSC Adv.*, vol. 7, no. 8, pp. 4580–4610, Jan. 2017, doi: 10.1039/C6RA25094G.
- [3] R. Desai, V. Mankad, S. K. Gupta, and P. K. Jha, "Size distribution of silver nanoparticles: UV-visible spectroscopic assessment," *Nanosci. Nanotechnol. Lett.*, vol. 4, no. 1, pp. 30–34, 2012, doi: 10.1166/NNL.2012.1278.
- [4] R. G. M. de A. Macedo, N. do N. Marques, J. Tonholo, and R. de C. Balaban, "Water-soluble carboxymethylchitosan used as corrosion inhibitor for carbon steel in saline medium," *Carbohydr. Polym.*, vol. 205, pp. 371–376, Feb. 2019, doi: 10.1016/J.CARBPOL.2018.10.081.
- [5] M. J. C. Lo, M. A. C. Pesebre, J. J. C. Riza, E. B. N. Samson, A. Prof, and C. O. Cruz, "CHARACTERIZATION OF POWDERED PECTIN FROM WATERMELON (*Citrullus lanatus*) RIND" vol. 6, no. 2, pp. 9–13, 2019.
- [6] S. E. Nataraja, T. V. Venkatesha, and H. C. Tandon, "Computational and experimental evaluation of the acid corrosion inhibition of steel by tacrine," *Corros. Sci.*, vol. 60, pp. 214–223, Jul. 2012, doi: 10.1016/J.CORSCI.2012.03.034.
- [7] Board on Chemical Sciences and Technology, "Physicochemical Properties and Environmental Fate - A Framework to Guide Selection of Chemical Alternatives -," National Academy of Sciences. p. 334, 2014. [Online]. Available: <https://www.ncbi.nlm.nih.gov/books/NBK253956/>
- [8] J. Singh, T. Dutta, K. H. Kim, M. Rawat, P. Samddar, and P. Kumar, "'Green' synthesis of metals and their oxide nanoparticles: applications for environmental remediation," *J. Nanobiotechnology* 2018 161, vol. 16, no. 1, pp. 1–24, Oct. 2018, doi: 10.1186/S12951-018-0408-4.
- [9] R. K. Singh, "The Corrosion Protection of Materials by Nanotechnology – Material Science Research India." <https://www.materialsciencejournal.org/vol8no2/the-corrosion-protection-of-materials-by-nanotechnology/>
- [10] X. Zhao et al., "Microwave-assisted synthesis of silver nanoparticles using sodium alginate and their antibacterial activity," *Colloids Surfaces A Physicochem. Eng. Asp.*, vol. 444, pp. 180–188, Mar. 2014, doi: 10.1016/J.COLSURFA.2013.12.008.
- [11] D. A. Dean, T. Ramanathan, D. Machado, and R. Sundararajan, "Electrical impedance spectroscopy study of biological tissues," *J. Electrostat.*, vol. 66, no. 3–4, pp. 165–177, Mar. 2008, doi: 10.1016/J.ELSTAT.2007.11.005.



PHILIPPINE WELDING SOCIETY, INC.

DOST-MIRDC Compound, Gen. Santos Avenue. Bicutan Taguig City

Tel. No.: (632) 8357-3167

Mobile No. (0917) 124-9881 / (0917) 909 0261

E-mail: pws@pws.org.ph URL: www.pws.org.ph



Brief History of the Society

Philippine Welding Society started as a vision of various industry professionals whose aim is: to advance the science and professionalize the practice of welding in the country. On September 19, 1991, encouraged by the government, business sector, educators and practitioners, twelve founding members from construction, manufacturing and inspection companies bonded together and established the Philippine Welding Society (PWS). On February 13, 1992, The Securities and Exchange Commission (SEC) registered the Philippine Welding Society as a non-stock, non-profit organization

The Objectives of the Organization are as follows:

(1.) To promote the advancement of the science and practice of welding and to advise and support government entities whenever possible on matters of standardization, public safety and health; (2.) To foster and maintain among members' high ideals of integrity, learning, professional competence, public service and conduct; (3.) To provide proper forum for meeting, exchanging of ideas and opinions, and to be involved in the solution of multifarious problems affecting the country in general and the welding profession; (4.) To conduct workshops and seminars for purpose of keeping its members abreast of progress in the welding field; (5.) To promote orderliness and effectiveness in the maintenance of good fellowship and occupational standards; (6.) To promote and organize research in all matters relating to the science and practice of welding technology; and, (7.) To promote consciousness among members of their serious responsibilities in helping our country move forward in our national development and to consolidate all gains already made.



TESDA ACCREDITED WELDING ASSESSMENT CENTER

Schedule: Monday – Friday (8:00 AM – 5:00 PM)

- SHIELDED METAL ARC WELDING (SMAW NC I & II)**
- GAS TUNGSTEN ARC WELDING (GTAW NC II & IV)**
- GAS METAL ARC WELDING (GMAW NC I & II)**
- FLUX CORED ARC WELDING (FCAW NC I & II)**

TRAININGS, SEMINARS AND SERVICES OFFERED:

- Welding Inspector's Seminar, Review, and Exam
- Welding Engineer Training Program
- Accreditations, Inspection, Training, Testing for Institutions and Industry
- Preparation and Qualification of Welding Procedure Specification (WPS)
- Qualification & Certification of Welding Personnel
- Provide Forum for Exchange of Ideas on Welding
- Annual Welding Competition and Convention
- Research and Development/ Special Reports
- Welders Performance Up-grading Course
- Free Technical Seminars & Workshops
- Maintenance Welding Training Course
- Welding Supervisor's Training Course
- Welding Trainer's Training Course
- Welding Repair and Maintenance
- Technical Welding Consultancy
- Conduct of Welding Inspection
- Welding Exhibits/ Trade Fairs
- Plate/ Pipe Fitters Course
- Welding Steel Fabrication
- Welding Safety Seminar
- Technical Bulletins
- Welding Library

MEMBER OF:



ASIAN WELDING FEDERATION





FIERCE.

FEARLESS.

FUTURE-READY.

FILIPINO.



Working together with the DOST-MIRDC for the C.O.B.R.A. Remote-Controlled Weapon Station (RCWS) project in support of the Self-Reliant Defense Posture Program (SRDP).



Game-changing innovations for winning battles and saving lives

www.battlelab.ph

EXPLOITING SCIENCE, TECHNOLOGY, AND INNOVATION FOR MILITARY APPLICATIONS.



BUHAWI

(JOINT PROJECT WITH THE PH NAVY)

an automated gun mount developed to increase the PN's firepower capability and ensure the operator's safety

RECOIL COMPENSATOR FOR BUHAWI 0.50 CALIBER MACHINE GUN



REMOTE CONTROL WEAPONS SYSTEM

improves the BUHAWI's firing and charging mechanisms



ENGAGING IN RESEARCH AND DEVELOPMENT;
UTILIZING CONVENTIONAL METALWORKING AND STATE-
OF-THE-ART TECHNOLOGIES TO CONTRIBUTE TO THE
ACHIEVEMENT OF A SELF-RELIANT DEFENSE POSTURE.

METALS INDUSTRY RESEARCH and DEVELOPMENT CENTER
Tel. No.: (02) 8837-0431 to 38
Email: mirdc@mirdc.dost.gov.ph
Website: www.mirdc.dost.gov.ph



Design of Plastic Bottle Shredder Machine with Monetary Reward System

Reherson D.V. Bugarin*¹, John Benedick D. Calising*², Irish Jem B. Dioso*³, Nolito Dominic M. Guanzon*⁴, Glorie P. Masagca*⁵, Ron Eric B. Legaspi*⁶, Mark Joseph B. Enojas*⁷, Jane E. Morgado*⁸, Hohn Lois C. Bongao*⁹, John Bryan S. Odiña*¹⁰, Jefferson C. Rufo*¹¹, Ruem G. Arribas*¹², Constancio Andong Jr.*¹³

Abstract

Polyethylene Terephthalate (PET) is a widely used form of plastic to make bottles for mineral water, soft drink, ketchup, pickle, etc. The global production of PET is expected to increase from 42 million tonnes (2014) to 72 million tonnes by 2020. The waste generated by PET packaging creates not only environmental issues but also disposal problems. Also, PET waste blocks drain leading to overflowing drains and sometimes flooding. There is no proper system of plastic waste collection and many people from the community are not into segregating plastic waste, especially PET bottles. The collection procedure in most developing countries presently is done manually by drop-off centers and buy-back centers but the mechanization of the other stages of the recycling process had received considerable research efforts in the past years. This paper presents the design of a plastic shredding machine that allow the user to receive monetary award. This is to engage the community in recycling waste especially in the PET bottles. The machine will have a display monitor that will prompt the user if the machine is in operation. The user will insert the PET bottle in the hopper, and it will direct it to the shredding blades. The machine will weigh the shredded PET bottle and compute how much is the equivalent amount, then the machine will dispense the said amount. The machine has a minimum of 1.37% weight discrepancy and a maximum of 1.56%. The machine makes a disbursement of 100% accuracy in 100 pieces of assorted 250ml bottles. The machine performance shows significant result with the weighing and dispensing of monetary amount expected.

Keywords: plastic bottle, shredding machine, monetary reward system

I. Introduction

PLASTICS have been one of man's means of bearing items or contents, widely used by the majority of the world. This material is readily used with ease because of its characteristics which include resilience, lightness, resistance to corrosion, and ease of processing [1]. In a developing country such as the Philippines, the demand for plastic usage is increasing in different applications in industry, household products, packaging, etc. In the Philippines, where budget and product availability are also considered in designing containers, plastic is used to store small quantities of goods and merchandise to increase the sale and profit of companies.

PET is one of the most commonly used plastics in both local and industrial thus contributing largely to the solid waste body [2]. This waste causes flooding and contamination of sewage system by blocking the flow. The collection procedure is done manually by drop-off centers and buy-back centers but the mechanization of the other stages of the recycling process had received considerable research efforts in the past years [3].

To solve this problem the proponents have decided to design a plastic bottle shredding machine with a

monetary reward system for community engagement in recycling. To identify the parameters needed for the design of a plastic bottle shredding machine. To fabricate and develop a program for the plastic bottle shredding machine. To assess shredder efficiency with the percent yield of the machine.

II. Methodology

A. Machine Design Components

The designs and systems applied to the machines were studied based on the existing and available designs based on the application and scale of shredding. The design and components shown in Figure 1 were carefully studied by the proponents which include the dimensions of the frame, the blades to be installed, motor performance, size of the output, and the load a community can provide on the target machine. The machine is tested according to its weighing scale accuracy, and reward system accuracy.

The machine combines hardware components like a power source, monitor, weighing scale, shredding device,

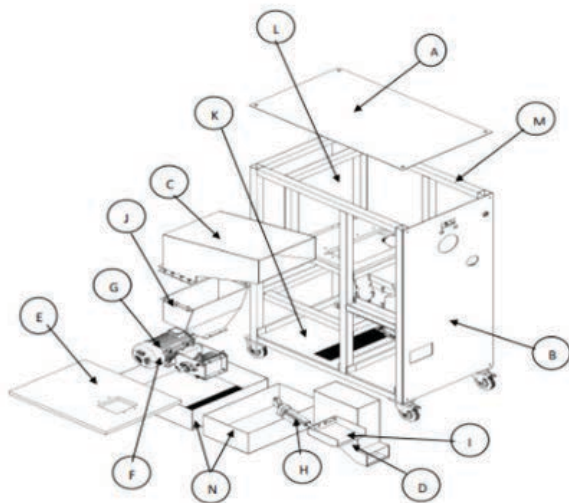
* Presented during the National Metals and Engineering Conference (NMEC), June 15, 2022.



*1, 2, 3, 4, 5,
Student
Batchelor of Engineering
Technological University of
the Philippines Taguig,
Taguig City, 1630, Philippines



*6
Professor
Batchelor of Engineering,
Technological University
of the Philippines Taguig



A	TOP COVER	H	LINEAR ACTUATOR
B	FRONT COVER	I	WEIGHING SCALE
C	BOTTLE HOPPER	J	FUNNEL
D	COIN HOPPER	K	BOTTOM PLATE
E	MIDDLE BASE PLATE	L	CONTROL PANEL
F	SHREDDER	M	FRAME
G	3 PHASE MOTOR	N	COLLECTOR BINS

Fig. 1. Machine Design Components

mesh screen, and moving platform with software that calculates rewards, prompts user inputs, and manages the recycling process. Users participate by depositing PET bottles into the machine, which then processes the bottles, rewards the user with monetary equivalent, and ensures that the recycling process is effective.

B. Machine Operation

1. Powering On: The machine is connected to a power source. Once it's turned on using the on/off button, it initializes its system and prepares for user interaction.
2. User Interface: The monitor displays easy-to-understand commands and options for users. The interface aims to guide users through the recycling process seamlessly.
3. PET Bottle Input: The user inserts PET bottles into the machine through a hole provided. These bottles are analyzed by a weighing scale incorporated into the system.
4. Weight Calculation and Reward Assignment: The machine's program calculates the weight of the deposited PET bottles using the weighing scale. Based on this weight, a predetermined algorithm assigns a value in peso as the monetary reward.
5. Reward Display: The machine's monitor could also display the calculated monetary reward amount to the user, ensuring transparency and providing immediate feedback on their recycling efforts.
6. Coin Catcher: The machine is equipped with a coin

catcher or a container where the calculated monetary reward, in physical coin or bill form, is placed. This can be a tray, a compartment, or another mechanism that securely holds the monetary reward until the user collects it.

7. Shredding Process: The PET bottles that are deposited are introduced into a shredding device. This device contains a set of blades and is configured to shred the bottles effectively based on the desired output.
8. Separation of Recycled Plastic and Foreign Material: The shredded plastic particles then move to a screen with a specified mesh size. This mesh screen is designed to separate the recycled plastic particles from any foreign materials, such as dirt and liquid.
9. Collection of Recycled Plastic: The recycled plastic particles, now separated from unwanted materials, are collected in a designated bin. This collection is facilitated by a moving platform that guides the plastic particles to the collection bin.

By combining both hardware and software components, this recycling machine streamlines the process of recycling PET bottles. It encourages participation by offering mobile load rewards, ensures the efficiency of the recycling process, and takes measures to separate the recycled plastic from unwanted foreign materials. The user-friendly interface and the incorporation of various components make the process smooth and accessible to users.

C. Testing and Evaluation

The testing and evaluation of the shredder involve the assessment of its performance and testing its efficiency in shredding PET bottles. The evaluation will determine if the output shredded PET bottles are weighed properly for the equivalent monetary reward to be met.

Figure 2 displays the shredded plastic particles with a diameter range of 4 to 8 mm, and it provides a comparison to the size of a one peso coin. Additionally, it is noted that the actual weight of the shredded plastic particles in the figure was 10.10g.

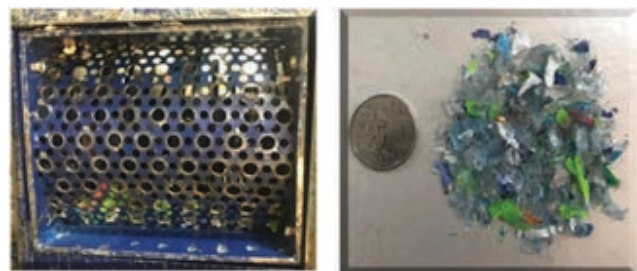


Fig. 2. Shredded output.



*7
Section Head
Mechatronics Technology,
Technological University of
the Philippines Taguig



*8, 9, 10
Professor
Electrical and
Allied Department,
Technological University
of the Philippines Taguig

III. Results and Discussion

A. Result of Weighing Scale Accuracy

The accuracy of a weighing scale can be affected by factors such as temperature, humidity, and vibrations. Ensure that the scale is used in a stable environment to minimize these influences. Precise measurements are crucial for the success of the recycling machine, as they directly affect the rewards given to users based on the weight of their PET bottles. Therefore, addressing and improving the scale's accuracy is essential for the overall functionality of the machine.

Table 1. Weighing Scale Accuracy Result

	Standard Weighing Test Piece	Theoretical Result	Actual Result	Variance	% Discrepancy
A	10-g	= 10g	9.85g	0.15g	1.5%
B	50-g	= 50g	49.22g	0.78g	1.56%
C	100-g	= 100g	98.63g	1.37g	1.37%

Table 1 indicates that the weighing scale's measurements are slightly lower than the theoretical weights for all test pieces. Additionally, the discrepancies seem to increase with larger weights. The % discrepancy values, ranging from 1.5% to 1.56%, suggest that the weighing scale is consistently underestimating the weights of the test pieces.

Table 2. Weighing Scale Accuracy Result

	Set of Bottles	Theoretical Reward Price	Actual Reward Price
A	40 Coke Mismo Bottles	P 5.20	P 5.00
B	100 Mismo Bottles (Assorted)	P 13.00	P 13.00
C	80 Mineral Bottles	P 7.60	P 8.00

Table 2 shows the actual reward price was accurately computed based on the output weight of shredded plastic. However, it is noted that the rewards were rounded off to the nearest peso, depending on the actual weight.

IV. Conclusion

The results of the weighing scale accuracy testing indicate an average discrepancy of about 1.47% across the three trials. This suggests that while the weighing scale was generally accurate, there was a small deviation between the actual weights and the measurements taken by the scale. The reward system's actual results demonstrated

accurate computation based on the output weight of shredded plastic. However, the rewards were rounded off to the nearest peso based on the actual weight. This rounding approach was likely chosen for simplicity and user-friendliness. The recycling machine's purpose and potential impact on the community are highlighted. The machine is expected to be especially beneficial for communities facing challenges such as improper waste segregation and financial limitations. By offering coin rewards for PET Plastic Bottles, the machine provides an incentive for individuals to participate in recycling efforts. The conclusion notes that the system is designed to provide coin rewards to users based on the type of PET Plastic Bottles they insert, and the quantity inserted per kilogram. This coin-based reward system aims to motivate users to recycle and contribute to environmental sustainability. Overall, the recycling machine is described as a potential solution that can address both environmental concerns (through recycling) and community needs (through financial support). It is positioned as a valuable resource for communities that lack proper waste management infrastructure and financial resources.

V. Acknowledgment

The authors of this study extend their gratitude to those who provided valuable insights, enabling the realization of this research. They also wish to acknowledge the Technological University of the Philippines Taguig Research and Extensions Services for their support in facilitating the presentation and publication of this research.

References

- [1] T. A. Olukunle, "Design Consideration of a Plastic Shredder in Recycling Processes," *Int. Sch. Sci. Res. Innov.*, vol. 10, no. 11, pp. 1824–1827, 2016.
- [2] A. David and J. . Oluwayomi, "Design and construction of a plastic shredding machine for recycling and management of plastic waste," *J. Multidiscip. Eng. Sci. Technol.*, vol. 9, no. 5, pp. 1379–1385, 2018.
- [3] S. Balasubramanian, S. D. Deshpande, and I. R. Bothe, "Design, development and performance evaluation of CIAE-millet mill," *AMA, Agric. Mech. Asia, Africa Lat. Am.*, vol. 51, no. 1, pp. 42–48, 2020.
- [4] A. Waleola Ayo, O. Olukunle, and D. Adelabu, "Development of a Waste Plastic Shredding Machine," *Int. J. Waste Resour.*, vol. 07, no. 02, pp. 2–5, 2017, DOI: 10.4172/2252-5211.1000281. [7] M. Muthukumaran, M. P. Murasoli, m. P. Selvam, s. S. Kumar, and C. Praveen, "Design and Fabrication of Plastic Waste Shredder Machine," *Int. J. Res. Dev. Technol.*, vol. 7, no. 4, pp. 210–214, 2017.



*11, 12, 13
Professor
Mechanical and Allied Department,
Technological University of the
Philippines Taguig

**COMPLEX FORMS NEED
STRAIGHTFORWARD SOLUTIONS:
VOLLMER - YOUR FULL-LINE SUPPLIER**



CHC 840
Sharpening machine
for circular saw blades



VGrind 3605
Grinding machine
for rotary tools

Whoever wants to shape the future will need forward-looking tools - and intelligent solutions for their production, processing and maintenance. VOLLMER supports you: with innovative sharpening and eroding machines to suit virtually every requirement. With economical automation options and strong services. For the highest possible flexibility, efficiency and quality of results.

The future takes shape: with precision from VOLLMER.

www.vollmer-group.com

Viability of Ammonia-pH-Temperature Model in Quantifying Ammonia Levels in Commercial Recirculating Aquaculture Systems (RAS)

Oscar Sheen M. Villaverde II^{*1}, Nicole Ann Portia U. De Luna^{*2}, Franz Joseph D. Libao^{*3}, Glen D. Espena^{*4}, Von Jansen G. Comedia^{*5}, Manuel O. Luna Jr.^{*6}, Ana Marie C. Atienza^{*7}

Abstract

Recirculating aquaculture systems (RAS) are seen as one of the solutions to fulfilling the demand for products in the aquaculture industry of the Philippines. These systems offer high stocking densities of fish in areas not meeting traditional aquaculture prerequisites, such as having a body of water to grow fish in. However, RAS requires close monitoring of parameters such as unionized ammonia, which requires expensive sensors that prevent potential users from adapting to RAS. A relatively cheaper ammonium sensor, and a model relating pH, temperature (K), and ammonia (mg/L) levels developed by [1] can be used as a proposed alternative. Samples from different aquaculture sites were analyzed on-site, with the results used to calculate the empirical value of ammonia-nitrogen (mg/L) to validate the model. 500 mL of each sample is then sent to a certified laboratory to measure the experimental ammonia-nitrogen levels. The empirical and experimental values are then compared using a Wilcoxon signed rank test. With $\alpha = 0.05$, the test revealed that $W_{stat} = 10$ is greater than $W_{crit} = 0$, concluding that ammonium sensors cannot replace ammonia sensors in RAS applications based on the result and methodology. The resolution of the test methods used is seen as a major factor in the results.

Keywords: ammonia, ammonium, recirculating aquaculture system, pH, temperature, Wilcoxon Signed Rank Test

I. Introduction

Aquaculture is one of Philippines' biggest industries in the food sector due to its archipelagic geography. However, the industry is lagging on the technology to keep up with the demand for fish, seafood, and other aquatic products. One of the solutions to keep up with the demand is high density fish farming using recirculating aquaculture systems (RAS). RAS is a closed-loop or semi-closed loop water treatment method that removes and captures wastes and enables water reuse. A key to successful water recirculation is maintaining the stability of critical parameters, such as temperature, pH, and ammonia [2]. This method, however, requires constant monitoring of critical parameters, especially ammonia. Ammonia, or unionized ammonia (NH₃), in elevated levels pose a threat to fish [3] [4]. This parameter represents the unionized ammonia present in fish excrement and uneaten fish feed [3]. Another parameter of interest is ammonium, or ionized form of ammonia (NH₄⁺). Ammonium is produced by the following equilibrium equation:

$$HV = 1854.4 \frac{L}{d^2} \quad (2)$$

The amounts of ammonia and ammonium combined is represented by a parameter called the total ammonia nitrogen (TAN) [3]. These parameters can be measured by different procedures available such as the phenate

method, salicylate, Nessler, and ion-selective electrode (ISE). The ISE method is the only method that can read real-time ammonia levels [5]. As such, this is the only method applicable in an automated RAS monitoring system. However, ISEs are relatively expensive as compared to the other alternatives. This makes it harder for micro, small, and medium enterprises (MSMEs) in the Philippines to adopt the technology. To address this problem, different attempts were made to model an automated RAS without ammonia sensors. [6] used the relationship of ammonia, pH, and temperature in their automated RAS. This relationship was derived from a study in 1975 by [1] which correlated temperature (K), pH, and ammonia (mg/L) in two equations, (2) and (3). Equation (4) was derived from the definition of f, where f is the ammonia fraction of TAN.

$$pK_a = 0.09018 + 2729.92/T \quad (2)$$

$$f = 1/(10^{pK_a - pH} + 1) \quad (3)$$

$$f = \text{ammonia (mg/L)} / \text{TAN (mg/L)} \quad (4)$$

Equations (2) and (3), cited by other literatures modeling RAS ponds [7], will now be investigated for its viability in a specific use-case scenario of an automated RAS pond in Roxas, Oriental Mindoro. Together with an ammonium sensor, these equations can be used to monitor real-time



^{*1} Science Research Specialist II
Metals Industry Research and
Development Center
Bicutan, Taguig City
Philippines



^{*2} Science Research Specialist II
Metals Industry Research and
Development Center
Bicutan, Taguig City
Philippines



^{*3} Sr. Science Research Specialist
Metals Industry Research and
Development Center
Bicutan, Taguig City
Philippines

ammonia levels in place of a more expensive ammonia sensor. In order to test the viability of this configuration in the specific use-case scenario, several aquaculture systems must be analyzed. These tests will support the idea whether the configuration of the equations and ammonium sensor will work on the said use-case scenario.

II. Methodology

To emulate the automated RAS pond, six major southern Luzon freshwater lakes with thriving aquaculture systems were sampled. The lakes are as follows: Taal Lake, Laguna de Bay, Sampaloc Lake, Tikub Lake, Caliraya Lake, and Lumot Lake. pH, temperature, and ammonia were measured on-site using Thermo™ TA-288 digital thermometer, Atlas Scientific™ pH lab grade sensor, and API™ Ammonia Test Kit, respectively. Three trials were made during the measurement of parameters per lake. The measurements were used as input to (2), (3), and (4) to calculate the empirical values for TAN. A portion of each sample was chilled and sent to a certified laboratory to measure the amount of TAN. The results from the laboratory testing were used as the experimental values for the same parameter. Due to the small sample size of $n = 6$, a non-parametric Wilcoxon Signed Rank Test was used to determine the statistical significance of the (1) and (2). A value of $\alpha = 0.05$ was used in the test.

III. Results and Discussion

Table 1 shows the measurements obtained on-site. The average of the three trials per lake was used on equations (2), (3), and (4). Temperature was measured in °C and ammonia in mg/L. After proper unit conversions were made, the amount of TAN in mg/L was calculated and was used as the empirical values for TAN.

Based on the data in Table 1, Sampaloc lake has the highest level of ammonia and pH measured while Tikub lake has the highest temperature recorded. It can be observed that the high levels of ammonia in Sampaloc lake can be attributed to the high levels of pH. This is validated by (2) and (3) which relates the increase of ammonia to the increase of pH and temperature. The temperature, although measured in different times, when converted in K are relatively close to each other and can be assumed constant across all lakes. Thus, pH accounts for the major fluctuations of ammonia levels.

The results of the laboratory tests done by the Department of Science and Technology - CALABARZON are shown on Table 2. The laboratory used a colorimetric method in measuring the TAN levels. However, the certified result indicated a range, instead of a specific

Table 1. Lake data

Lake	Trial	Parameters		
		pH	Temp.	Ammonia
Taal	1	7.733	26	0.25
	2	7.766	25.9	0.25
	3	7.778	26.3	0.25
	Average	7.759	26.06667	0.25
Laguna de Bay	1	7.299	27.5	0.125
	2	7.299	27.1	0.125
	3	7.303	27.4	0.25
	Average	7.300333	27.33333	0.166667
Sampaloc	1	8.288	26.5	1
	2	8.348	26.6	1
	3	8.35	26.7	1
	Average	8.328667	26.6	1
Tikub	1	7.204	27.8	0.5
	2	7.253	27.8	0.5
	3	7.259	27.7	0.5
	Average	7.238667	27.76667	0.5
Lumot	1	6.666	25.6	0
	2	6.676	25.5	0
	3	6.695	25.2	0
	Average	6.679	25.43333	0
Caliraya	1	6.902	25.1	0
	2	6.964	24.9	0
	3	7.037	24.8	0
	Average	6.967667	24.93333	0

Table 2. Laboratory TAN measurements

Lake	TAN Levels (mg/L)
Taal	less than 0.40
Laguna de Bay	less than 0.40
Sampaloc	less than 0.40
Tikub	less than 0.40
Lumot	less than 0.40
Caliraya	less than 0.40



*4 S&T Fellow II
Metals Industry Research and
Development Center
Bicutan, Taguig City
Philippines



*5 Science Research Specialist II
Metals Industry Research and
Development Center
Bicutan, Taguig City
Philippines



*6 Project Technical Specialist I
Metals Industry Research and
Development Center
Bicutan, Taguig City
Philippines

Table 3. Wilcoxon signed rank test values

Lake	Empirical	Experimental
Taal	7.37	0.4
Laguna de Bay	12.66	0.4
Sampaloc	8.39	0.4
Tikub	42.43	0.4
Lumot	0	0.4
Caliraya	0	0.4

value due to the limitation of the measuring method. The result showed that all lakes have a TAN level of less than 0.40 mg/L. It was assumed, for a conservative estimate, that 0.40 mg/L is the experimental level for TAN.

Table 3 shows the values used in the Wilcoxon Signed Rank Test calculations. Using $\alpha = 0.05$, the test resulted with $W_{stat} = 10$, greater than $W_{crit} = 0$. Implying that in this particular test, the empirical and experimental values are statistically insignificant.

IV. Conclusion and Recommendations

The study showed that the ammonium sensor, with (2) and (3), was not a suitable replacement in detecting ammonia levels of the automated RAS pond. The Wilcoxon Signed Rank Test showed that the empirical and experimental levels of TAN were not statistically significant. The two values were deemed too far apart to be considered as interchangeable methods of measuring TAN, and in turn, ammonia.

It is recommended to use a larger sample size to cater a parametric test. Moreover, it is also recommended to use a TAN measurement process that has a finer resolution that can detect trace amounts of TAN.

V. Acknowledgment

This project is funded by the Department of Science and Technology (DOST) through the Science for Change Program (S4CP) – Collaborative Research and Development to Leverage the Philippine Economy (CRADLE) and monitored by DOST – Philippine Council for Agriculture, Aquatic and Natural Resources Research and Development (PCAARRD) with Project No. 8816.

The authors would also like to acknowledge the DOST – Metals Industry Research and Development Center (MIRDC) as the research and development institute where the research was conducted.

References

- [1] K. Emerson, R. C. Russo, R. E. Lund and R. V. Thurston, "Aqueous Ammonia Equilibrium Calculations: Effect of pH and Temperature," *Journal of the Fisheries Research Board of Canada*, vol. 32, no. 12, pp. 2379-2383, 1975.
- [2] D. B. Almeida, C. Magalhães, Z. Sousa, M. T. Borges, E. Silva, I. Blanquet and A. P. Mucha, "Microbial community dynamics in a hatchery recirculating aquaculture system (RAS) of sole (*Solea senegalensis*)," *Aquaculture*, vol. 539, p. 736592, June 2021.
- [3] Y. K. Ip, S. F. Chew and D. J. Randall, *Ammonia toxicity, tolerance, and excretion*, vol. 20, Academic Press, 2001, pp. 109-148.
- [4] G. E. Elshopakey, H. H. Mahboub, N. I. Sheraiba, M. H. Abduljabbar, Y. K. Mahmoud, M. M. Abomughaid and A. K. Ismail, "Ammonia toxicity in Nile tilapia: Potential role of dietary baicalin on biochemical profile, antioxidant status and inflammatory gene expression," *Aquaculture Reports*, vol. 28, February 2023.
- [5] L. Zhou and C. E. Boyd, "Comparison of Nessler, phenate, salicylate and ion selective electrode procedures for determination of total ammonia nitrogen in aquaculture," *Aquaculture*, vol. 450, pp. 187-193, January 2016.
- [6] A. D. M. Africa, J. C. C. A. Aguilar, C. M. J. S. Lim, P. A. A. Pacheco and S. E. C. Rodrin, "Automated Aquaculture System that Regulates pH, Temperature and Ammonia," *IEEE*, 2017.
- [7] C. Wang, Z. X. Yuan, Y. Y. Liu, Q. Y. Wu and Y. X. Sun, "Relative developmental toxicities of reclaimed water to zebrafish embryos and the relationship with relevant water quality parameters," *Water Cycle*, vol. 2, pp. 85-90, January 2021.



*7 Project Technical Assistant I
Metals Industry Research and
Development Center
Bicutan, Taguig City
Philippines



COMPUTRENDS
Systems Technology, Inc.

AUTHORIZED
Reseller

 SOLIDWORKS

2D AND 3D

PRODUCT DEVELOPMENT SOLUTIONS

SOLIDWORKS —

SOLIDWORKS® solutions are trusted by leading engineers and designers to create, collaborate, and deliver innovative product experiences. It has the most efficient and powerful CAD design collection available for product and part assembly designers.

3DEXPERIENCE WORKS —

3DEXPERIENCE Works® is a business and innovation platform that connects people, ideas, data and solutions in a single collaborative cloud environment, empowering businesses - from startups to large enterprises, to innovate, produce and trade in entirely new ways.

Why should you connect SOLIDWORKS to 3DEXPERIENCE Works?

- ✓ Shorter Time to Market
- ✓ More Holistic Collaboration
- ✓ Faster Experimentation
- ✓ Greater Visibility into Projects and Processes
- ✓ Earlier Identification of Issues and Risk Mitigation

Other Solutions



SCAN THIS TO
CONNECT WITH US



Solar Powered Bio-Waste Recycler to Produce Fertilizer from Leftover Foods

Meyeth Jackeylhiz A. Titong^{*1}, Marc Moses R. Calamaya^{*2}, John Phillip E. Figares^{*3}, Agnes M. Idio^{*4}

Abstract

One of the major problems facing humanity today is the volume of municipal waste produced. This problem concerns the environment because of the many consequences it creates. With this, the Solar Powered Bio-Waste Recycler is an eco-friendly machine that households and municipalities can use to minimize food waste. The machine has three processes namely; heating, mixing, and odorizing that produce fertilizer from 1kg of leftover foods to 100g within three hours of operation. The machine will only consider leftover foods excluding bones and seeds. The aim of this study is to introduce a new product convenient for households and communities to solve problems of waste production, particularly in the Municipalities of Bacoor, Imus, and Dasmarinas Cavite, areas with an average of 350tons/day of waste produced. The machine was created through cutting, soldering, and assembling of materials. The machine has a size of 14.75inch x 12.25inch x 12.5inch with a detachable 100W solar panel. The development of this study provided our group with a greater interest in environmental solving and information for future researchers for further research.

Keywords: bio-waste, food recycler, fertilizer

I. Introduction

The amount of leftover food that is considered food waste in the Philippines is about 1.3 billion metric tons of food are wasted every year. Municipal Solid Waste (MSW) primary data in the Philippines, 2008-2013, Typical bio-waste consists of kitchen or food waste and yard or garden waste. From the available information, it could be estimated that 86.2% of compostable waste comes from food scraps. A projected waste generation 2008-2020, amount of waste in the country is expected to increase from 13.48 million tons in 2010 to 16.63 million tons in 2020.

Specifically, the city of Bacoor, Dasmariñas, Imus, Cavite, has a solid waste bulk density of 353kg/m³ consisting of fruits and vegetables with 56% according to Waste Amount and Composition Surveys (WACS)..

With these data, the proponents come to the idea of reducing the volume of food waste in the city of Bacoor, Dasmariñas, Imus, Cavite by the use of Solar Powered Bio-Waste Recycler to Produce Fertilizer.

II. Scope and Limitations

This study of Using Solar Powered Bio-Waste Recycler to Produce Fertilizer from Leftover Foods is restricted to the city of Bacoor, Imus, and Dasmariñas, located in the province of Cavite.

The study will only cover the device, its materials that will be used, the procedure for assembling, five (5) kg;

the possible amount of materials that is enough within the container, it should be dry, particularly meat, fish, shellfish, and poultry scraps, most fruit and vegetable scraps, cereals and grains, cheese, beans, seeds, and legume. Materials that can't the food recycler process are hard bones such as beef bones and pig bones, candy or gum, cooking oils or greases, hard pits (peaches, apricots), nuts, and other hard shells.

Application of solar panels within the device that is compatible by its voltage and how the output is produced particularly an organic fertilizer. The focus of this project is to design an easy production of organic fertilizer in just a short period of time.

III. Statement of the Problem

The Municipalities of Bacoor, Imus, and Dasmarinas Cavite have an average of 350tons/day of waste produced. The estimated average amount of garbage produced by the three municipalities are the following: Imus (85%), Dasmarinas (90%), and Bacoor (91%). Most of the food wastes are not being recycled and ends up in garbage areas and landfills.



^{*1, 2, 3}
Student
BS Industrial Engineering
University of Perpetual Help
Molino Campus, Cavite



^{*4}
Professor
College of Engineering
University of Perpetual Help
Molino Campus, Cavite

A. Objective

The primary source of food waste is the target participant, which includes households, restaurants/fastfood establishments, and barangays. With the help of the Business Permit and Licensing Office in the City of Bacoor, Imus, and Dasmariñas, Cavite, the researchers were able to determine the target market population and the possible number of samples/respondents.

IV. Conceptual Framework

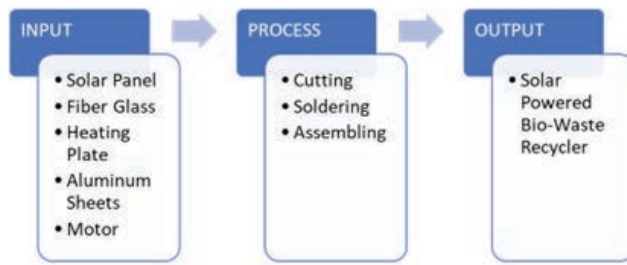


Fig. 1. Conceptual framework of the solar bio-waste recycler

V. Marketing Aspect

A. Marketing Objectives

Generally, the study aims to determine the marketability of the Solar Powered Bio-Waste Recycler to Produce Fertilizer from Leftover Foods through identifying potential demand. Specifically, the study aims to achieve the following: [1] To determine the target market of the business through market segmentation [2] To determine the best feasible market shares within the target market for the company's product. [3] To develop strategic marketing plans to promote the product.

B. Target Market

Household - Household is one of the main contributors of food waste in the Philippines, Solar Powered Bio-Waste Recycler's target market, particularly in the city vicinity of Bacoor, Imus, and Dasmariñas Cavite. Based on the data on the volume of residential wastes province of Cavite as of December 2015, the highest city is Bacoor with 284 tons per day, next is Dasmariñas with 252 tons per day and lastly is Imus with 133 tons per day. Not every household practices waste segregation as they usually place all types of waste in one bag and then let the municipal garbage disposal collect them.

Food Chain/Restaurant - Food chains and restaurant is also one of the main contributors to food waste as they have daily leftovers. The target locality has a high count of food chains/restaurants thus there can be a high probability of marketability in this type of market.

Local Government - local government has its different projects on how to lessen waste in their area. They had been trying different methods how to lessen and segregate waste. It had been identified as a target market due to the current projects of the target locality with regard to waste management.

C. Market Location

The next process is to find an ideal target location after knowing and identifying the target market of the Solar Powered Bio-Waste Recycler. Based on the data of the Provincial Government Environment and Natural Resources Office as of December 2015, the top three cities/municipalities of Cavite with the highest volume of waste per day in terms of tons are. Most of the wastes that were collected are biodegradable wastes comprising about half (52.31%) primarily consisting of kitchen or food waste.

D. Market Survey

A market survey is an important part of market research to define the market parameters of a business. With the help of the Business Permit and Licensing Office in the City of Bacoor, Imus, and Dasmariñas, Cavite we can now determine the target market population and the possible number of sample/respondents. The use of Slovin's Formula is a tool by us proponents to get the sample size with a 0.05% error tolerance.

Table 1. Numbers of samples per city

List of City	No. of samples
Imus City	399
City of Dasmariñas	400
Bacoor City	400

VI. Demand

The proponents went to the three city's municipalities particularly in Business Permits and Licensing Office (BPLO) to determine the demand.

Table 2. Number of demand from the target in Imus City

	Imus City		
	Barangay	Restaurant/FastFood	Household
2013	97	109	86,141
2014	97	119	97,466
2015	97	133	108,791
2016	97	147	120,116
2017	97	163	131,441

Table 3. Number of Demand From The Target In Dasmariñas City

Dasmariñas City			
	Barangay	Restaurant/FastFood	Household
2013	75	152	148,933
2014	75	176	154,547
2015	75	192	160,161
2016	75	249	165,775
2017	75	289	171,389

Table 4. Number of Demand From The Target In Bacoor City

Bacoor City			
Year	Barangay	Restaurant/FastFood	Household
2013	91	62	144,661
2014	91	73	152,768
2015	91	85	160,875
2016	91	98	168,982
2017	91	116	177,089

The BPLO of the cities of Imus, Bacoor, and Dasmariñas provides data on a number of barangays and restaurants while the household is through the Socio-Economic Sector of the official website of Cavite’s capital. The proponents can now compute the annual increase or decrease of the target market for the demand. It is simply the percentage growth divided by the number of years to get the annual percentage growth rate.

A. Projected Demand

Table 5. Projected demand of target market in Bacoor City (2018-2022)

BACCOOR			
Year	Barangay	Restaurant	Household
2018	91	132	186,279
2019	91	154	195,946
2020	91	180	206,115
2021	91	210	216,812
2022	91	235	228,064
Avg. rate of increase		16.96%	5.9%

Table 6. Projected demand of target market in Imus City (2018-2022)

IMUS			
Year	Barangay	Restaurant	Household
2018	97	180	146,096
2019	97	199	162,385
2020	97	220	180,490
2021	97	243	200,614
2022	97	268	222,982
Avg. rate of increase		10.59%	11.15%

Table 7. Projected demand of target market in in Dasmariñas (2018-2022)

DASMARINAS			
Year	Barangay	Restaurant	Household
2018	75	340	176,170
2019	75	400	181,085
2020	75	470	186,137
2021	75	552	191,330
2022	75	649	196,668
Avg. rate of increase		17.65	2.79%

VII. Supply

Currently, there are only 2 fertilizer machines in the target locality which are found at the city hall of Imus and Dasmariñas. There are no other fertilizer machines located or used individually in the target markets. From this, the current supply is only 2 units for the whole target market. For the past 5 years, these were the only fertilizer machines.

Based on the interview conducted, it had been determined by the researchers that there were 5 barangays planning to request/buy their own fertilizer machine by next year. Using this data, the researchers projected that there shall be an increase of 5 fertilizer machines yearly.

For the household and restaurants, there had been none who had planned to buy the currently available fertilizer machine as it is too big for their use.

Table 8. Projected demand of target market in Bacoor City (2018-2022)

Year	Projected Supply
2017	2
2018	7
2019	12
2020	17
2021	22
2022	27

A. Demand Supply Analysis

From the projected demand and supply, it can be determined if there had been demand left unfilled in the market.

Table 9. Unfilled demand for the fertilizer machine (2018-2022)

Year	Projected Demand	Projected Supply	Unfilled Demand
2018	509,457	2	509,457
2019	540,420	7	540,420
2020	573,852	12	573,852
2021	609,987	17	609,987
2022	649,085	22	649,085

From the data presented above, it can be seen that there is a large gap in the demand and supply of fertilizer machines as the current fertilizer machine is usually for commercial or mass production use and not for personal use. The high demand is coming from the household market.

The researchers decided to initially target 2% of the unfilled demand and increase it by another 2% yearly. The yearly projection of the target market share is presented in Table 10.

Table 10. Projected market share

Year	Unfilled Demand	Projected Market Share	Projected Unit
2018	509,455	2%	10,189
2019	540,413	4%	21,617
2020	573,840	6%	34,430
2021	609,970	8%	48,798
2022	649,063	10%	64,906

B. Current Marketing Condition/Practices

The target market such as the City of Imus, Bacoor, and Dasmariñas, Cavite is annually increasing its population, and this increase means increases in food waste produced. The bio-waste recycler is a newly invented machine introduced here in the Philippines where in consumers will be curious, about its design and function. The proponents find it as an opportunity to introduce the product and have an increase in demand.

VIII. Proposed Marketing Programs

A. Product Description

Terravon Manufacturing Corporation will introduce an innovative machine here in the Philippines, particularly in the Cities of Bacoor, Imus, and Dasmariñas, Cavite. This machine's function is to convert food waste into fertilizer, where the process of decomposing is only 24 hours with a process of heating and grinding.

The product will be pushed and advertised by the company as a bio-waste recycler where in it is a convenient machine for its size and it can be powered up by solar energy from the sun.

B. Place

This is where the location of the company will be placed. Most of the industry is nearly within the suppliers to be able to lessen the cost of transportation. The proponents decided to choose Noveleta, Cavite since the manufacturing is near the suppliers and also with the distributor.

C. Price

The product will sell at an affordable price to attract the target customer's attention. The price will be based on the cost of materials, processes of products, and expenses of the company for its continuous operation.

D. Promotion

The promotion of the product is through printed brochures, posters, and advertisements will be used is thru social media such as Facebook, Twitter, and Instagram to lessen the expenses in advertising. The company will also

create its own website where all the information about the company and products available is posted.

IX. Sales Projection

Considering that the company shall be able to meet the target market share, below is the projection of sales of the machine based on the projected unit price of Php. 10,526 per machine unit.

Table 11. Projected sales (2018-2022)

Year	Annual Supply in Pcs.	Projected Unit Price	Annual sales in Php.
2018	10,189	Php. 10,526	Php. 107,249,414
2019	21,617	Php. 10,526	Php. 227,540,542
2020	34,430	Php. 10,526	Php. 362,410,180
2021	48,798	Php. 10,526	Php. 513,647,748
2022	64,906	Php. 10,526	Php. 683,200,556

X. Production Aspect

The process of production and activities of manufacturing is discussed in this chapter. Machine and equipment are stated here for the producing the product. Identifying the business operation, plant layout, size, and structure is presented.

A.Product Description

Bio-waste recycler is a type of machine that produces fertilizer from leftover foods within 3 hours. It has a size of 14.75 inch x 12.25 inch x 12.5 inch with a detachable 100W solar panel. The machine has three simple processes namely- grinding, heating, and filtering the odor. It can reduce food waste by up to 90%.

The grinding blades are made of metal and It operates at 10 rpm. The food waste is crushed and dried through a heating process that has a temperature of 300 degrees Fahrenheit. And lastly, odors will be eliminated by the carbon filter.

B.Product Prototype

The following are the description and specifications of the product. A comparison of the existing product and the proposed product is presented (Table 12).



Fig. 2. Prototype design



Fig. 3. Fertilizer produced by the bio-waste recycler

Table 12. Comparison of the proposed product and the existing product

Specification	Description		
	Solared Bio-Waste Recycler	Smart CARA	Zera Food Recycler
Power Source	Solar	Electricity	Electricity
Size	14.75 inch (L) x 12.25 (W) inch x 12.5 inch (H)	30cm(L) x 27cm(W) x 35cm(H)	27(L) x 55cm(W) x 85cm(H)
Process Time	3hrs	3hrs	24hrs
Deodorization	Activated Carbon	Activated Carbon	Activated Carbon
Avg. Power Consumption	1.2KW/1,200W	34KW/34,000W	-

C. Production Process

Upon receiving the raw materials, the responsibility of the QA department shall inspect each material. Materials such as electric coil which must be 1,200W/230V, motor 24W, solar panel 100W, inverter 2,000W, and battery 12V20Ah/20HR/240W will be tested using a multimeter tester to assess the voltages. Solar Materials such as inverters, batteries, and the panel will proceed to the inventory. Parts of the machine will go through the assembly process which will depend on what part of the machine. Assembly 1 (Base): assembling of the base of the machine and heating plate, Assembly 2 (Body): assembling of a toggle switch, fiberglass, carbon filter, and stainless barrel. Assembly 3 (Top), assembling of the top cover and mixing metal for the mixing of food waste.

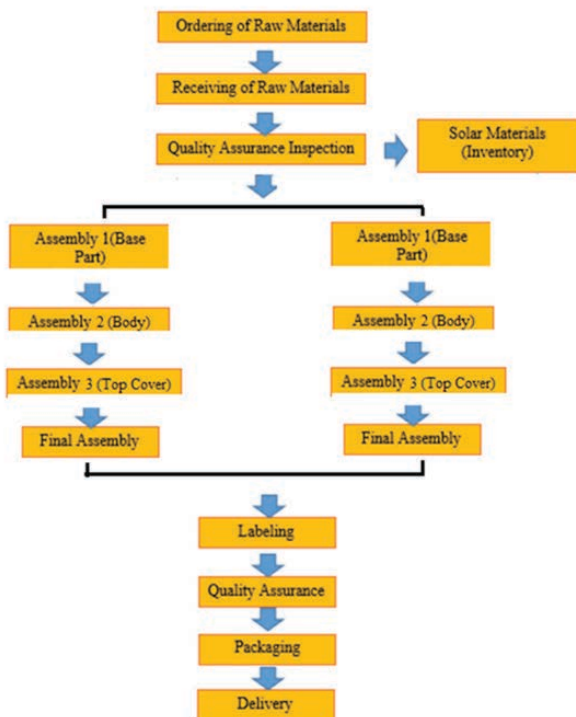


Fig. 4. Production process diagram

After the 3 processes, it will directly go to the final assembly for the assembling of assembled parts. The labeling process will label the product by indicating the manufacturing name. Then it will proceed to the final quality assurance inspection before the packaging of the product. Lastly, the product is ready, and it can be delivered. Our production has 2 production lines and each line produces 18 units with a cycle time of 27 mins. 13 sec.

D. Production Schedule

Production time will start at 8 am with 30 minutes of checking and calibrating of machines. The production of Bio-Waste recycler will be produced by batch.

Table 13. Production schedule

Daily (in pieces)	Weekly (in pieces)	Monthly (in pieces)	Annually (in pieces)
36	216	864	10,368

E. List of Materials

Below is the list of materials that are needed for the production.

Table 14. List of Raw materials with cost per unit

Materials	Qty	Cost
 Solar Panel with Inverter and Battery	1 unit	Php. 7,000.00
 48" x 24" Fiber Glass	1 unit	Php. 1,000.00
 Omega Wires #22	12 meters	Php. 180.00
 Heating Plate	1 unit	Php. 450.00
 Carbon Powder	1 unit	Php. 125.00
 DC Motor	1 unit	Php. 300.00
 Inner Cooking Pan	1 unit	Php. 300.00
 Angular Aluminum	1 meter	Php. 350.00
 3"x8" Tin Metal Sheets	1 unit	Php. 100.00
 Exhaust Fan	2 units	Php. 300.00
 Everbilt M6 1x25mm Screw	30	Php. 20.00

F. List of Suppliers

With the requirement needed for the specific materials, different suppliers from local and internationals are involved to able to make a high-quality Solar Powered Bio-Waste Food Recycler. Proper selection of suppliers is important to meet the standard requirement of each machine part.

Below is the list of possible suppliers of Solar Powered Bio-Waste Food Recycler based on the 2017 data provided by the www.cavite.gov.ph.

Table 15. Number of potential raw material suppliers in Cavite

	No. of Potential Suppliers	
	Hardwares	Battery Suppliers
District 1	14	-
District 2	19	-
Delgenta Solar	-	1
Natividad Ventures	-	1

XI. Financial Aspect

This chapter discusses the financial aspects needed to run the business. It contains the projected Income Statement, projected cash flow statement, and return on investment for the first five years of operations.

A. Projected Income Statement (5years)

TERRAVON MANUFACTURING COMPANY							
Income Statement							
January 2017- December 2022							
	Jan- Dec 2017	Jan- Dec 2018	Jan- Dec 2019	Jan- Dec 2020	Jan- Dec 2021	Jan- Dec 2022	Total
Sales	-	110,460,672.00	230,307,518.00	366,817,220.00	519,899,892.00	691,508,524.00	1,918,987,826.00
Less: Cost of Sales	-	102,429,667.00	226,027,822.45	359,289,001.00	510,000,000.00	679,000,000.00	1,876,746,490.45
Gross Profit	-	8,031,005.00	4,279,695.55	7,528,219.00	9,899,892.00	12,508,524.00	42,241,335.55
Gross Profit Rate	-	7%	2%	2%	2%	2%	2%
Less: Operating Expenses							
Gas and oil Expense		86,400.00	89,856.00	91,584.00	93,312.00	95,040.00	456,192.00
Repair and Maintenance		50,000.00	52,000.00	53,000.00	54,000.00	55,000.00	264,000.00
Taxes, Registration and Licenses		30,000.00	35,000.00	36,550.00	37,550.00	38,550.00	177,650.00
Insurance Expense		41,800.00	43,000.00	54,600.00	85,000.00	97,000.00	321,400.00
Miscellaneous Expense		158,000.00	158,000.00	158,000.00	158,000.00	158,000.00	790,000.00
Office Supplies Expense		114,340.00	118,913.60	121,200.40	123,487.20	125,774.00	603,715.20
Salaries Expense		2,611,700.00	2,611,700.00	2,611,700.00	2,611,700.00	2,611,700.00	13,058,500.00
Property Expense		1,650,000.00	1,650,000.00	1,650,000.00	1,650,000.00	1,650,000.00	8,250,000.00
Utilities Expense		150,000.00	156,000.00	159,000.00	162,000.00	165,000.00	792,000.00
Depreciation Expense		159,201.94	329,903.88	516,695.81	714,987.75	1,082,070.09	2,802,859.47
Net Operating profit (Loss)		2,979,563.06	(964,677.93)	2,075,888.79	4,203,855.05	6,430,389.91	15,253,018.88
Less: Provision to income taxes (30%)		-	(289,403.38)	622,766.64	1,261,156.51	1,923,116.97	3,523,636.75
Net Income after taxes		2,979,563.06	(675,274.55)	1,453,122.15	2,942,698.53	4,507,272.94	6,767,237.67
Net Profit Rate	0	3%	29%	40%	57%	65%	35%

B. Projected Cashflow

TERRAVON MANUFACTURING COMPANY							
Statement of Cash Flow							
January 2017- December 2022							
	Jan- Dec 2017	Jan- Dec 2018	Jan- Dec 2019	Jan- Dec 2020	Jan- Dec 2021	Jan- Dec 2022	Total
CASH FLOWS FROM OPERATING ACTIVITIES							
Net Income for the year	-	2,979,563.06	(675,274.55)	1,453,122.15	2,942,698.53	4,507,272.94	11,201,382.13
Adjustment for:							
Depreciation Expense		159,201.94	329,903.88	516,695.81	714,987.75	1,082,070.09	2,802,859.47
Operating income before working capital changes	-	3,138,765.00	(345,370.67)	1,969,817.96	3,657,686.29	5,589,343.03	14,004,241.60
Changes in operating assets and liabilities:							
Inventory		(102,429,667.00)	(123,598,155.45)	(133,261,178.55)	(150,710,999.00)	(90,000,000.00)	(600,000,000.00)
Prepaid Expenses		(145,000.00)	(68,083.00)	(231,833.00)	900,000.00	(400,000.00)	55,084.00
Accounts Payable		104,036,134.44	125,540,832.13	130,239,638.61	151,500,807.06	89,657,917.66	601,175,429.91
Var Payable		963,720.60	(450,157.13)	389,822.81	283,880.76	313,755.84	1,501,022.88
SSS, HDMF, PHIC Payable		262,338.00	-	-	-	-	262,338.00
Total Adjustments for non-cash income and expenses:	-	5,816,391.04	1,079,065.88	(893,732.16)	5,631,375.11	5,355,016.53	16,998,116.39
Net cash from operating activities	-	5,816,391.04	1,079,065.88	(893,732.16)	5,631,375.11	5,355,016.53	16,998,116.39
CASH FLOWS FROM INVESTING ACTIVITIES							
Delivery Equipment		(115,000.00)					(115,000.00)
Furniture and Fixtures		(60,146.00)					(60,146.00)
Machines & Equipment		(1,168,773.38)					(1,168,773.38)
Office Equipment		(248,100.00)					(248,100.00)
Net cash provided by (used in) investing activities	-	(1,592,019.38)	-	0	0	0	15,406,097.01
CASH FLOWS FROM FINANCING ACTIVITIES							
Opening Balance Equity	6,000,000.00	-	0	0	0	0	6,000,000.00
Terravon Capital	6,000,000.00	4,234,371.66					6,000,000.00
Net cash provided by (used in) financing activities	6,000,000.00	4,234,371.66					6,000,000.00
NET INCREASE (DECREASE) IN CASH	6,000,000.00	4,234,371.66	1,079,065.88	1,133,732.00	1,652,955.90	1,253,898.39	15,406,097.01
CASH AT BEGINNING OF YEAR	-	6,000,000.00	1,765,628.34	2,844,694.21	3,978,426.21	5,631,382.11	-
CASH AT END OF YEAR	6,000,000.00	1,765,628.34	2,844,694.21	3,978,426.21	5,631,382.11	6,885,280.50	15,406,097.01

Table 16. Cash flow schedule

PAYBACK PERIOD		
YEAR	CASH FLOW	CUMULATIVE CASH FLOW
0	(6,000,000)	(6,000,000)
1	1,765,628.34	(4234,371.66)
2	7,764,694.21	3,530,322.55
3	8,898,426.21	9,428,748.76
4	10,551,382	10,980,130.76
5	11,805,280.50	14,785,410.5

C. Return of Investment and Payback Period

Return of Investment (ROI) indicates how well the company is utilizing its equity. (inc.com). ROI can indicate good or poor management performances, capitalization, and the organization's approach to business. If the ROI per period is 10%-15% or higher, it means that the company is doing well in the business.

$$\text{Return of Investment} = \text{Income} / \text{Investment}$$

"Payback period is the length of time that it takes for the cumulative gains from an investment to equal the cumulative cost." (newleaf-llc.com). It is also considered that investments having shorter payback periods have a lower risk compared to long payback periods.

Where:

- A- The last period with a negative cumulative cash flow;
- B- The absolute value of cumulative cash flow at the end of period A.
- C- Total cash flow during the period after A.

XII. Conclusion and Recommendation

Solar Powered Bio-Waste Recycler to Produce Fertilizer from Leftover Foods target areas are the city of Bacoor, Imus, and Dasmariñas, specifically, Food-Chains/ Restaurants, Household particularly middle-class consumers, and local government. The maximum food waste that can be loaded into the product is five (5) kg; and it should be dry, particularly meat, fish, poultry scraps, fruit and vegetable scraps, cereals, and grains. Materials that cannot be in the food recycler process are hard bones such as beef bones and pig bones, candy or gum, cooking oils or greases, hard pits (peaches, apricots), nuts, and other hard shells. The maximum allotted time to create a fertilizer if the food waste is 2 kg-5 kg is 3 hours.

The proponents highly recommended the following: [1] Improving the design of the prototype, [2] Allowing to load hard waste such as hard bones.

References

- [1] Provincial Government of Cavite. (2014). Population and Population Growth Rate, Province of Cavite. Retrieved from http://cavite.gov.ph/home/wp-content/uploads/2017/06/9-SEPP2014_Chapter2_Human-Resource.pdf
- [2] Jimenea, A., Otera, A., & Napila, J. (n.d.). Comparative Study of Hinugasan ng Bigas, Manure and Compose as Soil Enhancer.
- [3] United States Environmental Protection Agency. (n.d.). Reducing Wasted Food At Home. Retrieved from <https://www.epa.gov/recycle/reducing-wasted-food-home>. Wikipedia. (n.d.). Leftovers. Retrieved from <https://en.wikipedia.org/wiki/Leftovers>.
- [4] Lee, N. (n.d.). Whirlpool's Zera Food Recycler turns food scraps into fertilizer. Weimar. (n.d.). Smart CARA. Retrieved from <http://www.weimariotech.com/web/cara.php?select=4>.
- [5] Lee, N. (n.d.). Whirlpool's Zera Food Recycler turns food scraps into fertilizer. Wikipedia. (n.d.). Organic Fertilizer. Retrieved from https://en.wikipedia.org/wiki/Organic_fertilizer. Wikipedia. (n.d.). Leftovers. Retrieved from <https://en.wikipedia.org/wiki/Leftovers>.
- [6] Lee, N. (n.d.). Whirlpool's Zera Food Recycler turns food scraps into fertilizer. Wikipedia. (n.d.). Organic Fertilizer. Retrieved from https://en.wikipedia.org/wiki/Organic_fertilizer. Wikipedia. (n.d.). Leftovers. Retrieved from <https://en.wikipedia.org/wiki/Leftovers>.
- [7] L. Freris and D. Infield, Renewable Energy in Power Systems (John Wiley & Sons Inc, Chichester, United Kingdom, 2008).

Exclusive Distributor:



PENTA TECHNOLOGY, INC.



CNC Machines
• Accuracy • Control
• Speed • Power
• Ecology

Easy to use, loaded with safety features



TAIKI[®]
Power Chuck & Soft Jaws

BARLOAD
Automatic Bar Feeder

Innovative Design
Humanified Control

Bar Feeder



HIWIN[®]
Motion Control and Systems Technology

Ball Screws



Linear Guideway



HAIMER
Passion for Precision



TAIYU

HI-CHIP Cutting Oil/ Coolant



SUGINO
CNC Drilling & Tapping Machine



FAGOR



Digital Readouts and
CNC Controllers

ZOLLER
expect great measures

Tool Presetter



“Quality of Production...Beyond Technology...Solutions is our Commitment”

22 El Rico Suites 1048 Metropolitan Avenue, Makati City 1205, Metro Manila
Tel. No.: (63-2)897-1287 • Fax: (63-2) 897-1313 • E-mail: pentech@info.com.ph

Development of an Innovative Arcade Game Operated with Polyethylene Terephthalate Bottle Shredder

Ymari John Florence N. Cometa*¹, Vicente P. Dela Cruz, III*², Ivone Tonie B. Ferrer*³, Sunshine T. Corpuz*⁴, Chris John Portos*⁵, Clark Ian A. Aclao*⁶, Veriann P. Alarde*⁷

Abstract

The rampant increase in plastic waste pollution has become an immeasurable problem in the present-day world. In the Philippines, several companies are high producers of plastics, specifically Polyethylene Terephthalate (PET) bottles, which cover almost 60% of waste products. To overcome the preceding problem, an arcade game with a shredder machine is designed and implemented in this article. The goal is to develop a functional machine that can encourage people to recycle plastic waste and help diminish the amount of PET waste with effective engagement through a fun and entertaining game. Two essential components, namely the arcade game and the shredder, are combined to create a machine that accepts PET bottles as a token to operate the Arcade Game. The shredder is capable of shredding 500 ml empty PET bottles into tiny pieces. The machine is equipped with components comprised of power transmission, 3D printed components, shredding system, and a frame for efficient utilization. The Arduino MEGA will control all of the machine's relevant procedures. In conclusion, this innovative approach can benefit communities by encouraging them to practice proper waste management and promoting recycling awareness. As a result, the machine has the capacity to shred a specific thickness and size of PET bottles. The functionality and shredding efficiency are the parameters used to evaluate the overall performance of the machine.

Keywords: PET, plastic shredding machine, arcade game

I. Introduction

In the present age, solid waste management is a crucial matter in various evolving communities due to the continuous expansion of waste annually. According to data from the World Bank, in the year 2020, the global solid waste production was estimated to reach a staggering 2.24 billion tons. This immense figure signifies a substantial ecological footprint, equating to approximately 0.79 kilograms of waste generated per person per day [2]. Also, according to the Environmental Management Bureau (EMB), from 2022 to 2025, the country's waste generation is projected to reach 92 million tons in total.

Plastic stands as both the most prevalent and harmful material in terms of environmental pollution. In fact, it has become so pervasive that the term "white pollution" has emerged to describe the widespread issue of plastic pollution [13]. Due to their slow degradation process and potential for toxic substance release, it is crucial to handle plastics in a specialized manner, as their disposal in landfills poses a significant risk of soil and groundwater contamination. With this project, it potentially exploits the opportunity for innovation in the design of the machine being studied. Representing the team, the goals of our team are primarily parallel with the project goals, which

are to devise a plastic bottle arcade game that shreds a certain type of plastic to manage waste into usable objects, to produce a safe and easy plastic shredder. In many areas of the country, local governments lack access to waste collection services and recycling facilities [15]. Collection of solid wastes is mostly being managed by the local government unit (LGU) [16]. The plastic market in the Philippines surpassed 1283.71 million US dollars in 2016. Furthermore, a projected compounded annual growth rate of 6.11% is forecasted for the period from 2018 to 2023 [14].

Plastic packaging constitutes approximately 48% of all packaging materials used (2017), and it is a significant contributor to the problem of marine litter and plastic pollution [17]. In regions where waste management systems are available, there are often inefficiencies in the stages of gathering, conveyance, handling, and elimination worsening the issue and further impacting wastewater and drainage systems. Consequently, this leads to the proliferation of marine litter and plastic pollution.

In low-income countries, it is common for over 90% of waste to be disposed of in unregulated dumps or burned



*1, 2, 3, 4
Student
BS in Mechanical Engineering,
Taguig City University

openly, which has negative health effects and leads to serious safety and environmental consequences. Effective waste management continues to be a major challenge for many developing countries and cities [21].

II. Project Development

The block diagram consisted of one major process, from inserting the PET bottles through the bottle depositor section, passing by the limit switch that will automatically trigger the motor for shredding system while also allowing the person to play the claw machine.

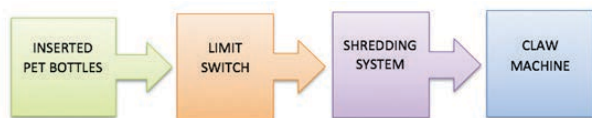


Fig. 1. System Flow Diagram

III. Hardware Requirement

The mechanical components used in making an Innovative Arcade Game Operated with PET Bottle Shredder comprises of Arduino MEGA as the main controller, claw machine system, shredder system, gear reducer (60:1), and AC motor (1 hp and 1750 rpm). Arduino Mega is a microcontroller board that has more pins, memory and speed to operate accordingly. It provides enough function that support the prototype. The AC motor is a single phase motor that supplies 1 HP. The size of the motor is 290mm x 175mm x 243 mm. It is the power source of shredding system. It is connected to the gear reducer and microcontroller. Limit switch is installed in the bottle depositor and will act as the sensor to give signal to shredding system and claw machine unit. It is also installed in the gantry area of the claw machine to control the axis of crane. The purpose of the shredding mechanism is to shred 1 bottle at a time. The size of the shredder is 270mm x 250mm x 162mm. It has 12 cutting blades that are arranged in "rectangular" shaped. The shaft is hexagonal shaped design and made of mild steel. The blades are assembled to the shafts with spacer between them. The material of the cutting knives is made from 4140 while the body of the shredder case is made from mild steel. The bottle acceptor unit is made of acrylic glass that accepts PET bottle as a token to play the claw machine. The prize dispenser unit is developed to dispense different prizes for every 3 bottles counted. The prizes are stored in claw machine unit. Gear reducer reduces the speed of the motor that will result to increase of torque. The size of the gear reducer is 150mm x 100mm x 180mm.

IV. Software Development

One of the main mechanism of the machine is to enable an Innovative Arcade Game with PET bottle shredder to use different microcontroller and various motors with Arduino IDE (Integrated Development Environment). Writing the necessary code control the game's behavior and interact with the hardware components. This study utilizes Arduino libraries, such as the "Servo" library for controlling servo motors or the "LiquidCrystal" library for interfacing with LCD displays. This study also establish communication between the Arduino board and the claw machine. This involves connecting the shredder's control circuit to the Arduino's digital or analog pins.

V. Computation of Parameters

Functional Testing

The system was tested to determine if it achieved a functionality level of 95%. This likely involved running the system through various scenarios and assessing its performance and consistency. The functionality of the limit switch, in claw machine, which returning the claw to its original position and allowing it to change the movement of axis, and in the bottle acceptor, which would trigger the shredder machine, is tested. The shredder assembly was tested to evaluate its efficiency in shredding. This test aimed to verify that the shredder assembly performed its intended function of effectively shredding materials. The Claw Crane functionality was evaluated to prove the overall performance of Claw Crane and to ensure proper integration. This test aimed to verify the Automation, Maneuverability and Sensitivity. The switch's ability to provide accurate indications to the Liquid Crystal Display (LCD) was the indicator used to test the functionality. This involved assessing whether the switch correctly detected and displayed relevant information on the LCD screen.

In order to determine the functionality, it is necessary to calculate the overall number of attempts. This can be achieved by employing the Fundamental formula of gambling.

$$N = \frac{\log(1-DC)}{\log(1-P)}$$

Where:

N = the number of trials

DC = the degree of certainty that the event will appear (95%)

p = the probability of the event (5%)

$$N = \frac{\log(1-95\%)}{\log(1-5\%)}$$

$$N = 4.32 = 5 \text{ trials}$$



*5, 6, 7
Student
BS in Mechanical Engineering,
Taguig City University

Overall Performance

To evaluate the functionality of the shredding process and measure its efficiency, a dedicated formula must be utilized. This formula involves comparing the weight of shredded PET bottles to the weight of PET bottles without water. By employing this formula, one can thoroughly assess and appraise the overall effectiveness of the shredding process.

$$SE = \frac{\text{output (g)}}{\text{input (g)}} \times 100\%$$

where:

Output = total weight of shredded PET bottles
Input = total weight of 500ml PET bottles without water.

VI. Summary of Findings

The Development of an Innovative Arcade Game Operated with PET Bottle Shredder involved assessing the functionality of machine in terms of Shredding and Claw Crane, and Overall Performance of the machine in terms of Shredding efficiency and Claw Crane functionability. Based on the results of the functionality tests and computations, after 5 successful trials for the shredder and claw crane, the system has achieved 100% functionality, exceeding the target 95% functionality.

In addressing the second research question, the overall performance in terms of Efficiency and Functionability, based on the findings derived from a comprehensive series of 5 shredding efficiency trials and computation conducted by the researchers, it has been determined that the shredding machine efficiency yields a notable efficiency rate of 85%. The PET bottle shredder demonstrated a high level of efficiency in terms of shredding PET bottles. It efficiently processed the bottles and converted them into recyclable shreds, allowing for effective waste management and recycling.

The researchers also evaluated the performance of an Innovative Arcade Game Operated with PET Bottle Shredder during the functionality testing and reported the results as "Ok" and "Not Okay". According to the observations, the machine passed all of the test criteria exhibiting automatic functionality, maneuverability and sensitivity.



Fig. 2.
Actual Photo of an Innovative Arcade Game Operated with PET Bottle Shredder

VII. Conclusion

In conclusion, the Development of an Innovative Arcade Game Operated with PET Bottle Shredder has shown remarkable results in terms of functionality and overall performance. The functionality tests conducted on the machine, including Shredding and Claw Crane operations gave a great result. This indicates that the machine performed exceptionally well in both shredding and claw crane functionalities.

Furthermore, the comprehensive series of shredding efficiency trials demonstrated that the PET bottle shredder achieved a notable efficiency rate. This highlights the machine's ability to efficiently process PET bottles and convert them into recyclable shreds, contributing to effective waste management and recycling practices. The researchers also assessed machine performance in terms of automatic functionality, maneuverability, and sensitivity. The machine successfully passed all test criteria, indicating its capability to exhibit these desired qualities. This suggests that the Arcade Game, integrated with the PET bottle shredder, operates smoothly and meets the expected standards for automatic functionality, maneuverability, and sensitivity.

Overall, the Development of an Innovative Arcade Game Operated with PET Bottle Shredder has proven to be highly functional, efficient in shredding PET bottles, and capable of meeting the desired performance criteria. By leveraging the positive findings from the assessment, the Arcade Game Operated with PET Bottle Shredder has the potential to make a significant impact in promoting recycling and sustainability while providing an enjoyable gaming experience.

VIII. Recommendation

Based on the outstanding results and observations from the Development of an Innovative Arcade Game Operated with PET Bottle Shredder, listed below are some recommendations to further improve the machine:

1. Although the Claw Crane functionality was reported as "Ok," it is essential to identify areas for improvement. It is important to conduct additional testing and analysis to refine the claw crane mechanism, ensuring smooth and precise movements. Adjusting factors such as grip strength will provide players with an optimal gameplay experience.
2. While the shredding machine efficiency yielded an impressive rate of 85%, it is worth exploring ways to optimize the recycling process further. By continuously researching and innovating methods, it will consistently produce high efficiency with compromising the quality of the shredding. This may include advancements in blade technology, optimizing motor and machine settings, or exploring alternative shredding techniques to improve energy consumption.
3. Conduct Long-Term Durability Testing: While the machine demonstrated functionality and performance during the testing phase, it is crucial to assess its durability over the long term. Conduct rigorous durability testing to ensure that the machine can withstand continuous operation and regular use without significant wear and tear.
4. When considering the overall mechanical components of the gantry assembly, it is crucial to ensure proper alignment and a suitable concrete size to prevent motor malfunctions. Instead of relying on the L298N motor driver, it is recommended to use the TB6600 stepper motor driver for enhanced precision and to prevent overheating. Furthermore, opting for the ESP8266 advanced microcontroller, rather than the Arduino MEGA, would be beneficial.
5. To ensure secure connections within the microcontroller, it is advisable to employ a soldering tool for fixing the wirings effectively. Additionally, while the prototype may perform adequately with limit switches, employing a photo-electric sensor is considered the optimal choice.
6. Rather than utilizing exposed type AC motors, it is preferable to select explosion-proof machines equipped with engineering plastic, which offers excellent safety features. Finally, it is recommended to adjust the speed reducer ratio from 60:1 to 50:1 to achieve the desired increase in RPM, specifically from 1740 to 1800 RPM.

IX. Acknowledgment

Conducting a study would not become possible without the help of these individuals. The researchers, would like to acknowledge and give our warmest gratitude to the following people:

To Engr. Salvador T. Gelilang, our Technical Adviser, we express our sincere gratitude for his dedication. He has not only provided us with technical expertise, but he has also been a source of our encouragement and support. His willingness to answer our questions and his patience with our mistakes are greatly appreciated. We are confident that his contributions made a significant impact on our study.

To Engr. Rico A. Geneta Jr. and Engr. John Renor P. Villarino, our professors who have exerted efforts in improving our study and believed that we will accomplish this study in time. Your invaluable insights and feedback have helped us improve our writing. We thank you for your willingness to give us an ample time to meet and discuss with you our progress.

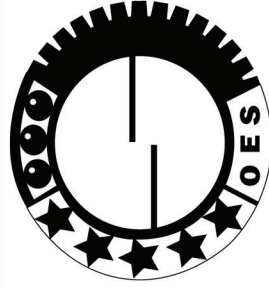
To Mr. Raul M. Yamon, Mr. Jim Ivan G. Lacorte, Mr. Mike Oliver Mondigo, and Mr. Louie Ocampo, for their priceless contribution to our thesis prototype. Their expertise, effort, and assistance in building our machine were essential to the success of our study. Their willingness to work long hours were truly inspiring. We are truly grateful for their help.

To Mr. Joseph and Mrs. Mary Grace Pelias, for their hospitality and generosity during our stay in their loving home. Their kindness and support made our time in their household a memorable one.

To our friends, they have been there for us through the tough times and so we celebrate our success with them. They are always there to cheer us, offering guidance and helped us to stay motivated. We are lucky to have them. To our amazing group, our thesis has been a tough and challenging journey. We have worked late nights, conducted tireless research, and faced many challenges. But we've shown unwavering dedication and always found a way to overcome them. We have stayed together, laughed together, and now celebrated our success together. I will cherish our lifelong friendship.

References

- [1] ACCOUNTING16 - Guide.pdf - Chapter 1 The Problem And Its Setting Background Of The Study Waste Generation Rates Are Rising. The Global Community Is Now Confronting The | Course Hero, March 17, 2021. [Online]. Available: <https://coursehero.com/file/84679224/guidepdf/>.
- [2] M. X. L. Bautista, "Arduino-Based Waste Detector with Alarm System," March 31, 2023. [Online]. Available: <https://ejsit-journal.com/index.php/ejsit/article/view/167>.
- [3] K. Choudhary, "Environment and economic impacts assessment of PET waste recycling with conventional and renewable sources of energy," 2019. [Online]. Available: <https://www.semanticscholar.org/paper/Environment-and-economic-impacts-assessment-of-PET-Choudhary-Sangwan/f9ad797312ccb80d72104b09a87d3303f153d379>.
- [4] A. Hafizi, "Eco-friendly Shredder Machine Project - Mechanical Engineering Design (Final Year) Project," 2021. [Online]. Available: https://www.academia.edu/44020866/Eco_friendly_Shredder_Machine_Project_Mechanical_Engineering_Design_Final_Year_Project.
- [5] A. Ikpe, "Design of Used PET Bottles Crushing Machine for Small Scale Industrial Applications," 2017. [Online]. Available: <https://www.semanticscholar.org/paper/Design-of-Used-PET-Bottles-Crushing-Machine-for-Ikpe-Ikechukwu/28134e07ddadc19a5927f3abec9c7c2d4eb3dd1c>.
- [6] N. D. Jadhav, "Development of Plastic Bottle Shredding Machine," 2018. [Online]. Available: <https://www.semanticscholar.org/paper/Development-of-Plastic-Bottle-Shredding-Machine-Jadhav-Patil/343d22f2f67b8a32a2caa4a84eb7704bdee245ae>.
- [7] A. Kooser, "This arcade machine runs on empty plastic bottles," CNET, April 30, 2014. [Online]. Available: <https://www.cnet.com/tech/gaming/bangladeshi-arcade-machine-runs-on-empty-plastic-bottles/>.
- [8] Mecvel Srl, "Electric linear actuators for recycling and waste treatment industries," MecVel Srl, April 17, 2023. [Online]. Available: <https://www.mecvel.com/recycling-industry/>.
- [9] Memorial University of Newfoundland, "Design, development and control of a new generation high performance linear actuator for parallel robots and other applications," Memorial University Research Repository. [Online]. Available: <https://research.library.mun.ca/11931/>.
- [10] J. M. C. Ongpeng, "Strengthening rectangular columns using recycled PET bottle strips," Animo Repository. [Online]. Available: https://animorepository.dlsu.edu.ph/faculty_research/2953/.
- [11] E. Pinter, F. Welle, E. Mayrhofer, A. Pechhacker, L. J. Motloch, V. Lahme, A. Grant, and M. Tacker, "Circularity Study on PET Bottle-To-Bottle Recycling. Sustainability," 13(13), 7370, 2021. [Online]. Available: <https://doi.org/10.3390/su13137370>.
- [12] N. H. A. Rahim and A. S. Khatib, "Development of PET bottle shredder reverse vending machine," International Journal of Advanced Technology and Engineering Exploration, 8(74), 24–33, 2021. [Online]. Available: <https://doi.org/10.19101/ijatee.2020.s2762167>.
- [13] regulusmachinery, "Waste plastic shredder crusher recycling machine hot sale," YouTube, [video], December 27, 2021. [Online]. Available: <https://www.youtube.com/watch?v=jFev6TEvpfw>.
- [14] SEA circular Project, "Countries Archive - SEA circular," SEA Circular. [Online]. Available: <https://www.sea-circular.org/country/>.
- [15] SEA circular Project, "Philippines - SEA circular," SEA Circular, Oct. 27, 2020a. [Online]. Available: <https://www.sea-circular.org/country/philippines/>.
- [16] SEA circular Project, "Philippines - SEA circular," SEA Circular, Oct. 27, 2020b. [Online]. Available: <https://www.sea-circular.org/country/philippines/>.
- [17] I. a. R. Silverio, "Filipino private sector steps up to tackle marine pollution," Maritime Fairtrade, 2022. [Online]. Available: <https://maritimefairtrade.org/filipino-private-sector-steps-up-to-tackle-marine-pollution/>.
- [18] E. So, "Shredding Machine Development for Recycling Process of Waste Plastic Bottles," [Open Access Journals], July 8, 2022. [Online]. Available: <https://www.rroij.com/open-access/shredding-machine-development-for-recycling-process-of-waste-plastic-bottles.php?aid=91688>.
- [19] R. Tiyyarattanachai, "Reverse Vending Machine and Its Impacts on Quantity and Quality of Recycled PET Bottles in Thailand," KMITL-Science and Technology Journal, 15(1), 2015. [Online]. Available: <http://www.tci-thaijo.org/index.php/kmitlsth/article/view/37699/31336>.
- [20] E. A. Villamer, M. T. Agrado, M. J. Delustre, R. Embestro, V. C. Mamano, C. Pante, R. Oliveros, E. Cabaltera, and V. S. Issac, "Concealed Automated Trash Bin with Shredder for Solid Waste," in Journal of Engineering and Emerging Technologies, 1(1), 1–7, 2022. [Online]. Available: <https://doi.org/10.52631/jeet.v1i1.45>.
- [21] World Bank Group, "Solid Waste Management," in World Bank, 2023. [Online]. Available: <https://www.worldbank.org/en/topic/urbandevelopment/brief/solid-waste-management>.



OPTIMIX ENGINEERING SERVICES

7-A Jacinto St., Brgy. Marulas, Valenzuela City

Tel. Nos. 291-8610; 444-9340; Fax 291-0009



MESCO

Since 1956

QUALITY MACHINE TOOLS AND ENGINEERING PRODUCTS

AMADA

ANCA

BIG
BIG DAISHOWA

CHEVALIER

Danfoss

EATON

ElektroPhysik
Meßgeräte für Oberflächentechnik • Surface Testing Instruments

EVERISING

FARO

FILTERMIST

HAIMER
Qualität gewinnt.



IHI

Realize your dreams

IMADA

ISCAR

Kemet



L&H MACHTECH CO., LTD.

Mazak

MITSUBISHI ELECTRIC
Changes for the Better

MITSUI SEIKI



Mitutoyo

MOOG

NIKKEN

OJIYAS

ORION

PALMRY

PRECISION TSUGAMI

RENISHAW
apply innovation™

RIVALIT

SCANTECH

SCHUNK

SEYI
PRESSING AHEAD

SUNNEN
ABOVE AND BEYOND HONING

system 3R

TOKIMEC
TOKYO KEIKI

Tungaloy

VICIVISION

VICKERS

Yawei

Y/G

Yushiro

MESCO Bldg., Reliance cor. Brixton Streets, Pasig
Tel No. 86311775 Fax No. 86314028 / 86350276
<http://www.mesco.com.ph>
email: mesco@mesco.com.ph



**STAMPFORM METALWORKS
INCORPORATED**

CONTACT INFORMATION:

MOBILE NUMBERS: 0998 582 7714 | 0998 555 4294

WEBSITE: WWW.STAMPFORM.NET

EMAIL: STAMPFORM@OUTLOOK.COM

WHAT WE CAN DO

DIE DESIGN & FABRICATION

TOOL DESIGN AND FABRICATION

LASER CUTTING

PLASMA CUTTING

WIRE CUTTING

METAL STAMPING

METAL BENDING AND FORMING

WELDING

TUBE BENDING AND FABRICATION



GRASCO

**ALLIED METALWORKS SPECIALIST,
INCORPORATED**

CONTACT INFORMATION:

MOBILE NUMBERS: 0917 700 8128 | 0917 548 0062

WEBSITE: WWW.GRASCOPH.COM

EMAIL: GRASCOPH.SALES@GMAIL.COM



PRODUCTS AND SERVICES:

CENTRIFUGAL BLOWERS

AXIAL FANS

IN-LINE FANS

JET FANS

ROOF EXHAUST FANS

WALL MOUNTED EFANS

CEILING CASSETTE FANS

BLOWER HOUSING AND SIDE PLATES

BLOWER WHEELS

DISCHARGE GRILLES

PROPELLER FANS

MAINTENANCE SERVICES

DESIGN SERVICES

ENGINEERING CONSULTANCY

REPLACEMENT PARTS FABRICATION

CNC Plasma Cutter with Ink Marker for Metal Plate Marking and Cutting

Hohn Lois Bongao^{*1}, Jane E. Morgado^{*2}, Harveen Bongao^{*3}, Mark Joseph B. Enoajs^{*4}, Kenneth D. Jalosjos^{*5}, Ciara Mae C. Lubay^{*6}, John Clifford C. Mallorca^{*7}, Jennylyn F. Maniacup^{*8}

Abstract

The computerized numerical control (CNC) machine is often coupled with a plasma torch when applied to cutting metal sheets. Prior to cutting, metal sheets are commonly marked manually using ink markers as a guide for bending and cutting. This manual marking has been observed to be time consuming and inconsistent. Therefore, integration of ink markers to the CNC plasma cutter is needed to create efficient cutting. In this work, an ink marker is integrated to a CNC plasma cutter that can be used for marking prior to the bending and cutting process. An inkjet marker is attached to a stepper motor for the marking mechanism. A MACH3 controller board is used for the control of the marking sequence. The developed machine is tested based on its cutting efficiency, processing speed, and acceptability. A work piece with a 40x40 mm² dimension is used to test which resulted in an average cutting efficiency of 0.585% error. The speed of processing was significantly improved, from an average of 16 minutes to 1.05 minutes. This was also tested for evaluation and acceptability to an engraving and tooling services company which uses manual marking process prior to cutting and bending of metal sheets. Out of the five users, three of them agreed that the machine is useful and can improve their processes, while two of them have a neutral response. This setup can be used for both marking and cutting.

Keywords: plasma cutter, CNC, ink marker, metal plate, manufacturing

I. Introduction

Arcenal Machine Engravers and Tooling Services is a local, small, and medium-sized enterprise (SME) that belongs to the metal industry. Among its fabrication services, metal sheet cutting and bending are the most in demand. In their present operation, manual markings are made onto the metal surface using basic patterning methods which incur high turnover time and low cutting accuracy. Afterwards, it is followed by a traditional way of searing metal sheets through stamping pressure known as cold sheet cutting. However, this traditional process is limited by the thickness of the metal sheets as it is directly proportional to the applied stress [1].

Nowadays, different metal cutting methods have been developed as substitutes for stamping through the use of different cutting media: laser, waterjet, and plasma. Laser cutting is an advanced technology having high cutting precision and accuracy [2]. Its major advantages include low kerf size and fast processing among others. However, it is limited by the material density and thickness of 2-3 millimeters (mm) for mild steels [3]. Waterjet on the other hand is capable of cutting over a wide range of surface roughness, thickness, and material type. Although the water is a low-cost source, the major drawback of using waterjet cutters is the turnover time and cost of producing immense pressure to facilitate the cutting process [4].

Plasma arc cutting is a scalable and versatile process dedicated for metal fabrication. In terms of processing cost, plasma arc generation is the most affordable and adaptable for SMEs. Producing the plasma arc involves three major system components that are readily available: gas source, power supply, and torch. The power supply generates the required energy to transform the ejected gas particles into plasma state which all transpires inside the torch [5]. In terms of cutting specifications, it has a maximum cutting thickness of up to 50 mm, as well as effectiveness in cutting stainless steel and aluminum sheets which is a common material requested by customers [6]. The main disadvantages of the plasma arc system are the heat-affected zone (HAZ) and surface discoloration therefore, a waterbed is located below the work piece, and final polishing is performed to address the issues, respectively.

In this work, an automated plasma cutter with integrated inkjet marking via computer numerical control (CNC) is designed and constructed in partnership with Arcenal Machine Engravers and Tooling Services. The present system is only intended for marking and cutting stainless steels and aluminum sheets with a maximum of 5 mm thickness.



^{*1, 2, 3}
Professor
Electrical and Allied Department,
Technological University of the
Philippines Taguig



^{*7}
Section Head
Mechatronics Technology,
Technological University of
the Philippines Taguig

II. Methodology

A. Design and Fabrication

The design of the machine is based on the standard plasma cutting machine table used in the industry built with modifications for the integration of a marker. The frame used for the table machine is made of an aluminum extrusion profile. The aluminum extrusion used in industrial grade machines must have flexibility and strength. The main reason for the modification of the frame is to create linear rails for the 3-axis plot or the X, Y, and Z axes of rotation, which aims to create a good foundation for the machine, as well as to carry and support the weight of the waterbed frame. The researchers considered the convenience of the machine when it comes to assembling. The frame made with an aluminum extrusion profile makes the machine fixture easier to assemble and disassemble. The water pan is composed of a curve slot which serves as the cooling system and reduces the warp caused by the effect of heat. The inkjet marker is attached below the plasma cutting torch that is meant for metal plate marking, to ease the time-consuming process.



Fig. 1. Isometric view of the CNC Plasma Cutter

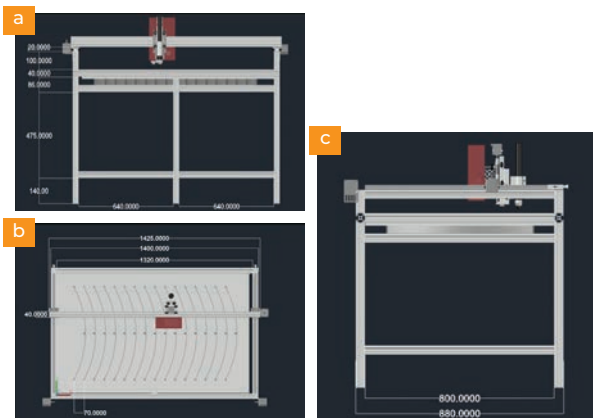


Fig. 2. Conceptual Design with dimensions of the CNC Plasma Cutter with Ink Marker – with measurements (a) Front view (b) Top view (c) Side view

B. The ink-marking device

Figure 3 displays the ink marking system housing with selected components inside. The Ink marking system housing is made of a tinted acrylic material and cut by a laser machine. The acrylic is required to be lightweight and is mounted at the back of the z-axis aluminum profile.

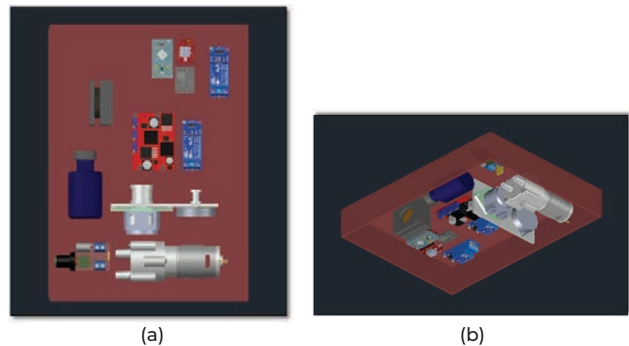


Fig. 3. Ink Marker Layout (a) Front view (b) Isometric view

Figure 4 shows the wiring connections between the electronic components such as Mach3 controller board, Stepper driver, relays, power supply, emergency stop, plasma machine, and Inkjet system. The positive output of the power source will supply voltage to the stepper motor driver. The A+, A-, B+, and B- of each motor driver are connected to the four-stepper motor. The input and output ports are used for the various processes supported by the mach3 controller. The 24 volts of the microcontroller are linked in the pin 1 of the two relays and connected to the stepper driver. Emergency stop pinouts are coupled in DCM ground and input 1 of the mach3. The DCM ground of mach3 and driver ground are both linked

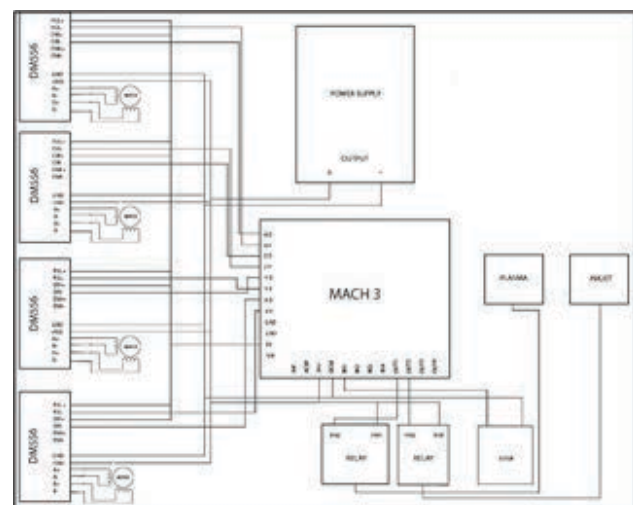


Fig. 4. Ink Marker Layout (a) Front view (b) Isometric view



*5, 6, 7, 8
Student
Electrical Engineering and Allied Department
Technological University of the Philippines Taguig

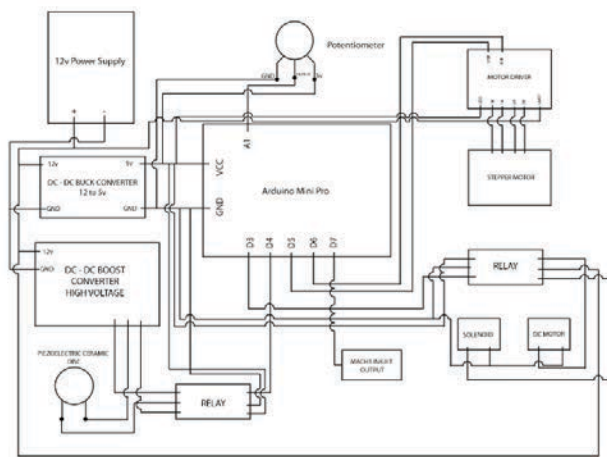


Fig. 5. Schematic diagram of Ink Marker Hardware Device

in the negative power source. The relay 1 is attached in the plasma cutter and relay 2 is intended for the inkjet marker.

The positive pinout of the power supply is connected to the DC-DC buck converter and DC-DC boost converter which supplies 12 volts of power as shown Figure 5. The piezoelectric ceramic disc is linked to the DC boost converter and relay 2. The GND pinout of potentiometer is connected to the ground of Arduino min pro and DC-DC buck converter ground. The 5 volts pin of potentiometer is wired for Arduino's VCC and buck converter, while the output is connected to the A1. To be able to drive a stepper motor the motor driver's pinout including 1A, 1B, 2A, 2B is wired in the motor. The Digital pin 3, 4, 5, 6, and 7 are connected to the following components: Relay 1, Relay 2, motor driver step, motor driver direction, and mach3 injket output.

C. Test and Evaluation

Functionality test will be done to know the capability of the developed prototype. It will also be evaluated in terms of its repeatability and cutting accuracy, by the end users.

III. Results and Discussion

A. Fabrication Result

The prototype developed is presented in Figure 6. The inkjet marker was embedded in the plasma cutting machine as shown in Figure 6a and 6b shows the electronic parts of the control system. The machine is built sturdy to prevent unnecessary shaking, vibrations, and movements during the cutting process. In a closer look, the inkjet marker can be seen in Figure 7.

B. Test and Evaluation

Comparative analysis was conducted for different settings such as testing with and without probing and by changing nozzle feed rate. Table 1 shows the test cuts using consumables for cutting a metal plate which have

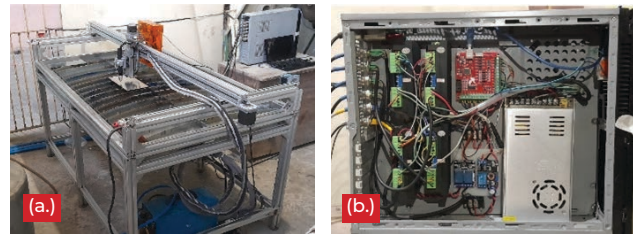


Fig. 6. The prototype (a) Inkjet marker embedded on the plasma cutter (b) electronic parts

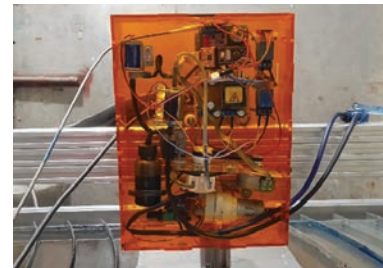


Fig. 7. Inkjet marker embedded in the plotter.

Table 1. Test cutting using consumables without probing

Test no.	Ampere	Z-distance (mm)	Thickness (mm)	Plunge rate (mm/min)	Feed rate (mm/min)
1	30	1.5	1.5	350	2000
2	30	2	1.5	350	2000

Table 2. Test cutting using new consumables without probing

Test no.	Ampere	Z-distance (mm)	Thickness (mm)	Plunge rate (mm/min)	Feed rate (mm/min)
3	35	2	1.5	350	2000
4	35	1.5	1.5	450	2000
5	40	1.5	1.5	450	2500
6	40	1.5	1.5	450	4000

Stainless steel, 70 psi

Table 3. Test cutting new consumables with probing

Test no.	Ampere	Z-distance (mm)	Thickness (mm)	Plunge rate (mm/min)	Feed rate (mm/min)
1	35	2	1.5	350	2000
2	35	1.5	1.5	450	2000
3	40	1.5	1.5	450	2500

Stainless steel, 70 psi

the same material and material thickness as well as the settings for the ampere, pressure (psi), plunge rate, and feed rate while having different z-distances. Different values in the functionality test of parameters were assigned and the test cut output is analyzed to determine the constant settings for the plasma cutting machine. The first test is conducted to analyze the quality of output using a used consumable without the probing. The z-distance was changed from 1.5 mm to 2 mm.

Table 2 shows the comparison data of test cuts in which the nozzles used are new consumables and are recorded as test cuts without probing. The current was increased from 30 to 40 ampere while the pressure of the

compressor remains at 70 Psi. The distance between the metal sheet is varying from 2 mm to 1.5 mm. In the fifth and sixth trial the feed rate changed from 2000 to 400 mm/min.

Table 3 shows the comparison between test cuts using new consumables and is recorded as data gathered with probing. The three trials have the same current of 35 amperes, pressure of the compressor with 70 Psi, Z-distance of 1.5 mm length, plunge rate of 350 mm/min, and feed rate of 2000 mm/min which is compared to the input value of other data tables.

C. Repeatability test

Six trials were made for the repeatability test at each axis. A dial indicator was mounted to obtain the precise measurement for the ink markings of the marker embedded in the CNC plasma machine. The desired distance is 10 mm and the actual distance measured was 9.98 mm, which got an average of 0.2% error for the x-axis. Same experiment is done in the y-axis which has an impressive average of 0.067% error. The z-axis test has an average of 0.0167% error. The z-axis test results are significant since it carries the plasma torch attached to it. It must have a minimal error to maintain its accuracy.

D. Cutting accuracy

Five trials were made to test the cutting accuracy by measuring the actual cut distance and compared to the desired cut distance. The work piece has an actual dimension of 40 mm x40 mm. In result, an average of 0.585% error was measured. A comparative analysis is done in terms of marking and cutting time in a metal plate where 4 trials are made for each test. The manual marking and cutting process takes an average of 16 minutes while the automated marking and cutting has an average of 1.05 minutes.

E. User perception

Five respondents evaluated the developed prototype. Based on the survey conducted from the machinists of Arcenal Machine Engravers and Tooling Services, having an automated cutting machine will help them ease their work and which will lessen the human error in terms of manually plotting the lines or marks on the metal sheet. One of the most common problems that the machinists' encounter is making mistakes in cutting metal sheets using manually operated cutting machines which later results in wastes and downtime.

IV. Conclusion and Future Work

In this study, an inkjet marker was embedded in the plasma cutting machine to eliminate the manual marking and cutting on plain metal sheets. This addresses problems such as the inaccuracy of manual marking and cutting and yet minimizes the warping of the work pieces when prolonged exposure to the torch. In result, it was found out that the developed prototype is faster in terms of the combined marking and cutting compared to the erratic manual process. In the future, this model can be developed further into a more accurate one by using a different ink marker. This can avoid clogging on the nozzle.

V. Acknowledgment

The authors would like to acknowledge the Technological University of the Philippines Taguig Research and Extensions office for its support in the conduct of this research.

References

- [1] H. Wang and Z. Wang, "Theoretical Forming Limit Diagram Based on Induced Stress in the Thickness Direction," *Metals (Basel)*, vol. 13, no. 3, p. 456, 2023.
- [2] Y. He et al., "Laser Cutting Technologies and Corresponding Pollution Control Strategy," *Processes*, 2022.
- [3] M. Sobih, P. L. Crouse, and L. Li, "Laser cutting of variable thickness materials - Understanding the problem," *ICALEO 2006 - 25th Int. Congr. Appl. Laser Electro-Optics, Congr. Proc.*, no. January 2015, 2006.
- [4] J. M. Llanto, M. Tolouei-Rad, A. Vafadar, and M. Aamir, "Recent progress trend on abrasive waterjet cutting of metallic materials: A review," *Appl. Sci.*, vol. 11, no. 8, 2021.
- [5] L. Kudrna, J. Fries, and M. Merta, "Influences on plasma cutting quality on CNC machine," *Multidiscip. Asp. Prod. Eng.*, vol. 2, no. 1, pp. 108–117, 2019.
- [6] J. Kechagias, M. Petousis, N. Vidakis, and N. Mastorakis, "Plasma Arc Cutting Dimensional Accuracy Optimization employing the Parameter Design approach," *ITM Web Conf.*, vol. 9, p. 03004, 2017.

Portable Coconut Dehusker with Breaker

Dahlia Gay A. Bunolna*1, Chosme Jones D. Aggihao*2

Abstract

The Philippines is one of the producers of coconut products. In Ifugao we are known of our delicacy which uses coconut milk to enhance our products. Having coconut trees in almost every province including the Indigenous peoples of the north, particularly the Ifugao are recognized for their creativity as well as the Banaue Rice Terraces. It is not surprising, that coconut is a major component in Filipino cuisine, appearing in everything from appetizers to the main dish to desserts. However, due to lack of processing technology, numerous procedures are used to peel the coconut until recently. Even now, the use of traditional method is practiced. The development of dehusking machines with breaker is essential to resolve these problems. These methods are extensively used to remove the coconut husk, although numerous issues and limits are employed with this equipment. These issues have an impact on rate at which coconuts are dehusked. To overcome the current machine's limitations and issues, a way that is both automated and efficient to the user is required. This study focuses on the development and fabrication of a Portable Coconut Dehusker with Breaker. A dehusking with breaking machine is introduced and constructed to solve these restrictions, improve automation, and provide operator safety. The portable coconut dehusker with breaker appears to be worthwhile and economical. The quantity of coconuts processed per hour is determined by the limp time and roller unit swiftness. The coconut dehusker with breaker is simple to operate and maintain, and it is also low-cost to maintain. The equipment can dehusk 93% of coconut compared to manual processing.

Keywords: coconut, dehusked, Ifugao, coconut dehusking machine

I. Introduction

In plight of the country's goal to build and improve economic status of the country thru recovery of the small-scale business, technology development is a need to help cope with the requirements of today's quantum era. *Cocos nucifera* commonly known as coconut is a common Southeast Asian fruit that are commonly planted and produced in Asian countries such as Malaysia, Indonesia, and the Philippines. Coconut trees are common in almost every province of the Philippines including the Indigenous peoples of the north, particularly the Ifugao who are recognized for their creativity as well as food delicacies prepared using coconut milk. Coconuts are famous for their expediency, as proved by a variety of old-fashioned routines ranging from food, fuels and as cosmetics, as well as numerous homes, commercial, and industrial applications of various parts. Coconut production is a significant contributor to the Philippine economy and that about one-third of the Filipino population is supported by the coconut business.

As seen in **Figure 1**, a coconut is made up of an external thick skin covering, a thick sinewy wool known as husk, and a solid shielding case known as shell.

The diameter and length of the coconut range from 136 to 200mm. On the end of the coconut is three black pores that are soft known as the eyes. A hard thick white and



Fig. 1. Composition of coconut fruit

soft white meat that depends on the age and kind of the coconut is attached on the shell is called the coco meat or "copra". The nut's inside is dull and half occupied with "coconut juice," a watery liquid. When young, the meat is soft and juicy, but as it matures, it becomes tough (**Figure 1**). Coconut juice is abundant in young coconut fruits, but as they seasoned the juice becomes less. The shells are maximized by some as fuel, and shell gasifiers and an alternative source of heat energy. Coir products are all made from the husk.



*1 Dean
College of Engineering and Technology
Ifugao State University Lagawe, Ifugao



*2 Instructor I
College of Engineering and Technology
Ifugao State University Lagawe, Ifugao

Processing coconut products implore same methods in all manufacturing and processing industry that includes picking, de-husking, and shell-breaking for coconuts. Coconut dehusking is one of the most tough tasks in the coconut industry. While coconut is one of massive pecuniary ideal to entrepreneurs and the locals, dehusking of the coconut is the dangerous and toughest stage in the process. Coconuts are manually husked with a machete or a spike. Aside from dehusking of coconut, the shell breaking process is currently manual and there is a potential of mishaps when using a manual technique. The price of the product includes the cost of labor as well. These methods necessitate specialized labor, are exhausting to use, take time, and entail human labor, training, and endurance. This project solves this issue by developing a coconut dehusking machine with a coconut shell breaker that is hydraulically operated and useful to laborers and producers. The principal purpose of the fabrication and development of the Portable Coconut Dehusker with Breaker is to mechanize the dehusking and the breaking process for safety purpose and efficiency as the highest goal. This coconut dehusking and breaking machine uses mechanically controlled dehusking equipment to eliminate the husk and detached them from the shell, resulting in a dehusked coconut fruit that is to be cracked into two pieces by the breaker. This helps and reduces the threats, dangers, and menaces of dehusking the coconut in a way that is efficient, less hazard, and simple to operate. This machine requires less human interaction and aids in the reduction of drudgery. This machine is benign to use than the manual conventional dehusking and breaking instruments that were often employed in our province because it does not require direct human vigor as compared to the traditional method.

II. Materials and Method

The research used applied research design for the gap analysis phase and its design phase; the project development design phase for its fabrication and assembly stage where all necessary parts were assembled; functionality testing with all the mechanical parts are done; prototype development phase; and technical evaluation stage. The study used personal interviews and survey for the acceptance and its economic impact of the developed coconut dehusker with breaker.

The Portable Coconut Dehusker with Breaker operates by electricity for the motor to rotate the blades and remove the coconut husk and automatically be pushed to the exit panel for the breaking of the shell. The coconut juice is then extracted thru a pin straw and are funneled to the juice catcher for processing into "buko juice" for consumption. The husked coconut is break with the mechanical breaker that divides the coconut for further processing. The processing time of a coconut from dehusking to breaking takes 70 seconds depending on the size and the quality of dryness of the coconut.

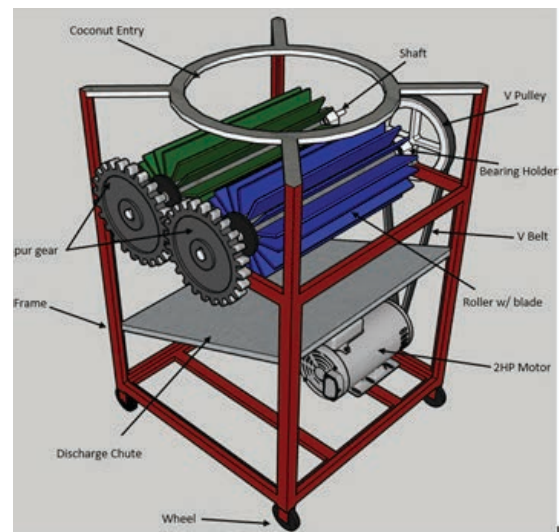


Fig. 2. Major parts

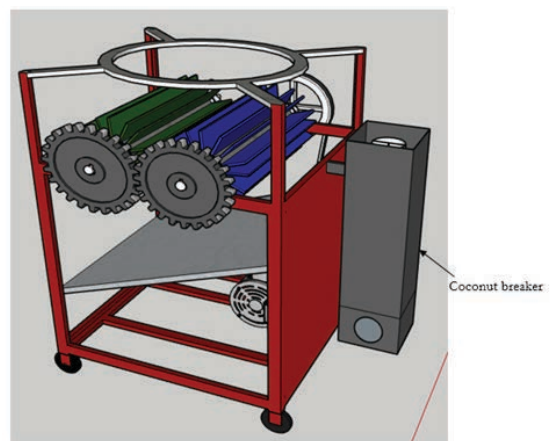


Fig. 2.1

III. Results and Discussion

The Portable Coconut Dehusker with Breaker is developed in Ifugao State University, Lagawe Ifugao. The major parts are the frame, de-husking, discharge chute, metal plates, bearing and the breaking unit as shown in Figure 2.

The mainframe serves as the main support assembly of the fabricated machine. It is connected thru welding of 600mm in length, 500mm in width, and 750mm in height made of a 50x50x5mm angle bar. The dehusking part makes up of two pin rollers, two pin roller shafts, gears, and four bearing holders. The rollers was connected thru welding twenty-eight metal blades (carbon steel plates) of 50.8mm in height and 495.3 in mm length. A pulley is attached at the left of the roller shaft that is operated by a 2HP motor together with the v belt that is connected. Simple operation and management is necessary in the used of the machine. When the motor is turned on, the roller blade revolves in inward motion to remove the husk. The breaker unit is composed of a blade that will crack the coconut shell into two pieces.

Overall, the coconut dehusking machine is functional with an energized 2HP motor. The motor will turn the spur gears that forcibly removed the coconut husk separating it from the coconut shell, the removed husk are now pushed to the bottom of the machine while the coconut will be pushed to the side in preparation for breaking.

Fabrication Process

Cutting is done with chisels and cutting machines (all of which have powered and manual variations). The chopped pieces are joined together using welding, riveting, and threaded fasteners. The standard beginning components for fabrication are structural steel angle bars, welding wire, flux, and fasteners that will connect the cut parts. Welding is mostly used for in fabricating steel. The assembled and tacky-welded shaped and machined parts are then double-checked for correctness. The welding is done as per the engineering drawings. The manufactured machine is given wheels in order to make it portable. The iron components are properly painted to keep them from rusting.

Dehusking and Breaking Process

In the course of De husking coconut, the machine is driven by a motor that uses strategically positioned rolling blades on shafts to strip the husk from the coconut. Two rollers with blades over them make up a coconut husking. The coconut is slid through the top holes and falls onto the rollers, which rotate in opposing directions inwards. One roller's blades hold the husks in place, while the other's blades shred the husk. After the coconut is de-husked, the husk will fall on the discharge chute. The husked coconut will immediately be put in the cutting mechanism. When the husked coconut puts on the cutting base, it will activate the pneumatic cylinder, which will then push the husked coconut toward the pointed blade. The husked coconut will be cut into two.

Coconut Dehusker Design

As shown in Figure 3, the body is made up of metals. It has a height of 930 millimeters, a width of 500 millimeters, and a length of 600 millimeters. The body is made by the combination of an angle bar, flat bar, flat sheet, stainless pan and etc.

On the bottom of the machine, there are four wheels, which makes the machine move conveniently. The machine top part will be covered with a flat sheet in order to avoid any hazards or danger when placing the coconut fruit. After putting the coconut into the coconut entry, the roller with a blade works and husks the coconut, and the husk will fall over to the flat sheet.

The results of the performance of the machine are about 90% efficacy in the test case as projected. It is estimated, that the total coconut that will be husked per hour in pieces, depending on the movement of the operator. However, on average an operator can de-husk 60 plus nuts per hour with this machine. While the capacity of the

tool to break the coconut shell is 1 coconut in 10 seconds depending on the capacity of the operator. The machine has the particular benefit of being able to de-husk and cut a mature coconut in 60 seconds as opposed to a competent person who would need an average of 180 seconds to complete the task.

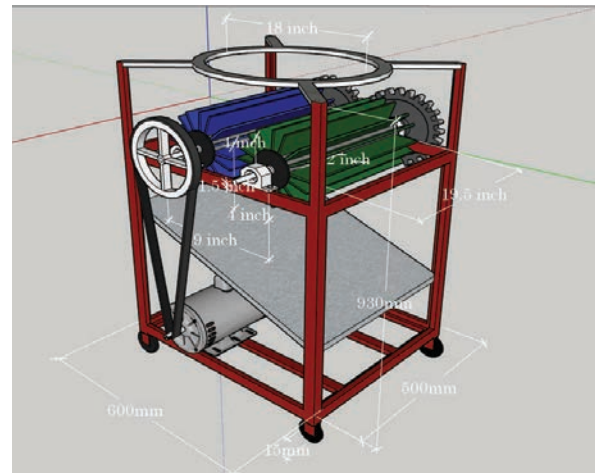


Fig. 3

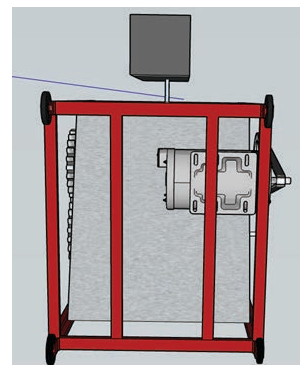


Fig. 3.1

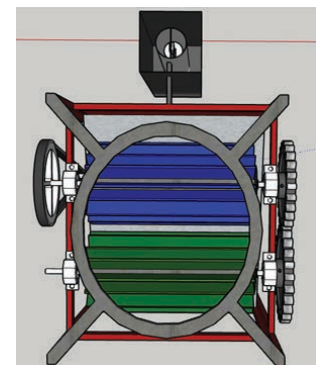


Fig. 3.2

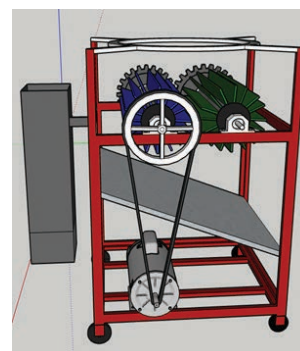


Fig. 3.3

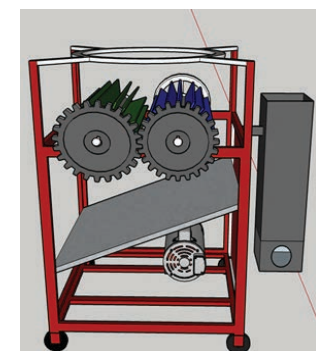


Fig. 3.4

IV. Conclusion

The low cost portable coconut de-husking with breaking machine is a breakthrough in the field of coconut industry especially to our small scale coconut business owners/ manufacturers. In this quantum agriculture the fabrication of the machine as a revolution to increase yield and reduce the necessity for skilled manpower and safety has been unraveled. The pecuniary status and cost has been a problem of farmers in adapting such innovation. The fabricated machine is easy to use and has a dehusking efficacy of 90% and a minimum of 60 plus nuts per hour, respectively. The machine has the particular benefit of being able to cut the dehusked coconut in 50-70 seconds. Just unlike the manual equipment, such as the keramithra and the foot-operated dehusked, which is time-consuming and can lead to harm if dehusking is done without concentration. The introduction of this equipment into farm areas can lessen the risk of using a spike to dehusk coconuts while also eliminating the need for experienced people. The equipment can also be combined with the nuts' subsequent processing phases, such as copra production. The machine can be further combined with the Portable Coconut Grating Machine with Presser to maximized the processing of the coconut in the industry.

V. Acknowledgment

The authors would like to thank the Metals Industry Research and Development Center (MIRDC) of the Department of Science and Technology (DOST) for entrusting and funding this research, as well as the IFSU-MEIC Team for extending their profound knowledge and effort towards the realization of this study.

References

- [1] Nwankwojike BN, Onuba O and Ogbonna U. 'Development of a Coconut Dehusking Machine for Rural Small-Scale Farm Holders', International Journal of Innovative Technology & Creative Engineering, 3(2), pp1-7, 2012.
- [2] Foale, M.A. The Coconut Palm. In: Chopra, V.L. and Peter K.V. edited Handbook of Industrial Crops. Haworth Press, New York, 2005.
- [3] APCC. Coconut Food Process – Coconut Processing Technology. Informantion Document. Arancon, Jr, R.N., ed. Asian and Pacific Coconut Community. Jakarta, Indonesia, 1996.
- [4] Thampan, P.K. Handbook on Coconut Palm. Oxford & IBH Publishing Co., New Delhi. 1996.

Design and Development of Coconut Coir and Coco Peat Extraction Device

Abel T. Mendoza*

Abstract

Coconut husks are valuable byproducts of the coconut industry, but they are time-consuming and labor-intensive to process. In this study, we devised and built a coconut coir and coco peat extraction apparatus that can extract coir and peat from coconut husks economically and effectively. Our prototype machine uses a 2hp electric motor and can process 20kgs of coconut husks per hour. Our findings reveal that the initial prototype is functional and successful at extracting coconut coir and coco peat. However, more research is required to maximize the machine's performance and capacity. Additional methods are required to separate the harvested coir and peat, which can be optimized in future study. Our coconut coir and coco peat extraction system can help to ensure the sustainability of the coconut industry by lowering labor costs and increasing efficiency. Overall, our research shows that employing a machine to extract coconut coir and coco peat is feasible, and it lays the framework for future research and development in this field.

Keywords: decorticator, coconut husk, cocopeat, coconut coir, design and development

I. Introduction

Coconut (*Cocos nucifera*) is an extensively cultivated palm tree found in tropical regions like the Philippines, and it is renowned for its various applications in food, medicine, and industry (Ferreira et al., 2018). As a result of coconut processing, a substantial amount of waste in the form of coconut husks is generated. These husks, which consist of the fibrous outer layer and the inner woody shell, pose significant environmental challenges due to their slow decomposition and accumulation in landfills (Al-Tabbakh et al., 2020). However, these waste husks also present an opportunity for resource recovery and the development of sustainable materials.

Metals Industry Research and Development Center Nueva Ecija University of Science and Technology Coconut coir and coco peat, extracted from coconut husks, have gained increasing attention as valuable raw materials for a wide range of products. Coconut coir refers to the fibrous material obtained from the outer layer of the husk, while coco peat refers to the finer particles. These materials possess remarkable properties such as high lignocellulosic content, water-holding capacity, and biodegradability, making them suitable for applications in agriculture, horticulture, and various industries (Rufus et al., 2021).

The extraction of coconut coir and coco peat traditionally involves manual labor, which is time-consuming and labor-intensive. In recent years, there has been a growing interest in the development of mechanized extraction devices to streamline the process and enhance productivity. These devices aim to efficiently separate

the coir fibers and coco peat particles from the coconut husks, contributing to waste reduction and promoting the utilization of these valuable by-products.

The utilization of waste coconut husks through the extraction of coconut coir and coco peat presents numerous environmental and economic benefits. By repurposing this abundant waste material, we can reduce the strain on landfills, contribute to sustainable resource management, and provide raw materials for industries in need of sustainable alternatives. This research not only showcases the feasibility of mechanized extraction but also serves as a foundation for further optimization and advancement in the field.

In this study, we employ the design and development research (DDR) method to create a device for coconut coir and coco peat extraction. This device offers a promising solution to address the challenges associated with manual extraction. The device utilizes innovative mechanisms and a 2hp electric motor to achieve efficient extraction with a capacity of 20 kilograms per hour. Furthermore, we investigate the subsequent processing steps required to separate the coir fibers and coco peat particles effectively.

Specifically, this study has the following objective:

1. Design a coco peat and coconut coir extraction device, based on the patented technology with consideration on the locally available materials;
2. Perform casting of some parts of the device and fabricate it in the Nueva Ecija University of



*1 Assistant Professor III
Metals Engineering and Innovation Center,
Nueva Ecija University of Science and Technology,
Cabanatuan City, Nueva Ecija, Philippines

- Science and Technology - Metals Engineering and Innovation Center; and
- Evaluate the initial prototype in terms of its capacity, effectiveness and efficiency.

In the following sections of this manuscript, we will discuss the materials and methods employed, present the results of our experiments, and provide a comprehensive analysis of the extracted coconut coir and coco peat. Furthermore, we will explore potential applications for these materials and discuss their implications for sustainable development.

II. Materials and Method

This study falls in the product and tool research category of the Design and Development Research (Richey and Klein, 2007). Data collection methods employed were needs assessment, expert interviews, tool development, expert validation, participant interviews, focus group interviews, and evaluation methods.

This study underwent in the following process:

- Identification of a research worthy problem which is expressed by researchers in peer reviewed research literature and patented technology;
- Describing the purpose of the research to ensure that it aligned with the problem statement;
- Writing of research questions to align with the problem and purpose statements; and
- Creating of the following documents:
 - Needs Assessment;
 - Measurable Goals and Objectives;
 - Description of the product;
 - Technology selection; and
 - Evaluation Plan.

To address the first objective of the project, the researcher reviews available literature published in journals and books to gain theoretical knowledge applied in the design and development of the device.

Then, the researcher conducts patent search to review existing technology applied in the extraction of coco peat and coconut coir. The researcher also seeks existing coconut husk decorticator device and evaluate their capacity, effectiveness and efficiency in order to find opportunities for improving its design. The governing rules followed by the designer in the design of the prototype is the capacity of the 2HP electric motor already available at the time of designing phase.

After designing process, the researcher reviews the design and list all the materials needed in fabrication of the device prototype. The researcher consults casting and fabrication experts and operators of existing decorticators to gain knowledge and seek for their advice on improving the initial design. Then, the researcher revise the initial design to incorporate the gathered information and suggestions from the experts.

The researcher then, perform artificial evaluation through

computer simulations using NovaCast and Solidworks. Then perform minor changes in the design. Afterwards, the canvas of all the needed materials and fabrication tools based on the design and fabrication methodology was performed and seek for the approval of budget and procurement.

After all the needed materials and tools was procured the device was fabricated and tested in the Metals Engineering and Innovation Center of the Nueva Ecija University of Science and Technology.

The conceptual framework applied in the design and development of the device was presented in Figure 1.

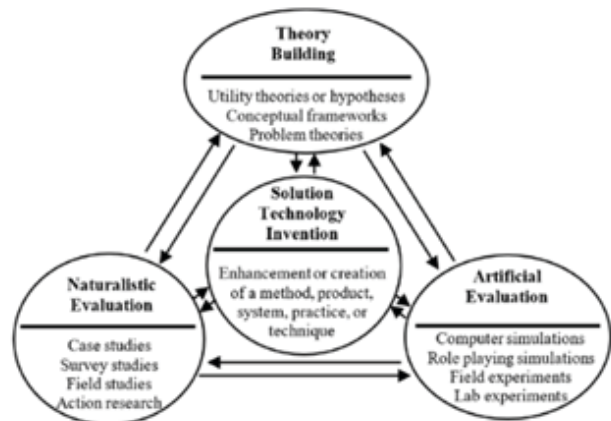


Fig. 1. Conceptual framework for DDR method

III. Results and Discussion

The Philippines ranks second worldwide in 2021 as shown in Figure 2 base on the data from Food and Agriculture Organization (FAO) that reach a total of 14.7 million tons and a coconut plantation area of more than three million hectares with approximately 500 million coconut trees that produce an estimated amount of six million tons of coconut husk annually.

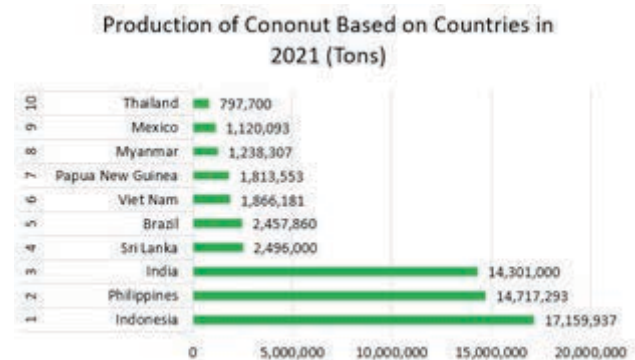


Fig. 2. Production of coconut based on countries (2021)

Currently, there are nineteen companies around the Philippines that is processing coconut husk as reported in the List of Companies in World Wide website. But, still coconut husk utilization in the country is very low and processing machines are very critical in this problem.

To address this problem and help our country utilize this valuable product we employ the Design and Development Research (DDR) method to create a device to extract coconut coir and coco peat from coconut husk.

A. Designing the Coconut Coir and Coco Peat Extraction Device

In the design phase of the project, the researcher gathered valuable information from the related literature published in journals and patented technology. The researcher also employed Solidworks as CAD software to draw the initial design of the device as show in the **Figure 3**. These software helps the researcher to identify different parts of the device and decide sizes and geometric shape of each part. The drawing also helps in discussion and gathering information from the experts in the field.

The researcher also employed the Novacast software to help us decide on blades and pulley sizes and shapes. **Figure 4** shows the simulation trial results from Novacast which the researcher used to decide the size and shape of the pattern and mold for the casting of the decorticator blade.

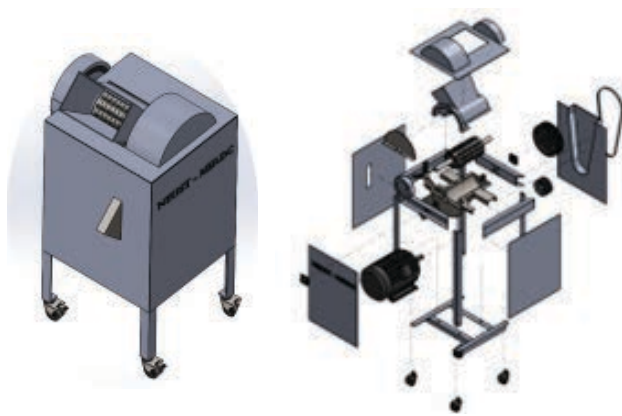


Fig. 3. Design of the coconut coir and coco peat extraction device

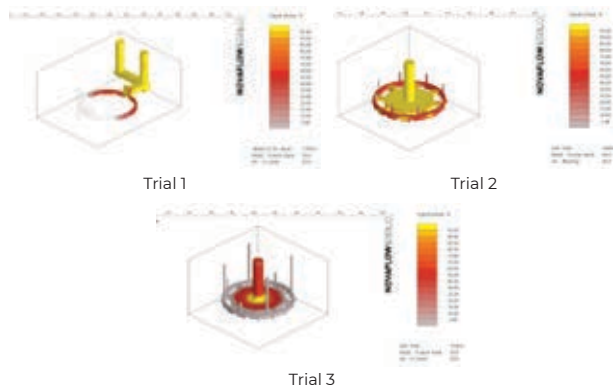


Fig. 4. Different simulation trials using Novacast software

B. Casting and Fabrication of the Device

After the design was finalized and verified by consultation from the experts in the field and simulations, the casting and fabrication phase followed. This has two major goal. First, is that the designed device is possible to fabricate and second, the Nueva Ecija University of Science and Technology – Metals Engineering and Innovation Center (NEUST-MEIC) is capable in fabricating it.

Fabrication of the device employs various fabricating methods like wood working, 3D printing, pattern making, mold making, casting, sand blasting, welding, bending, machining, cutting, grinding and painting. **Figure 5** shows various activities during the fabrication and casting phase.

This phase took the longest part of the project implementation which is almost one year. The material used in casting of the pulley and blade was cast iron. We employed an induction furnace in melting of the cast iron and used a silica sand as mold. We create a pattern from wood and fabricate other parts using mild steel. Angle bars were use for the frame and mild steel plate for the body of the device. Other parts like bearings, shafts, V-belts, caster wheel were purchased from the hardware.

There was also some minor revision from the final design of the device that's why the fabricated device does not looks like in the design.

Revision is due to fabrication limitations, specially in the machining of the designed blade.



Fig. 5. Fabrication of the coconut coir and coco peat extraction device.

C. Testing and Evaluation of the Device

After all of the handwork, the researcher evaluates the device in terms of its capacity, effectivity and efficiency. A single phase, 220VAC, 2HP motor with a rated speed of 1,725 revolution per minute was used to power up the device and the researcher gathered two types of coconut husk for testing, the brown husk which is obtained from mature coconuts and green husks from immature coconuts. Before testing we measure the weight of each samples. The brown husk was submerged first in water before processing. Each of the samples weighted 20kg before testing. The brown coconut husk took 1 hour before fully processed, while the green husks took 47 minutes. The processing time includes stoppage due to malfunction of the machine. The energy used by the motor was also included in the observation. The data gathered during the test was shown in Table 1. It shows that the machine is more efficient when processing green husk.

Table 1. Data gathered during the testing of the coconut coir and coco peat extraction device

	Brown Husk	Green Husk
Mass	25kg	25kg
Total processing time	60 mins	47 mins
Down time	35 mins	25 mins
Operating Time	25 mins	22 mins
Motor Used	Single phase, 230VAC, 2 horsepower, 1725 rpm	
Ave. Amps.	8 Amps	7.5 Amps
Estimated Motor Efficiency	75%	75%
Energy Used	0.47kWh	0.41kWh

The fabricated device can be used to extract coir and peat from the husk but still need to undergo another process to separate the coir from the peat. The picture of the processed coir was shown in Figure 6.

After extraction procedure the product was sieved to separate the coir from the peat. The resulting product was shown in Figure 7.



Fig. 6. Coconut husk coir and peat after processing in the extraction device



Fig. 7. Separated coir (left) from peat (right)

IV. Conclusion and Recommendation

After the conduct of this study, the researcher provide evidences that the coconut husk can be processed using the disigned and developed device to extract coconut husk's coir and peat.

The researcher can also prove that the NEUST-MEIC is now capable to design and fabricate devices like the Coconut coir and peat extraction device and now ready to cater community needs.

It is then be recommended that the developed prototype to be further improved to meet commercialization requirement and support coconut industry to be more profitable.

The developed prototype can be the basis of the design of future decorticator devices. This study is just a single step forward to open opportunities for Filipino people, where they can earn money and improve lives by turning waste into valuable products. This initial steps have lots of improvement needed to cater vast amount of resources available. Larger capacity coconut husk's coir and peat extraction devices, physical plant with automated processing facilities, supply chain and high quality product must be met for us to compete in the international market.

V. Acknowledgment

The researcher wants to acknowledge Engr. Nathaniel S. Olivero, the head of NEUST-MEIC, Dr. Felician P. Jacoba the President of NEUST and my Colleges in the NEUST-MEIC for your support and encouragement.

The researcher also want to thank the Metals Industry Research and Development Center and Nueva Ecija University of Science and Technology for funding this research.

References

- [1] Al-Tabbakh, H. A., Razzaque, M. A., & Ibrahim, M. H. (2020). Coconut biomass waste: A review of potential value-added products. *Journal of Cleaner Production*, 268, 122255.
- [2] Ferreira, J. L., Soares, A. G., Nascimento, R. A., & Aguiar, E. M. (2018). Coir fiber waste: an agricultural waste with great potential for use in the treatment of domestic wastewater. *Environmental Technology & Innovation*, 10, 198-207.
- [3] Rufus, S. L., Kalimuthu, P., Saravanakumar, R. A., Alharbi, N. S., & Rajaram, R. (2021). Application of coconut coir in sustainable materials: A review. *Journal of Cleaner Production*, 286,125440.
- [4] Richey, R. C. & Klein, J. D. (2007). *Design and Development Research*. Routledge.
- [5] Minatogawa, Vinicius & Franco, Matheus & Duran, Orlando & Quadros, Ruy & Holgado, María & Batocchio, Antonio. (2020). Carving out New Business Models in a Small Company through Contextual Ambidexterity: The Case of a Sustainable Company. *Sustainability*. 12. 2337. 10.3390/su12062337..
- [6] Daquil Jr, E. M. (2016). Coconut Husk Decorticator, (PH12015000144A1). Philippines.
- [7] Dagaas, F. M. (2016). An Improved High-Capacity Coconut Husk Decorticator (PH22013000650U1). Philippines.
- [8] Cherian, J. V. & Thamizhchelvan, P. (2012). A Process for the Defibering of Coconut Husk (WO2012150610A2 (A3)). India.




Colt Commercial Inc.

Colt Commercial Inc. has been providing technical services and supplying industrial cutting tools for more than 30 years. Colt Commercial Inc. is a major player in the supply of industrial cutting tool products in the Philippines and has been the exclusive distributor of major cutting tools manufacturers in the world – TaeguTec Ltd., HPMT Industries Sbn. Bhd., and Whizcut of Sweden AB.



The former Korea Tungsten Company was born from the mines in Gangwon Province in the northern part of South Korea in 1916. Since then, TaeguTec has grown to become not only South Korea's largest and most innovative industrial cutting tool manufacturer, but also an important provider of tungsten powders, solid carbide rolls and specialized industrial products to the world at large.



HPMT cutting tools are made for specific applications and are sold both locally in Malaysia as well as overseas. Today HPMT prides itself as an innovator in the three categories of high precision solid carbide cutting tools. The universal tools, the specialised tools and the customized tools categories. All with in-house R&D facilities committed to perfecting the art of precision tool innovation right from today's advanced manufacturing hub of the technology-driven South East Asia.



WhizCut is the leading manufacturer of cutting tools specially developed for CNC Swiss type automatics. WhizCut offers a complete range of carbide inserts for turning, boring bars, thread mills and micro drills. With this precision tooling WhizCut will help you improve productivity and reduce interruptions in production in your Swiss lathe.



BAOJE industrial Ltd. Co. is a leading manufacturer of high quality micro boring tools with 30 years experience. BAOJE focuses on what you need and endeavor to research the best quality of tools for your industry. These are some patents which include CNC grinding tool machine, sectioning machine, precision boring tools along with toolholders to satisfy your needs.

Transfer of Technology Through Innovated Machine Shop Training Table for Benchwork Operation

Rey Roland G. Macauba*¹, Mark Anthony Partosa*², Jonathan O. Mañas*³

Abstract

The effective transfer of technology is crucial in technical education, as it enables students to acquire the necessary skills and knowledge to succeed in the industry. In this study, an innovated training table was developed to address the need for more efficient and effective machines that can facilitate the transfer of learning in machine shop training. The innovated training table was designed to have four (4) different features and purposes: a four (4) jaw independent chuck, a rotary surface plate, a crankshaft truing stand, and a welding clamp positioning tool. The study evaluated the innovated training table through a survey of 38 respondents, composed of both students and faculty members from the research location. The results of the survey showed that the innovated training table received a qualitative description score of 95-100% in scoring procedures, as corresponded to its weighted mean. This indicates that the respondents and users of the training table found it to be highly acceptable and promising. The innovated training table offers a more efficient and effective way of teaching and learning in machine shop training, as it enables students to work with various machines and tools in a single table. It also enhances the transfer of technology, as it allows students to gain practical skills and experience through hands-on training. Finally, the innovated training table offers a promising tool for technology transfer in technical education, as it enhances the efficiency and effectiveness of machine shop training. It is recommended that further studies be conducted to explore the full potential of the innovated training table and its impact on technical education.

Keywords: Industrial Technology, Innovated Machine Shop Training Table, Developmental Research

I. Introduction

Throughout the 20th century, mechanical technology continued to boom, particularly in the industrialized nations. It became the key in making and developing project plans and research in many fields that involve from foundry metallurgical designs down to mass productions and its uses. Bulky technologies from spaceships, space satellites, missiles, aircraft, airplanes to earth moving equipment like huge cranes and cars, down to smallest piece part of a wristwatch, were considered products of mechanical technology development [1]. As also published in www.rise.edu.pk, mechanical technology and progress of a country were considered directly proportional to the well-being and living standard of a society. With the complexity of its technologies, the present world is facing a shortage of able technicians.

Just about everything we eat, see, feel, and hear, smell and touch, had used metal in its manufacture. Since metal played such a prominent role in our daily life, it would appear that everyone knows metal. Technical programs were continuing to boom because of these matters [1]. As observed, almost every school in different developing countries gave importance to their technical programs such as in mechanical engineering and technology.

Learning mechanical technology involved hands-on experience with machines in which students would be able to hone their ability in identifying materials, testing new materials, creating product projects based on research, performing accurate measurements, and do troubleshooting and repair. Other concepts like hand tools skills, metallurgy, blueprint reading, welding, and basic manufacturing skills were also taught in mechanical technology under courses.

In mechanical technology, every course of a particular program needed some tools and equipment in order to gain more knowledge about specific concepts. Basic machines that were used for productions like a metal shaper, vertical slot machine, milling machines, lathe machine, welding machines, and grinding machines, were commonly be seen inside the shop room for lecture and demonstration purposes [5]. While some professors kept their job simple from following the book and dictated words for machine manuals, some professors of different schools of particular program tended to create their own tools and machinery that they believed could make their students learning easier and much faster. Machines that could not be seen inside the classrooms or shops or job



*² Professor
College of Technology
Eastern Visayas State
University, Tacloban City



*³ ITSO Coordinator
Eastern Visayas State
University, Tacloban City

shops that the main purpose was to help the trainee in their works were considered improvised machine trainers.

It is believed that the desire to make such improvised training machines was invented upon knowing the term machine itself. "In history, Archimedes discovered the mechanical advantages by using pulley, lever, and screw. More philosophers took advantage and pursued the discovery, maximizing each mechanical system's parts. The classic rules of sliding friction in machines were discovered by Leonardo da Vinci [2]. As cited in en.wikipedia.org, starting the later part of the 18th century, there began a transition in parts of Great Britain's previously manual labor and drafts-animal based manufacturing. As posted in summer-sad.blogspot.com, it started with the mechanization of the textile industries, the development of iron-making techniques and the increased use of refined coal.

There are other technology innovations that were created in order to speak to workers or trainer's need for enhancing their abilities. These outputs were machine trainers more often observed in some classroom shops across countries that gave importance not only to the mechanical engineering technology field but also to other situational aspects as it concerned. These trainers were made for the reasons to faster the learning system of their trainees, lessen the time of consumption, and much of positive productions. But also other reasons suited that, unavailable of learning materials because of its purchasing costs, such reasons could affect the learning ability of such trainer to the trainees [3].

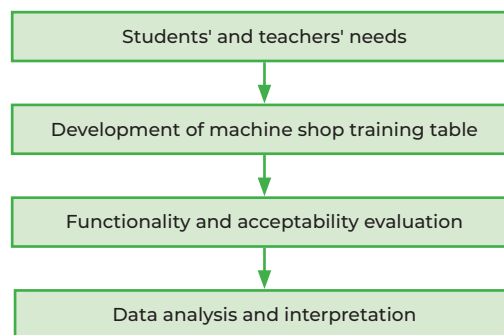
Furthermore, the Eastern Visayas State University (EVSU-Main) was offering technical programs like Bachelor in Mechanical Technology with majors of Welding Technology, Automotive Technology, and Machine Shop. The said programs produced skilled and competitive workers and entrepreneurs around the globe based on the department's attributes on the graduates. It corresponded to the said program offered by the school were the laboratory facilities that supported the learning inputs of the program.

Through the years, such machines and equipment available were the only learning materials for the students. Professors preferred sometimes into laboratory trainers. These machines were made for the purpose of lectures and application of learnings [1-3]. Say for example, in Automotive Technology Laboratory, they used different mock-ups of engine builds and driving wheel trainer for understanding driving more and also for application purposes like researches, etc. The professor understood the need for such machine trainers inside their classrooms.

In the named major courses of Bachelor in Mechanical Technology, there was a need for having additional "machine trainers" as observed inside the laboratory rooms of the said program. Therefore, a research had to be conducted to be able to fulfil the need for these materials and trainers to be used for the students and professors.

The Machine trainer would provide coverage of the three majors which were Welding Technology, Automotive Technology, and Machine Shop Technology. The Machine Trainer would provide the students for practice angles in welding positioning, jigs, and fixtures for welding and machine shop, and adjustable Bench Centers for Welding, Machine Shop, and Automotive Trainee.

II. Methodology



III. Materials and Methods

The Innovated Training Table is made up of several important parts which is discussed below.

1. The Table

The table is made up of angle bars (75 x 75mm width, 6mm thickness) build frame with built in metal drawer as tool box itself at its side, and both , 5mm thickness heavy duty surface plate at lower and upper side of table.

2. Four Jaws Independent Chuck

The four jaws chuck is a 7" diameter with 3" length jaws that use to clamp a rounded-shape and even an irregular shape for the purpose of centering operations layout purposes.

3. Rotary Surface Plate

The Rotary plate is a 5mm thickness 254mm diameter steel plate with patterned slots for clamping device during users welding operations or layout purposes.

4. Crankshaft Truing Stand

The Crankshaft Truing Stand was made up of (75 x 75mm width, 6mm thickness) fabricated with attached bearings (25mm outside diameter, 12mm inside diameter) attached to the angle bars through fasteners and weld. It is equally constructed using laser lights in order to secure crankshaft centers and even cylindrical shaftings, detecting its bents or in machinist called Truing operation.

5. Crankshaft Truing Slide

The Crankshaft Truing Slide was made up of (75 x 75mm width, 6mm thickness) angle bars with lead screw attached underneath as crankshaft truing stand adjusters in locating the length of work piece or crankshaft to true.

6. Welding Positioning Plate

The welding positioning plate was made up of 5mm thickness with 203mm x 304mm steel plate with patterned slots for insert butt clamps used in welding operation welding positioning training. The Welding positioning plate is adjustable in angle applicable to 1G, 2G, 3G and 4G welding positions (Butt joint).

IV. Design and Consideration

Technical Requirement

The "Machine Shop Training Table" was a bench table innovated to be a laboratory tool that was utilized in the teaching and learning process. There were many types of bench table available in the market that also made to address the need of the industrial uses and other fabricating or leisure purposes. In ProQuest, there was an innovated welding table, adjustable bench table, and other innovated types of tool listed that were used for easier transfer of learnings.

As needed and observed in the present Machine Shop Laboratory, some technical requirements had been set in order to address the problem and for further utilization of the Innovated Training Tool.

The users must easily understand the functions and importance of every part in the "Machine Shop Training Table". The machine was user-friendly and had an equivalent manual that contained all the procedures or steps and operations of the parts. The parts were detachable and accurately working for moving and adjusting for certain locations.

The Innovated Machine must be completed with the attachable parts corresponded to its devices needed to start the operation. The Machine had four (4) principal parts with each playing an important role for training the users, namely; Independent Chuck for Centering operations, the rotary workspace for layout, the adjustable angle Welding position learning, and the Crankshaft Center Stand for Crankshaft truing. Each part was completed with devices that were needed for every operation. These included Dial gauge indicators, Butt Clamps, and Wrenches. These tools and other devices could be seen in the Manual provided.

The Machine must have appropriate elevations for the comfort of users. The machine's height was set for all users. As could be seen below, the table with each part was accessible and easy to handle for every operation followed by the rules according to the guidelines stated in the manual provided.

Design and Fabrication

The design and fabrication of the Innovated Machine Training Table was the result of collecting the information inspired by the need of the locations of this research for such a machine. The design of the machine could be described as "Solid but Accessible". The materials that had been used must match its functioning role and operations were done on it. It was heavy with weight approximately up to 80-90 kilos but very accessible as the parts could be easily moved and adjusted for locating works. The design must be secured that all the technical learning would be transferred to the users.

Every part was designed and tested with its durability under operations. The accessibility of tools on each part, the clamps, the moving jigs, the centering tools like dial gauge indicator, and other materials were provided in order to operate properly the "Innovated Machine Shop Training Table".

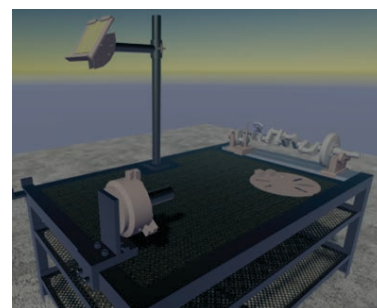


Isometric view of product

V. Functionality of Project

Benchwork

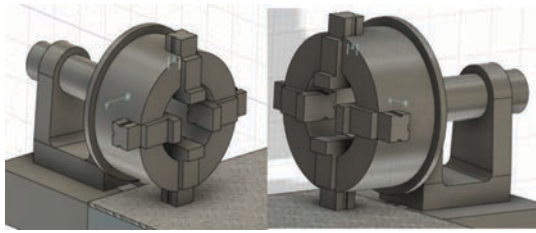
The rotary plate has patterned slots for clamping device in a work, fixing it to undergo other operations such as welding, layout works and other benchwork operations.



Rotary plate

Centering Operation

Now that there was a "Training Table" provided with four jaws chuck, the enhancing of skills for centering procedures could be maximized since the location of research was lacking tools and equipment for instructional purposes, the researcher saw it as an opportunity to

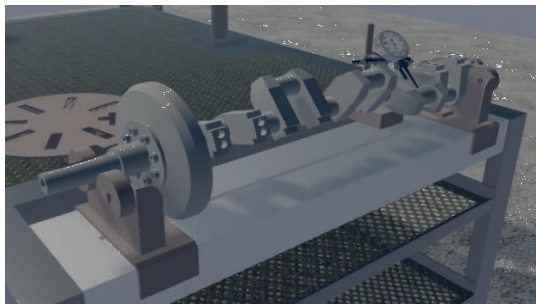


Four jaw independent chuck

make and indulged into this type of research. Centering procedures could be done on the Layout work for tinsmith purposes, or for Lathe turning.

Crankshaft Truing

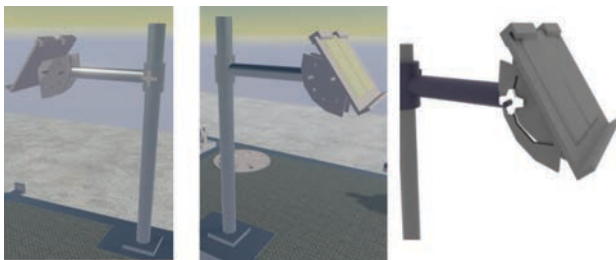
The Crankshaft Center Stand or Truing Stand was basically the first Center stand for Crankshaft in the School and would be used for instructional purposes. As it could be observed that the weight on its functions had the highest weight respondents gave was 4.84 weighted average on the checking of ovalness and taperedness. This would be useful in diagnosing crankshaft's journals and alignments. The Crankshaft Truing Stand has tolerance of plus/minus 0.02mm centers.



Crankshaft truing simulation (thru; Fusion 360)

Welding Angle Positioning

The Welding Angle in accordance to the welding positioning plate is a type of clamping device for welding procedures 1G, 2G, 3G and 4G butt joints significant joints in welding operation as preparation for students in more of welding and fabrication industry.



Welding positioning plate (Fusion 360)

VI. Results and Discussions

The "Machine Shop Training Table" was a type of bench table innovated in order to be used for training students and instructional purposes. The product would provide easier transfer of learning to its users and it also offered quality constructions of its parts and features, accessible, and movable parts.

The said machine shows quality results with "excellent" in its overall mean for "Functionality" and "Acceptability" Evaluation. Specifically, it is assessed as "excellent" in terms of its Benchwork Operations done in Training Table, the construction of the machine, its parts and features, and overall functions.

FIGURE 1 LEVEL OF FUNCTIONALITY		
BENCH WORKS OPERATIONS DONE IN TRAINING TABLE	MEAN	INTERPRETATION
CENTERING OPERATION	4.71	EXCELLENT
ROTARY SURFACE PLATE	4.79	EXCELLENT
CRANKSHAFT TRUING	4.80	EXCELLENT
WELDING PLATE POSITIONING	4.82	EXCELLENT
GENERAL AVERAGE WEIGHTED MEAN	4.76	EXCELLENT

FIGURE 2 LEVEL OF ACCEPTABILITY		
CONSTRUCTION OF TRAINING TABLE	MEAN	INTERPRETATION
MATERIALS USED IN FABRICATION	4.32	EXCELLENT
ASSEMBLED PARTS INTO BENCH TABLE	4.34	EXCELLENT
ACCESSIBLE HEIGHT OF THE TABLE FOR OPERATIONS	4.18	EXCELLENT
ADJUSTABLE PRINCIPAL PARTS	4.16	EXCELLENT
GENERAL AVERAGE WEIGHTED MEAN	4.49	EXCELLENT

VII. Conclusion

Based on the results of the data gathered, it could be said that the Innovated Training Table for the Machine Shop Students was a complete package for being a trainer on its users. The design of constructions, the features offered, and the transfer of learnings that could be offered in the training table could verdict as very helpful for the program, the Bachelor of Science in Mechanical Technology.

The level of acceptability and the level of functionality of the Training Table of the Machine Shop were evaluated as "excellent".

References

- [1] Walker, J. R. (2004). Modern Metalworking Workbook. Goodheart-Willcox.
- [2] <https://www.mpoweruk.com/history.htm>
- [3] Harvey, J. A. (2004). Machine Shop Trade Secrets. Industrial Pr.
- [4] Piazza, M., Alexander, S., & Notaro, M. (2015). Machining: A Summary of the Literature. Maxine Goodman Levin School of Urban Affairs Publications, 1-3, 1320.
- [5] Bergek, A., Jacobsson, S., Carlsson, B., Lindmark, S. & Rickne, A. (2008a).
- [6] Analyzing the functional dynamics of technological innovation systems: A Scheme of Analysis. Research Policy, 37, 3, 407-429

A Design of Shredder Machine for Scrap Material for Meter Assembly and ECU Assembly

Jane E. Morgado*¹, Mark Joseph B. Enojas*², Hohn Lois C. Bongao*³, Ruem G. Arribas*⁴, Jefferson C. Rufo*⁵, Tatyana A. Macarimbang*⁶, Joshua James Q. Aguilar*⁷, Jayson D. Ramirez*⁸,

Abstract

Shredding is a widely used process of stripping or cutting scrap materials into smaller pieces in the manufacturing industry. Before disposal, it is required for companies to shred the scrap material for destruction and data protection. This study aims to improve the proper disposal of scrap materials, develop an efficient method for destroying them, and reduce costs associated with returning them to the owner. The traditional method of destroying scrap samples using tools like hammers and tables is eliminated through the creation of a shredding machine. This machine reduces the time needed for preparing scrap materials for disposal from 45 minutes to 15 minutes and significantly improves the quality of the output produced from shredding. The fabricated shredding machine for scrap material for meter and ECU assembly was designed and tested for functionality and effectiveness. The average sizes of the measured output sizes of PCB and IC from the testing meet the standard size for shredder cut data destruction, which is 12.7mm (0.5 inches). The findings indicate the effectiveness of the fabricated machine in shredding scrap materials, outperforming existing literature in terms of output size reduction and utilization of the shredding process alone. This study provides a practical solution to the proper disposal of scrap materials while improving the efficiency of operations compared to the manual method.

Keywords: shredding machine, scrap materials, material disposal, Meter assembly, ECU assembly

I. Introduction

The retention of meter assembly and scrap materials in a company's storage or warehouse is crucial to ensure the security of data and information associated with prototypes. Specifically, the meter assembly and ECU assembly being evaluated are still in the prototype stage and require a protected environment. Once the evaluation is complete, the prototypes are returned to the owner for the disposal of scrap materials. With this, it is required to destroy these scrap materials through shredding for data protection and to prevent unauthorized copying [1]. Shredding machines are known for reducing the sizes of paper, plastic, electronic, and agricultural scrap materials into smaller pieces used for waste management, material recovery, and as value-added products of a company [2-4].

Companies traditionally use the conventional ways of scrap material destruction by using hammers or vise. However, these methods have proven to be ineffective and failed to meet the required standards for shredding scrap materials [5]. In addition, they have caused damage to company properties and posed risks of injury to workers due to flying debris. To address the challenges of the manual method, the researchers have proposed the design, development, and fabrication of a shredding machine for scrap materials for meter and ECU Assembly. This shredding machine aims to efficiently shred the scrap materials until they become unrecognizable, ensuring

complete destruction and protection of confidential information.

Implementing an automated shredding process for the disposal of scrap materials will result in reduced costs associated with returning these materials to the customer. Furthermore, the workers and manpower within the company will benefit from the study as it eliminates the fatigue and potential injuries associated with manual labor for scrap material destruction. The designed shredding machine includes features such as a safety sensor to ensure operator safety during machine operation, a machine signal light to detect errors, manual and forward/reverse switch functions to handle jamming situations, and to notify the machine operator when the shredder drawer bin is full, a bin level sensor is utilized.

By addressing the challenges and fulfilling the objectives outlined, this study aims to enhance the process of scrap material disposal, shorten processing time from 45 minutes to 15 minutes, improve efficiency, and increase productivity while maintaining the confidentiality and security of the meter assembly and its associated data through the use of the fabricated shredding machine.

This study utilized three related works of literature to evaluate the performance of the fabricated shredding



*1, 2, 3
Professor
Electrical and Allied
Department
Technological University of
the Philippines Taguig



*4, 5
Professor
Mechanical and Allied
Department
Technological University of the
Philippines Taguig

machine in terms of output size and method of shredding used. The first study emphasizes the extraction of valuable metals like nickel, copper, and zinc from circuit boards, revealing that finer shredding enhances metal recovery [6]. The second study focuses on SSD disposal and underscores the need for a secure shredder, reducing SSDs to a maximum size of ½ inch to prevent data retrieval [7]. Lastly, the third study explores PCB recycling, showcasing shredder and crusher systems that efficiently reduce PCBs to sizes as small as 1mm [8]. These studies collectively advance electronic device waste management, enabling the recovery of valuable materials, ensuring data security, and optimizing recycling efficiency for a sustainable future.

Furthermore, this study follows the recommended measurement of shredded scrap materials by NSA also known as the National Security Agency for data destruction which should be less than ½ inch for the companies that give services of data destruction through shredding of materials that is according to the standards of NAID (National Association for Information Destruction) [9].

II. Methodology

A. Machine Design Components

This study was conducted in the area where the scrap materials are destroyed and stored. The machine design and components shown in Figure 1 were incorporated into the project to ensure efficient and safe shredding of scrap materials for meter assembly and ECU assembly.

A single-phase motor was utilized as the power source of the machine for operational efficiency. The machine was equipped with manual and forward/reverse switches, allowing the operator to control its functions and reverse the shredder's rotation. This also ensures

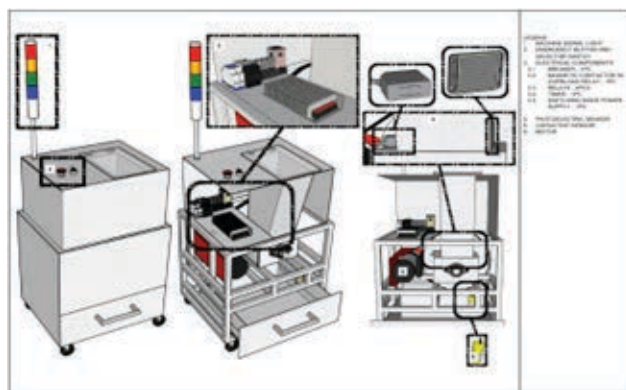


Fig. 1. Machine design and components

smooth operation and handles potential jamming incidents. Several measures were implemented for safety considerations. An emergency power button (EPB) was incorporated, enabling the operator to immediately stop the shredding process during emergencies. The shredded materials were collected in a drawer bin with a capacitive sensor, which provides real-time feedback to the operator regarding the bin's fill level. Once the bin reached its capacity, the blue light will be activated in the tower light system notifying the operator. Additional signal colors were added in the tower light for visual indications: a red light denoting that the power supply is on but shredding stopped, a green light indicating that the shredding process is in progress, and a yellow light indicating an overload trip.

Additionally, a photo sensor was integrated into the machine to detect the presence of materials in the shredder's hopper. A limit switch, positioned behind a transparent door, automatically halted the shredding process if the door was opened. Caster wheels with brakes were also installed on the machine to make it portable and stable. These components can be seen in Figure 2. By seamlessly integrating these machine design elements and components, the shredding process for scrap materials in meter assembly and ECU assembly was efficiently and safely accomplished.

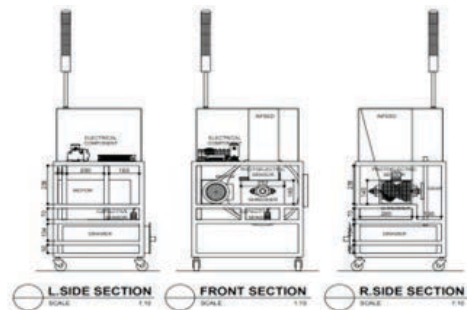


Fig. 2. Machine design & components sectional views

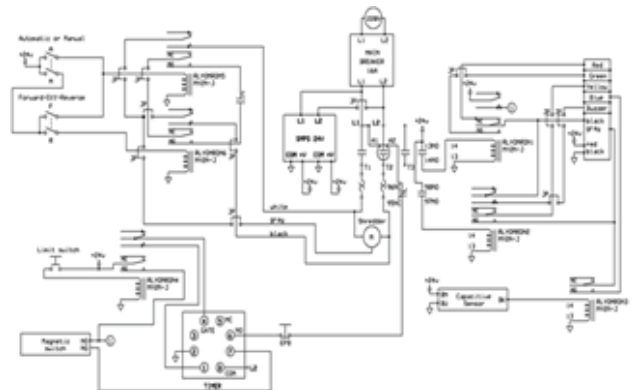


Fig. 3. Schematic diagram of the machine



*6, 7, 8
Student
Bachelor of Engineering
Technological University of the Philippines Taguig

The schematic diagram of the machine is presented in Figure 3 which illustrates the overview and interconnections of various elements and components incorporated for its efficient operation.

B. Machine Fabrication

The fabrication process is the most important part of this study which encompasses essential processes in creating a functional and efficient shredding machine in meter and ECU assembly. This involves a series of steps, from the design phase and the collection of machine parts to the construction of individual components and assembly of the machine.

The fabrication of the device started with the assembly of the tubular components, ensuring precise alignment and utilizing a welding machine to secure them firmly in place. The shredder mechanism was installed alongside the electric hoist. An 80-teeth gear was incorporated into the shredder assembly together with a 14-teeth gear in the electric hoist to enhance its torque. A custom-made hopper was installed to facilitate the feeding of scrap materials into the shredder. The final step was the application of a coat of paint to the tubular parts to protect the metal components from corrosion and ensure their durability. This will protect the machine from potential environmental factors that could cause future damage. Through these steps, the shredding machine was successfully fabricated, as depicted in Figure 4, following the proposed design and specified functions.



Fig. 4. Fabricated shredder machine in meter and ECU assembly



Fig. 5. Actual fabricated prototype

C. Testing and Evaluation

The testing and evaluation of the fabricated shredding machine involve the assessment of its performance and testing its efficiency in shredding scrap materials in meter and ECU assembly. To evaluate the machine's capabilities, relevant literature on shredding scrap materials, and manual method in terms of the methods employed for shredding and the size and appearance of the scrap materials shredded was conducted. The evaluation will determine if the output shredded scrap materials for meter and ECU assembly met the data destruction standard. A combination of 10 printed circuit boards (PCB) and 7 integrated circuits (IC) with the size of 20x10cm subject for destruction were shredded in the fabricated machine and the outputs were measured using a caliper shown in Figure 6.

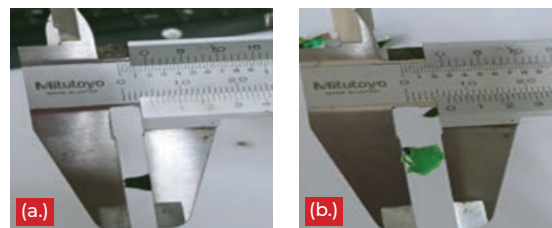


Fig. 6. (a) PCB and (b) IC output size measurement using a caliper

The comparison is illustrated in tables that validate the machine's performance and ensure its alignment with the intended objectives. By assessing the shredded output sizes from the fabricated device based on the established standards, the machine's effectiveness was verified in achieving the desired shredding outcomes for the scrap materials commonly utilized in meter and ECU assembly.

Table 1. Comparison of the fabricated machine to related literature

	Literature 1	Literature 2	Literature 3	Design of Shredder Machine for Scrap Material for Meter and ECU Assembly
METHOD	Cutting & Shredding	Shredding	Crushing & Shredding	Shredding
OUTPUT SIZE	8x4cm 3.9mm 2.1mm	12.7mm (1/2 inch)	30mm 25mm	PCB - 6.47mm IC - 2.14mm

Table 2. Output sizes of shredded scrap materials from the testing

NO.	OUTPUT SIZE
PCB SAMPLES	
PCB No. 1	6.8mm
PCB No. 2	5.8mm
PCB No. 3	6.1mm
PCB No. 4	6.5mm
PCB No. 5	6.4mm
PCB No. 6	6.8mm
PCB No. 7	5.5mm
PCB No. 8	7.3mm
PCB No. 9	7.4mm
PCB No. 10	6.6mm
Average:	6.47mm
IC SAMPLES	
IC No. 1	4mm
IC No. 2	2.7mm
IC No. 3	4.7mm
IC No. 4	2.6mm
IC No. 5	4.4mm
IC No. 6	4.8mm
IC No. 7	5.7mm
Average:	4.12

III. Results and Discussion

A. Fabricated vs. Existing Shredding Machine Output

To evaluate the performance of the fabricated shredding machine, the outputs were compared to three relevant literature in shredding scrap materials, in terms of the

methods and materials in various sizes used for shredding, and output sizes. The results of the comparison can be seen in Table 1. The following literature was used for comparison: "Effect of Shredding and Particle Size in Physical and Chemical" (Literature 1), "Why does Size Matter for SSD Shredding" (Literature 2), and "Shredder and Crusher Systems for Size Reduction" (Literature 3).

With the results presented in Table 2, it is observed that the measurements for the shredded output of PCB and IC from the fabricated machine are significantly smaller compared to the output in the relevant literature. Additionally, the machine achieved these outputs through the process of shredding alone compared to existing literature that involves cutting, crushing, and shredding. The machine produced a minimum output size of 2.6mm and a maximum output of 5.7mm for IC and a minimum output size of 5.1mm, and a maximum output size of 7.4mm for PCB.

The average sizes of the measured output sizes of PCB and IC were calculated which can be found in Table 1. The average size of the PCB was determined to be 6.47mm, while the average size of the IC was found to be 4.12mm in width. Comparing these averages to the standard size for shredder cut data destruction, which is 12.7mm (equivalent to 0.5 inches), all the output from the machine met the required size according to the standard of data destruction for shredding scrap material.

These findings indicate the effectiveness of the fabricated machine in shredding scrap materials outperforming the existing literature in terms of output size reduction and utilization of the shredding process alone.

B. Manual vs Fabricated Machine Shredding

In Figure 7, it can be observed that the components of scrap materials shredded from manual labor (shredding) are still intact and confidential information are still visible and copy-able. While in the fabricated shredding machine, the shredded output is in smaller pieces, and the circuit boards are destroyed totally. With this, the automated shredding machine for scrap materials for meter and ECU assembly produced output that can already be disposed of, hence, more efficient in shredding scrap materials compared to the manual method.

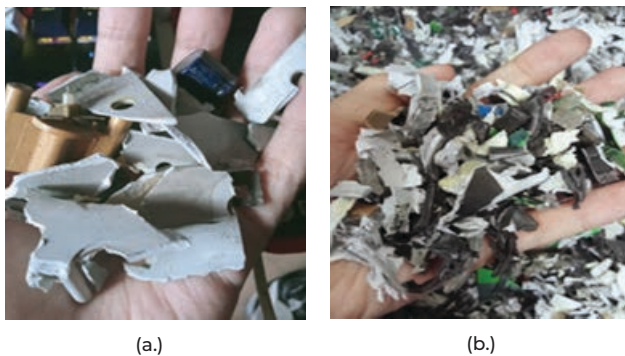


Fig. 7. Manual and fabricated machine shredding machine output comparison

IV. Conclusion

The successful development and fabrication of a shredder machine intended for scrap material for meter and ECU assembly have yielded remarkable outcomes. This innovative machine implementation has not only reduced recycling costs but also significantly minimized labor-intensive work. Additionally, the machine operation requires a moderate skill level, leading to substantial cost reductions for the company. With its functionality, the machine surpasses manual labor in terms of efficiency, completing the shredding process in just 15 minutes per meter compared to the laborious 45 minutes required by manual methods. The utilization of this fabricated machine is more efficient in shredding scrap materials which produces smaller output sizes as compared to other relevant literature. This means the security and protection of confidential information upon disposal of scrap materials.

V. Acknowledgment

The authors of this study acknowledge the people who contributed valuable insights to make this research possible and the Technological University of the Philippines Taguig Research and Extensions Services for allowing this research to be presented and published.

References

- [1] Bennison, P. F. and Lasher, P. J. "Data security issues relating to end of life equipment," IEEE International Symposium on Electronics and the Environment, 2004. Conference Record. 2004, Scottsdale, AZ, USA, 2004, pp. 317-320, doi:10.1109/ISEE.2004.1299737.
- [2] Oladejo, A. E., Manuwa, S. I., and Onifade, T. B. "Design and fabrication of a shredder," IOP Conference Series: Earth and Environmental Science, vol. 445, no. 1, p. 012001, 2020. doi:10.1088/1755-1315/445/1/012001
- [3] Wong, J. H., Gan, M. J. H., Chua, B. L., Gakim, M., and Siambun, N. J., "Shredder machine for plastic recycling: A review paper", in <i>Materials Science and Engineering Conference Series</i>, 2022, vol. 1217, no. 1. doi:10.1088/1757-899X/1217/1/012007.
- [4] Brusa, E., Morsut, S. and Bosso, N. (2013) 'Dynamic behavior and prevention of the damage of material of the massive Hammer of the Scrap Shredding Machine', *Meccanica*, 49(3), pp. 575-586. doi:10.1007/s11012-013-9812-x.
- [5] Dora, V., Ventakesh, P., Sai Yugendhar, S., Prasanth, S., Sai Kumar, D., and Ramesh Naidu, J. "Design and Fabrication of Plastic Shredder Machine", in *International Journal of Research Publication and Reviews*, 2023, vol 4, no. 6, pp 1816-1821.
- [6] P. A. Oliveira, F. Taborda, C. E. W. Nogueira, and F. Margarido, "The Effect of Shredding and Particle Size in Physical and Chemical Processing of Printed Circuit Boards Waste," *Materials Science Forum*, vol. 730-732, pp. 653-658, Nov. 2012, doi: 10.4028/www.scientific.net/msf.730-732.653.
- [7] M. Milligan, "Why Does Size Matter For SSD Shredding?," *Securis*, Jun. 2022, [Online]. Available: https://securis.com/news/why-does-size-matter-for-ssd-shredding/?fbclid=IwAR0jc63GI4epDXyOAIbKIWM1kVb8Ln3775L_NI8neuMBjhGWgh_oO3GnkM
- [8] RecyclingInside, "Shredder & Crusher Systems for Size Reduction," *RecyclingInside*, Oct. 2020, [Online]. Available: <https://recyclinginside.com/shredder-crusher-systems-for-size-reduction/>
- [9] M. Milligan, "What is a Certificate of Data Destruction?," *Securis*, Jun. 2022, [Online]. Available: https://securis.com/news/what-is-a-certificate-of-data-destruction/?fbclid=IwARIQkwx3Dqs_zHsczuWrfLb_IUUR-GnDvUPPjix_dVtwnB3zxaYIbFLb8

Development and Evaluation of Spring Suspension Compressor Tool for Automobile Suspension System

Christopher T. Estopin*¹, Jonathan O. Mañas*², Jake A. Algo*³

Abstract

This study was conducted to develop a suspension spring compressor tool for automobile and evaluate the level of functionality among chosen coil spring type of suspension system particularly; Sedan, Sports Utility Vehicle (SUV), Utility Van (UV) and to determine the cost of the project. The Null hypotheses of this study which states that the overall functionality level of the developed suspension spring compressor is FUNCTIONAL after a series of trials on different types of vehicles used coil spring type of suspension system was tested and accepted. This study utilized the Quantitative research methods and an experimental research design. There were a series of three tests made on suspension spring compressor. The evaluation was done by five panels of expert, each of them were given an evaluation guide sheets to record its evaluation

Keywords: suspension system, coil spring suspension, coil spring compressor

I. Introduction

The manufacturing and servicing of the automobiles have become the key elements of industrial economy. The automobile has an engine which is the main source of power, and sometimes called as the heart of automobiles and it is the automotive vehicle power plan and prime mover. It converts chemical energy in the form of reciprocating and rotating forces which propelled the vehicle. Without the engine, the vehicle cannot move or run from one place to another. It is made of stationary and moving parts working as a unit to produce power which is transmitted by the clutch, transmission, universal joints, propeller shaft, and differential and drive axles systems where the wheels are attached [1].

Other part is the suspension system, it is a system of tires, tire air, springs and shock absorber and linkages that connects a vehicle to its wheels and allows relative motion between the two. Suspension system must support both road holding/handling and ride qualities which are at odds with each other [1].

There are several types of suspension system that are used in an automobile now a day among which identified are the air suspension that uses an airbag, leaf spring that uses several sizes of leaf metals set into one and bolted in common, torsion bars that uses metal round bar and twist once the wheels encounter irregularities on the road surface, and spring suspension that uses a coil spring. All of these holds the function to; maintain correct vehicle ride height, reduce the effect of shock, support vehicle

weight and most of all keep the tires in contact to the road [2].

Aside from the leaf spring because of its simplicity, coil spring type of suspension system was widely used in an automobile especially in front wheel suspension system.

A suspension strut is actually a shock absorber that is already mounted inside a coil spring, essentially two suspension components in one. This type of dampening structural supports for the car's suspension system [2].

As the coil spring continuous to work, its size will be shortening, force will be lessening and practically cannot perform its function well and add danger to a running vehicle, these parts should be taken care and be replaced.

In taking out of size and damage coil spring from a strut shock absorber is quite easier. However, in replacing it back with a new one is more difficult there is a need of a devise for compressing a strong force of the coil spring suspension which was not available in our automotive technology department.

Along this notion, the researcher became interested in developing a devise known as Suspension Spring Compressor in trying to experiment and evaluate its level of functionality among chosen coil spring suspension system.



*1 Project Manager, DML Eastern Visayas State University, Tacloban City



*2 ITSO Coordinator Eastern Visayas State University, Tacloban City



*3 Head, Industrial Technology Department, Eastern Visayas State University, Tacloban City

Objectives of the Study

1. Develop and fabricate a suspension spring compressor for automotive technology;
2. Evaluate the level of functionality of the project among chosen coil spring type of suspension system particularly:
 - 2.1. Sedan
 - 2.2. Sports Utility Vehicle (SUV)
 - 2.3. Utility Van (UV)
3. Determine the cost of the project.

Conceptual framework of Study

Any spring, whether it's a leaf, torsion or coil spring, must compensate for irregularities in the road surface, maintain the suspension system at a predetermined height and support added weight without excessive sagging. Each of those functions is extremely important in providing comfort, precise handling and load-bearing capability in the modern vehicle. As a vehicle gains speed, the springs begin to absorb the impact of striking irregularities in the road surface. As vehicle speed increases, a stiffer spring rate is required to keep the axles and wheels in contact with the road surface. This is why high-performance vehicles tend to use stiffer suspension systems than regular passenger vehicles. Because a compressed spring will extend in a violent fashion, shock absorbers must be used to dampen the spring's compression and extension cycles. Without dampening, a spring's violent compression and extension would cause a vehicle to lose control on a rough road surface [3].

A coil spring (also called helical spring) is a kind of torsion spring which can store energy and release it later when needed. It can also absorb shock and maintain the force between two contracting surfaces together with a shock absorber, coil springs are pre-assembled as one coil over unit installation [4] as shown in Figure 1.

Coil springs expand and contract countless times whenever a vehicle is driven, absorbing the bumps and turns encountered along the way. They work along with the shock absorbers, soaking up bumps and roughness while the shock absorbers limit up-and-down movement. Over time, though, coil springs eventually wear out from old-fashioned metal fatigue. When they do, the vehicle tends to sag, droop, and handle poorly. Changing your coil springs can restore the vehicle's suspension and significantly improve vehicle ride, handling, and safety. Standard practices include replacing coil springs in pairs, and also replacing the shocks at the same time. Before starting this project, you should also check the spring insulator pads, which may also be worn out [5].

Figure 2 on the succeeding page shows a disassembled coil spring suspension. Figure 3 on the succeeding page illustrates the schema showing the concepts of the study following the input, process, and output. The inputs are the disassembled parts of a coil spring suspension system. The process is consisting of the developed suspension spring compressor which compresses the strong force



Fig. 1. Pre-assembled coil spring suspension



Fig. 2. Disassembled coil spring suspension

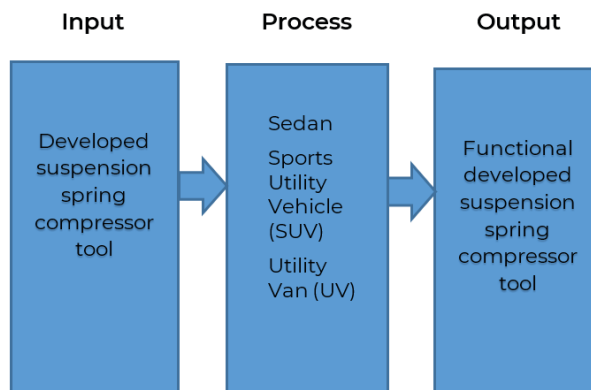


Fig. 3. Schema showing the concept of the study

of the spring suspension. With the sufficient input and carefully done through process, its output produces a pre-assembled coil spring suspension system.

A suspension spring compressor as presented in Figure 4 on the succeeding pages is a device having a hydraulic unit used for compressing a strong force of the coil springs suspension. It includes a fixed base plate, a movable plate attached to a hydraulic unit, an adjustable head base suitable for different height of suspension springs, two posts where these bases are mounted and some feet to where it stands.



Fig. 4. Schema showing the concept of the study

Scope and Delimitation of the Study

This study focused on suspension system of the automobile because the researcher believe that this is the only system that was directly affected by suspension spring compressor. The researchers also found out that there were several types of suspension system that were used in an automobile, among which identified were the air suspension, leaf springs, torsion bars, and spring suspension. All of these holds the function to; maintain correct vehicle ride height, reduce the effect of shock, support vehicle weight and most of all keep the tires in contact to the road. The developed spring compressor was made used to compress the coil spring of a coil spring type suspension of Sedan, Sport Utility Vehicle (SUV), and Utility Van (UV) only.

This experiment was conducted on an actual development of suspension spring compressor. The evaluation of the developed coil spring compressor was made in the Eastern Visayas State University main campus Automotive Laboratory of the College of Technology. The researcher chose this place because all the needed tools and equipment were made available.

Significance of Study

The results of this study are beneficial to the automotive students, automotive teacher, vehicle owner, the automotive industry.

Definition of Terms

Coil spring suspension. A type of suspension system that uses coil spring. [6]

Shock absorbers. An integral part of a vehicle's suspension system. It is designed to absorb or dampen the compression and rebound of the springs and suspension. [7]

Suspension spring compressor. A tool used to compress the coil spring of a suspension system spring compressor. [8]

Spring. A device on the suspension system to cushion and absorb shocks and bumps and to keep the vehicle level on turns. After the stress or pressure exerted by the flexing of the spring has been removed, the spring returns to its original state. [9]

Related literature

Some coil spring compressors are designed to be used with air-powered wrenches. Coil spring compressors are tools that are used to service certain types of automotive suspensions. Some vehicles use components known as struts, which combine a shock absorber and spring into an integral component of the suspension system. The springs are very strong, and under significant tension, so simply taking a strut apart can be quite dangerous. To safely accomplish this task, and to facilitate the reassembly of a strut, a coil spring compressor is typically required. Struts have three primary components, which are a housing, cartridge, and coil spring. The housing typically bolts up to a steering knuckle and a strut tower, and the cartridge fits inside. A strut plate typically sits on top of the cartridge, and a coil spring is installed between the housing and the plate. In most cases, some type of bushing will also be installed between the plate and the tower. A coil spring compressor is usually required to permit the replacement of items such as cartridges and bushings.

The purpose of a coil spring compressor is to remove the tension from a strut assembly so that it can be safely disassembled for service and then reassembled afterwards. This is accomplished by inserting the feet or hooks of the compressor into the spring, and then tightening it with a pneumatic ratchet or hand tool. When the coil spring compressor is tightened, its feet or hooks cause the spring coils to draw closer together. That effectively removes the tension from the strut assembly so that the plate can be unbolted, and the cartridge may safely be replaced. It is sometimes possible to take a strut assembly apart without this type of tool, if the technician is careful and works very slowly, though it is typically dangerous to attempt this. Since the coils are very strong, and under extreme pressure, they may move suddenly when the pressure is released. If a technician is in the way when that happens, severe injury, or even death, may occur. Moreover, at that point it would be difficult or impossible to put the assembly back together with a new shock absorber cartridge. Consequently, it is generally much safer and more practical to use a coil spring compressor when servicing strut assemblies [10].

Springs and shock, they come together in suspension kits. They go hand in hand. the springs are the foundation of a suspension system. It allows the up and down movement of the wheels with minimal impact on the chassis and the rest of the vehicle. The primary job of springs, though, is to hold the weight the vehicle and its cargo. As the spring rate increases the more weight it takes to compress the

spring, and thus the more weight the spring can hold. A higher spring rate does not necessarily mean that it will add any height and handle more weight. However, using a spring with a much higher rate than needed will contribute to a harsh ride, and using one with a rate that is lower than needed will result in the spring being partially compressed at ride height. The latter situation will reduce ride height and the spring failed to manage the weight so it will compress more easily, leading to excessive and abrupt contact with the dumper. Spring rate is primarily dictated by thickness of steel used for the spring. For coil springs, the thicker the diameter of the coil, the higher the rate. Understanding shocks is more challenging. This is because most of the shock works is hidden inside the tube. Also, most shock manufacturers won't share their specifications. Another option is an adjustable shock. The most important thing to remember, though, is that shocks do not hold weight. The purpose of the shock is to control or dampen the motion of the spring. Shocks are essentially hydraulic pumps. A piston is attached to the shock rod. As the shock compresses and extends, this piston moves up and down inside hydraulic fluid. Orifices in the piston dictate how easily the piston moves by varying how much fluid is allowed to transfer from one part of the chamber to another. This converts the kinetic energy of the spring into heat, which is then dissipated through the shock fluid. The variables that affect how much dampening there are the volume of the chambers, the diameter of the piston, the size of the orifices, and the type of fluid and gas used. And that's in the simplest design. Shocks can be either twin-tube or monotube design. Twin-tube shocks hold the hydraulic oil and gas (usually nitrogen) in the same chamber. As the name implies, there are two tubes, and the mixture of fluid and gas moves from one into the other as the piston moves up and down. These are simple, lower-cost shocks. One drawback is that they can overheat when used in heavy vehicles or ones with very heavy axles and tires. There are gas-charged versions of twin-tube shocks that have a small chamber filled with low-pressure nitrogen gas to minimize aeration, reducing overheating issues.

Monotube shocks are considered high-performance. They separate the hydraulic fluid from the gas, significantly reducing the opportunity for aeration. They do this by introducing a floating piston in addition to the piston attached to the shock rod. The gas charge under the floating piston is at high pressure. A variation of the monotube shock that is very popular for off-roading is one with a remote reservoir. This locates the gas charge and floating piston in a separate canister. This provides more capacity for fluid and gas for better heat dissipation and the potential for different tuning options. Within each of these designs, the tech that sets one shock apart from another is the specific valving. Custom shock builders can configure the valving for the weight of your vehicle, the weight of the axle, wheels and tires (unsprung weight), and how you use the vehicle. High-speed desert racing requires much more attention to shock tuning than rock crawling does [1].

II. Related Studies

The study done by Hareesh Sunil Rawool et al. on their study Design, development, and manufacturing of hydraulically operated coil spring compressor for MacPherson type suspension system discusses the purpose of this tool is for use on, a MacPherson-type independent suspension assembly of a vehicle, the tool includes upper and lower C-shaped pressure brackets which for receiving spaced coils of the spring intermediate the opposed connected ends of the spring. Lower bracket is linearly adjustable for initial alignment with the spaced spring coils. A bottle jack is positioned below the lower bracket. Hydraulic pressure is provided through bottle jack mounted on the base for moving the bracket toward one another to compress the spring and for releasing the spring [12].

The present study is similar to The study done by Hareesh Sunil Rawool et al. for it uses a bottle jack positioned below the lower bracket and a provide a hydraulic pressure resulting to move these bracket towards each other compressing the spring and for releasing the spring [12]. However, the present study has same idea and only differ in the construction of the spring compressor.

Another study conducted by Roger C. McWilson in titled Stress Analysis and Fatigue Testing of a Hermetic Compressor Suspension Spring, his paper describes the use of high-speed motion photography and experimental strain measurements to describe the performance of helical compression-type suspension springs during the stopping motion of a hermetic refrigerator compressor. Operating stress ranges were used to relate accelerated life test loading to service loading and to appraise the quality of the springs in relation to expected fatigue behavior. The feasibility evaluation, and confirmation of performance by experimental strain measurements, of a spring fatigue test is described [13]. The present study is to compress the suspension spring so it can be release for disassemble and returned it back for reassemble. Roger C. McWilson on his study showed similar manifestation in terms of compressing the suspension spring. However, it differs on the purpose of investigation he used suspension spring compressor for stress analysis and fatigue testing of a Hermitic Suspension spring.

III. Research Method

This study utilized the Quantitative research methods since it emphasized objectives measurements and the statistical numerical analysis of data collected through researcher made observation guide sheets questionnaires, and by manipulating pre-existing statistical data using computational techniques [14]

Research Design

An experimental research design was used in this study. The discussed device was made and designed to respond to the needs of a compressor that will compress the suspension spring at high resistance force so it can be removed, replaced and/or return to its original position before it goes into a wander and create any accident to shop workers/ students during Automotive laboratory shop works particularly on suspension system.

The researchers used three sets of spring suspensions, one for sedan, one for SUV and another one spring suspension for Van UV type of vehicles tested in same suspension spring compressor.

Variables of the Study

The average level of functionality of suspension spring compressor of different coil spring suspension represents independent variable. The dependent variable is the developed suspension spring compressor used in this study.

Data Gathering

The data gathered are as follows:

1. Average level of functionality of spring compressor on Sedan suspension spring.
2. Average level of functionality of spring compressor on Sports Utility Vehicle (SUV) suspension spring;
3. Average level of functionality of spring compressor on Utility Van (UV) suspension spring.
4. Total cost of the project.

The evaluation of different types of vehicles with coil spring suspension and number of trials per panel member were recorded.

Experimental Procedures

First Stage of the study (Developmental Stage) Preparation of Suspension Spring Compressor

A full skills and knowledge in measuring, welding, heating, and cutting out of materials was prepared by the researchers, including the particular tools and equipment needed.

Second Stage of the study (Experimental Stage) Evaluation of Suspension Spring Compressor

The evaluation was made on the suspension spring compressor. There were a series of three tests, and per test, suspension spring compressor was evaluated. The evaluation was done by five panels of expert that are composed of two (2) automotive technicians and three vehicle owners each of them were given an evaluation guide sheets to record its evaluation on the said device.

Methods of Scoring

The researchers used five levels of functionality as criteria for evaluation of suspension spring compressor, the levels are weighted and analyzed as follows.

Analysis	Weight
Highly Functional	5
Functional	4
Moderately Functional	3
Slightly Functional	2
Not Functional	1

Statistical Analysis of the Data

The statistical tool used in this study was weighted mean.

Mean (\bar{x}) or arithmetic mean is average obtained by adding all the arithmetical values or data then divide by the number of observations. Such tool was used to determine the mean level of functionality for the number of tests, and the mean level of functionality per suspension spring tested [15].

IV. Results and Discussions

FUNCTIONALITY LEVEL OF SUSPENSION SPRING COMPRESSOR FOR SEDAN

The evaluation of suspension spring compressor on sedan type of vehicle having coil spring as the system of suspension. It indicates that the total evaluation of panel number 1 was 5, panel number 2 was 4, number 3 was 5 another 5 from panel number 4 and the last but not the least an evaluation of 4 given by panel number 5. Among these mean evaluations, a total mean of 23 was recorded and a weighted mean of 4.6, this result gives a level of functionality of FUNCTIONAL as per as the criteria was concerned.

FUNCTIONALITY LEVEL OF SUSPENSION SPRING COMPRESSOR FOR SPORTS UTILITY VEHICLE (SUV)

The evaluation of the developed suspension spring compressor tool on SUV type of vehicle by panel number 1 gives a mean of 4, panel number 2 for another 4, panel number 3 is 4, panel number 4 is 5 and another 5 evaluated by panel number 5. All of these resulted to a total mean of 22, this total mean of 22 has a weighted mean equivalent to 4.4, as bases from the criteria 4.4 has fall to a functionality level of FUNCTIONAL.

FUNCTIONALITY LEVEL OF SUSPENSION SPRING COMPRESSOR FOR UTILITY VAN (UV)

The evaluation of suspension spring compressor on utility van type of vehicle. Panel number 1 gave a mean number of 4 likewise the two following panels number 2 and 3. Panel number 4 and 5 give credit of 5 as their evaluation. All the evaluation done by all of the panels achieved a mean evaluation 22. This number 22 reached the weighted mean of 4.4 and the level of functionality of FUNCTIONAL.

To have this devise a skillful hand of the researchers and a six thousand eight hundred twenty Philippine currencies were needed, a very minimal amount as to compare the uses, safety and comfort of the workers doing the job on suspension spring compression.

V. Summary of the Findings

1. The total mean of suspension spring compressor on sedan was 4.6 weighted and analyzed as functional;
2. The total mean of suspension spring compressor on Sports Utility Vehicle (SUV) was 4.4 weighted and analyzed as functional;
3. The total mean of suspension spring compressor on Utility Van (UV) was 4.4 weighted and analyzed as functional;
4. Total cost of the project was Php6,820.
5. The overall functionality level of the developed suspension spring compressor was 4.47 weighted and analyzed as FUNCTIONAL.

VI. Conclusions

1. The functionality level of suspension spring compressor on SUV was functional.
2. The functionality level of suspension spring compressor on Sedan was functional
3. The functionality level of suspension spring compressor on UV was functional
4. Total cost of the project was P 6,820.
5. The overall functionality level of the developed suspension spring compressor was FUNCTIONAL.

VII. Recommendations

1. The developed suspension spring compressor must be used for SUV;
2. Suspension spring compressor must be used for sedan suspension system services;
3. Having a functionality level of Functional, suspension spring compression must be used for UV vehicles.
4. It is further recommended that this study be conducted on other type of vehicles using coil suspension spring as their suspension system.

References

- [1] (<https://www.quora.com>)
- [2] (www.carbide.com)
- [3] <https://www.tirereview.com> › the-role-of-springs-in-sus.
- [4] www.carparts.com.
- [5] <https://shop.advanceautoparts.com> ›
- [6] <https://www.ijera.com> › papers ›
- [7] <https://www.abletireandbrake.com>
- [8] <https://www.testingautos.com> › car_care
- [9] <https://www.howacarworks.com>
- [10] [www.tire truck.com](http://www.tiretruck.com)
- [11] <https://www.motortrend.com>

Comparative Performance of Motor-powered and Conventional Blower Furnace Using Charcoal as Fuel

Noel A. Baguilod*¹

Abstract

The investigation determined the performance of motor-powered blower furnace. Specifically, the study sought answers to the following objectives: (1) Design and fabricate a proto-type charcoal furnace; (2) Determine the performance of a conventional and motor-powered blower furnace; (3) Determine the time spent to reach the desired temperatures; and (4) Determine the significant difference of the time spent between the conventional and a motor-powered blower furnace in the heating process. The study advanced tested the null hypothesis which state that there is no significant difference in the performance of a prototype charcoal fired motor-powered blower furnace in terms of level of temperatures produced, and time to produce specific level of temperature and there is no significant difference on the time spent between the conventional and the motor-powered blower furnace along the following heating process annealing, hardening, normalizing, spheroidizing, and tempering. The findings of the study revealed that the motor-powered blower produced higher level of temperature on its corresponding weight of fuel than conventional furnace and the time spent to produce specific level of temperature was lower using the motor-powered blower furnace. There was significant difference of the performance in the temperature produced and the time spent required to reach the desired temperature between the two types of furnaces using charcoal as fuel. The prototype charcoal furnace has lesser time to spent to reach the desired temperature in heat treating processes (annealing, hardening, normalizing, spheroidizing, and tempering).

Keywords: annealing, charcoal-fuel, hardening, heat-treatment, normalizing, spheroidizing, tempering, time spent

I. Introduction

Blacksmith industry in the Philippines is one of the country's industries that promotes pride and economic growth. This produces different products such as local farming tools, garden tools, knives and even sharpened weapons. Some of the high-quality products are exported to other countries like sword with its tempered blade.

But this field of industry is rarely seen and seldom engaged and practiced among persons who have knowledge in blacksmithing. Some parts of our country like Batangas are still preserving this field of specialization. Others are found in Carigara, Leyte and some parts of Region VIII who supplies the needs of the farmers and for household chores purposes. As technology continually evolve, blacksmith shops most often are still using conventional type and blacksmithers are practicing traditional steps and methods in making such products.

In Leyte, Carigara is one municipality where blacksmith industries are mostly found. It is located along the highway wherein several and different products are being displayed. Mostly furnaces are in conventional type, and some equipped with improvised blower. Conventional furnace is made from ordinary wood. It looks like dirty

kitchen with clay on top and filling materials that serves as the pot for the heat treatment. The blower is made of wood shaped like a box and tied with cloth gasket to produce air. It is operated manually by pushing and pulling the blower handle (Carigara Journal 2012).

With the use of the conventional furnace in heat treatment, the air is not equally distributed to the charcoal, the main fuel of the furnace. This causes improper application of temperature to the metals that are being treated. There is unsustainability of air in the pot burner because it is driven manually. The unsustainability of air in the pot furnace causes improper application of temperature and the quality of the treated metals are affected. Moreover, more time is consumed during the process of heat treatment.

The study conducted by Aderoba and Fapeto (2000) stressed that to improve local blacksmith process, one thing to consider is the performance of blacksmith furnace. It is emphasized also that the common problems met during the blacksmith process are the improper application of temperature caused by the unequal distribution of air to the fuel where metals are being



*¹ Professor
Industrial Technology Department Eastern
Visayas State University, Tacloban City, Leyte

treated, and the constant waste of fuel that is used during the process because air pressure is not controlled. The problems facing local blacksmiths were also highlighted and the probable solutions to the identified problems which invariably lead to the design of air duct and the pot burner for closed furnace, the design of blower that sustain air pressure and heat treatment bath to replace the bellow, open furnace and water pot respectively, to effect mechanization of the local blacksmith. This design will actual lead to improved quality and time reduction in producing any blacksmithing product. The result of test of the fabricated furnace shown improved hen quality and the quantity of product in local blacksmith to some extent.

As an answer, the researcher fabricated a motor-powered blower furnace using charcoal as fuel that simply adapted what is latest technology today particularly on the concern of product quality. This furnace is designed to improve the performance of conventional furnace in terms of level of temperatures produced and the time spent during the heat treatment process of metals. Improving the temperatures produced, the fabricated furnace has a motor-powered blower that maintains sustainability of air to the pot burner. Its model is SY03, the size of pipe for the passage of air or tuyere is 2 1/2", 50/60 cycles, 220 volts, 1.8 amperes, and with 3000/3600 R.P.M. or revolvment per minute. The use of this motor-powered blower will increase combustion efficiency and shorten the process time since this blower has an attached rheostat to control the speed of the motor.

Moreover, it is also concerned with the comfort of the owners and workers because the fabricated furnace is designed with a semi portable machine that can easily be transferred from one place to another. Finally, improvement of mechanization process was also considered, and the fabricated furnace is designed with spacious pot burner and multiple small holes, and a 1/4" thick heat resistant steel plate where the charcoal fuel is placed. Therefore, in this study, improved furnace performance was hypothesized and hence, the study was conducted.

II. Methodology

The experimental method of research was used to test the performance of the propto-type motor-powered blower furnace using charcoal as fuel. The study employed t-test to see whether the difference between the mean performance of charcoal-fired motor-powered and conventional furnace is significant (Fraenkel et. al.,1993).

Development of the Proto-type Furnace:

The following procedures in the fabrication and assembling the charcoal-fired motor-powered blower furnace are illustrated in Figure 1.

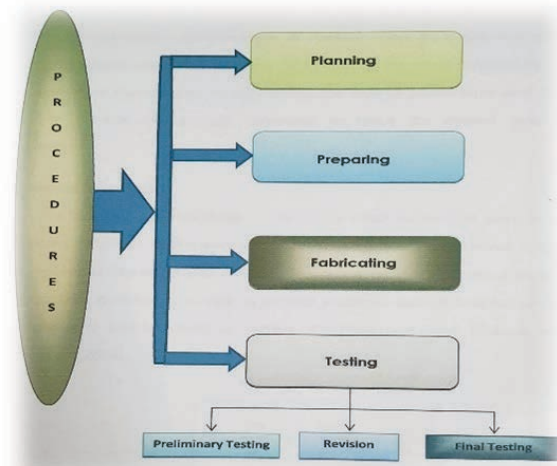


Fig. 1. Procedures in the fabrication

III. Materials and Design

The following are the materials used in the fabrication of motor-powered blower machine:

Materials, Tools, and Equipment Used

Materials	Tools	Equipment
Angle Bar 2"X2"	Tape Rule	Drill Press
Steel Plate	Try Square	Portable Drill
Plain Round Bar	Vernier Caliper	Bench Grinder
Gencord Welding Rod	Hacksaw	Portable Grinder
G.I. Pipe Gauge 20	Open End Wrench	Electric Motor Blower
Bricks	Hand Gloves	Welding Machine
Portland Cement	Center Punch	Infrared Thermometer
Corrugated Bar	Chipping Hammer	
Tie Wire	Welding Mask	
Bolt and Nut	Mechanical Pliers	
Paint QDE	Vise Grip	

Design of the Machine

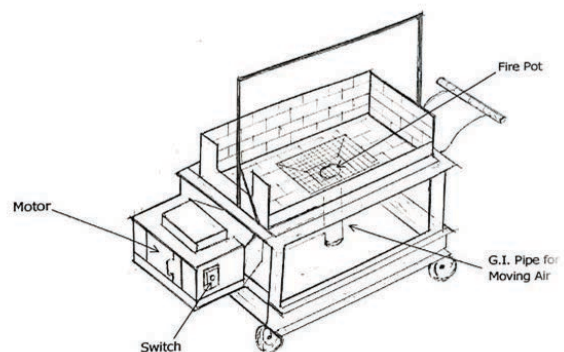


Fig. 2. Design of the motor-powered blower furnace

IV. Findings and Discussions

The study obtained the following findings:

On the Temperatures Produced. The motor-powered produced higher in all the five levels of weight in fuel having 662.7 °C for ¼ kg, 725 °C for ½ kg, 759.28 °C for ¾ kg, 847.14 °C for 1 kg, 934.9 °C for 1 ¼ kgs. On the other hand, the conventional furnace produced a little bit lower temperature compared to the prototype having 659.44 °C for ¼ kg, 723.2 °C for ½ kg, 755.7 °C for ¾ kg, 842.18 °C for 1kg, and 924.96 °C for 1 ¼ kgs.

Time Spent to produce Specific Temperature. The Conventional furnace required a little bit more time to produce specific level of temperature than the motor-powered blower furnace with 36.05 seconds for ¼ kg of fuel, 47.72 seconds for ½ kg, 49.06 seconds for ¾ kg, 47.52 seconds for 1 kg. of fuel, and 53.57 seconds for 1 ¼ kg of fuel. On the other hand, the motor-powered blower furnace required 32.18 seconds for ¼ kg, 45.15, 46.46, 45.57, 49.77 seconds using ½, ¾, 1, and 1 ¼ kgs. respectively.

Difference of Performance in terms of Temperature between the conventional and the Proto-type. The result of the t-test computation revealed that there was a significant difference of performance in terms of temperature of the two types of charcoal furnaces in all levels of weight fuel used to produce the desired temperature the t-ratios were -33.982 for ¼ kg of charcoal fuel, -23.705 for ½ kg of fuel, -55.986 for ¾ kg of fuel, -81.177 for 1 kg of charcoal fuel and -198.493 for 1 ¼ kgs of charcoal fuel which were all below the p-level at .05 (.000) level of significance with df=4.

Difference in Time Spent between the Conventional and the Proto-type Furnace. The result of t-test computation yielded values that were below p-level <.05 (.000), the computed t-test values were 101.393 for ¼ kg of fuel, 84.409 for ½ kg, 95.170 for ¾ kg of fuel, 130.810 for 1 kg., and 147.135 for 1 ¼ kgs. of fuel.

Time Spent to Reach the Desired Temperature for Heating Process. The data revealed a slightly longer time spent to reach the desired temperature for the conventional furnace having 51.50 seconds for annealing, 55.75 seconds for hardening, 58.34 seconds for normalizing, 52.53 seconds for spheroidizing and 49.81 seconds for tempering. While the fabricated motor-powered blower furnace required 48.52, 52.43, 55.77, 48.97, and 45.91 seconds for annealing, hardening, normalizing, spheroidizing, and tempering, respectively.

Difference of Time Spent in the Heat Treating Process between the two types of Furnaces. The Yielded values after the t-test was computed were all lower than the .05 (.000) level of significance, therefore there was a significant difference between the conventional and the fabricated proto-type motor-powered blower furnace in terms of time spent in the heat treating process. The t-ratio were 48.180 for annealing, 60.779 for hardening,

16.962 for normalizing, 74.272 for spheroidizing, and 41.418 for tempering.

V. Conclusions

Based on the findings of the Study, the following conclusions are made:

1. The motor-powered blower furnace produces higher level of temperature on its corresponding weight of fuel than conventional furnace.
2. The time spent to produce a specific level of temperature is quite lower using the motor-powered blower furnace.
3. There was a significant difference of performance in the temperature produced and time spent required to reach the desired temperature between the two types of furnaces.
4. The proto-type charcoal furnace has less time spent to reach the desired temperature in heat treating process (annealing, hardening, normalizing, spheroidizing, and tempering).
5. There was a significant difference on the time spent required to reach the desired temperature in heat treating process between the two types of furnaces using charcoal as fuel.

References

- [1] Walker, J. R. Modern Metalworking Workbook. The Goodheart-Willcox Co., Inc. USA, 2004.
- [2] Albert F. Check, Steve F. Krar, and Mario Rapisarda, Machine Tool and Manufacturing Technology. Delmar Publishers, USA, 2010
- [3] Jack R. Fraenkel and Normal E. Wallen, How to Design and Evaluate Research in Education. McGrawhill-Hill Inc. San Francisco State University, San Francisco California, USA, 2004.
- [4] Larry D. Hesel, and John R. Wright, Introduction to Materials and Processes, Delmar Publisher, Albany, New York, USA, 2006
- [5] James V. Lieberman, Introduction to Forging, American Technical Society, Chicago, USA, 2003.
- [6] Aderoba, A.A., Fapetu, O.P., Oke, Peter Kayode, 2000 An Evaluation of Improved Local Blacksmith Process, Federal University of Technology, Akure, Futa.
- [7] Daoud, Jihad and Nipl, Igor 2000 Enhanced Control Visualization and Process Characteristics: Video Monitoring of Coal Powder Injection in Blast Furnace, Tekniska Publisher, Lulea University of Technology, Lulea, Sweden.
- [8] Gustavsson, Joel R. 2004 Reactions in the Lower Part of the Blast Furnace with Focus on Silicon, Published Dissertation, Roya Institute of Technology, Stockholm, Sweden.
- [9] Grant, Michael G. 2006 Factors Affecting the Mechanical Properties of Blast Furnace Coke, East Mall Publisher, University of British Columbia.
- [10] Rafidi, Nabil E. 2005 Thermodynamic Aspects and Heat Transfer Characteristics of Hitac Furnaces with Regenerators, Stockholm Publisher, Sweden.



CHOMARUNITRADE
SERVICES CO. LTD.



NEW

FLUKE
Ti480U

**IS YOUR TRUSTED AND
RELIABLE PARTNER
FOR QUALITY METROLOGY
INSTRUMENTS**



WE ARE AN AUTHORIZED DISTRIBUTOR OF



For more information about our company, list of our products and free demos, visit our website at

 www.chomarunitrade.com

FOLLOW US ON SOCIAL MEDIA!



fb.com/chomarunitrade



linkedin.com/company/chomarunitrade



CONTACT US



(+63) 2 7949 2618



sales@chomarunitrade.com



West City Plaza Bldg., 66 West Ave., Quezon City



ADVANCED MANUFACTURING CENTER

MATERIAL EXTRUSION: PELLETS



**ERECTORBOT
EB2088HD**



GIGABOT X XL



COSINE AM1

MATERIAL EXTRUSION: FILAMENTS



ULTIMAKER S5



**INTAMSYS
FUNMAT PRO
410
HIGH TEMP**



**LEAPFROG
XCEL
TOWER TYPE**

MATERIAL EXTRUSION: VISCOUS SOLUTION

**HYREL HYDRA
16AS**



VAT PHOTOPOLYMERIZATION PHOTOCURABLE RESINS

**FORMLABS
FORM 2**



WE CAN PRINT:

- Standard Plastics
- Engineering Plastics
- Composites
- Resins
- Metals
- Ceramics

WE ALSO OFFER:

- R&D Collaboration
- Training
- Consultancy

EOS M290

POWDER BED FUSION: METALS

MATERIALS:

- Stainless Steel
- Maraging Steel
- Aluminum
- Titanium
- Cobalt Chrome



CERAMAKER 900 FLEX

VAT
PHOTOPOLYMERIZATION:
CERAMIC PASTE

MATERIALS:

- Alumina
- Zirconia
- Fused Silica
- Cordierite
- Silicore



Development and Verification of a Laterite Ore Refining Equipment

Lemuel N. Apusaga^{*1}, Jasmine Marie O. Gamboa^{*2}, Frederick N. Campoy^{*3}, Earl John T. Geraldo^{*4},
Edrhea B. Villas^{*5}, Mikee C. Tre-Inta^{*6}, Karen C. Santos^{*7}

Abstract

Laterite ore is identified as a feasible source for iron. This is critical to the process of developing steel which is widely used in different products in different sectors globally. There is a limitation, however, in the use of laterite ore in converting them to pig iron as doing so directly yields high amounts of sulfur and phosphorus, which are detrimental to the structure of steel. Hence, this study developed a refining equipment for desulfurization and dephosphorization of pig iron. The equipment was based on the Induction Furnace-Basic Oxygen Furnace process for refining and is suitable for low-capacity production. The designed equipment was able to refine the laterite-based pig iron to the quality of high-purity pig iron, having sulfur and phosphorus content of 0.02% and 0.04% respectively.

Keywords: laterite-based pig iron, steel refinement, desulfurization, dephosphorization

I. Introduction

Steel is a substantial part of material science and a key material in product development in modern technological advancement, being used in thousands of different grades of products and being produced in millions of tons a year globally[1][2]. However, due to its increasing demand over the millennia, manufacturers need to cope with the decreasing amount of raw material deposits of iron ore, coke, and coal. The reserves are limited, and most better-quality raw materials have already been used.

One of the feasible sources of iron is laterite ore. Laterite ore is the most abundant nickel source in the world. It is rich in iron oxide minerals like goethite and hematite, and also contains valuable metals used in the iron and steel industry such as nickel, iron, chromium, and cobalt. The Mines and Geoscience Bureau (MGB) reported estimated laterite reserves of 1.9 billion metric tons in the Philippines. Recently MGB, in collaboration with the Department of Science and Technology –Philippine Council for Industry, Energy and Emerging Technology Research and Development (DOST-PCIEERD), developed a technical feasibility study of converting low-grade laterite ores to nickel pig iron or pig iron. This pig iron is a vital component in stainless steel production[3].

The produced pig iron, as it is, however, cannot be used directly for steel production as it contains impurities such as sulfur, phosphorus, and silicon. These impurities are detrimental to the production of steel. There are varieties of methods that have been developed in refining, one of which was in used in desulfurization. This was by a Japanese company, Nippon Steel, who developed the

Kanbara Reactor (KR) process in 1963[4]. KR is a hot metal pre-treatment system for the desulphurization process in which a reaction takes place by the addition of reagents and mixing through the mechanical stirring refractory impeller. It utilizes the efficiency of lime (CaO) as lime is cheap and easily available[5]. Compared to the Injection system it is a very simple process and the treatment time is very short.

The co-injection process is a method that combines the advantages of reagents used. Common reagents used in the process are magnesium (Mg) and CaO. Magnesium enables fast desulfurization while lime allows for low final sulfur concentrations[4]. Sometimes lime is replaced with calcium carbide (CaC₂), which is more efficient, but due to some safety issues of CaC₂, this option is hardly used nowadays[6]. The reagents are stored in different dispensers and are only mixed inside the injection line. It is then injected into the hot metal via a straight lance with one opening at the bottom or two or four openings at the side.

A basic oxygen furnace (BOF) is made of a vertical vessel lined with basic refractory; it consists of parts namely spherical bottom, a cylindrical shell, and an upper cone. The main principle of BOF is to decrease the carbon content in liquid metal to produce desired steel. Moreover, phosphorus removal is favored in the BOF converter[7]. In a typical top-blown BOF operation[8], the hot metal is first transported from the blast furnace to BOF through torpedo vessels, and then the hot metal is poured into the furnace, which takes around 5 mins. Usually,



^{*1} Sr. Science Research Specialist
Metals Industry Research and
Development Center
Bicutan, Taguig City
Philippines



^{*2} Science Research Specialist II
Metals Industry Research and
Development Center
Bicutan, Taguig City
Philippines



^{*3} Science Research Specialist II
Metals Industry Research and
Development Center
Bicutan, Taguig City
Philippines

scrap metal is added to the furnace prior to hot metal addition to avoid splashing. Then, the additions of flux components commonly the usage of CaO as burnt lime and Magnesium Oxide (MgO) as dolomite. This is followed by oxygen blowing in three batches:

- 1) High lance height and low oxygen blowing to initiate oxidation (large metal dispersion) and heat generation reaction without touching the scrap;
- 2) Medium lance height and medium oxygen blowing rate for increased reaction rates and controlled slag formation; and
- 3) Low lance height and high oxygen blow rate to promote optimum carbon removal.

This present study focuses mainly on desulfurization, dephosphorization, and production of steel through the developed ore refining equipment based on the Induction Furnace (IF)- BOF process to meet the demand for steel in the country. Furthermore, at present, there is no commercially available steel-making equipment for low-capacity production which will be considered in the development of the refining equipment

II. Materials and Methods

The development of the ore refining equipment was separated into the reagents delivery system, the mini BOF and the oxygen lancing equipment. Apart from the developed equipment, an induction furnace was also utilized and is essential in the development of a lab-scale iron refinement facility. The developed equipment serves a different purpose in the refinement process, as summarized in Figure 1, and further explained in the following sections.

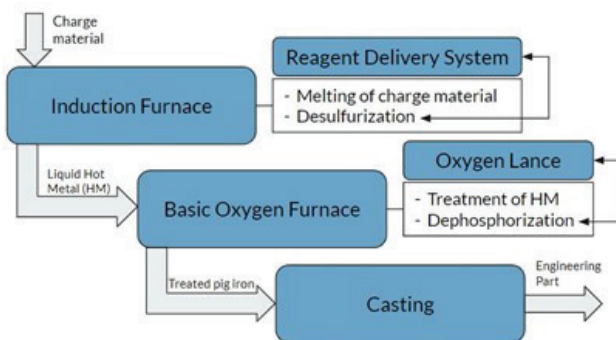


Fig. 1. Summary of process and equipment in refining

A. Scientific Basis

Based on a previous study[3], the pig iron composition from laterite ores were acquired as can be seen in Table 1. The study found these pig iron had excessive amounts of phosphorus (target of 0.08-0.15%) and sulfur ($\leq 0.05\%$) which are undesirable. Steel grades however differ in application and composition depending on which standard is followed (i.e., European Standards (EN), Japanese Industrial standards (JIS), Germany Steel Grades (DIN), etc.[9]). The refining focus of this study, therefore, has been split into two chemical processes: desulfurization and dephosphorization of the laterite ore to produce viable pig iron for steel making.

Table 1. Composition of samples

Element	Zambales sample	Isabela sample
Fe	89.3	89.7
C	2.74	1.80
Ni	1.36	1.69
Cr	3.45	2.63
Si	0.624	0.135
Mn	1.22	0.187
Co	0.193	0.138
S	0.450	0.125
P	0.192	0.200

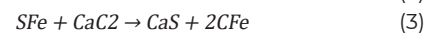
1) Desulfurization process

The presence of sulfur negatively influences both mechanical and corrosion properties in steel[11]. During desulphurization, the sulfur in the metal bath is reduced into the slag phase accompanied by the oxidation of oxygen into the metal bath[10]. A general reaction can be written as follows:



Where S and O are dissolved sulfur and oxygen in the hot metal respectively, and XO and XS are oxide and sulfide in the slag. Usually, there is a desulfurizing agent added to react with sulfur and mostly it is directly injected into the melt.

According to [4], the commonly used desulfurization agents are CaO, CaC₂, and Mg. These reagents are sometimes used individually, in a combination with two, or mixed with three. Mixing of reagents into the hot metal is commonly done with either the Kanbara reactor (KR) process or the co-injection process[4]. All processes are based on the following chemical reactions:



*4 Project Technical Specialist I
Metals Industry Research and
Development Center
Bicutan, Taguig City
Philippines



*5 Science Research Specialist II
Metals Industry Research and
Development Center
Bicutan, Taguig City
Philippines

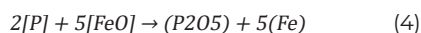


*6 Project Assistant I
Metals Industry Research and
Development Center
Bicutan, Taguig City
Philippines

The study [4] found that reaction (4) is 20 times faster than reaction (2). This means that magnesium is a much faster desulfurizing agent than lime and prevents resulfurization. Mg also has a high vapor pressure which leads to violent reactions when injected, which is why it is usually combined with other desulfurizers[10]. The formed Calcium Sulfide (CaS) and Magnesium Sulfate (MgS) after the reactions between the reagents and dissolved sulfur will rise to the surface to form a slag layer. Hence, when this layer is skimmed off, the sulfur is effectively removed from the liquid hot metal.

2) Dephosphorization process

Phosphorus is mostly an unwanted substance in both regular and stainless steel. Phosphorus reduces the plasticity and toughness of the steel if the content is too high[8]. Common oxidation of phosphorus in a metal bath follows Eq. (5), where phosphorus in the bath reacts with dissolved oxygen and oxygen ions of the slag phase (Figure 1).



The common flux components that are added include CaO as burnt lime and MgO as dolomite. CaO plays a very important role in dephosphorization and MgO is usually added to minimize the wearing of the converter wall linings [12].

B. Reagent Delivery System

The reagent injector was used for injecting reagents used for desulphurization. Initially identified reagents are lime, magnesium and calcium carbide. The desulphurization reagents need to be injected as they are less dense than the molten metal. If they are simply introduced at the top of the molten metal bath, the reaction with the sulfur in the bath would be limited only with the melt in the surface. Those in the bulk will not be affected. Initial activation tests of the reagents indicate that they react at temperatures above 1450 °C. It was then decided to conduct the desulphurization operation in the induction furnace for temperature control. Industrial desulphurization practices are conducted in a separate treatment ladle. But then they have significantly large volumes with massive heat content that can retain melt temperatures over a longer period of time. Our experimental setup is only 50 kg. At this quantity, the melt would rapidly lose temperature well below the activation temperatures of the reagents. As a result, special operational considerations were taken to ensure that the furnace lining would not be damaged by the desulphurization operation.

C. Basic Oxygen Furnace (BOF) Vessel

The BOF vessel will be used for the dephosphorization process. During this process, the molten metal is blown with high pressure and high-volume oxygen gas to oxidize the phosphorus, along with some other elements. The BOF vessel should be able to withstand the treatment parameters and the high temperatures that will be generated with the oxidation of carbon, silicon and other elements in the laterite pig iron. The original concept for this equipment proved to be sufficient for the actual operations to which it was subjected with some modifications.

D. Oxygen Lance

The oxygen lance works in conjunction with the BOF in the dephosphorization process and is combined with it in the designing process. The oxygen lance will introduce oxygen gas to the molten metal for the dephosphorization process. In terms of performance, the lance needs to deliver a high volume of oxygen gas at supersonic speeds. The lance will be exposed to the high temperature generated by the oxygen lancing process.

III. Results and Discussion

The following sections separate the different developed equipment and the iterations of the components. In conjunction with this equipment, the process parameters and design of experiment was developed. The development of the process parameters will be reported in a different avenue.

A. Reagent Delivery System

This equipment eventually contained five (5) distinct components that underwent several design iterations and development to achieve the target performance. These are the splash shield, injection mechanism, mechanical injector, injector lance pipe and tip, and injector lance cladding. In addition, a support equipment, a water model setup, was designed and built to test the injector and its components and identify as many reagent injection operating parameters as possible prior to actual testing with the molten metal. This is made possible as the viscosity of molten metal at 1500°C is the same as that of water at 25°C.

1) Splash shield

The initial design target performance for the pneumatic injector system was to be able to inject the reagents at carrier gas pressures and flow rate low enough to achieve target rate of injection but at controlled splash over. This



*7 Science Research Specialist II
Metals Industry Research and
Development Center
Bicutan, Taguig City
Philippines

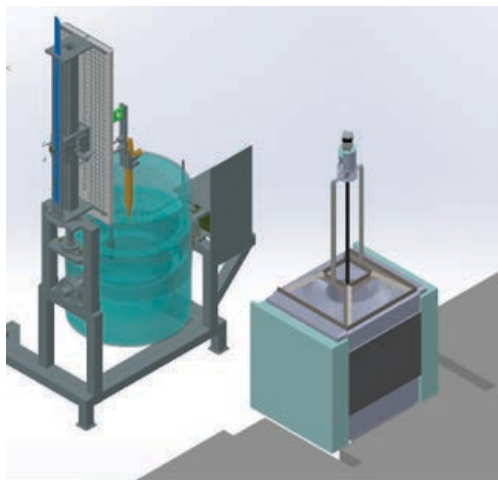


Fig. 2. Initial design of refining equipment

is because the injected carrier gas into the molten metal will eventually bubble up the surface. As the volume of gas injected increases, the possibility of splash over also increases, hence the splash shield was developed to protect the operator and equipment from molten metal splash out during injection, at higher carrier gas pressures and flow rates. The final splash shield design has the following features and functions:

- Redundant splash liners to contain and direct blowout in one direction.
- Base seal to contain molten metal if it got past the splash liners.
- Replaceable lance seal to protect injector and operator.
- 50 kg total weights to hold down the shield unto the base seal.

2) Injection mechanism

This is the part of the injector responsible for driving the reagents onto the lance and eventually into the molten metal bath. The first design involves a pure pneumatic drive - the nitrogen gas acts as carrier gas to drive the powdered reagents. Tests with the water model indicate very low injection rates - it would take at least an hour to inject the expected dosage of reagents. With the improvement of the other components, the prototype performance improved significantly to be used in the final design of experiment runs.

The injector chamber also had several features to achieve the following functions:

- Batch type injector - the chamber contained enough dosage.
- Fast charging and recharging of reagents.
- Seals to control carrier gas leakage.

3) Mechanical injector

After the initial injection mechanism prototype, the design already incorporated an additional mechanical driver to assist the carrier gas. This was because it was discovered

that the carrier gas alone is not enough to inject the powder at the required speed. The mechanical injector features a rotating screw driven by a motor.

The prototype features a 3D printed rotating plastic screw to push the reagents down the injector lance. Initially a stepper motor was used to drive the screw, but a servo motor was used instead as it provided faster injection rates. It was also determined that using coarser grained reagents significantly improved injection rates compared to powdered reagents. This may be because coarser grained reagents are more affected by gravity, hence they readily go down the injector instead of being blown inside the injection chamber by the pressurized carrier gas.

4) Injector lance pipe and tip

The lance pipe is the portion of the injector being immersed into the molten metal to deliver the reagents at the depth of the molten metal bath. The initial performance requirement is for the reagent to exit uniformly around the bath to reach as large volume as possible. In addition, the reagent jet is preferred to be only of a certain length or a certain distance from the furnace walls. Initial chemical reaction analysis between the alumina lining and nitrogen gas indicates a possibility of increased erosion of the alumina lining. Initial water model tests indicated that at carrier gas pressures and flow rates being used, the jet profile and length did not vary with different tip configurations. In addition, cladding of the tips for protection from high temperatures was a more critical design consideration. Tip configurations other than a simple straight tip pose a significant challenge to cladding. The lance and tips need to be cladded with a refractory coating to delay its melting at least for a few seconds until all reagents have been injected. Finally, a straight and open tip for its injector lance was used in consideration of the cladding constraints.

During initial tests, the lance pipe was found to only last a few seconds before being melted by the molten metal. To further reduce pipe consumption, the injector pipe has been redesigned to be a 2-piece pipe. Only half of the lance needs to be replaced after each injection.

5) Injector lance cladding

To delay the melting of the injector lance pipe during injection, the pipe needs to be cladded with an effective refractory coating. Several options were tested such as ceramic fiber, with and without zircon wash, zircon wash only and high alumina plastic refractory. Uncladded pipe was also tested with the assumption that the carrier gas flow would be enough coolant to delay melting of the pipe. The uncladded pipe melted almost immediately. Ceramic fiber offered protection for a few seconds while the alumina plastic cladded pipe offered the longest delay which was still only for a few seconds. In addition to the high consumption of lance pipes, once the pipe has melted, the reagents also seem to freeze inside the injection chamber, stopping the injection altogether.

The last design tested was by using paper tube cladding and the lance pipe lasted for 1 - 2 minutes without melting. The time is enough for the bulk of the reagents to be injected. However, reagents containing magnesium proved to be a challenge to inject. Typically, 3 to 4 cladding changes are needed before all measured dosages are fully injected.

B. BOF Vessel

Most of the modifications were conducted during the design phase as a result of rigorous review of concept of operations. The following aspects were thus improved: oxygen lance, mobility, preheating, melt depth measurement, lance attachment, lance height setting, length of operation, periodic sampling and periodic melt temperature measurement and melt stirring.

1) Oxygen Lance

According to industrial practices, the lance is a complicated and expensive device and is not meant to be consumable. Hence it needs to be protected from extreme heat generated during its operation. In terms of performance, the lance needs to deliver a high volume of oxygen gas at supersonic speeds. The design execution of these requirements is beyond the project capabilities and constraints hence the team decided to use an off-the-shelf device that can deliver gases to supersonic speeds, a machine cutting torch. The design could then focus on the protection of the torch from heat damage during lancing operations.

To some extent, the design has been successful in the use of the machine cutting torch as oxygen lance. Nevertheless, two torches were still destroyed during the testing of the design. The damage was caused by the failure of the refractory cladding, at treatment operations lasting for more than 5 minutes. This is because during lancing operation, the lance needs to be moved around the BOF vessel to reach more areas of the melt. Incidentally, during lancing a thick foamy slag is generated by the reaction of oxygen with the iron in the melt. It is the assumption that moving the alumina cladded machine cutting torch in the hot foamy slag hastens the erosion of the alumina cladding. Once enough cladding has been eroded, the cutting torch itself will be melted. As a result, only a maximum of five minutes oxygen lancing treatment was decided to prevent destroying the pricey machine cutting torches.

2) Preheating

Preheating the BOF is necessary to reduce heat loss of the molten metal upon its transfer from the induction furnace to the BOF ladle. Preheating is a matter of the maximum ladle temperature that can be attained which means that higher ladle temperature has lower associated heat loss. Heat loss is also time dependent, where the longer the duration from stopping the preheating to charging of molten metal equates to more heat loss.

Two design options were considered, a stationary ladle preheater or a mobile preheater. With the stationary ladle preheater, the BOF will be brought to the preheater then once preheated, will once again be moved and positioned in front of the induction furnace to receive the molten metal for the dephosphorization treatment. The final design used was the stationary one as it reached higher temperatures and was more fuel efficient.

3) Mobility

The BOF needs to be mobile to be flexible in terms of preheating and maintenance. Initial designs considered the use of built-in caster wheels. Subsequent design reviews found this solution to be unstable and unwieldy - there may be challenges in relocating the heavy BOF especially after preheating when it's already hot. The final design included Features to accommodate a pallet truck to move the BOF around as necessary.

4) Lance Attachment, Melt Depth Measurement, and Lance height setting

The oxygen lance needs to be easily deployable and removable. During preheating, the oxygen lance is not attached. It will be attached right after charging the BOF with molten metal. This is because the oxygen lance is connected to the oxygen and nitrogen lines which will be cumbersome to move as the BOF is relocated from the ladle preheater to the induction furnace. It should be easily attachable to minimize delay and heat loss of the molten metal. In this regard, the attachment mechanism design enables very fast deployment of the oxygen lance by utilizing a single pin connection with loose sliding fit.

During oxygen lancing, the lance needs to be positioned at a certain height above the molten metal bath. To be able to do that, the initial level of molten metal needs to be established. The final design involved the use of wood as a molten metal as a level indicator coupled to a dial that runs by an adjustable ruler. Once the molten metal level was determined, the ruler is adjusted, and accurate distance readings can be used to move the lance at the desired height.

According to published literature, the oxygen lance needs to be positioned at certain heights during various stages of injection. During initial runs, the project team tried oxygen lancing at different heights above the molten metal. However, one indicator of correct lancing height is the generation of foamy slag. When lancing at a distance, no foamy slag is generated. After several trials, it was discovered that foamy slag is generated when the lance is slightly immersed in the molten metal, approximately 5-10mm. Succeeding treatments then were conducted with this lance depth setting. It is possible that the lance operating pressure and velocity is not high enough to generate foamy slag at a distance from the molten metal level.

5) Periodic Melt Temperature Measurement

A complementary component of periodic sampling for chemical analysis is the periodic measurement of the molten metal temperature while oxygen lancing is also ongoing. To achieve this the project team modified the immersion pyrometer to be able to conduct this.

6) Melt Stirring

To rectify the issue of the production of the required foamy slag as indicative of good dephosphorization, the improvement of stirring of the melt for the lance to uniformly react with all the molten metal was considered. The simplest solution was by swinging the lance holder back and forth in an arc during the oxygen blowing.



Fig. 3. Prototype of final design of reagent delivery system



Fig. 4. Prototype of final design of BOF and oxygen lance

C. Results

Figure 5 show runs (A and B) conducted with the final design. Two samples (a and b) were taken at four different phases of the refining process which were before and after the ferromanganese (FeMn) injection, after desulfurization and after oxygen lancing.

Table 2 summarizes the percent by weight content (particular to sulfur and phosphorus content) of the refined laterite-based pig iron (averaged between the runs) as compared to other materials.

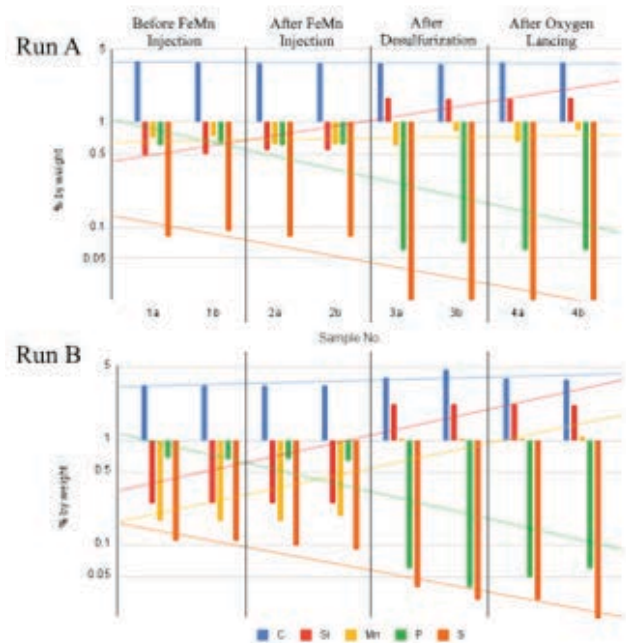


Fig. 5. Graphs on composition for runs A and B

Table 2. Comparison of composition of different materials

Material	% Sulfur	% Phosphorus
Refined Laterite-Based Pig Iron	0.02	0.04
Basic Pig Iron	≤0.05	0.08-0.15
Foundry Pig Iron	≤0.04	≤0.12
High Purity Pig Iron	≤0.025	≤0.035
Steel	0.02 - 0.1	≤0.12

IV. Conclusion and Recommendations

Both runs exhibited a trend of reducing sulfur and phosphorus throughout the sampling with the last samples showing the least amount of sulfur and phosphorus. Both sulfur and phosphorus concentrations were reduced in the treatment used. Based on these runs, the yield was able to achieve cleanliness comparable to that of a commercial high purity pig iron and steel as can be seen in the following table. This indicates that the design was effective in the refinement of the laterite ores.

Although the developed equipment is of sufficient performance, durability, and safety to accomplish the project objectives, significant improvements are needed to ensure reliability, repeatability, efficiency, and effectiveness of desulfurization and dephosphorization operations. In addition, it is also desired for the equipment to have higher capability in terms of the range of operational parameters that it can handle.

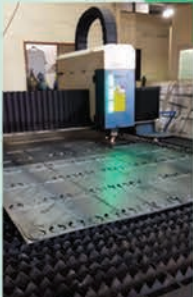
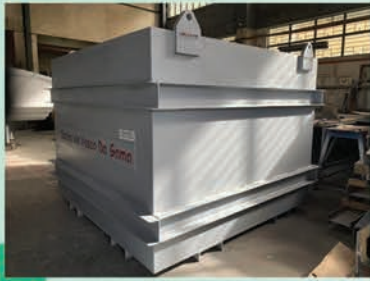
V. Acknowledgment

The project team would like to thank the Philippine Council for Industry, Energy and Emerging Technology Research and Development (PCIEERD), Mines and Geosciences Bureau - Department of Environment and Natural Resources, Steel Asia, Inc., and Pag-asa Steel Works, Inc. for their contribution to the success of this project.

References

- [1] S. F. Mayowa, "MASTER ' S THESIS Improvement of the Desulphurisation Process by Slag Composition Control in the Ladle Furnace," 2009.
- [2] D. Janke, L. Savov, H.-J. Weddige, E. Schulz, "CRAP-BASED STEEL PRODUCTION AND RECYCLING OF STEEL," 2000.
- [3] B. Bitanga, M. L. Sajonas, and C. Arnejo, "Pilot Scale Production of Nickel Pig Iron Using Low Grade Laterite Ores," 2019.
- [4] F. N. H. Schrama and B. van den Berg, "Comparison of Kanbara Reactor Magnesium Mono-Injection and Co-injection," *Millenium Steel*, vol. 16, no. 1, pp. 26–33, 2015
- [5] K. C. Mahendra, V. G. H, A. Kompil, K. Muniswami, K. Honnuraswamy, and R. N. Shivaraj, "Hot Metal De-Sulphurisation by KR Process," vol. 5, no. V, pp. 1556–1565, 2017.
- [6] F. Schrama, G. van Hattum, and B. van den Berg, "the Leading Hot Metal Desulfurization Methods: a Comparison Between Kr, Mmi and Co-Injection," pp. 323–332, 2017.
- [7] A. Ghosh and A. Chatterjee, *Ironmaking and Steelmaking Theory and Practice*, vol. 20. 2008.
- [8] A. Andersson and E. Wendel, "Parameters affecting dephosphorization of stainless steel," p. 10.
- [9] <https://www.purdue.edu/bidc/wp-content/uploads/2021/08/ISOGrade.pdf>
- [10] A. F. Yang, "A pre-study of Hot Metal Desulphurization," no. October, p. 60, 2012.
- [11] Lindstrom, S. Karamoutsos, and S. Du, Study on desulphurization of hot metal using different agents, no. April. 2015.
- [12] M. Owais and P. Metallurgy, "Desphosphorization in ironmaking and oxygen steelmaking," *Aalto Univ.*, vol. 358, no. 0, pp. 1–42, 2018.

SAMPLE PRODUCTS



"Your Complete FABRICATION Partner and Service Provider"

About us:

HDN TECHNOLOGY & RESOURCES INC. is a manufacturer of highly quality products made of STAINLESS STEEL & other metallic and non metallic materials.

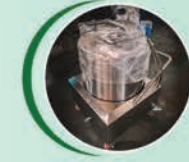
The Company was established in Year 2010. It employs a team of highly skilled employees to fabricate & produce best products & services. We strive to meet the expectation and needs of our valuable clients in a professional and timely manner.

PRODUCTS (Custom Made)

- *Blending Machine
- *Lockers, Cabinet, Racks, Table, Carts
- *Tanks, Mixers, Tumbler
- *Conveyors
- * Construction Items
- *Hotel Items
- *Kitchen Lavatory
- *Signages
- *Toolings & Machining Items
- *Jigs, Gears, Die
- * Others Metal Products

SERVICES OFFERED :

- *Bending
- *Shearing
- *Laser Cutting
- *Cutting
- *Rolling



HDN Technology & Resources Inc.

📍 B149 Lot I-C, 5th St. Golden Mile Business Park Maduya Carmona Cavite Philippines

☎️ (046) 482-0300 / (046) 683-5831

📞 0917-572-0300 / 0917-586-2071 / 0998-5332057

✉️ hdn_metalfabrication@yahoo.com

🌐 <https://www.facebook.com/HDNtechnology.ph>

Electropolishing Optimization for Additively Manufactured Aluminum Alloy

Keziah M. dela Rama*¹, Marvin Louise Carpena*², Ulysses B. Ante*³

Abstract

Additive Manufacturing (AM) process helps reduce or avoid machining of parts with complex geometries. However, the surface roughness of an AM component is very high. Reducing the surface roughness of AM component is one of the most critical factors in determining its suitability. To address this issue, a versatile alternative is the use of electropolishing, which is an anodic dissolution process, used to reduce surface roughness and obtain a bright and smooth finish. This study aims to develop an Electropolishing process for Additively Manufactured Aluminum Alloy and compare the results to Cast Aluminum. The aluminum alloy was 3D printed using Direct Metal Laser Sintering EOS M290 and the cast aluminum used as the comparison is A356. It was observed that the main process factors (concentration of solution, current density, temperature, and electropolishing time) determines the optimum electropolishing parameters. The samples were characterized by Atomic Force Microscopy (AFM), Profilometer, Tensile Test, and Corrosion Test before and after the electropolishing process. The tests demonstrated that electropolishing is a good surface treatment for the resistance to corrosion and reduction of surface roughness in additively manufactured aluminum but have a contrasting result on cast aluminum samples. The surface roughness of AM samples is significantly reduced by 62.40 percent according to the profilometer readings and up to 34.13 percent according to the AFM test. On the other hand, the cast aluminum becomes rougher as the electropolishing time increases due to its material.

Keywords: electropolishing, additively manufactured, AlSi10Mg, direct laser metal sintering, aluminum alloy

I. Introduction

Additive Manufacturing (AM) methods can produce nearly ready to use highly complex engineering components. However, the major problem of additively manufactured components is the surface finish of as produced metal parts is significantly rough and this surface roughness prohibits the direct utilization of AM components for the intended applications. A smooth and contamination-free surface is often required and can be obtained by a series of surface treatments including mechanical polishing, chemical etching and ultrasonic cleaning. Mechanical polishing may induce residual stress and introduce contaminants which are critical to some AM components. Conventional surface finishing may not be suitable for complex additively manufactured components with large internal surface areas. A versatile alternative is the use of electropolishing, which is an anodic dissolution process, used to reduce surface roughness and obtain a bright and smooth finish. Electropolishing has been utilized in many prototyping methods, including investment casting, photochemical machining, injection molding, laser cutting, metal stamping, 3D printing, direct metal laser sintering and electrical discharge machining.

Electropolishing is often referred to as a “reverse plating” process. Electrochemical in nature, electropolishing uses a combination of rectified current and a blended chemical electrolyte bath to remove flaws from the

surface of a metal part. The electropolishing method utilizes the electrochemical reaction between the anodic and cathodic electrodes, when the current is switched on with a DC/AC power supply, it removes the material from the surface of workpiece. In the literature, electrolyte composition is formulated according to the type of metal.

Aside from bright polish left on the surface, some important benefits include deburring, size control, micro finish improvement, ultraclean finishing, corrosion resistance and others. These metal improvement benefits are highly desirable to design and production engineers for cost savings and product lifespan improvement. It is also more convenient than conventional mechanical polishing for small and complex shape components. Vast engineering applications of electropolishing in many fields, includes food, medical, pharmaceutical, semiconductor, aerospace, automotive, medical devices and other metal working industries.

This study aims to optimize electropolishing process for additively manufactured Aluminum Alloy. This is in line with the Harmonized National R&D Agenda and the Mandate of MIRDC to strengthen the Metals & Engineering Industry through research and development (R&D) support.



*1 Science Research Specialist II
Metals Industry Research and
Development Center
Bicutan, Taguig City
Philippines



*2 Metals Technologist II
Metals Industry Research and
Development Center
Bicutan, Taguig City
Philippines



*3 Sr. Science Research Specialist
Metals Industry Research and
Development Center
Bicutan, Taguig City
Philippines

II. Methodology

Sample Preparation

The aluminum samples were additively manufactured using Direct Metal Laser Sintering EOS M290 and is composed of AlSi10Mg alloy. The cast aluminum used as the comparison for the additively manufactured is A356. The additively manufactured and cast aluminum specimen geometries were formed following the specifications outlined in ASTM D-638 for the type IV tensile specimens, see **Figure 1**. The build orientation of the additively manufactured aluminum is up-right.

The chemicals used for preparation of solutions were of technical grade and proprietary. Sample preparation was conducted on the part specimens to ensure a clean metallic surface. The sample specimens are properly mounted to a rack or jig to ensure the current will flow smoothly, which is then submerged in an acidic electrolyte solution. As printed samples were subjected to electropolishing directly, as well as the as cast samples and the results are compared. The samples were fully characterized before and after electropolishing.

Experimentation and Testing

Electropolishing was conducted in a glass beaker with an acidic electrolyte solution composed of a mixture of phosphoric, sulfuric acid and proprietary polyether. The solution was kept under constant agitation by rotating a magnetic stirrer at 200 rpm to avoid the accumulation of the etching solution on the surface of the sample. The process was held at an elevated temperature of about $85 \pm 10^\circ\text{C}$ while a 4.5 to 5 A current was maintained for 10 to 30 minutes. Stainless steel was used as the counter electrode for this electropolishing process. The surface area of the stainless steel counter electrode was maintained to be higher than sample surface area. The optimum electropolishing parameters were based on prior studies [1][2][3]. The electropolishing was carried on 30 samples each of additively manufactured and cast aluminum. The electropolishing behavior of additively manufactured Aluminum alloy and Cast Aluminum was observed and compared. **Figure 2** shows a simple electropolishing set up and **Figure 3** shows the actual electropolishing set up in this study.

For this study, the main parameters of electropolishing were examined such as current density, electrolyte concentration, temperature and electropolishing time to obtain the desired surface finishing of the sample specimens [4][5] [6]. To better understand the impact of electropolishing on the surface properties of additively manufactured aluminum alloy, the samples were characterized by Atomic Force Microscopy (AFM), Profilometer, Tensile Test, and Corrosion Test.

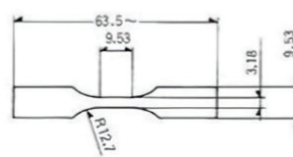


Fig. 1. ASTM D638, Type IV dog bone specimen

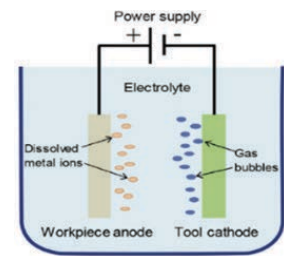


Fig. 2. Simple electropolishing system



Fig. 3. Actual electropolishing system

III. Discussion of Results and Findings

Main Process Factors

Electropolishing is based on Faraday's laws of electrolysis. It states that the amount of a material deposited or etched on an electrode is proportional to the amount of electricity used and the number of different substances liberated by a given quantity of electricity is proportional to their electrochemical equivalent (or chemical equivalent weight) [7][8]. The amount of metal removed in electropolishing depends on the specific bath concentration, temperature, current density, electropolishing time and the metallic workpiece being electropolished [9].

Concentration of Solution

In choosing the type of acid electrolyte to be used in electropolishing, we should consider that aluminum is generally separated to two main categories: casting and wrought alloys. The casting alloys are composed of high amounts of silicon that leads to their low melting points and decent fluidity and at the same time lessens their desirable smooth finish. On the other hand, wrought alloys have significantly different compositions and microstructures from casting alloys, that make them exhibit an improved shiny surface when electropolished [10]. There is silicon content on the additively manufactured AlSi10Mg and cast A356, thus the electropolishing finish produced is not shiny as compared to a wrought alloy that produces a mirror finish.

The electrolyte used in electropolishing is normally a concentrated acid media having a high viscosity. The samples are immersed in a glass beaker containing an

acidic electropolishing bath composed of a mixture of 90% phosphoric acid, 5% sulfuric acid and 5% polyether. The amount of phosphoric acid used in an electropolishing bath influences the operating conditions. Lower amounts of phosphoric acid ranging downwardly from about 60%, may require a relatively greater electropolishing time, increased voltages, and higher bath operating temperatures. The polyether forms a foamy film over the part to be electropolished, protecting it from chemical attack by the acidic electrolyte while being polished [1].

Current Density and Temperature

In electropolishing processes, the current density determines the optimum electropolishing parameters and it is largely affected by the type of material and electrolyte used in the process. The current would increase approximately in linear form at low voltage until it reaches a plateau in which the current keeps constant as the voltage increases. At this stage, the ions diffuse through the surface layer at a stable rate, creating electropolishing current that is little dependent on the voltage level [1] [12]. When the voltage is sufficiently high, the current will start to increase again in a more drastic rate, and chemical pitting on the surface will occur [13][14]. The first step of the electropolishing experiment would be to establish the current density to avoid surface damage. To limit the number of factors and make our optimization study manageable, we fixed the current density around 4.5 to 5 A/dm².

Other factors such as temperature [15][16] have significant effect on electropolishing. Low temperature reduces the solubility of ions in solution, resulting in an additional effect on the reducing the current density [17]. Higher temperature promotes the mass transportation because of low viscosity and facilitates the polishing reaction, however, uncontrolled, it will cause unwanted decomposition reactions. In this study, the solution was kept under constant agitation by rotating a magnetic stirrer at 200 rpm to avoid the accumulation of the etching solution on the surface of the sample. The process was maintained at an elevated temperature of about 85 ± 10° C.

Electropolishing Time

The surface roughness of the sample specimens tended to improve as the electropolishing time were increased. The surface roughness decreases fast at the beginning of polishing, and the decrease rate becomes slow with the increasing electropolishing time. In this study, the process was held at an elevated temperature of about 85 ± 10° C while a 4.5 to 5 A current was maintained. The additively manufactured and cast aluminum samples were electropolished for 10, 20 and 30 minutes.

Tensile Test

The tensile test was conducted to determine if the electropolishing of additively manufactured & cast aluminum will influence its mechanical property values,

particularly the tensile strength. For tensile test, the specimen geometries followed specifications outlined in ASTM D-638 for the Type IV tensile specimens. Shimadzu Universal testing machine with 50kN capacity were used to conduct the test. The samples were subjected to pulling until it reaches the maximum stress that it can bear before breaking, see Tables 1 and 2. In the results conducted on additively manufactured specimens, it is shown that electropolishing has a very minimal to no effect on the tensile strength. On the other hand, the results on Cast A356 shows that electropolishing weakens the material significantly, Figure 4.

Salt Spray Test

The salt spray test is done to verify how the additively manufactured aluminum and the cast aluminum will behave under a highly corrosive environment for 240 hours. The test was conducted in accordance with ASTM B 117-19 (Standard Practice for Operating Salt Spray (Fog) Apparatus) using Cyclic Corrosion Chamber, ATLAS CCX 2000, S/N: 25131. The actual test conditions were consisting of 5% Sodium Chloride (NaCl) Solution with a pH of 6.54 – 6.65, a temperature of around 35.3 – 35.6° C, and an air pressure of 17.0 to 18.0 psi.

At the end of the test, all the samples have appeared to exhibit moderate amounts of white corrosion products developed on the surface. The longer the electropolishing time of the electropolished specimens of the additively manufactured aluminum showed lesser signs of corrosion. The test therefore demonstrated that electropolishing is a good surface treatment for the resistance to corrosion in additively manufactured aluminum. However, the cast aluminum exhibits a contrasting result due to its material and form. As the electropolishing removes material from the cast aluminum, it reveals the porous structure of the sample, thus making it more prone to corrosion. This result signifies that the longer the electropolishing time of the electropolished specimens of the cast aluminum showed more signs of corrosion.

Table 1. Tensile test for AM aluminum

Additively Manufactured Aluminum, AlSi10Mg				
Sample Designation	Not Electropolished	10 mins Electropolishing	20 mins Electropolishing	30 mins Electropolishing
Thickness, mm	3.69	3.61	3.59	3.56
Width, mm	3.49	3.39	3.4	3.33
Cross-sectional area	12.88	12.24	12.21	11.85
Tensile Strength, Mpa	353	359	362	362

Table 2. Tensile test for cast aluminum

Cast Aluminum, 360-F				
Sample Designation	Not Electropolished	10 mins Electropolishing	20 mins Electropolishing	30 mins Electropolishing
Thickness, mm	3.38	3.37	3.32	3.29
Width, mm	3.21	3.14	3.12	3.12
Cross-sectional area	10.85	10.58	10.36	10.26
Tensile Strength, Mpa	160	104	128	131

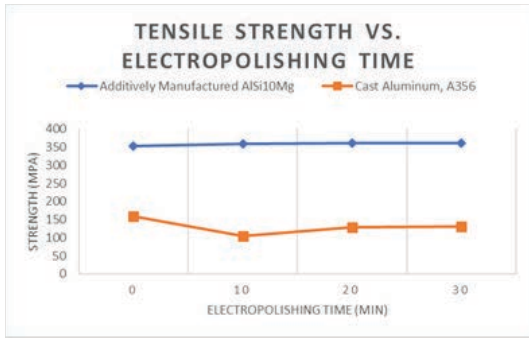


Fig. 4. Tensile strength vs. electropolishing time

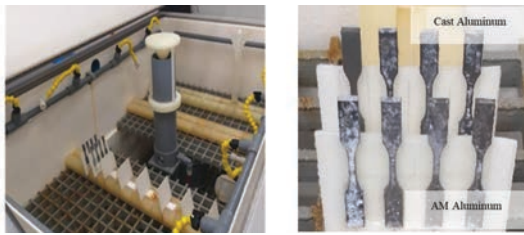


Fig. 5. Salt spray test set-up and actual results

Profilometer Test

Profilometers are used to measure surface roughness or surface finish. Contact profilometer has a stylus lightly dragging across the surface. The tip of the stylus rides in a line on the surface, moving vertically over the peaks and valleys. Changes in the stylus' height are registered electrically and tracked against position as the stylus moves, creating a measured profile, see Figure 6. Surface roughness was evaluated with a Mitutoyo SJ-201 contact profilometer, Figure 7.

Five different points were measured across the sample specimen and recorded the average roughness in Ra. The additively manufactured Aluminum shows significant reduction in the surface roughness as the time of electropolishing increases, see Figure 8. On the other hand, the cast aluminum exhibits a different result due to its material and the way it was made. As the material draws away from the surface of the electropolished cast iron, it reveals the porous structure of the sample, thus making it more rough as the electropolishing time increases, see Figure 9.

Material Loss

The electropolishing process works by removing thin layers of material from the surface of a metal part to achieve a smooth finish that is easier to clean and resistant to corrosion. There are many variables involved such as time, amperes, temperature, and bath chemistry. Material removal can be increased by adding more time and/or direct current to the process. These variables can be controlled to create a consistent, reliably controlled surface finish. On average, the surface roughness of parts can be reduced between 25-35% assuming a moderate amount of material removal [18][19]. In this study, the

effects of electropolishing on the thickness of additively manufactured and cast aluminum is observed by weighing and measuring the dimensions of the sample specimens before and after the process, see Figure 10 and Figure 11. Results show that the amount of material that is removed by electropolishing is directly proportional to the electropolishing time.



Fig. 6. Profilometer diagram



Fig. 7. Mitutoyo SJ-201 contact profilometer

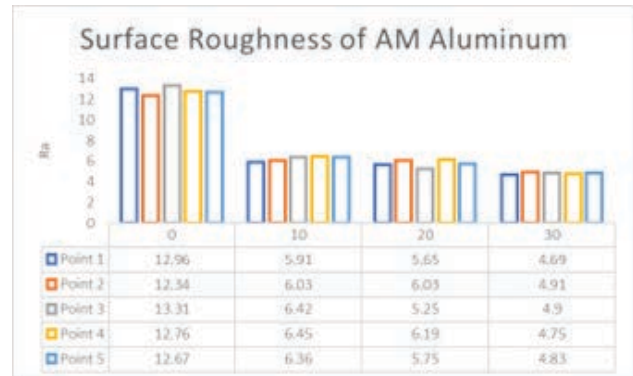


Fig. 8. Surface roughness of AM aluminum

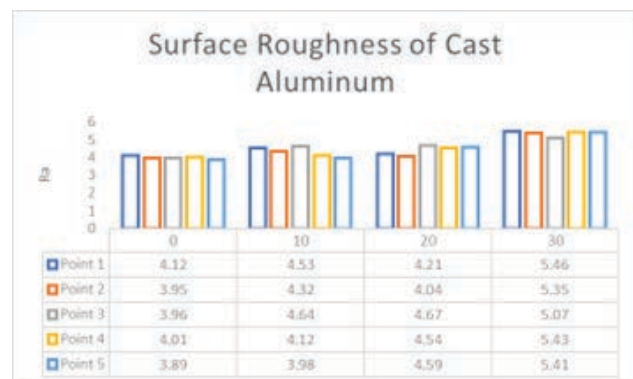


Fig. 9. Surface roughness of cast aluminum

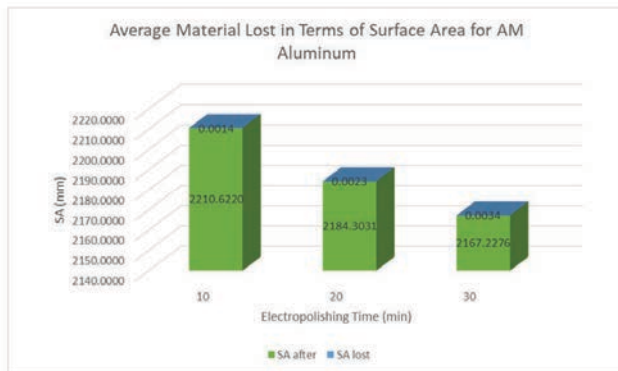
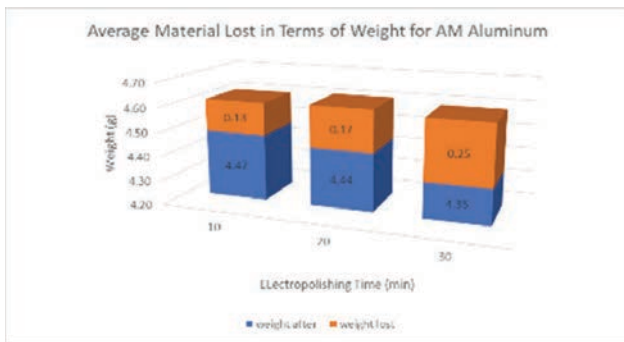


Fig. 10. Material lost of AM aluminum in terms of (a) weight and (b) surface area

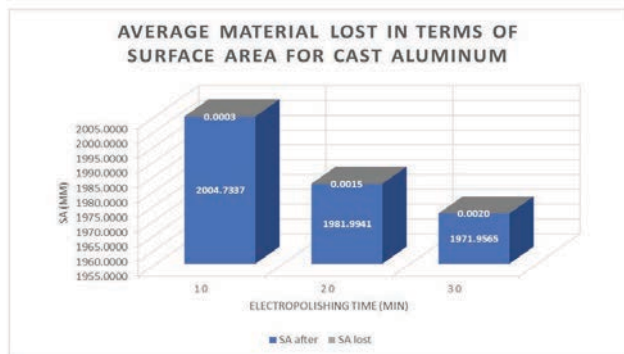
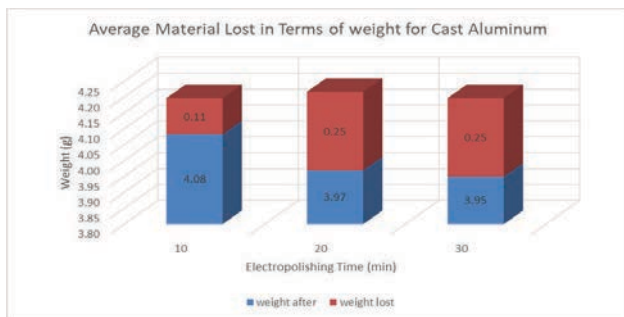


Fig. 11. Material lost of cast aluminum in terms of (a) weight and (b) surface area

Atomic Force Microscopy

The three-dimensional representation of the surface topography of the electropolished samples are obtained using Atomic Force Microscopy. AFM can measure the height profile, or roughness of the workpiece after electropolishing. One of many important applications of AFM in evaluating the electropolishing metal surface is to directly offer the information of the sample surface roughness, which cannot be fulfilled by electron microscopes [20][21][22]. The images were obtained by scanning an area of 12.5 μm x 12.5 μm. The surface roughness of the additively manufactured Aluminum is decreasing as the time of electropolishing increases. The surface roughness is inversely proportional to the electropolishing time. Conversely, the cast aluminum was observed to have a result that is different to the additively manufactured aluminum. The surface roughness of the cast aluminum increases as the electropolishing time increases and as the material draws away from the surface because it reveals the porous structure of the sample.

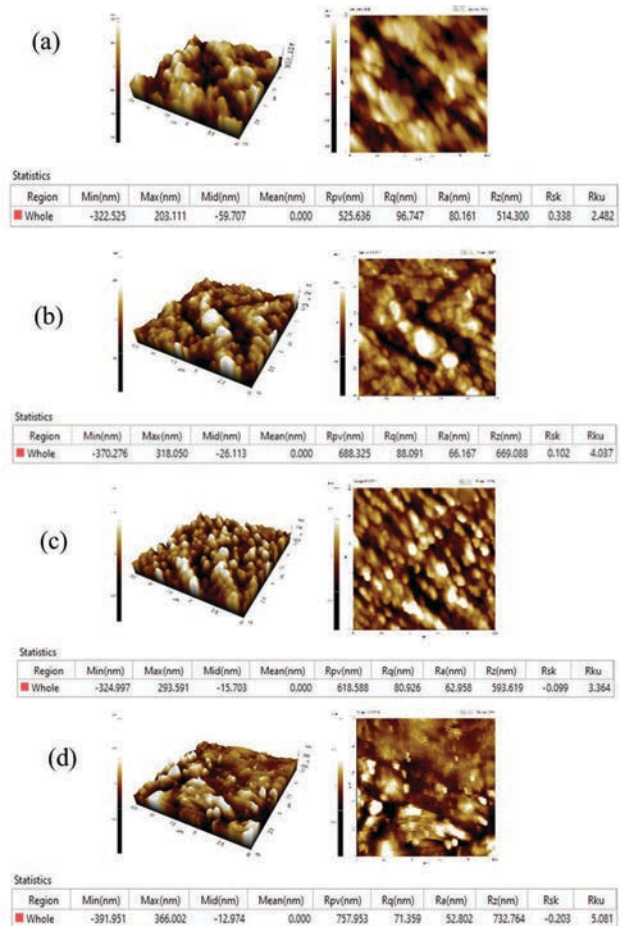


Fig. 12. AFM three dimensional images and height profiles of AM aluminum samples (a) unpolished (b) 10 mins electropolishing time (c) 20 mins electropolishing time (d) 30 mins electropolishing time

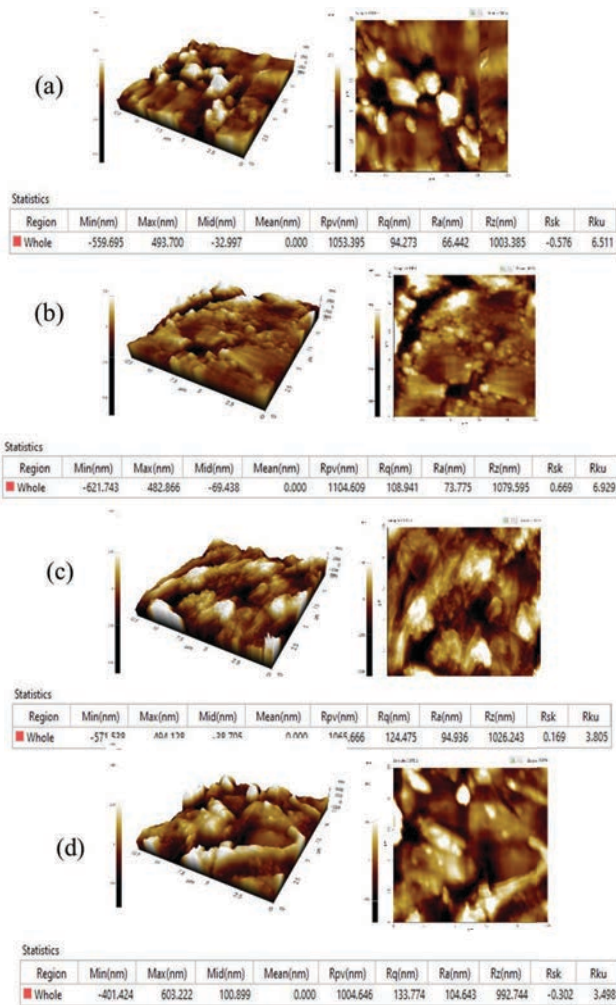


Fig. 13. AFM three dimensional images and height profiles of Cast aluminum samples (a) unpolished (b) 10 mins electropolishing time (c) 20 mins electropolishing time (d) 30 mins electropolishing time



Fig. 14. Photographs of electropolished AM aluminum samples: unpolished (left), and electropolished (right)

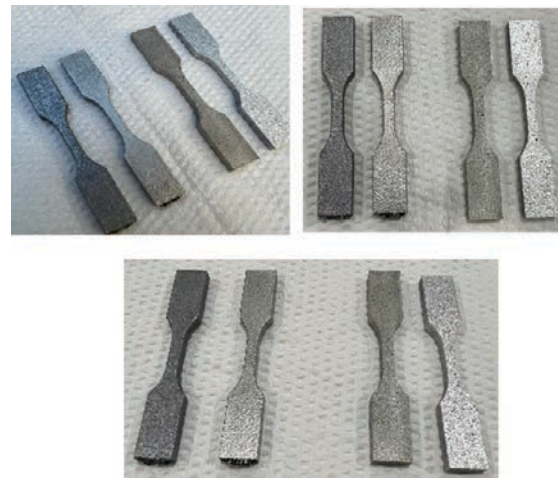


Fig. 15. Photographs of electropolished AM and cast aluminum samples (left set) before and after electropolishing of AM aluminum (right set) before and after electropolishing of cast aluminum

IV. Conclusion

The additively manufactured Aluminum shows significant reduction in the surface roughness as the time of electropolishing increases. The experimental data shows that the surface roughness (Ra) can be reduced to up to 62.40% according to the profilometer readings and up to 34.13% according to the AFM test. On the other hand, the cast aluminum exhibits a different result. As the material draws away from the surface of the electropolished cast iron, it reveals the porous structure of the sample, thus making it more rough as the electropolishing time increases.

In the results conducted on additively manufactured aluminum, it is shown that electropolishing has a very minimal to no effect on the tensile strength. On the other hand, the results on Cast aluminum shows that electropolishing weakens the material significantly. The longer the electropolishing time of the electropolished specimens of the additively manufactured aluminum showed lesser signs of corrosion. However, the cast aluminum exhibits a contrasting result, as the electropolishing removes material from the cast aluminum, it reveals the porous structure of the sample, thus making it more prone to corrosion.

The tests therefore demonstrated that electropolishing is a good surface treatment for the resistance to corrosion and reduction of surface roughness in additively manufactured AlSi10Mg alloy but not on cast A356 aluminum samples.

V. Recommendation

It is recommended for the future work to thoroughly investigate the impact of surface finishing methods on the mechanical properties of additively manufactured aluminum samples by conducting fatigue, creep and toughness test. Further studies are needed to achieve better control of the electropolishing process and better understanding of the key parameters.

References

- [1] S. Martin, "Electropolishing aluminum and aluminum alloys," US3970529A, Jul. 20, 1976 Accessed: Sep. 22, 2023. [Online]. Available: <https://patents.google.com/patent/US3970529A/en>
- [2] "Standard Guide for Electrolytic Polishing of Metallographic Specimens," ASTM-E1558. [Online]. Available: https://www.researchgate.net/profile/Bala_Guniputi2/post/Procedure-for-Electro-etching-of-sintered-TiAl-alloys/attachment/5d386be6cfe4a7968db8cc43/AS%3A784197769768961%401563978726493/download/E1558.30063.pdf
- [3] G. Yang, B. Wang, K. Tawfiq, H. Wei, S. Zhou, and G. Chen, "Electropolishing of surfaces: theory and applications," *Surf. Eng.*, vol. 33, pp. 1–18, Jul. 2016, doi: 10.1080/02670844.2016.1198452.
- [4] F. Nazneen, P. Galvin, D. W. M. Arrigan, M. Thompson, P. Benvenuto, and G. Herzog, "Electropolishing of medical-grade stainless steel in preparation for surface nano-texturing," *J. Solid State Electrochem.*, vol. 16, no. 4, pp. 1389–1397, Apr. 2012, doi: 10.1007/s10008-011-1539-9.
- [5] Z. Ur Rahman, K. M. Deen, L. Cano, and W. Haider, "The effects of parametric changes in electropolishing process on surface properties of 316L stainless steel," *Appl. Surf. Sci.*, vol. 410, pp. 432–444, Jul. 2017, doi: 10.1016/j.apsusc.2017.03.081.
- [6] T. Hryniewicz, K. Rokosz, and R. Rokicki, "Electrochemical and XPS studies of AISI 316L stainless steel after electropolishing in a magnetic field," *Corros. Sci.*, vol. 50, no. 9, pp. 2676–2681, Sep. 2008, doi: 10.1016/j.corsci.2008.06.048.
- [7] T.-R. Lin and C.-R. Su, "Experimental study of lapping and electropolishing of tungsten carbides," *Int. J. Adv. Manuf. Technol.*, vol. 36, no. 7–8, pp. 715–723, Mar. 2008, doi: 10.1007/s00170-006-0895-6.
- [8] M. Matlosz, S. Magaino, and D. Landolt, "Impedance Analysis of a Model Mechanism for Acceptor-Limited Electropolishing," *J. Electrochem. Soc.*, vol. 141, no. 2, pp. 410–418, Feb. 1994, doi: 10.1149/1.2054741.
- [9] M. Datta and L. T. Romankiw, "Electrochemical tool for uniform metal removal during electropolishing," US5217586A, Jun. 08, 1993 Accessed: Sep. 22, 2023. [Online]. Available: <https://patents.google.com/patent/US5217586A/en>
- [10] "Aluminum Electropolishing Service | Able Electropolishing." <https://www.ableelectropolishing.com/alloys-electropolished/aluminum/> (accessed Sep. 22, 2023).
- [11] O. Piotrowski, C. Madore, and D. Landolt, "The mechanism of electropolishing of titanium in methanol-sulfuric acid electrolytes," *J. Electrochem. Soc.*, vol. 145, pp. 2362–2369, Jul. 1998.
- [12] J. Pelleg, "Electropolishing of titanium," *Metallography*, vol. 7, no. 4, pp. 357–360, Aug. 1974, doi: 10.1016/0026-0800(74)90015-9.
- [13] E. Mahé and D. Devilliers, "Surface modification of titanium substrates for the preparation of noble metal coated anodes," *Electrochimica Acta*, vol. 46, no. 5, pp. 629–636, Jan. 2001, doi: 10.1016/S0013-4686(00)00646-0.
- [14] J. Lausmaa, B. Kasemo, H. Mattsson, and H. Odellius, "Multi-technique surface characterization of oxide films on electropolished and anodically oxidized titanium," *Appl. Surf. Sci.*, vol. 45, no. 3, pp. 189–200, Oct. 1990, doi: 10.1016/0169-4332(90)90002-H.
- [15] T. P. Hoar and J. A. S. Mowat, "Mechanism of Electropolishing," *Nature*, vol. 165, no. 4185, pp. 64–65, Jan. 1950, doi: 10.1038/165064a0.
- [16] K. Tajima, M. Hironaka, K.-K. Chen, Y. Nagamatsu, H. Kakigawa, and Y. Kozono, "Electropolishing of CP Titanium and Its Alloys in an Alcoholic Solution-based Electrolyte," *Dent. Mater. J.*, vol. 27, no. 2, pp. 258–265, 2008, doi: 10.4012/dmj.27.258.
- [17] X. Zhao, S. G. Corcoran, and M. J. Kelley, "Sulfuric acid–methanol electrolytes as an alternative to sulfuric–hydrofluoric acid mixtures for electropolishing of niobium," *J. Appl. Electrochem.*, vol. 41, no. 6, pp. 633–643, Jun. 2011, doi: 10.1007/s10800-011-0276-1.
- [18] "How Much Material Does Electropolishing Remove?" <https://neelectropolishing.com/how-much-material-does-electropolishing-remove/> (accessed Sep. 22, 2023).
- [19] C.-C. Lin, C.-C. Hu, and T.-C. Lee, "Electropolishing of 304 stainless steel: Interactive effects of glycerol content, bath temperature, and current density on surface roughness and morphology," *Surf. Coat. Technol.*, vol. 204, no. 4, pp. 448–454, Nov. 2009, doi: 10.1016/j.surfcoat.2009.08.005.
- [20] C.-C. Lin and C.-C. Hu, "Electropolishing of 304 stainless steel: Surface roughness control using experimental design strategies and a summarized electropolishing model," *Electrochimica Acta*, vol. 53, no. 8, pp. 3356–3363, Mar. 2008, doi: 10.1016/j.electacta.2007.11.075.
- [21] A. M. Awad, N. A. A. Ghany, and T. M. Dahy, "Removal of tarnishing and roughness of copper surface by electropolishing treatment," *Appl. Surf. Sci.*, vol. 256, no. 13, pp. 4370–4375, Apr. 2010, doi: 10.1016/j.apsusc.2010.02.033.
- [22] W. Simka, M. Kaczmarek, A. Baron-Wiecheć, G. Nawrat, J. Marciniak, and J. Zak, "Electropolishing and passivation of NiTi shape memory alloy," *Electrochimica Acta*, vol. 55, no. 7, pp. 2437–2441, Feb. 2010, doi: 10.1016/j.electacta.2009.11.097.



MACHINERIES AND INDUSTRIAL SUPPLIES



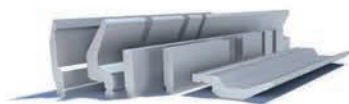
HAAS FACTORY OUTLET

A DIVISION OF KAYA MACHINERIES



HIGH-QUALITY MACHINE TOOLS, PARTS & AFTER SALES SERVICE

CNC Machines, Conventional Machines, CNC Press Brake, Hydraulic Shearing, Laser Machines, Plasma Cutters, Cutting Tools, Machine Accessories and Consumables.



Kaya Machineries and Industrial Supplies

E-mail: sales@kayamachineries.com

Website: www.kayamachineries.com

Tel. Nos. : (02) 8742 0590 / 0925-787-0818

Improved Patternwax Material for Investment Casting Using Fillers

Karen C. Santos*¹, Florentino J. Lafuente*², Celso L. Aguisanda*³

Abstract

In 2019, the Metals Industry Research and Development Center (MIRDC), formulated a pattern wax material composed of paraffin, carnauba, and beeswax. In this project, the compatibility, and effects of fillers such as polyethylene terephthalate (PET), cellulose acetate (CA), polyethylene wax (PW) and hydroxyethyl cellulose (HEC) on the property of base pattern wax were observed. Among the trial proportions used, the combination of 87 percent base wax, 10 percent PW and three percent HEC exhibited superior quality and performance in terms of bending strength, volume shrinkage, quality of pattern produced and cost.

Keywords: pattern wax, investment casting, fillers

I. Introduction

Investment casting remains to be the preferred method in producing high-precision parts with wax being the most desired material for pattern making[1]. The quality of the pattern wax material directly affects the quality of the final cast parts. Some of the defects linked to pattern wax are issues with dimensional accuracy, cavitation, filling, surface finish, etc. Hence, the efforts to improve pattern wax materials continue to progress. One of the ways to improve pattern wax materials is by introducing fillers and additives.

Fillers are playing an increasingly important role in the main task to modify the properties of the original blends. The addition of a filler ranging from 5 to 50 parts by weight of total wax composition¹ may improve tensile or compressive strength, thermal and dimensional stability[2].

The use of polyethylene terephthalate (PET) as the filler material is effective for controlling the expansion and contraction properties of the wax composition providing a high degree of dimensional accuracy[3]. It can contribute to fast cycle time due to its high thermal conductivity which allows the wax composition to cool quickly. It is relatively inexpensive compared to other inert filler materials and does not react with mold. It can be easily removed from the mold with less probability of crack occurrence.

Polyethylene wax (PW) is high crystalline in nature, it is known for low viscosity, high hardness, high melting point, excellent thermal stability, and provides lubrication.

Ethyl cellulose when mixed with waxy material results in a low softening point and low viscosity in the fluid state

at a temperature it was injected into the pattern die. It also acts as a toughening agent which enhances the cast pattern flexibility and its mechanical shock resistance. This material further decreases both the amount of sag and the load deflection of the formed melt pattern.

Through a contract research project in 2019, the Metals Industry Research and Development Center (MIRDC) successfully formulated a pattern wax material comparable to the ones sold in the market using locally available waxes: paraffin, carnauba, and beeswax. This study explored on introducing fillers for an improved property of pattern wax material. The MIRDC formulated wax will be used as the “base wax.”

II. Materials and Methods

The project explored the use of fillers that are locally available: Recycled PET, cellulose acetate (CA), hydroxyethyl cellulose (HEC), and polyethylene wax (PW). Recycled PET was derived from grinding used PET bottles and collecting dust particles. PW was ground to desired particle size (mesh 100).

The base wax is a mixture of 65% paraffin wax, 25% beeswax, and 10% carnauba. Each filler was observed on how its particles are distributed and remain suspended in the mixture. Considering the melting temperatures of the wax and filler materials, as shown in Table 1, and the wax pattern was to be produced using the gravity pouring technique, the base wax blend was melted under the temperature range of 80-150°C[4].



*1 Science Research Specialist II
Metals Industry Research and
Development Center
Bicutan, Taguig City
Philippines



*2 Supervising Science Research Specialist
Metals Industry Research and
Development Center
Bicutan, Taguig City
Philippines



*3 Metals Technologist V
Metals Industry Research
and Development Center
Bicutan, Taguig City
Philippines

Each filler was introduced one by one into the base pattern wax and the mixture was continuously agitated using a magnetic stirrer within a holding time of approximately 8-10 minutes. The following performance indicators were observed: mixability of fillers into the base wax, pourability and cooling time.

Given the significant difference in the melting points of base waxes and fillers CA and PET, as indicated in Table 1, and the particle shape and size of PET, it was noted that both fillers did not mix well with the base pattern wax, ended clumped together or coagulated. However, PW and HE were both successfully mixed with the base wax. Table 2 shows different formulations of filled pattern waxes using PW and HEC.

Table 1. Melting points of different base waxes and fillers

Material		Melting Point
Base Waxes	Paraffin	46-68°C
	Beeswax	62-65 °C
	Carnauba	82°C
Fillers	PET	260 °C
	CA	230-300 °C
	HEC	140 °C
	PW	90-140 °C

Table 2. Filled pattern wax trial proportions

Mixture	MRDC Base Wax (%)	PW (%)	HEC (%)
A	95	5	-
B	90	10	-
C	85	15	-
D	80	20	-
E	97	-	3
F	95	-	5
G	90	-	10
H	88	-	12
I	85	-	15
J	90	5	5
K	85	5	10
L	75	10	15
M	85	10	5
N	87	10	3
O	92	5	3

Test coupons measuring about 1x1x6cm for each filled wax formulation were subjected to bending strength using Compressive Strength Tester (3-point test) as shown in Figure 1. This test is done by putting the sample horizontally on two support points (A&B). The loading force (C) is applied in the middle and the bending strength is determined by the force at which the specimen breaks.

Figure 2 shows that the bending strength peaks at 22.5 kg/cm² for wax that has 10% PE Wax and drops down as the PE Wax content is further increased.

Figure 3 shows that the bending strength peaks at 26.25 kg/cm² for wax that has 5% HEC and begins to decline as the HEC content exceeds 5%.

Based on the results of bending strength tests conducted on samples that are added with a single type of filler, further tests were conducted to observe the effects on the bending strength when the two fillers were combined. Finally, the mixture N composed of 87% base pattern wax, 10% PW, and 3% HEC exhibited the highest bending strength of 33.75 kg/cm² which is 7% higher than that of the base pattern wax which is 31.5kg/cm², as shown in Figure 4.

The samples were tested for volumetric shrinkage by measuring the difference between the mold volume and the wax pattern volume using a digital caliper. Five (5) samples for each formulation were measured to get the average shrinkage.

Based on the results, mixture N has an average of only 9% volumetric shrinkage which is the lowest amongst the samples, followed by mixture M at 10%. For comparison, the shrinkage percentage of MIRDC unfilled pattern wax was measured at an average of 10.5%, as shown in Figure 5.

It can be recalled that the mixtures N & M also showed the highest bending strengths of 33.75 and 24 kg/cm², respectively. These two formulations were both used in the production of wax patterns. Mixture N produced wax patterns with lesser touch up required, as shown in Figure 6 and Figure 7.

Bending strength is one of the key characteristics of a pattern wax material. It eases handling and allows the wax pattern to withstand forces in the investment casting process, specifically during the ceramic coating stage[5].

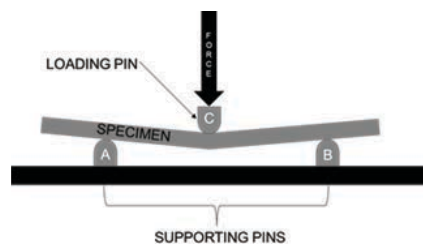


Fig. 1. Compressive strength test model

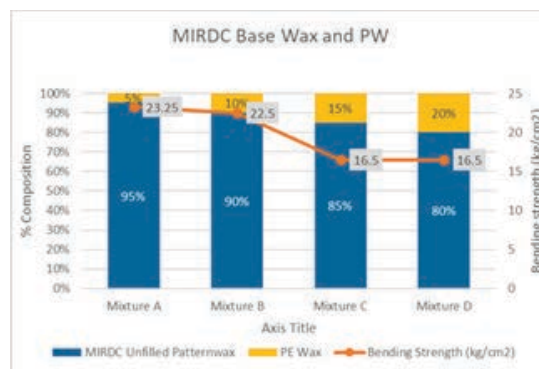


Fig. 2. Bending strength of pattern wax filled with PW

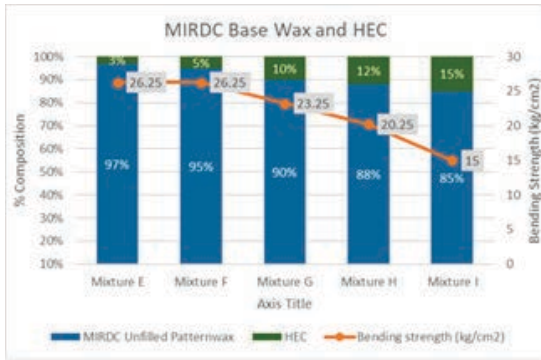


Fig. 3. Bending strength of pattern wax filled with HEC

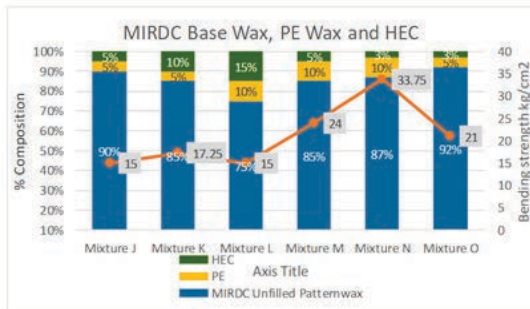


Fig. 4. Bending strength of pattern wax filled with HEC

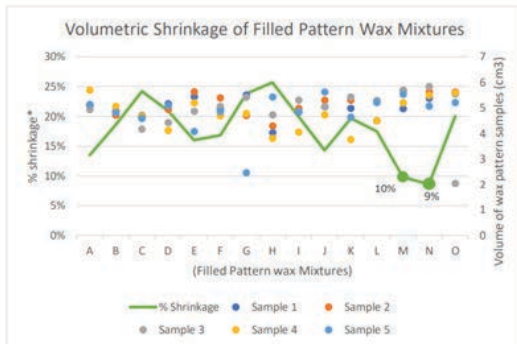


Fig. 5. Volumetric shrinkage of filled pattern wax mixtures

Mixtures M and N were tested in the actual casting investment, using Stainless Steel 316. Although both mixtures generally performed well in the whole casting process, Mixture N showed higher pattern wax quality, as shown in Figure 8. And the final casting produced did not have any noticeable defects and no repairs were needed.

Additional tests on the pattern wax materials produced to determine the ash content using gravimetry and melting point using Shimadzu TGA-DTA Analyzer (DTG-60H). All samples have less than 0.05% ash content and a melting range as shown in Table 3.

Table 4 shows the overall comparison among the three pattern wax materials: Commercially available wax material, MIRDC base wax and mixture N.

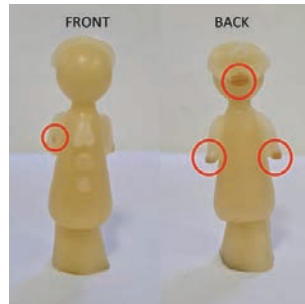


Fig. 6. Wax pattern using mixture M

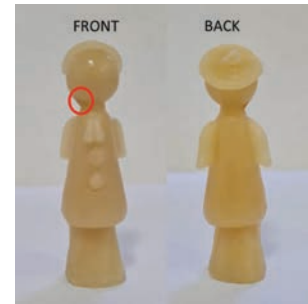


Fig. 7. Wax pattern using mixture N



Fig. 8. Final cast parts produced using (L-R), 100% base wax, mixture M and mixture N

Table 3. Melting ranges of waxes

Mixture	Melting Range (°C)
Commercially available	45-55
MIRDC Base Wax	52-64
Mixture N	50-65

Table 4. Comparison of waxes

Specification	Casting Wax / B 2025 USA	MIRDC Base Wax	Mixture N
Cost per kg.	Php 750.00	Php 540.00	Php 525.00
Bending strength (kg/cm ²)	33.42	31.73	33.75
Average Volumetric Shrinkage	-	10.5%	9%
Melting Range (°C)	45-55	52-64	50-65
% Ash content	<0.05	<0.05	<0.05

III. Conclusion

The study aimed to improve the properties of pattern wax material formulated by MIRDC in 2019. Based on the results, base wax added with fillers: 10% polyethylene wax and 3% hydroxyethyl cellulose exhibited 7% higher bending strength, and 14% lower volume shrinkage as compared to unfilled base wax. The new formulation was used in the actual investment casting process and the ease of use and the quality of the final cast part is comparable to the pieces produced using MIRDC base wax and store-bought pattern wax.

In addition, this wax is 2.78% cheaper than the MIRDC base wax and 30% cheaper than the commercially available wax material as shown in Table 4.

IV. Acknowledgment

This work was funded by the Metals Industry Research and Development Center (MIRDC). The project team would like to thank the following individuals for their invaluable support in the success and completion of the project: Robert O. Dizon, Agustin M. Fudolig, Fred P. Liza, Juanito V. Mallari, Paul John V. Luna and Carlo U. Rasco

References

- [1] N.Senthilkumar, N.Arul, and K.Soundararajan, "A Study on Blended Wax Pattern in Investment Casting Process," *Int. J. Creat. Res. Thoughts IJCRT*, vol. 6, no. 2, p. 18, Apr. 2018.
- [2] Guinn, Paul, "Filler Material and Wax Composition for Use in Investment Casting," US 6,485,553 B1, Nov. 26, 2022
- [3] Dorota Czarnecka-Komorowska, Krzysztof Grzeskowiak, Paweł Popielarski, Mateusz Barczewski, Katarzyna Gawdzińska, and Mikołaj Popławski, "Polyethylene Wax Modified by Organoclay Bentonite Used in the Lost-Wax Casting Process: Processing-Structure-Property Relationships," *Multidiscip. Digit. Publ. Inst.*, vol. 13, no. 10, May 2020, doi: 10.3390/ma13102255.
- [4] Omkar Bemblage and D. Benny Karunakar, "A Study on the Blended Wax Patterns in Investment Casting Process," in *Proceedings of the World Congress on Engineering 2011 Vol I*, London, U.K., Jul. 2011.
- [5] Robert K. Tewo, Hilary L. Rutto, Walter Focke, Tumisang Seodigeng, and Lawrence K. Koech, "Formulations, development and characterization techniques of investment casting patterns," *Gruyter*, p. 15, Apr. 2018, doi: <https://doi.org/10.1515/revce-2017-0068>.

Prototyping of the Mechanical System of a Local Oxygen Concentrator with Parts Designed Using Design for Additive Manufacturing (DfAM)

Leif Oliver B. Coronado*¹, Marc Adrian O. Yu*², Ronald Joaquin B. Javate*³, Alvin M. Buison*⁴

Abstract

The medical field has a demand for a reliable medical oxygen concentrator (MOC) apparatus which was exacerbated during the height of the COVID 19 pandemic. The cost of the unit itself and the serviceable parts are a vital concern to the device's accessibility in the Philippines. The rise of additive manufacturing (AM) technology will revolutionize the way things are manufactured. Design for additive manufacturing (DfAM) methodology has been developed to produce optimized parts to take advantage of AM. One of the research gaps in this field is the lack of studies on the effects and mechanical behavior of parts created by DfAM. This paper focuses on the rapid prototyping and design for additive manufacturing aspects of the components for oxygen concentrator parts. The material is selected through Technique for Order of Preference by Similarity to Ideal Solution (TOPSIS). The design is optimized for fabrication using AM technology, specifically material extrusion, and is validated using Finite Element Analysis (FEA) which shows the behavior of the optimized parts. The results establish the advantage and limitation of using AM in part production.

Keywords: additive manufacturing, fused granular fabrication, design for AM, medical oxygen concentrator

I. Introduction

Severe acute respiratory syndrome coronavirus 2 (SARS-CoV-2) is a contagious, novel coronavirus first reported in Wuhan, China at the end of December 2019. SARS-CoV-2 is the primary culprit for the pulmonary disease strain called COVID-19. [1] The most severe cases of COVID-19 required intubation to directly substitute the patient's respiratory functions. Cases with pulmonary complications that included difficulty breathing and damage to the lungs required ventilator devices which aid in breathing through continuous positive airway pressure [2]. High-flow oxygen therapy was also shown to bring relief to these patients helping them also avoid intubation [3]. Low-flow oxygen therapy aided in mild COVID cases and oxygen concentrator devices were critical in situations where medical oxygen tanks were difficult to come by. [4] Medical grade oxygen can be acquired by hospitals through oxygen generating plants, liquid oxygen in bulk storage tanks, and oxygen concentrators, helping increase blood oxygen levels in patients.

At the height of the COVID pandemic in 2021, the Philippine Department of Health (DOH) reported that the average consumption of medical oxygen was around 5,366 tons per month, with 179 hospitals reporting to have experienced a shortage in oxygen tanks daily, 15 facilities had the same problem at least once weekly, while 63 others hospitals said they faced shortages at least once a month [5], [6]. The Philippine Department of Trade and Industry (DTI) recommended a protocol for the

fast ramp-up of oxygen supply to bolster the production capacity of local producers, reported at around 11,000 tons per month, and increase this buffer in the case of a surge. [7] The Philippine Confederation of Industrial Gases Inc. (PCIGI) affirmed that the local suppliers indeed have the capability to keep up with the oxygen demand, however there was still a problem with the turnaround, stating that a cylinder of oxygen can be used up in about 2 hours, but it takes 10 days for it to be returned to the supplier. [8]

A medical oxygen concentrator (MOC) is a machine used to provide low flow oxygen, typically at around 5-20 L/min, by extracting oxygen from the ambient air and separating it from the other gasses, mainly nitrogen. The system begins with a compressor that draws air in. It may be passed through some filters, heat exchangers, and dehumidifiers, as the heat and vapor coming from compression are detrimental to the nitrogen adsorption process. The compressed air is then directed to one of two beds which are packed with a molecular sieve composed of zeolite, sized specifically to trap nitrogen. The flow to the beds is controlled by a solenoid valve, alternating the flow from bed 1 and bed 2. The valve pushes air through the sieve bed leaving oxygen at the outlet, a fraction of which is directed to purge nitrogen in the opposite bed, the majority of the oxygen however is placed into a collector tank which ensures that there is a steady flow rate of oxygen to the patient.



*1 Science Research Specialist II
Metals Industry Research and
Development Center
Bicutan, Taguig City
Philippines



*2 Project Technical Specialist I
Metals Industry Research and
Development Center
Bicutan, Taguig City
Philippines



*3 Project Technical Specialist I
Metals Industry Research and
Development Center
Bicutan, Taguig City
Philippines

The MOC can provide a continuous supply of oxygen, particularly in long term oxygen therapy situations which may require the machine to run at least 15 hours per day. [9] Efforts have been made to open-source the technology for emergency medical device use by initiatives such as ShieldMission with their OxiKit, which was adopted for use as far as India by a group called Technido [10], [11]. Commercial oxygen concentrators are readily available for import, but there are still currently no local manufacturers of the equipment in the Philippines [12].

Table 1 shows the advantages of 3D printing through prototyping by employing Design for Additive Manufacturing (DfAM), which results in a more lightweight and cost-effective design. It takes advantage of the ability of 3D-printing to produce highly intricate parts. Thus, material can be reduced or optimized based on the actual strength needs of the parts [13], [14].

This paper explores the fabrication of this specialized medical equipment with the context of introducing additive manufacturing (AM) in the prototyping workflow. The design ideation stage will involve identification of major components, determination of commercial off the shelf parts (e.g. fittings), determination of candidate parts for AM fabrication process, material selection and technology selection for AM, assembly and integration of parts, and performance validation of the prototype.

Table 1. DfAM related work [12] [13]







Ref.	Conventional design	DfAM
1		
2		
3		



Fig. 1. OxiKit - DIY Oxygen Concentrator [10]



Fig. 2. Commercial Philips EverFlo Oxygen Concentrator [12]

II. Methodology

A. Mechanical System and Components

The primary mover of pressure in the system is the compressor unit, driving the pressure swing adsorption (PSA) of nitrogen in ambient air. The chosen setup of PSA does not include any vacuum pressure stages, meaning that adsorption in the sieve bed will occur at higher than atmospheric pressure, while desorption or purging of trapped nitrogen for regeneration of the zeolite sieve would occur at ambient outside pressure [15]. Designs would typically size the compressor at 0.5 to 2.0 horsepower depending on the desired output in liters per minute of oxygen, and for compact use, a silent and oilless positive-displacement reciprocating compressor would be an ideal choice. For the process to occur, the inlet feed air would necessarily have to be dry and free of CO₂ [16] thus a dehumidifier and a heat exchanger are included before the sieve beds. These components are readily available as commercial off the shelf parts, except for the heat exchanger component which would have to be manufactured and coiled to size out of copper or aluminum tubing. AM is a viable candidate for space saving heat exchange designs but the current space of additive manufacturing of metals would make mass production prohibitively expensive.

The sieve bed is where the adsorption of nitrogen present in ambient air occurs. Zeolite minerals serve as the molecular sieves in MOC devices, typically synthetic Zeolite 13X and 5A. A study in Jordan evaluated their local natural zeolite, determining that 0.55 - 0.75 mm grain size of zeolite with 48.0% SiO₂ and 10.8% Al₂O₃ delivered the highest oxygen purity. [17] The container for the molecular sieves would experience around at least 1.5 bars of pressure during the adsorption step. In the case of commercial MOCs, there would typically be two sieve beds, and these can be manufactured from aluminum or stainless steel tubes of around 7 to 10 centimeters in diameter. The ends would have different combinations of screws, spring loaded mechanisms, O-rings, and other design features in order to ensure a good pressure seal whilst leaving the beds open to access if the zeolite needs to be replaced. The emergency DIY kits substituted the aluminum for more readily available but sufficiently thick PVC pipes and end caps. Due to the nature of the pressure loading and the size of the sieve beds, additive manufacturing is not recommended for these components except for maybe creating custom brackets to the frame which conforms well to the round bed, minimizing overall design vibrations.

Other components such as the control solenoid valves, quick connectors, flow meters, oxygen meters, tubings, etc. are readily available as off-the-shelf components



*4 Sr. Science Research Specialist
Metals Industry Research and
Development Center
Bicutan, Taguig City
Philippines

for creating a prototype MOC. In order to determine the form factor of the MOC device, especially if it is intended to be portable, additive manufacturing can be employed in order to create component mounts and enclosures. Composite construction of the form can be made by making the frame out of a rigid metal structure, but the design of which would have to account for mounting the AM printed panels. Such panels when in mass production would be produced with injection molding instead. The size of the MOC would make typical AM machines cumbersome because of the limitations to build volume. Fused granular fabrication (FGF) is a subset of material extrusion additive manufacturing technology. These machines utilize pellets or flakes as feedstock, allowing for larger extrusion nozzles, which translates to more deposition of the material at a faster flow rate. The total buildable size with pellet machines is greater than the more common filament based machines, at the cost of not being able to attain fine details. The speed of production for the enclosure set to be printed with an FGF printer is governed by the print process parameters while the performance is heavily dictated by the material selection.

B. Material Selection via Multi Attribute Decision Making

Multiple Attribute Decision Making (MADM) is employed for the selection of materials for the AM printed oxygen concentrator enclosure, ensuring that considerations are made for strength, manufacturability, compatibility with other parts, and appropriateness for medical device applications. MADM techniques allow one to easily handle the many complexities in a transparent and objective manner. Technique for Order of Preference by Similarity to Ideal Solution (TOPSIS) will be used as it considers both the best and worst case solutions making it less sensitive to small variations in the criterion values.

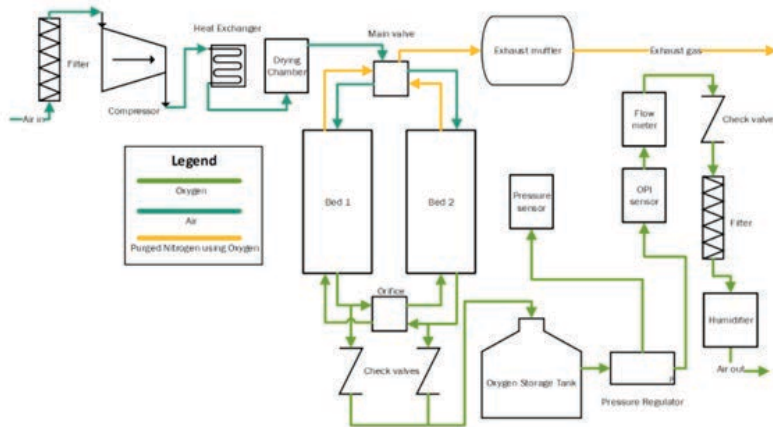


Fig. 3. Schematic for proposed mechanical system

The workflow for TOPSIS first involves the selection of candidate solutions and the appropriate selection criteria, these are then placed into a matrix and then the values are normalized, additionally a weight for each criterion may be determined. Next the distance of the candidate solution to the best and worst solution must be evaluated.

The values of the ideal/best solution are all the largest values among the choices in a maximization case (e.g. highest value is best for mechanical properties), and all the smallest values in minimization cases (i.e. lower density is best for compartmentability); and vice versa for the worst solution. The distance of the candidate to the best and worst can be computed in many ways but the simplest would be the multi-dimensional Euclidean distance. The rank of the solution is finally determined from the closeness value, or the ratio of its distance to the ideal solution over the sum of its distances to the best and worst solutions [18].

Fused granular fabrication is diverse in its option for feedstocks, most pellets that are used for traditional injection molding are compatible for the FGF process. Plastics such as acrylonitrile butadiene styrene (ABS), polycarbonate (PC), and acrylonitrile styrene acrylate (ASA) are widespread in home appliances and consumer electronics. Another common polymer is polyethylene terephthalate (PET) used in plastic bottles, wherein a sister polymer also exists with glycol added (PETG), which improves the overall flowability of the polymer. Polylactic acid (PLA) is one biopolymer that started to gain more and more use due to the rise of additive manufacturing as it melts at a relatively lower temperature making it easy to work with for non critical components. PLA [19], PETG [20], ABS [21], ASA [22], and PC [20], will be the candidate materials that will be compared against using TOPSIS as they are available in bulk pellet form for FGF as well as filament form in case any detailed work needs to be done on the design.

The tensile strength of polymers relates to the performance of the material when experiencing tension loading; the value is taken at the peak of the stress-strain curve before the material experiences permanent and significant deformation. Pellet batches are tested in tension using coupons to ensure consistency of product following ASTM D638 or ASTM D882. Flexural strength similarly tests the material but this time in bending load, following standards such as ASTM D790. The higher mechanical strength in tension and bending is of course desired. Melt flow index (MFI) is a test done specifically for evaluating pellets under constant load exiting a small extruder orifice, standardized in ASTM D1238. MFI is a useful metric for injection molding and also additive manufacturing because high flow feedstock can be extruded faster, meaning AM toolpaths can be traversed at higher movement speeds; however, too high flow may cause issues for dimensional stability, cooling, interlayer adhesion, and other unique considerations for AM. The temperature in which the melt flow index test is done is usually slightly higher than the known melting point of the polymer, and is a good approximation for the recommended printing temperature setting for the hot end of AM printers. A lower and more manageable printing temperature is

Table 2. Setup of TOPSIS

Kind of Polymer	Brand	Tensile Strength (MPa)	Flexural Strength (MPa)	MFI (g/10min)	MFI Temp. (degC)	HDT (degC)	Specific Gravity (g/cm3)
PLA	Ingeo 4043D	60	83	6	210	55	1.24
PETG	PolyCore PETG 1000	50	71	11	240	62	1.3
ABS	LGChem ABS AF365S	47	77	7.5	220	87	1.16
ASA	LGChem ASA LI912	49	79	12	220	86	1.07
PC	PolyCore PC 7100	59.7	94.1	7	260	100	1.2
Theoretical Best		60	94.1	12	210	100	1.07
Theoretical Worst		47	71	6	260	55	1.3

desired in AM, specifically melt based material extrusion technologies, as it causes parts to be less prone to warping, shrinkage and delamination that occurs due to the time lag of deposition from one layer to the next, which is even more exacerbated with large scale prints, it also marginally lowers the energy requirements of the printing process. Heat deflection temperature (HDT) is the maximum temperature a polymer can handle before reaching a set deflection with a weight acting upon it, this is correlated to the glass transition temperature of a polymer. Higher HDT is therefore desired to resist heat loads such as those coming from the compressor. Density or specific gravity is also a factor that is evaluated, minimizing such to save on overall device weight. These values for each candidate were tabulated in Table 2.

C. Design for Additive Manufacturing (DfAM) Methodology

The external structure of the oxygen concentrator was designed for AM fabrication thru FGF. The size of the enclosure was printed on a medium to large format 3D printer -the Gigabot X XLT and the Cosine AM1. The design of the main enclosure focused on contours that can be printed flat and direct to the build plate or shapes that can be easily printed in a spiralized manner, eliminating the need for sharp seams caused by abrupt Z- height movements (otherwise called as vase mode printing).

There are internal components of the oxygen concentrator as well that are suitable for topology optimization. These include the brackets, supports and holders of the manifolds, sieve bed canisters/ tanks, etc. These components were optimized thru generative design for volume reduction.

D. Behavior and Performance of the Machine

The design with DfAM was compared with initial non-DfAM design through Finite Element Analysis (FEA). The change in volume, stress and strain is collected for comparison. Additionally, functional observations will be conducted on the optimized design which was conducted while the device is in operation.

III. Results and Discussion

A. TOPSIS Selection Results

The material selection results is one of the precursory steps aside from design. As listed previously, candidate materials were chosen based on certain criteria and scored using the TOPSIS workflow. The candidate with the highest score, summarized in Table 3, was the LGChem ASA LI912, followed closely by LGChem ABS AF365S. These scores agree with the general criterion as the particular brand of PETG has generally low scores in terms of tensile and flexural strength, PLA scored less because of its low heat deflection temperature, and PC although being the closest to theoretical best in terms of strength and heat deflection was affected by its high printing temperature which makes it more susceptible to warping. The results of the TOPSIS are unique to these particular brands of pellets as even across similar polymers the properties can have large variations.

Table 3. TOPSIS results

Kind of Polymer	Brand	Distance to Best	Distance to Worst	Overall Closeness Score
PLA	Ingeo 4043D	46.7358	53.0378	0.5316
PETG	PolyCore PETG 1000	54.5771	21.9773	0.2871
ABS	LGChem ABS AF365S	27.3983	51.5972	0.6532
ASA	LGChem ASA LI912	25.3970	51.6242	0.6703
PC	PolyCore PC 7100	50.2504	52.1623	0.5093

B. Design of AM Printed Enclosure and Printing

The FGF printed enclosure was designed to be bolted around a metal frame, as seen in Figure 4. The thicknesses of parts that were designed to print 90 degrees perpendicular to the build plate were set to be twice that of the nozzle width, this is to ensure the success rate of the print, allowing it to build its height without sagging and print in a spiralized manner. Prints that were done flat and parallel to the build plate also were set to two or three times that of the layer height. Features that were to interface with more complex components, such as the control screen and a humidifier bottle connected to the cannula were cut out from the FGF print and were done separately, so as to minimize unnecessary overhang and support features. These interfacing features were also printed using more traditional filament printers, giving better accuracy to these more critical parts. The FGF printers used, the Gigabot X XLT and the Cosine AM1, shown printing in Figure 5, were set at a higher but still manageable 240 degrees Celsius for the printing temperature at the nozzle for ASA pellets. A large enough brim and some weights were also used to prevent warping and peeling off from the build plate.

C. DfAM - Topology Optimization and FEA

Topology optimization of DfAM is a technique that optimizes the geometry and design of the part through structural computation for a given design space. This results in compliance with a decrease in volume or mass that can still withstand the load given in a design. Moreover, this technique needs to specify boundary conditions to be met in order to have a reliable result. For the components of the oxygen concentrator, topology optimization was investigated for the internal brackets. The load and the physical constraints were applied depending on their function. Figure 6 shows the summary of topology optimization results for the sieve bed top and bottom bracket guide.

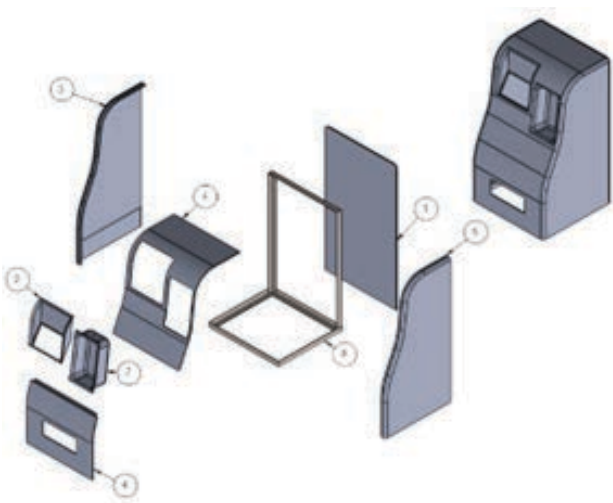


Fig. 4. Design of the enclosure

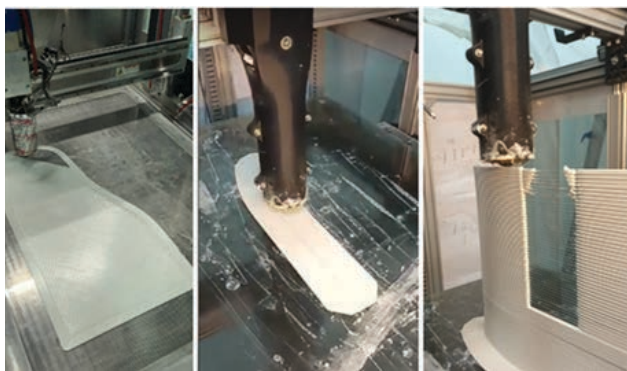


Fig. 5. FGF of the external enclosure of the oxygen concentrator

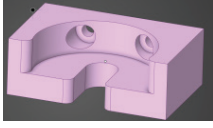
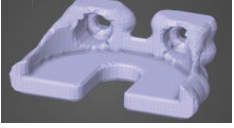
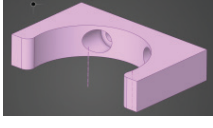
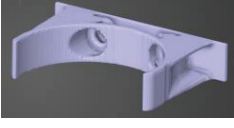
Specs.		Conventional design	DfAM
3D part	A		
	B		
Volume (mm ³)	A	1,129,654	429,547
	B	459,794	186,538
Max. Displacement (m)	A	5.11x10 ⁻⁶	9.36x10 ⁻⁶
	B	9.87x10 ⁻⁶	1.74x10 ⁻⁵
Max. Stress (Pa)	A	0.53x10 ⁵	1.02x10 ⁵
	B	1.43x10 ⁵	1.17x10 ⁵

Fig. 6. Results from DfAM and conventional design

Figure 7 shows the actual printed enclosure and internal parts of the oxygen concentrator printed using additive manufacturing. The internal brackets still follow the non-topology optimized design, however the optimization software shows a significant decrease in volume which may lead to lower costs. The results also show minimal change in stress and strain concentrations between the topology optimized and non-topology optimized design. There is a slight increase in the displacement due to the thinner members of the part resulting from topology optimization. Results are summarized in Figures 8, 9, 10, and 11 respectively.

Functional tests were conducted to evaluate the structural stability of the 3D printed parts, as well as the functionality of the oxygen concentrator by allowing the MOC to run for an extended period of time, subjecting the machine to the compressor vibrations and heat loads. The 3D-printed parts show no sign of unstable mechanical characteristics, as well as showing that the ASA material was able to deflect heat and not deform. Also, the structure can fully withstand the weight and the dynamic load from the vibrations coming from the compressor. Figure 12 exhibits the functional testing of the researchers and the final assembled output for the oxygen concentrator.

The MOC was able to deliver a consistent 90+% purity of oxygen throughout the test runs conducted, measured using an externally connected oxygen meter.

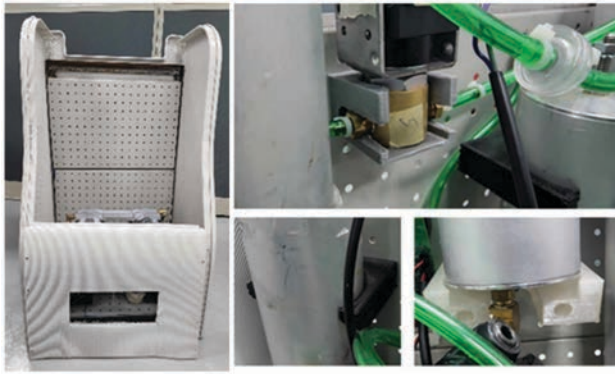


Fig. 7. Sub-assemblies of the oxygen concentrator with 3D-printed components

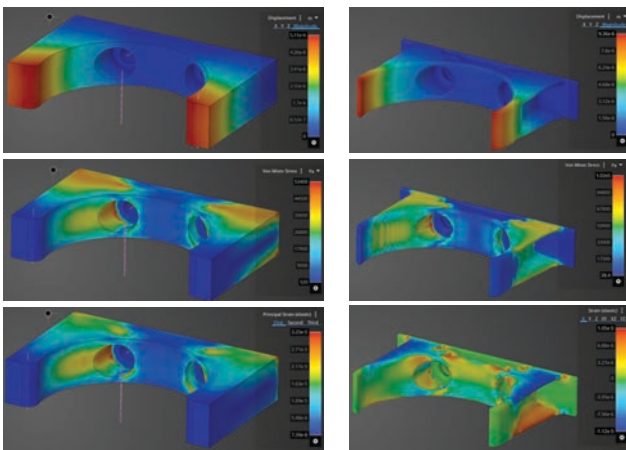


Fig. 8. Displacement, von-Mises stress and strain of 3D-printed oxygen concentrator sieve bed top bracket/guide (non-DfAM)

Fig. 9. Displacement, von-Mises stress and strain of 3D-printed oxygen concentrator sieve bed top bracket/guide (DfAM)

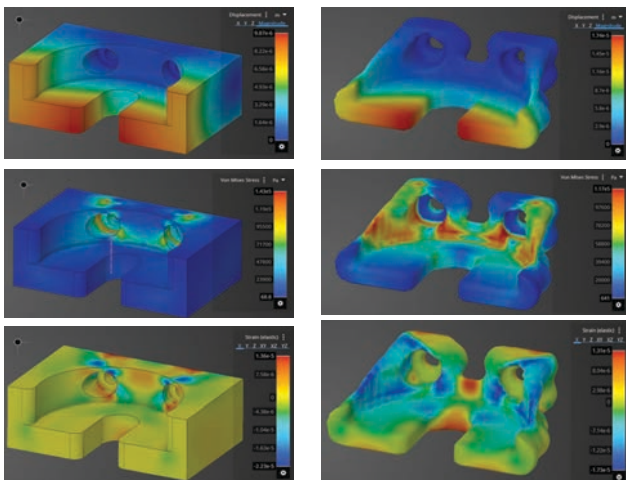


Fig. 10. Displacement, von-Mises stress and strain of 3D-printed oxygen concentrator sieve bed bottom support (non-DfAM)

Fig. 11. Displacement, von-Mises stress and strain of 3D-printed oxygen concentrator sieve bed bottom support (DfAM)



Fig. 12. The final completed assembly of the prototype MOC

IV. Conclusions

The paper was able to demonstrate that parts of a medical oxygen concentrator device can be manufactured via a combination of commercial off the shelf parts and additively manufactured parts. Proper sizing and cross comparison with open source and commercial designs allow the device to deliver the adequate oxygen output.

Additive manufacturing also demonstrates an effective method of device prototyping, allowing faster development times. The techniques of design for additive manufacturing like optimization of print orientation, minimization of overhang and support structures, and topology optimization allow for higher success rate of prints. The mechanical performance of the parts can also be suitably dictated through the appropriate material selection techniques and verified through finite element analysis simulations and functional testing.

V. Acknowledgment

The authors would like to express their utmost gratitude to the Metals Industry Research and Development Center - Advanced Manufacturing Center (MIRDC-AMCen), the Philippine Council for Industry, Energy and Emerging Technology Research and Development (PCIEERD) of the Department of Science and Technology (DOST) for their invaluable support in funding and overall guidance of this research. This work is partially funded by the Department of Science and Technology (DOST) with Project No. 19-007-01-08-96, 2023. The researchers would also like to extend their appreciation to the EPDC team and DOST-ITDI team for sharing their expertise to the project throughout this endeavor.

References

- [1] N. Zhu et al., "A Novel Coronavirus from Patients with Pneumonia in China, 2019," *New England Journal of Medicine*, vol. 382, no. 8, Jan. 2020, doi: <https://doi.org/10.1056/nejmoa2001017>.
- [2] K. Iyengar, S. Bahl, Raju Vaishya, and A. Vaish, "Challenges and solutions in meeting up the urgent requirement of ventilators for COVID-19 patients," *Diabetes & Metabolic Syndrome: Clinical Research & Reviews*, vol. 14, no. 4, pp. 499–501, Jul. 2020, doi: <https://doi.org/10.1016/j.dsx.2020.04.048>.
- [3] C. Panadero et al., "High-flow nasal cannula for Acute Respiratory Distress Syndrome (ARDS) due to COVID-19," *Multidisciplinary Respiratory Medicine*, vol. 15, no. 1, Sep. 2020, doi: <https://doi.org/10.4081/mrm.2020.693>.
- [4] Phee Kheng Cheah, Evelyn Marie Steven, Khai Keam Ng, Muammar Iqbal Hashim, M. Hakimi, and Nicholas Paul Roder, "The use of dual oxygen concentrator system for mechanical ventilation during COVID-19 pandemic in Sabah, Malaysia," *International Journal of Emergency Medicine*, vol. 14, no. 1, May 2021, doi: <https://doi.org/10.1186/s12245-021-00354-9>.
- [5] "More serious COVID-19 cases on the rise, oxygen supply shortage in the regions," CNN. <https://www.cnnphilippines.com/news/2021/10/19/COVID-19-cases-hospital-admissions.html> (accessed Aug. 31, 2023).
- [6] K. Domingo, "257 hospitals report oxygen tank shortage amid pandemic, PH eyes deal with manufacturers: DOH," ABS-CBN News, May 07, 2021. <https://news.abs-cbn.com/news/05/07/21/257-hospitals-report-oxygen-tank-shortage-amid-pandemic-ph-eyes-deal-with-manufacturers-doh> (accessed Aug. 31, 2023).
- [7] "DTI-BOI assures adequate oxygen supply in PH," BOI, May 11, 2021. https://boi.gov.ph/dti-boi-assures-adequate-oxygen-supply-in-ph/?utm_source=rss&utm_medium=rss&utm_campaign=dti-boi-assures-adequate-oxygen-supply-in-ph (accessed Aug. 31, 2023).
- [8] L. Desiderio, "Oxygen supply enough, but tank turnaround slow," Philstar.com. <https://www.philstar.com/headlines/2021/08/15/2120064/oxygen-supply-enough-tank-turnaround-slow> (accessed Aug. 31, 2023).
- [9] T. W. Evans, J. Waterhouse, and P. Howard, "Clinical experience with the oxygen concentrator.," *Br Med J (Clin Res Ed)*, vol. 287, no. 6390, pp. 459–461, Aug. 1983, doi: <https://doi.org/10.1136/bmj.287.6390.459>.
- [10] "OxiKit - DIY Oxygen Concentrator," OxiKit, 2020. <https://oxikit.com/> (accessed Aug. 31, 2023).
- [11] "Marut - India's First Open Source Oxygen Concentrator," Technido, 2021. <https://www.technido.com/marut> (accessed Aug. 31, 2023).
- [12] "EverFlo Home oxygen system | Philips Healthcare," Philips. <https://www.usa.philips.com/healthcare/product/HC0044000/everflo-home-oxygen-system> (accessed Aug. 31, 2023).
- [13] [X] Veiga, F.; Suárez, A.L.; Aldalur, E.; Goenaga, I.; Amondarain, J. Wire arc additive manufacturing process for topologically optimized aeronautical fixtures, 3D print. In *3D and Additive Manufacturing*; Mary Ann Liebert, Inc.: Larchmont, NY, USA, 12 July 2021.
- [14] [Y] Suárez, A.; Veiga, F.; Bhujangrao, T.; Aldalur, E. Study of the Mechanical Behavior of Topologically Optimized ArcWire Direct Energy Deposition Aerospace Fixtures. *J. Mater. Eng. Perform.* 2022.
- [15] A. Sami et al., "Oxygen Concentrator Design: Zeolite Based Pressure Swing Adsorption," in *IEEC 2022, MDPI*, Aug. 2022, p. 26. doi: 10.3390/engproc2022020026.
- [16] S. W. Chai, M. V. Kothare, and S. Sircar, "Rapid Pressure Swing Adsorption for Reduction of Bed Size Factor of a Medical Oxygen Concentrator," *Ind. Eng. Chem. Res.*, vol. 50, no. 14, pp. 8703–8710, Jul. 2011, doi: 10.1021/ie2005093.
- [17] A. F. Al-Shawabkeh, N. Al-Najdawi, and A. N. Olimat, "High purity oxygen production by pressure vacuum swing adsorption using natural zeolite," *Results Eng.*, vol. 18, p. 101119, Jun. 2023, doi: 10.1016/j.rineng.2023.101119.
- [18] P. Patel, F. Defersha, and S. Yang, "Resilience Analysis of Additive Manufacturing-enabled Supply Chains: An Exploratory Study." *Frontiers in Manufacturing Technology*, vol. 2, 2022, doi: 10.3389/fmtec.2022.884164.
- [19] "Ingeo™ Biopolymer 4043D Technical Data Sheet - 3D Printing .." https://www.natureworksllc.com/-/media/Files/NatureWorks/Technical-Documents/Technical-Data-Sheets/TechnicalDataSheet_4043D_3D-monofilament_pdf.pdf (accessed: Aug. 31, 2023).
- [20] "Polycore™ - Polymaker" <https://polymaker.com/polycore/> (accessed: Aug. 31, 2023).
- [21] "Grade : AF365S | LG Chem On ABS." https://www.lgchemon.com/s/abs/grade/a4z2x000000RpbAAE/af365s?language=en_US (accessed: Aug. 31, 2023).
- [22] "Grade : LI912 | LG Chem On ABS." https://www.lgchemon.com/s/abs/grade/a4z2x000000RnbAAE/li912?language=en_US (accessed: Aug. 31, 2023).



RAMCAR TECHNOLOGY INC.

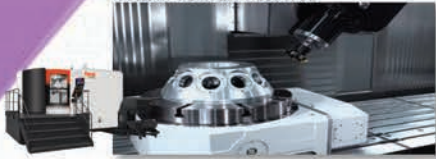
Sta. Maria Industrial Park, Brgy. Bulac, Sta. Maria, Bulacan.



Mold/Die, Tooling and Critical Parts Machining

5 AXIS - MILLING MACHINES

MAZAK VORTEX I-630V/6S



DMG DMU80P



MAZAK VRX 600C



3 AXIS - MILLING MACHINES

AWEA LP-2516YF



MAZAK FJV35/60



DMG DMC 1150V



DMG-MORI CMX600



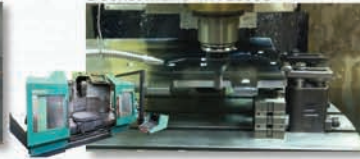
HAAS VF-1



Victor Taichung VCenter 20S



Deckel Maho MH 1600S



Deckel Maho DC100V

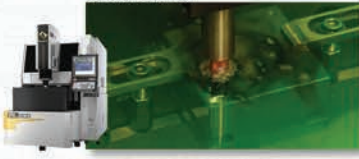


Deckel Maho 64V Linear



EDM MACHINES

Sodick AL60G



Sodick AG40L



DAVI MCA 4 ROLLS



Tube Bending



Sheet Metal Rolling and Pipe/Tube Bending

LATHE MACHINES

Gildemeister CTX 500



Victor Taichung VTURN 26



Victor Taichung VTURN P16



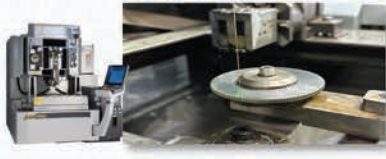
Tool Cutting Machine

ANCA FX-5



WIRECUT MACHINES

Sodick ALN400G



Mitsubishi MP4800



Surface Hardening and Treatment

HEAT TREATMENT MACHINE

Electric Chamber Furnace



PVD COATING MACHINE



Sheet Metal Forming and Cutting

LASER CUTTING MACHINE

Salvagnini L5



WATERJET CUTTING MACHINE

Flow Waterjet Mach 500



BENDING MACHINES

Compact Panel Bender - P1



TruBend 5230

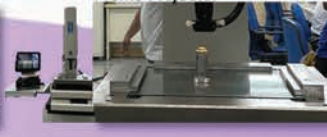


Quality Control Measuring Tool

CMM Zeiss Prismo



Profile Projector



Desktop CNC Wegstr



UV Exposure box



Ferric Chloride Shaker



XRF Analyzer



Roughness Tester



Hardness Tester



Portable Hardness Tester



Oscilloscope RIGOL DS1102E



Digital Multimeter Fluke 287



Microscope Dino Lite AD7013MT



Component Tester and Desktop Oscilloscope Prof 1A GeFA0039F-1



Soldering Station Weller WES51



Hot Air Rework Station X-tronic 6040



PCB Repair and Fabrication

Design Improvement of Gear Shifting Mechanism for Riding-Type Rice Transplanter

Dominic S. Guevarra*¹, Joiein L. Luces *²

Abstract

In 2019, Rollmaster Machinery and Industrial Services Corp. requested assistance from DOST-MIRDC in the improvement of shafts and bevel gear for the spindle drive of the power transmission gearbox. The intervention significantly increased the machine's performance in terms of durability and mobility in the deep mud field. However, there are still machine components that needed to be improved. One of these is the gear shifting mechanism of the rice transplanter's power transmission. Hence, this project was implemented with the general objective of improving the design and developing a gear shifting mechanism for the riding-type rice transplanter. With the existing design, to change the speed of the gear transmission, the shifting gear slides along the shaft to mate with the other gear. The process produces a grinding sound because of the unsmooth engagement of gears. In the developed design, the pair of gears with different speeds are constantly engaged. Two gears on one shaft comprise corresponding bearings to allow free rotation along the shaft. Engagement with the shaft happens when a shifting mechanism sliding along the shaft's spline engages with the spline of the gear. This allows the shaft to rotate in unison with the speed of the engaging gear. This process facilitates the smooth shifting of gears.

Keywords: gear shifting mechanism; rice transplanter; transmission system

I. Introduction

The Philippine Rice Research Institute (PhilRice) has implemented an initiative under the agricultural machinery development program in collaboration with the Metalworking Industries Association of the Philippines (MIAP) through Rollmaster Machinery and Industrial Services Corp. They localized a Vietnamese transmission and installed it in the front portion of a rice transplanter.

In 2016, initial pilot testing of the local riding-type rice transplanter was conducted by PhilRice thru the funding from DOST-PCAARRD. Using the design of the second prototype, Rollmaster Machinery and Industrial Services Corp. started the fabrication of the two pilot test units. However, the completion was delayed due to some design improvements and issues relating to government procurement policy. In 2018, the two pilot test units were completed and field-tested at PhilRice. Problems encountered during field tests were mainly from the power transmission of the machine e.g. sliding clutch, disengaging shifting gears, grinding noise, and breakdown of shafts and bevel gears.

In 2019, the manufacturer requested assistance from the Metals Industry Research and Development Center (DOST-MIRDC) in the improvement of shafts and bevel gear for the spindle drive of the power transmission gearbox. MIRDC approved the request and collaborated

with the improvement of the transmission gearbox by providing technical analysis of the gearbox and fabrication of spiral bevel gears.

The technical assistance of DOST-MIRDC in the design, simulation, and fabrication of spiral bevel gears for the power transmission thru contract research agreement with Rollmaster Machinery and Industrial Services Corp. significantly increased the machine's performance in terms of durability and mobility in the deep mud field. However, there are still machine components that needed to be improved. One of these is the gear shifting mechanism of the power transmission for riding-type rice transplanter. Hence, this project was implemented with the general objective of improving the design and develop a gear shifting mechanism of the said machine.

II. Methodology

Review of Relevant Literature/ Data Gathering

Literature and technical articles relevant to the proposed improvement in the transmission system were considered during the implementation of this project. The existing gear shifting mechanism of the rice transplanter transmission system was documented to serve as the



*1 Sr. Science Research Specialist
Metals Industry Research and
Development Center
Bicutan, Taguig City
Philippines



*2 Science Research Specialist II
Metals Industry Research and
Development Center
Bicutan, Taguig City
Philippines

benchmark and reference for the improvement of the transmission system.

Design Improvement and Development of a Rice Transplanter Gear Shifting Mechanism

The improved design of the machine was based on the existing transmission system of rice transplanter being developed both by Rollmaster and PhilRice. The gear shifting mechanism with gear pair combinations was developed using NX CAD software and KISSsoft. The gear ratio for each gear pair was based on the documented gearbox. The final design of the gear shifting mechanism of the rice transplanter transmission system was based on the 3D model and simulation made using the NX CAD and KISSsoft gear design software. Likewise, a technical drawing was made in preparation for the fabrication of the gear box.

Fabrication of the Rice Transplanter Transmission

The fabrication of the rice transplanter transmission was simultaneously undertaken at MIRDC and Rollmaster Machine Shop in conformity with the prepared detailed drawing. All gear components were made of AISI 4140 steels and were manufactured using CNC gear hobber. Preparation of gear blanks was done using other CNC machine operations.

Transmission Housing. The transmission housing of the rice transplanter was made of mild steel plates whose individual components were fabricated using a CNC milling machine and assembled using SMAW welding process.

Gear Shifter Components. Not only gears were manufactured using various processes but also the other major parts necessary to operate the whole system properly. The first process to produce the gears was the preparation of specified materials. This was done by cutting AISI 4140 round bars into appropriate thickness using a bandsaw. The next process was gear blanking. Gear blanking was done using CNC lathe machine. Actual gear thickness and diameter were attained during this process. The gears underwent the process of internal splining, as necessary. This was done to keep the gears move together with the shafts having corresponding splines during its rotary motion. The final stage of gear manufacturing was gear cutting which was done using CNC Gear Hobber.

Gear Shafts. The gear shafts that hold the gears in place were fabricated using two processes. One is shaft blanking which forms the cylindrical profile of the shaft using a CNC turning machine. The other is the splining, also similar to gear cutting, which was done using a CNC milling machine with an attached gear cutter at the end of the tool holder along with the dividing head. Shaft splining was done to prevent the gears from slipping off the shafts while rotating.

Functional Testing

Functional testing was done to determine the initial performance of the developed gear shifting mechanism. This was based on the requirement as agreed with the industry partner.

III. Results and Discussion

Design Development of the Gear Shifter

Design Conceptualization. The conceptual design of the developed gear shifting mechanism was the product of several activities conducted. Among which are the conduct of preliminary visit to the industry partner (Rollmaster Machineries and Industrial Services Corp.).

The project team gathered information pertaining to the problems encountered in using the existing transmission system (Figure 1). The team learned that the drawbacks with the existing transmission system is the difficulty in shifting of gears.



Fig. 1. Meeting with the industry partner

Design Improvement. With the existing design, to change the speed of the gear transmission, the shifting gear slides along the shaft to mate with the other gear. The process produces a grinding sound because of the unsmooth engagement of gears.

In the developed design, the pair of gears with different speeds are constantly engaged. Two gears on one shaft comprise corresponding bearings to allow free rotation along the shaft. Engagement with the shaft happens when a shifting mechanism sliding along the shaft's spline engages with the spline of the gear. This allows the shaft to rotate in unison with the speed of the engaging gear. This process facilitates the smooth shifting of gears.

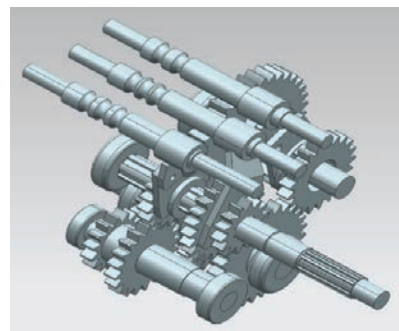


Fig. 2. The existing gear shifting mechanism

Fabrication and Assembly of the Gear Shifter

The gear shifting mechanism together with the gears and shafts was fabricated using various machine operations such as cutting, milling, turning and other required machine operations. After it was completed, the components were assembled in a gearbox developed by Rollmaster.

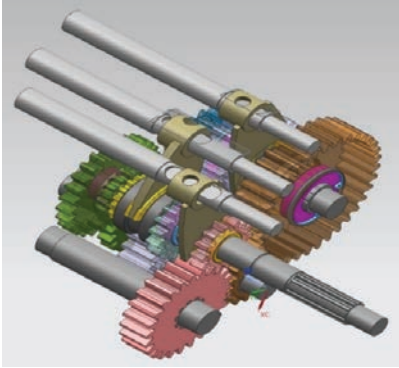


Fig. 3.
The improved gear shifting mechanism

Functional Testing and Debugging

After the assembly of the gear shifter, testing automatically commenced. Vital components that were found to be nonconformity were automatically repaired and adjusted. Functional testing was completed successfully however, the researchers observed various conditions in the process that need to be improved. The said improvements are depicted in the Recommendations section of this report.



Fig. 5.
Testing of the improved gear shifting mechanism



Fig. 4. Fabrication and assembly of the gear shifter

IV. Summary and Conclusion

This project originated from the previous project of MIRDC together with Rollmaster Machinery regarding the improvement of a rice transplanter transmission system. However, during field testing, it was observed that the transmission's gear shifting mechanism needed also to be improved. Hence, this project was conceptualized and implemented.

The general objective of the project was to improve the design and develop a gear shifting mechanism for the riding-type rice transplanter transmission system. Specifically, this project aimed to 1) Simulate the developed gear shifter design using computer-aided design (CAD) modeling and simulation software; 2) Develop a prototype and conduct technical evaluation of the developed gear shifting mechanism; and 3) Validate the modifications to improve the gear shifting system based on the actual field test and performance.

The researchers concluded that the CAD model of the gear shifting mechanism was successfully developed and put into reality by conducting actual fabrication based on the detailed drawing. The developed gear shifting mechanism was also tested for functionality however, due to limited time, field testing was not pushed through as agreed with the industry partner due to unavailability of the existing rice transplanter which is under repair and adjustment.

V. Recommendations

Based on the results of the study, the researchers recommend the following:

1. Increase the width of the gearbox to accommodate the different sizes of improved gears and to facilitate the ease of assembly process.
2. Conduct field testing of the gear shifting mechanism considering the above modification.

References

- [1] Can Yang, Lin Hua, Zhou Wang and Yaohua He. 2014. "Shift Performance Test and Analysis of Multipurpose Vehicle". *Advances in Mechanical Engineering*. Hindawi Publishing Corp.
- [2] Anoop Dixit, R Khurana, Jaskarn Singh, and Gurusahib Singh. 2007. "Comparative Performance of Different Paddy Transplanters Developed in India- A Review". *Agric. Rev.*, 28 (4), pp.262-269.
- [3] Yong-Joo Kim, Sun-Ok Chung, and Chang-Hyun Choi. 2013. "Effects of Gear Selection of an Agricultural Tractor on Transmission and PTO load during Rotary Tillage". *Soil & Tillage Research* 134, pp.90–96.
- [4] Types of Transmissions and How They Work. *Transmission Repair Cost Guide*. <https://www.transmissionrepaircostguide.com/types-of-transmissions/>. Accessed February 5, 2018.
- [5] Shiheng Sun, Huiting Shi. 2018. "Design and Optimization of Automatic Shifting Mechanism for the Tractor". *MATEC Web of Conference* 153.
- [6] Sangamesh Bhure. May 2015. "Optimization and Analysis of Mechanical Gear Shifting System using Kinematic Methodology". <https://www.researchgate.net/publication/275955555>.
- [7] <https://mechanicalenotes.com/constant-mesh-gearbox/> April 28, 2020.

Comparative Study of Sand Casting Pattern Fabrication Lead Times Using Conventional and Additive Manufacturing Processes

Jose Bernardo L. Padaca III^{*1}, Hannah H. Ramos^{*2}, Alvin M. Buison^{*3}, Earl John T. Geraldo^{*4}, Fred P. Liza^{*5},
Leif Oliver B. Coronado^{*6}

Abstract

Traffic conditions in urban communities are worsening because of the sheer volume of vehicles on the road. More vehicles mean more pollution. Thus, alternative means of transport are sought. Methods such as carpooling, mass transportation and personal mobility devices are introduced to reduce the volume of vehicles. This is where personal mobility devices such as electric scooters come into play. The rear lid of the deck of an electric kick scooter is difficult to fabricate due to its intricate geometry. Sand casting is one of the common methods used for fabricating this type of design but creating the pattern for it is usually a tedious process and may take time to finish by conventional means. In this study, the capability of additive manufacturing (AM) to compete with conventional manufacturing in terms of lead-time was investigated. Fused Deposition Modeling (FDM), an AM technology, is used to fabricate the mold pattern for casting as a replacement to the conventional process. Computer Aided Manufacturing (CAM) using Solidworks is applied to get the manufacturing time of the conventional process. It was found that AM could significantly decrease lead-times when producing mold patterns for sand casting compared to conventional manufacturing. The results showed that AM was able to reduce lead times for the deck rear lid pattern parts by more than 50 %. For future studies, the researcher will analyze the economic and environmental aspects of this proposed hybrid process.

Keywords: additive manufacturing, electric scooter, sand casting, pattern fabrication, lead time

I. Introduction

Patterns for the sand casting process can be made from various materials including aluminum, wood, ferrous metals, plastics, etc., but traditionally, these are made of wood [1,2,3]. These materials have different advantages and disadvantages, but wood was mainly used since it is easier to machine than metal. However, this relied on highly-skilled craftsmen to be able to design a pattern as accurate as possible to the dimensions of the part to be cast [2]. For this, the patternmaker needs to be aware of critical information in order for the pattern to function properly.

The shrinkage tendency of the metal will need to be considered in order to apply a certain scale that the patternmaker will use depending on the material to be cast. This is done using shrink rules which are rulers that have various enlarged scales such as by factors of 15:1000 or 10:1000, selected as appropriate to the casting material. This has to be done by the patternmaker for each dimension specified in the shop drawing during the actual pattern layout. Without shrink rules, the patternmaker will need to multiply each dimension by the shrinkage compensation factor to be used on a regular ruler [3].

Apart from this, the patternmaker will need to be mindful of undercuts and internal cavities. An extensive knowledge of working with pattern drafts and parting lines, coupled with the craftsman's experience and creativity, is vital in coming up with a design that ensures that the pattern can be stripped off easily during molding. The pattern will also need to be kept very smooth, as pattern surface quality will be directly reflected by the final cast product. From a manufacturing standpoint, the patternmaker and the foundryman should also work together to come up with a gating and feeding design to ensure that possible casting defects can be minimized or eliminated [3].

With these things to keep in mind, it usually takes weeks to months to be able to craft a pattern out of wood, depending on the size of the part and the intricacy of the design.



Fig. 1. Conventionally fabricated wooden patterns



^{*1} Project Senior Technical Specialist
Metals Industry Research and
Development Center
Bicutan, Taguig City
Philippines



^{*2} Project Technical Assistant IV
Metals Industry Research and
Development Center
Bicutan, Taguig City
Philippines



^{*3} Sr. Science Research Specialist
Metals Industry Research and
Development Center
Bicutan, Taguig City
Philippines

With the advent of newer technology, fabrication of patterns is now much easier compared to when everything had to be done by hand. Using Computer Aided Design (CAD) software, accurate 3D models of the parts to be cast can be easily prepared and worked on. Modern CAD solutions such as Solidworks have features that let the engineer design molds easily. Scaling the model to compensate for shrinkage will need just a few computer commands. Undercuts in the pattern can also be seen easily as the software includes a feature that color-codes the surface topography of the 3D model to easily check which portions will need to have drafts applied. Applying drafts can also be readily done inside the software. For intricate designs that may not be possible to be split using a simple, straight parting line, the software can suggest a parting surface that follows a path where the positive and negative draft values of the pattern meet. Gating systems and feeders can then be added to complete the casting design. From these, a comprehensive design of the pattern, as well as core boxes (if any) can easily be achieved.

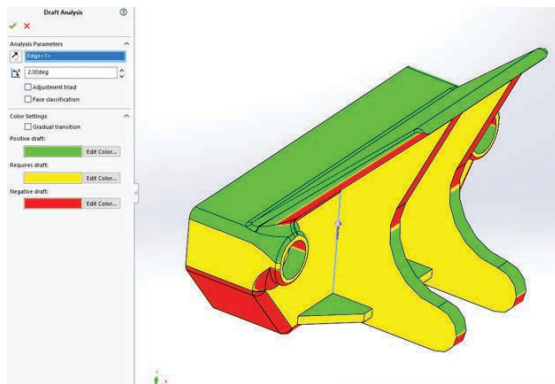


Fig. 2. Draft Analysis feature to evaluate sufficiency of drafts as well as undercuts

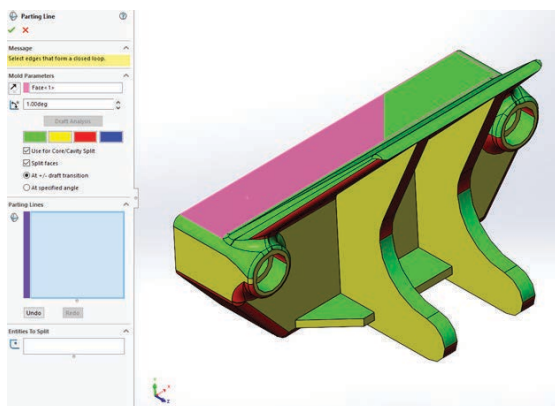


Fig. 3. Parting line recommendation feature

This 3D model can also be used with Casting Simulation Software such as Magma or Novacast, which have the ability to predict possible defects by simulating the metal casting process. This gives the designer a huge advantage in that testing out the casting design need not entail making the actual pattern and doing actual casting in order to validate the effectiveness of the design. This allows the designer to easily modify and improve the casting design readily in the CAD software and simulate again. The design can be changed as appropriate based on the simulations, as many times as needed, without incurring too much costs. Once simulation results are deemed satisfactory, only then will the pattern need to be fabricated.

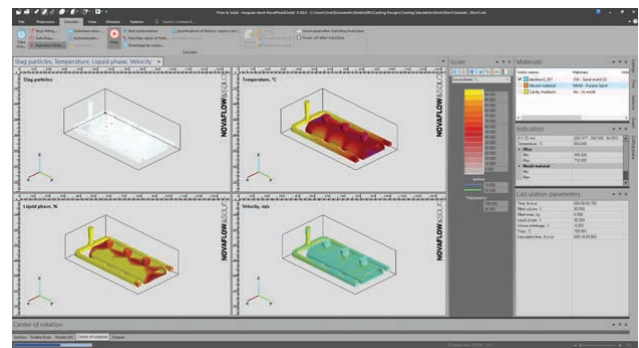


Fig. 4. Casting simulation software to help identify possible defects in the casting design

This 3D model can then be used to make 2D drawings that can be used by patternmakers and employ traditional woodworking processes. But with the availability of newer technology that can make use of 3D CAD models as input, more dimensionally accurate patterns can be achieved. One of these technologies is Computer Numerical Control Machining or better known as CNC. With CNC machining technology, a part can be manufactured from the 3D model which will ensure that the finished product will be dimensionally faithful to the drawing. It does this by beginning with a block of material and removing material by cutting, using a tool path program made up of lines of machine codes derived from the input 3D model. Equally important to dimensional accuracy is that machining can achieve faster fabrication times compared to traditional handmade patterns, as the patterns will be made with fully automated machines that can work non-stop. Nowadays, CNC machined patterns are quickly becoming a more popular choice by foundries due to the aforementioned advantages, coupled with the fact that there now seems to be a very short supply of able conventional patternmakers probably as a result of the availability of newer technologies, as well as younger generations also leaning to learn these new technologies.



*1 Project Technical Specialist I
Metals Industry Research and
Development Center
Bicutan, Taguig City
Philippines



*2 Chief Science Research Specialist
Metals Industry Research and
Development Center
Bicutan, Taguig City
Philippines



*3 Science Research Specialist II
Metals Industry Research and
Development Center
Bicutan, Taguig City
Philippines



Fig. 5. CNC machined pattern using a horizontal 3-axis milling machine

Another process that can promise high dimensional accuracy and fast lead times is Additive Manufacturing (AM) or 3D printing, which works the other way around compared to CNC machining. It also uses the 3D CAD model as an input but rather than a subtractive approach, the part is built from the ground, layer by layer until the entirety of the part is printed. In theory, this can achieve even shorter lead times than CNC machining because of the fewer amount of material being worked on. In AM, the material consumption is almost equal to the actual part volume, with minor additional weight used to make print supports. This is as opposed to machining where a block of material is used and is cut to make the final product, thus starting with more material than how much is needed for the actual part. In addition to this, AM is a one-step process once the build process begins. With CNC machining, depending on the complexity of the shape of the part being produced, several stages of machining operations which involves unloading the workpiece and clamping it in another orientation may be needed, which significantly add to the total manufacturing time.

This study aims to compare the fabrication lead times of CNC Machining and Additive Manufacturing to explore whether Additive Manufacturing can be used as a viable alternative in pattern fabrication, especially in the context of product development where timeliness is a crucial part of a product's success on its way to being commercially available.

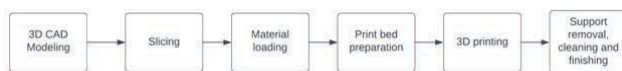


Fig. 6. Process flowchart for 3D printing

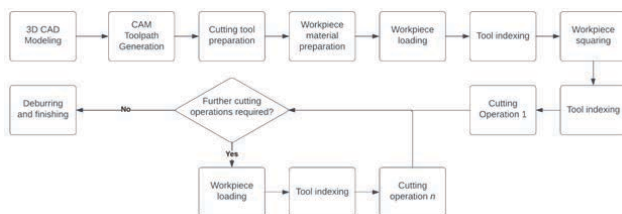


Fig. 7. Typical process flowchart for CNC Machining

II. Materials and Methods

For this study, the pattern of a rear lid of the deck of an electric kick scooter was made from Polylactic Acid (PLA) plastic filament feedstock using Fused Deposition Modeling (FDM).

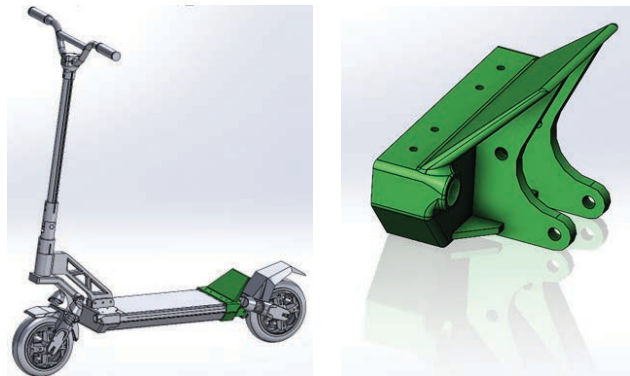


Fig. 8. Left: The Local Electric Kick Scooter (LEKS) showing the cast rear lid of its deck in green. Right: The rear lid of the scooter deck to be made by sandcasting

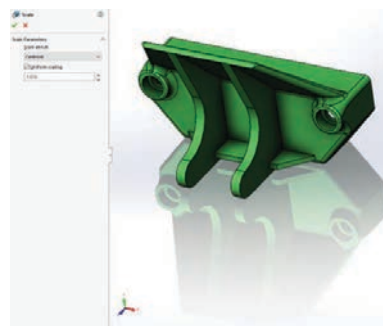


Fig. 9. The Scale feature that can be used to apply the shrinkage compensation factor in designing patterns

The 3D model of the deck rear lid was made using Solidworks. From this base design, the shrinkage compensation factor was accounted for using the "Scale" feature, to enlarge the part by a factor of 1.015, which is appropriately selected for the casting to be made out of aluminum alloy A356.

Since the part geometry is intricate, a simple, straight parting line will not be possible. As such, an offset parting surface was made using the software. From here, the drag and mold halves of the pattern were designed, as well as the gating and feeding design.

As an additional step to ensure the quality of the parts to be cast, the casting design was run through a casting simulation software, Novacast Flow and Solid.

Once the simulations show satisfactory results, the components of the pattern were prepared for 3D printing. The preliminary step to 3D printing is slicing, which is used to set the printing parameters that will affect the quality of the print such as print resolution, density, orientation, and many other parameters that dictate the durability as well as surface quality of the pattern to be made. For this particular part, the main pattern cavity for the rear lid, which is the main part of the pattern assembly, was

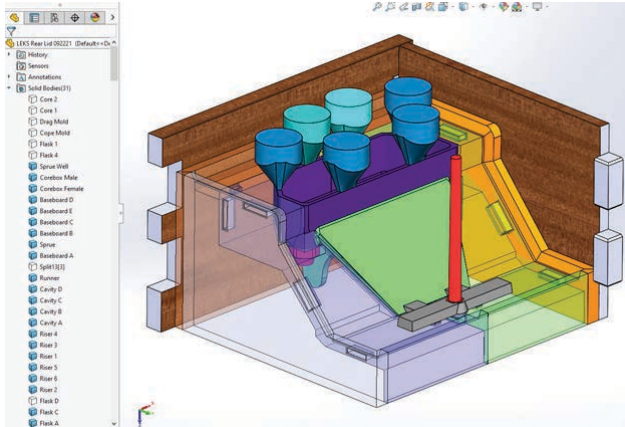


Fig. 10. The assembly 3D model of the whole casting design of the rear lid, color-coded to indicate distinct components

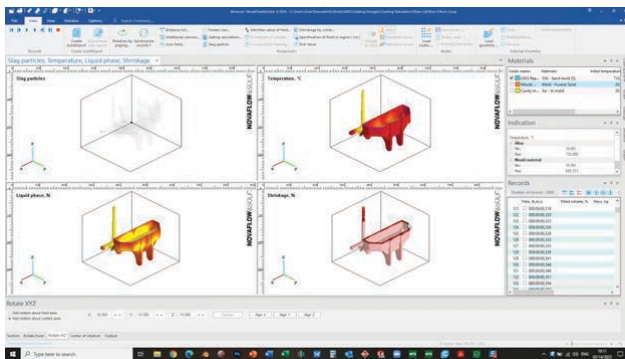


Fig. 11. Casting simulation software to help identify possible defects in the rear lid casting design

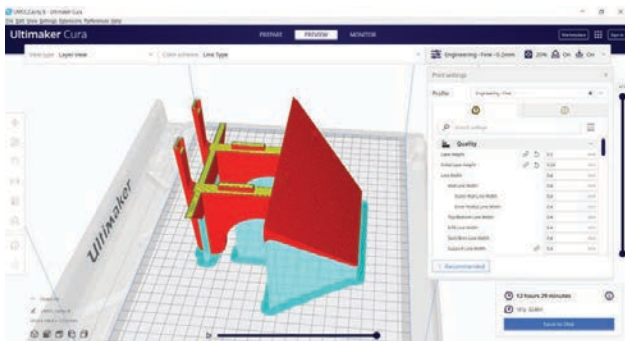


Fig. 12. Slicing of the cavity of the rear lid pattern using Ultimaker Cura software

printed with tighter tolerances and higher resolution, with a layer height of 0.2mm, in order to ensure a good surface quality casting. Other ancillary parts such as risers, sprue, runners, the follow board and flasks were printed with lower resolution, with a layer height of 0.3mm, to achieve even faster print times as they will not be part of the final product.

All the components of the rear lid pattern assembly were printed using the Ultimaker S5 desktop FDM 3D printer, using PLA plastic filament. After printing, post processing was performed to clean up the prints and remove unnecessary material such as print supports and brims. The pattern components were also coated with hard

automotive primer and sanded to achieve a smoother surface. This coating protects the pattern from abrasion from the molding sand as well as chemical degradation that may be caused by the acid catalyst present in the furan no-bake binder used in molding.



Fig. 13. 3D printing of the pattern components of the rear lid

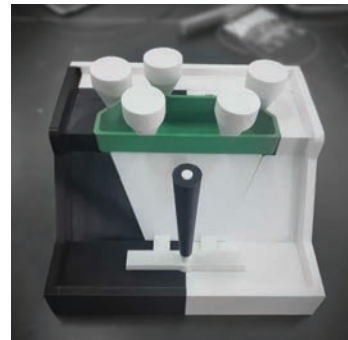


Fig. 14. Assembly of the as-printed pattern of the rear lid



Fig. 15. Application of primer in order to improve abrasion/wear and chemical resistance of the 3D printed pattern



Fig. 16. The assembled 3D printed pattern of the rear lid ready for molding

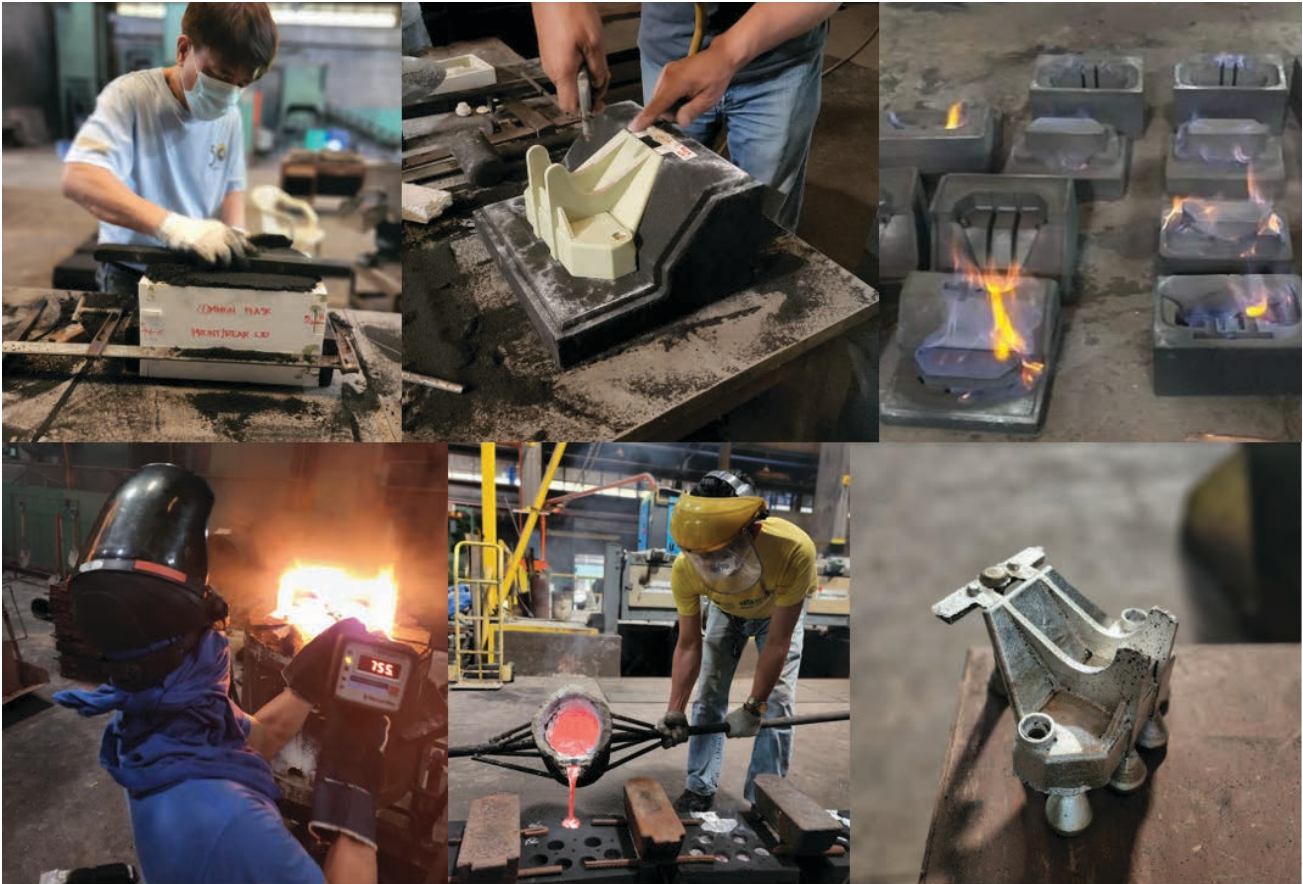


Fig. 17. 3D printing of the pattern components of the rear lid

The pattern was then used in molding 5 units of the rear lid castings.

In order to compare the lead times of the pattern fabricated through 3D printing, the same 3D pattern design was used in a Computer-aided Manufacturing (CAM) software. This software can predict the fabrication time of a product using machining processes. This takes

into account the geometry of the part as well as the material in order to identify the required cutting processes and sequences. This will determine the total time it takes for the machining process to finish. Three components were studied for the process cycle time comparison - one single piece cavity for the rear lid and two split cavities A and B that will be assembled together to form a single cavity.

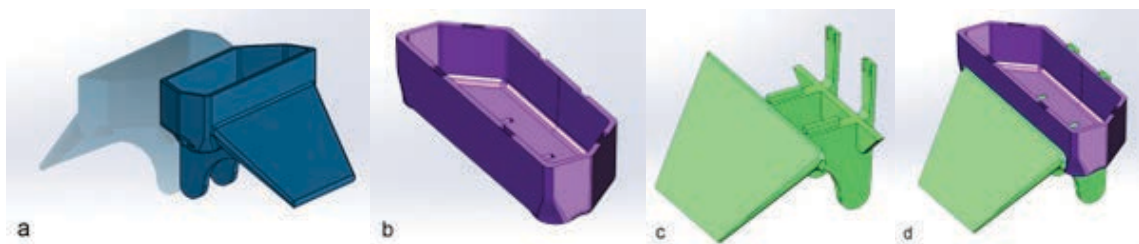


Fig. 18. (a) Rear lid single-piece cavity, (b) Rear lid split cavity A, (c) Rear lid split cavity B, (d) Rear lid split cavity A and B - assembled

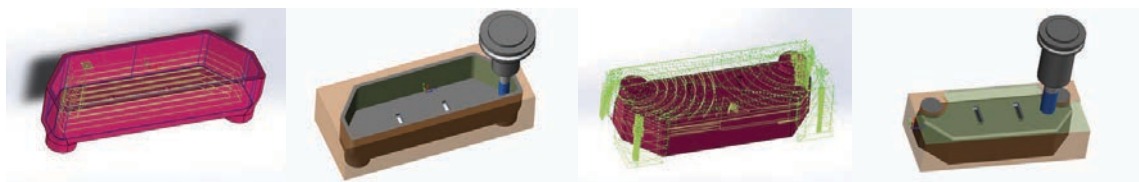


Fig. 19. CAM software showing the toolpath in machining the rear lid split cavity A

III. Results

Table 1 shows the results of the cycle time simulations using CAM software compared to actual printing time of the rear lid pattern cavity.

tool preparation, workpiece preparation, tool indexing and workpiece clamping - processes which add significant time to the total machining fabrication process - are effectively increased twofold.

V. Conclusion

Additive manufacturing is a viable option for fabrication of patterns for the sand casting industry. However it should not be looked at as a replacement for other existing fabrication technologies such as machining or traditional woodworking. Rather it should be treated as a complementary process and the choice of process or combinations thereof will highly depend on the judgment of the designer, depending on the requirements of the product in terms of design complexity, dimensional accuracy and production volume. For intricate parts, additive manufacturing using plastic material will suffice for low-volume production parts. However, as the volume increases, plastic components may not be able to last as long compared with metal patterns with excellent mechanical properties to withstand wear. For these instances, it may be a better option to select CNC machining as presently, metal additive manufacturing is a more costly process due to the high prices of raw materials and operation.

Table 1. Cycle times of 3D printing and CNC Machining of Rear Lid Pattern Cavity

Pattern Component	Fabrication Process	Technology	Sub-process	Cycle Time, min	Total cycle time, hr
Rear Lid Single-piece Cavity	Additive Manufacturing	Fused deposition modeling	3D Printing	1563.0	26.05
	CNC Machining	3-axis Vertical Milling	OP10 Rough Cut	2020.0	56.25
			OP10 Finishing	60.0	
			OP20 Rough Cut	1267.0	
			OP20 Finishing	28.0	
Rear Lid Split Cavity A	Additive Manufacturing	Fused deposition modeling	3D Printing	563.0	9.38
	CNC Machining	3-axis Vertical Milling	OP10 Rough Cut	940.0	23.69
			OP10 Finishing	19.3	
			OP20 Rough Cut	460.0	
			OP20 Finishing	2.0	
Rear Lid Split Cavity B	Additive Manufacturing	Fused deposition modeling	3D Printing	749.0	12.48
	CNC Machining	3-axis Vertical Milling	OP10 Rough Cut	1501.6	25.66
			OP10 Finishing	26.8	
			OP10 Finishing 2	11.2	

IV. Discussion

As can be seen in Table 1, the total cycle time for 3D printing the pattern cavities are significantly shorter than that of CNC machining, with the former's cycle times reaching up to less than half of the latter's cycle time. It is to be noted that for this study, only the cycle times of the actual building processes are taken into consideration. This does not take into account the various preparation and set-up procedures before and in between each step of the build process. As can be seen in the comparison of the process workflows presented in Figure 6 and Figure 7, a significantly longer time will be added on top of the total build cycle time for the CNC machining process as it involves more sub-processes (e.g. tool preparation, workpiece preparation, tool indexing, loading and unloading for different cutting operations) whereas 3D printing is a single-step build process.

For the single piece cavity, the total 3D printing cycle time is 26.05 hours, which is a 53% reduction in build cycle time from CNC Machining with a 56.25-hour build time. Splitting the pattern into two pieces may make it easier to orient the workpieces in directions where the build cycles can be reduced. Such is the case for both 3D printing and CNC machining where the total build cycle times are 21.87 hours and 49.35 hours respectively. However, the reduction in these build cycle times may not be enough to offset the additional preparation and set-up times for each of the components for both processes. This is especially true for CNC machining where procedures like

VI. Acknowledgments

The authors would like to acknowledge the support of Mayatech, Inc. in this endeavor in providing all the needed materials as well as technical inputs in the design of the kick scooter. The authors would also like to extend their gratitude to the MIRDC Technical Solutions Services Section for their support in metal casting and further processing of the rear lid and other scooter components.

References

- [1] Anakhu, Peter & Bolu, Christian & Abioye, Abiodun & Azeta, Joseph. (2018). Fused Deposition Modeling Printed Patterns for Sand Casting in a Nigerian Foundry: A Review. *International Journal of Applied Engineering Research*. 13. https://www.researchgate.net/publication/324601411_Fused_Deposition_Modeling_Printed_Patterns_for_Sand_Casting_in_a_Nigerian_Foundry_A_Review.
- [2] M. M. Ganganallimath, K. Vizayakumar and U. M. Bhushi, "Quality Improvement of Sand Castings through Implementation of 3D-Printing Technology," 2022 *Advances in Science and Engineering Technology International Conferences (ASET)*, 2022, pp. 1-6, doi: 10.1109/ASET53988.2022.9734939. <https://ieeexplore.ieee.org/abstract/document/9734939>.
- [3] W. Wang, H. Stoll, J. Conley. 2010. "Rapid Tooling Guidelines For Sand Casting." Springer. pp. 1-7. doi: 10.1007/978-1-4419-5731-3.

Development of Automatic Trash Rake in Malabon-Tullahan River System

Maybelyn D. Rivera*¹, Rodnel O. Tamayo*², Nestor Q. Colibao Jr.*³, Vincent Boy E. Manabat*⁴

Abstract

Solid waste management is one of the pressing concerns in Malabon that leads to pollution and flooding. Among the dominant concerns that lead to pollution and flooding are improper wastes disposal, inefficient wastes collection, and lack of disposal facilities. The DOST – Metals Industry Research and Development Center (MIRDC), in cooperation with the Department of Natural Resources Environmental Management Bureau – National Capital Region (DENR EMB-NCR) developed the Automatic Trash Rake Facility in Malabon that will serve as a possible source of alternative technology to help the flooding problem caused by clogged waterways. A series of functional tests were conducted to test the performance and functionality of the equipment. Results showed that the ATR can collect an average of five cubic meters of garbage, which is better compared with the existing manual method previously used. However, further innovation of the trash rake is towards an unmanned facility. It can be remotely controlled or can be operated on a pre-programmed operation or more complex continuous system operation.

Keywords: trash rake, waterways, automatic, WQMA

I. Introduction

Solid waste management has been one of the greatest challenges the Philippines is facing, as the country's garbage is way beyond the solid waste management capacity [1]. This is also a result of improper waste disposal, lack of disposal facilities, and inefficient waste collection that leads to pollution and flooding [2].

One of the best ways to prevent the accumulation of garbage, specifically in waterways, is by using trash traps and trash rakes. Trash rakes are raking devices used to remove large or rough debris. They protect pumping equipment at electrical generating plants, pump stations, and flood control projects and may be used as a preliminary screening device to protect finer screens [3].

The idea of this project is pursuant to Section 5 of RA 9275 otherwise known as the Clean Water Act of 2004, wherein the DENR Environmental Management Bureau-National Capital Region (EMB-NCR) has proposed the designation of Malabon-Navotas-Tullahan-Tinajeros River System as Water Quality Management Area (WQMA) in the National Capital Region.

Basically, this aims to establish one (1) Automatic Trash Rake Facility along Malabon-Tullahan River System.

Specifically, to (1) keep floating debris, leaves, and other solid waste from entering; (2) reduce pollution loading discharges in Malabon; and (3) establish a partnership mechanism that will coordinate approaches to the management of the area.

II. Related Literature and Studies

Trash rakes existed as soon as the hydroelectric power plants were established. These are heavy equipment used to remove debris from screens at hydropower facilities. It consists of one or more stationary rakes and a screen raking mechanism. There is a variety of raking mechanisms available for use in a variety of configurations, including installation on vertical buildings and dam walls. Rakes may also be mounted on fixed structures or may be suspended from an overhead gantry [4].

There are different types of trash rakes namely: cable-operated rakes, chain-operated rakes, and hydraulically-operated rakes. A cable-operated rake system consists of a cable winch and rake arm that scrapes across the screen to remove large pieces of debris that are to be deposited in a trash bin. Chain-operated rakes use tooth rakes or debris lifters mounted on strands of chain, operating overhead and foot sprockets. On the other hand, hydraulically-operated rakes are commonly used in hydropower plants, wastewater treatment plants, and other industrial applications. This system can run without the use of chains, guides, and sprockets [5].

Automated trash rack cleaning has been proven to improve efficiency and reduce costs. In Europe, Verbun upgraded its hydroelectric plants along the Mur River with fully automated systems in 2005. The plants have been unmanned ever since and working very efficiently.



*1 Science Research Specialist II
Metals Industry Research and
Development Center
Bicutan, Taguig City
Philippines



*2 Chief Science Research Specialist
Metals Industry Research and
Development Center
Bicutan, Taguig City
Philippines



*3 Engineer I
Metals Industry Research and
Development Center
Bicutan, Taguig City
Philippines

One of the most noticeable benefits of the automatic trash rake system is the operators' safety. Manual trash raking is inherently risky, and automated systems reduce that risk. Also, it offers many operational and financial benefits. Evidence of these benefits can be seen in the upgrades being done to hydroelectric plants around the world [6].

The first automatic trash rake project developed by DOST-MIRDC was installed in Balingasa Creek along Gregorio Araneta Ave., cor. Mauban Street in Barangay Manresa Quezon City. It was installed to collect the garbage before the water goes to adjoining major creeks leading to the San Juan River. The project was entitled "Improvement of Flood Control Facility through the Development of Automatic Trash Rake". The Balingasa creek is the main tributary to the San Juan River and 86 percent of the wastes from upstream pass through it. The setting up of the facility has remarkably abated clogging of the San Juan River and reduced the amount of debris washed out in Manila Bay during typhoons. The facility is capable of collecting an average of 5.1 cubic meters of trash in an 8-hour shift. It has its own backup generator and has three trained operators [7].

III. Methodology

Collaboration and site identification

The project was a collaboration between the DOST - Metals Industry Research and Development Center (MIRDC) and the Department of Environment and Natural Resources (DENR) wherein the beneficiary is the Local Government of Malabon. A memorandum of agreement was signed by all parties which paved the way for the construction and fabrication of the Automatic Trash Rake facility.

The site was identified by Malabon LGU. Prior to the design phase, the following data were gathered and taken into consideration.

- The width of the creek is 9.1 meters.
- The depth of water level from the ground level is 2.40 meters
- The proposed site is surrounded by numerous inhabitants
- There is possible access for the dump truck
- Located on the other side of the road
- Near the pumping station

The sustainability of the facility such as storage of garbage collected, accessibility of garbage trucks during collection, and the number of barangays served were also considered.



*4 Science Research Specialist II
Metals Industry Research and
Development Center
Bicutan, Taguig City
Philippines



Fig. 1. Identified location of the ATR - Letre Creek, P. Aquino Avenue, Brgy. Tonsuya, Malabon City

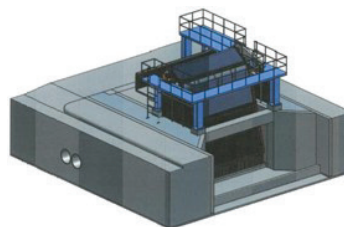


Fig. 2. Design of the Automatic Trash Rake Facility



Fig. 3. Training of LGU personnel

Facility design

The design of the Automatic Trash Rake was based on the previous project installed in Balinghasa Creek, Quezon City. With the support of the Engineering Department of Malabon LGU, the structural/civil design was finalized based on the soil test analysis results. On the other hand, the MIRDC focused on the preparation and finalization of the mechanical design.

Implementation (Construction and Installation)

The R2M Construction Corporation was awarded the construction and fabrication of the Automatic Trash Rake facility based on the design of the MIRDC project team. An operation and maintenance manual for the ATR operation was also prepared to be used by Malabon LGU.

Testing and Training

After the complete construction and installation of the facility, functional and performance testing was conducted. Moreover, 3 personnel from LGU Malabon were trained for the operation and maintenance of the facility.

IV. Results and Discussion

The DOST-MIRDC developed the Automatic Trash Rake (ATR) in Malabon in response to the proposal of DENR EMB-NCR to designate the Malabon-Navotas-Tullahan-Tinejeros (MaNaTuTi) River System as WQMA in the NCR under the Clean Water Act of 2004. The primary objective of the project is to design and develop an automatic trash rake in Malabon-Tullahan River System as an alternative solution to flooding and to improve the waste management system. The ATR facility was constructed in Malabon City.

With the help of Malabon LGU, DENR EMB-NCR, and MIRDC were able to identify the needed requirements of the site making it easier for the project team to address the problem and consider it during the designing stage. According to the CENRO of Malabon, the identified location is the most feasible since it is near the pumping station and where abundant trash from different barangays accumulates.

The design concept of the project was based on the specifications of the previous Automatic Trash Rake Facility constructed in Quezon City, which was also installed and implemented by MIRDC. However, the design was modified based on the width of the creek. The mechanical design is based on the civil/structural design prepared by the Malabon Engineering Office considering the result of the soil test analysis.

Functional and performance testing was conducted and results showed that the Automatic Trash Rake can collect an average of 5 cubic meters of trash per day.



Fig. 4. Automatic Trash Rake Facility

Table 1. Specifications of the Automatic Trash Rake Facility installed at Letre Creek, Malabon

ITEM/PART	SPECIFICATIONS
Number of Rakes	6 sets
Width of Rake	6 meters
Linear Speed of Rake	0.3 meters per second
Rake Conveyor Sprocket	
Pitch	200 mm
Pitch Diameter	636 mm
Number of Teeth	10
Material	SS 304
Rake Conveyor Chain	
Pitch	200 mm
Material	SS 304
Drive Motor	Gear Motor: 10 HP, 240 VAC, 3 phase, 40 rpm
Drive Sprocket	
Gear Motor Shaft	#8014
Drive Shaft	#8048
Generator set	
Fuel	Diesel
Rating	33 kVA
Output	240 VAC, 3 phase

Table 2. Collection results of the functional testing

Day	Collection Rate	Remarks
1	4.5 m ³	Without rain
2	4.5 m ³	Without rain
3	6 m ³	Without rain
4	5 m ³	Without rain
5	5 m ³	Without rain
Total	25 m ³	
Average	5 m ³	

V. Conclusion

Towards the completion of the project, in partnership with Malabon City LGU, DENR EMB-NCR, the Automatic Trash Rake Facility was designed and built at Letre Creek P. Aquino Ave. Brgy. Tonsuya, Malabon City. The design of the automatic trash rake facility was planned through the collaboration of the MIRDC project team and the Malabon City Engineering Department.

The project team conducted a series of functional testing of the equipment as witnessed by the Malabon City Environment and Natural Resources Office (CENRO) and the initial test was considered a successful one. The equipment underwent complete performance and endurance testing conducted by the Malabon

City Personnel. The trash rake facility already collected an average of 5 cubic meters of garbage a day, which is better compared with the existing manual method previously used.

The DOST-MIRDC has officially turned over the management and operation of the automatic trash rake facility to Malabon City Government during a brief ceremony held at the Penthouse Malabon City Hall.

The use of technology will enable the collection of garbage in the waterways faster and easier, especially during the critical times of the rainy season. It was installed to collect garbage before the water goes to adjoining major creeks leading to the Malabon-Tullahan River system.

With the success of the project during this test period, the DENR EMB-NCR expressed interest to construct another two (2) trash rake facilities in different local government units in Metro Manila to further improve its garbage collection mechanism.

VI. Recommendations

Research and Development Breakthrough

The Automatic Trash Rake Facility installed in Malabon is the second ATR implemented and developed by the DOST-MIRDC. As part of its continuous development, below are the recommendations for future R&D works:

1. The trash rake facility must be adopted by the LGU to be deployed in small river systems or creeks. The project is geared towards raising public awareness of the government's research and development initiatives, as well as promoting the ATR as a machine that could capture the trash and debris in the waterways.
2. A further innovation of the trash rake is towards an unmanned facility. A facility with no operator on site. It can be remotely- controlled or can be operated on the pre-programmed operation or more complex continuous system operation.

References

- [1] Department of Environment and Natural Resources, 2018. "National Solid Waste Management Report". <https://emb.gov.ph/wp-content/uploads/2019/08/National-Solid-Waste-Management-Status-Report-2008-2018.pdf>
- [2-3] 2018, <https://www.lakeside-equipment.com/how-do-hydropower-trash-rakes-work/>
- [4] 2018, <https://www.lakeside-equipment.com/how-do-hydropower-trash-rakes-work/>
- [5] Screening Equipment Handbook for industrial and municipal water and wastewater treatment, 2nd ed., Thomas M. Pankrats, CRC Press, 1995.
- [6] <https://www.streetdirectory.com/etoday/-wffep.html>
- [7] Improvement of flood Control Facility through the Development of Automatic Trash Rake, Philmetals Vol. 4, Bathen, Gharry M., 2017

CNC MACHINING & FABRICATION SERVICES



Capabilities

- > Design & Fabrication
- > Rapid mass pro & prototyping
- > 3D & 5 Axis machining technology
- > Industrial Automation

CONTACT US NOW!

Tel: 049 544 2506

Cp: 0917 8096 628

Email:

sales.hantverk@gmail.com

www.hantverkphils.com



Hantverk Technologies

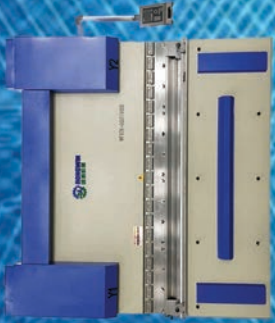
www.hantverkphils.com

Engineering Sourcing Solution Across the Globe

Email: sales@hantverkphils.com / sales.hantverk@gmail.com



RONGWIN



Press Brake Machine

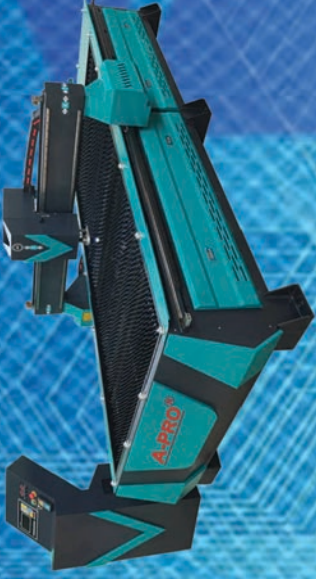


Hydraulic Shearing Machine



Rolling bending Machine

A-PRO[®]



CNC PLASMA CUTTING MACHINE



Freezer Dryer



Vacuum fryer



Spray Dryer



Water Retort

BEMATO



CONVENTIONAL LATHE



VERTICAL LATHE



VERTICAL MILLING MACHINE



UNIVERSAL MILLING MACHINE



CNC Lathe Machine GS 150



CNC Milling Machine GX 600



#17 Mars St. Congressional Subd. II Tandang Sora Quezon City Philippines 1116
Admin@gecarmachine.com, Sales@gecarmachine.com, Marketing@gecarmachine.com

Mobile No. : +63 922 855 7222
+63 922 855 7333

Phone No. : +632 8928 8307
Fax No. : +632 8928 8307

www.gecarmachine.com

Augmented Poultry Egg Hatchery

Arvin Yan V. Pacia*¹, Angeluzel Tonido-Reyes*², John Michael P. Alipio*³

Abstract

The global demand for poultry products, driven by population growth and dietary shifts, has surged, prompting the poultry industry to optimize processes for greater efficiency. Key to this is the incubation of poultry eggs, where manual methods have limited yield and hatching effectiveness. To address this, researchers developed an "Augmented Poultry Egg Hatchery," an automated incubator controlling temperature, humidity, ventilation, and turning of egg, creating an optimal hatching environment. The study aimed to assess the effectiveness of this automated incubator in enhancing hatchability. The project was focused on incubation, candling, and hatching phases, integrated features like a built-in candling light for egg analysis and a motor for automatic turning. The incubator's design also included a hatching area with egg baskets. Poultry farmers and hatcheries, reliant on high hatchability for operational success, benefit significantly. The automated incubator increased hatchability, reduced manual labor dependence, and ensured consistency of efficient production. The study's success is evident in the incubator yielding 418 live chicks from 528 viable eggs, achieving an efficiency rate of 79.17%. Lastly, the recommendation emphasizes upgrading the power supply to a renewable energy source to reduce energy consumption.

Keywords: arduino-based, augmented, automated, candling, efficiency, egg, engineering, hatchery, incubator, turning, optimization, poultry, sustainable, system

I. Introduction

The Philippines boasts a thriving agricultural sector, particularly in poultry farming, where continuous monitoring and management are essential for the healthy incubation of eggs. The incubation phase, crucial for embryo development demands consistent heat, and deviations in parameters can hinder normal growth. In the current era, global demand for poultry products has surged, pressuring the industry to optimize processes. Pivotal to this is poultry egg hatching, where traditional manual or semi-automated methods are labor-intensive and yield inconsistent results.

Technological advancements, specifically in the field of technology and controller systems are subject for innovation, present opportunities to revolutionize egg incubation. This study, entitled "Augmented Poultry Egg Hatchery," explores the integration of automation and embedded technology to create an adaptable and highly efficient incubation environment. In the context of sustainable agriculture, the incorporation of nanotechnology and Arduino-based control systems promises improved hatch rates, and enhanced productivity, aligning with global efforts for sustainable food production and minimized environmental impact.

The research takes a comprehensive approach, beginning with a study of fundamental incubation principles and technology's potential advantages. It progresses to the design, development, and testing of the Augmented Poultry Egg Hatchery system, evaluating its performance against traditional methods. Practical implications and

economic feasibility for widespread adoption are also considered.

Despite increasing demand, the Philippines' chicken production has not significantly shifted since 2020, according to Philippine Statistics Authority (2020), attributed to the pandemic, bird flu outbreak, and underdeveloped manual egg hatching technology. This manual operation restricts egg production, potentially resulting in an ineffective hatching rate of 50-65%. Unsatisfactory incubators can significantly impact hatching rates, causing premature hatching, deformities, and contamination.

The study cites Mousa-Balabel et al.'s findings on microorganisms penetrating eggshells, impacting embryo development and causing mortality in hatcheries with poor hygiene. To address these challenges, the researchers introduce the "Augmented Poultry Egg Hatchery" an automated system aiming to increase hatching viability by precisely controlling temperature, humidity, ventilation, and egg turning. The device includes visual indicators for convenience, aiming to achieve a 90-95% survival rate through the hatching stage.

As researchers navigate an era demanding technological innovation and sustainability in food production, this study promises to transform the poultry industry, introducing efficiency, eco-friendliness, and economic capability to poultry egg hatchery operations.



*1 Sr. Science Research Specialist
Metals Industry Research and
Development Center
Bicutan, Taguig City
Philippines



*2 Assistant Professor III
University of Rizal System
JP Rizal St., Brgy. Sampaloc,
Tanay, Rizal, Philippines



*3 Instructor III
Rizal Technological University
Boni Avenue, Mandaluyong City
Philippines

II. Materials and Methods

Process Narrative

The researchers used the descriptive and developmental research methods to assess an egg incubator's effectiveness. Descriptive research gathers information about the subject, while developmental research aims to improve instructional and technical design of the system device. The researchers applied both methods to evaluate an automated incubator, aiming to enhance chick hatching efficiency and reduce human errors.

The researchers initiated this project to automate the incubation process, improving the efficiency of producing high-quality chicks. This machine focuses on fertile chicken eggs, operating continuously without direct human involvement except for candling and transferring. Comprehensive information about the incubation and hatching process is provided.

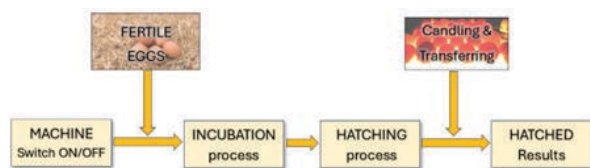


Fig. 1. Process Block Diagram for the Augmented Poultry Egg Hatchery

Incubation Process

The incubation process begins with thorough cleaning of the incubator to maintain proper hygiene. Temperature and humidity are adjusted, and eggs are placed in the incubator. Regular egg turning prevents issues and enhances embryo development, while fumigation sterilizes the eggs. The operator monitors the condition from day one to seven, with candling on day seven, settings are maintained until day twelve. Then, second candling occurs on day twelve, and a final one on nineteenth day. After candling, automatic turning of egg stops, and suitable eggs move to the hatching area.

Hatching Process

In the hatching phase, which occurs in the last two to three days, egg turning stops. On the eighteenth and nineteenth day, the chick positions itself to consume remaining yolk and only then can be moved to the hatching area after stabilizing temperature and humidity. Fumigation is done to protect the embryo.

The incubator door is closed on day twenty, maintaining hatching conditions. By day twenty-one, the chick cracks the shell, and another twenty-four hours for drying, hatched egg chicks can be removed if over 90% are dry. This process ensures the successful production of healthy chicks.

Control Narrative

Before incubation, fumigation and sanitation are critical to eliminate contaminants. Fumigation involves using powdered chemicals to generate smoke that passes through the incubation area. This process is followed by ventilation and a 30-minute machine pre-warming.

III. Materials and Specifications

The specifications of the materials and components used in the construction of the system device, along with the quantity needed and estimated prices are specifically plotted by the researchers. The total expense on the development of the system device was sixty-two thousand three hundred forty-nine pesos and fifty-three cents.

IV. Design, Fabrication, and Construction of System Device

The system device consists of two major parts which are based on the stages needed to have a successful incubation, namely Incubation Process and Hatchery. The two sides of the machine are intended for the two stages, and these are made from different materials.

System device's Different Point of View

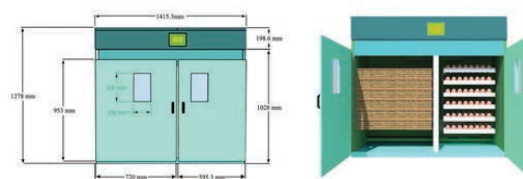


Fig. 2. System Device's Dimensions (Open and Close View)

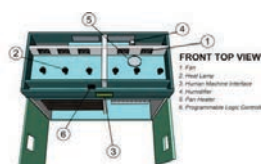


Fig. 2.1. Cross-section of the System device

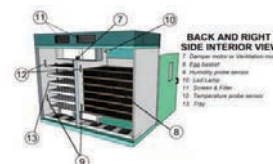


Fig. 2.2. Cross-section of the System device

Figure 2 on the left provides the dimensions of the unit while on the right shows the components inside the machine such as the egg basket, egg tray, HMI, and ventilation fan. Next Figure 2.1 shows the front top cross-section of the system device. It consists of six parts or components namely a ventilation fan, heat lamp, Human-Machine Interface, humidifier, pan heater, and Programmable Logic Controller.

Figure 2.2 shows the back and right-side cross-section of the system device. It consists of seven parts or components namely the damper motor, egg basket, humidity probe sensor, LED lamp, screen and filter, temperature probe sensor, and egg tray.

V. Results and Discussion

The researchers successfully developed an Arduino-based incubator for poultry eggs that improves production efficiency. The system device went through several stages, including design, material selection, procurement, assembly, component installation, testing, and adjustments. The incubator, controlled by an Arduino Mega, has an LCD display showing real-time temperature, humidity, date, and time. It regulates temperature, humidity, egg turning, and ventilation to create ideal conditions for egg hatching.

The results and discussion highlight the changes and improvements made during the system device's development. Overall, the automated incubator has enhanced egg hatching efficiency and success in both commercial and research settings by maintaining a stable incubation environment. Below is the actual image of the system device entitled Augmented Poultry Egg Hatchery.

The researchers worked on improving the design of an automated egg incubator. The various stages of development start from conceptualizing the design and selecting the appropriate modules. Initially the planned was to use a Programmable Logic Controller but switched to an Arduino Mega as the main controller since it can already handle the program tasks and more convenient to use. Part of the design is an egg tray trolley for easier egg placement. The power source was modified to include a generator with an Automatic Transfer Switch for uninterrupted power supply.

Exhaust fans were added to dissipate heat, and aluminum foam insulation was used for better heat retention. Marine plywood was chosen for its durability and resistance to moisture. The details of the later stages are discussed further in the following section.



Fig. 3. Actual System Device of the Augmented Poultry Egg Hatchery

Level of acceptability in terms of the selected criteria (ISO/IEC 25010 Standard).

The survey result evaluates the level of acceptability of the developed Augmented Poultry Egg Incubator in terms of functional suitability, performance efficiency, compatibility, usability, reliability and maintainability.

As evaluated by the respondent's functional suitability has an average mean of 4.37 and is verbally interpreted as "Very Much Acceptable". While performance efficiency

has an average mean of 4.38 and verbally interpreted as "Very Much Acceptable". Compatibility gathered 4.33 average mean and is verbally interpreted as "Very Much Acceptable". Usability collected 4.32 average mean and is verbally interpreted also as "Very Much Acceptable". And reliability collected a 4.19 average mean and is verbally interpreted as "Very Much Acceptable". Lastly, maintainability has an average mean of 4.31 and is verbally interpreted as "Very Much Acceptable". Through the given interpretations the perception of the end-users and experts imply that the developed Augmented Poultry Egg Incubator was very much acceptable in all aspects.

The calibration and testing of temperature sensors used in the incubation area are also conducted. This test aimed to check the accuracy of measurement of DS18B20 Temperature Sensor. The result shows that DS18B20 sensor 1, DS18B20 sensor 2 and type-K thermocouple with temperature rating of 37.5 C to 37.7 C have passed the tolerance. The tolerance limit from the measured values is only between 0.2 and -0.2 Celsius. Following the temperature rating test, the researchers proceeded to carry out a test for the component of the humidifier. In the process of egg incubation, it is recommended that the relative humidity falls within the range of 55-70% RH. The researchers set the standard for the relative humidity only between 55- 70%RH as it is the required value for the relative humidity inside the machine. Evidently the study achieved this by using two humidifier-nebulizers, resulting in a relative humidity value ranging from 67.6-68.4%RH. This confirms that the desired range was reached and achieved a successful outcome.

The component used to provide heat in the incubation machine is the ceramic heat lamp, and a test was conducted to determine the number of ceramic heat lamps needed to suffice the heat needed inside the egg incubator. The table below shows the result of heat lamp testing conducted by the researchers. The table presents results from heat lamp testing for an incubation machine. Originally, the design called for six ceramic heat lamps to maintain a temperature between 37-38°C inside the machine.

Table 1. Heat Lamp Test

No. of Heat Lamps	INCUBATION AREA		HATCHING AREA	
	Temperature Reading (°C)	Remarks (37-38°C = passed)	Temperature Reading (°C)	Remarks (37-38°C = passed)
1	34.5	Failed	34.2	Failed
2	37.5	Passed	37.6	Passed
3	39.7	Failed	Not Tested	N/A
4	44.6	Failed	Not Tested	N/A
5	Not Tested	N/A	None	N/A
6	Not Tested	N/A	None	N/A

However, during testing, a single heat lamp only reached 34.5°C, which was inadequate. Two heat lamps achieved a suitable temperature of 37.5°C, while using three or four resulted in excessive heat. Therefore, it was determined that two ceramic heat lamps are sufficient to maintain the required temperature inside both the incubation machine and the hatching area.

The responsiveness of limit switches used in egg turning are also tested. This aimed to check if the limit

switches are functioning properly and could support the asynchronous motor used in egg turning. Results show the limit switch installed at the front failed two times and this led to purchasing a new limit switch. The researchers purchased new limit switch and conducted another trial, which have passed. Due to the results, the researchers provided another set of limit switches and placed under the main to ensure the safety of eggs during the process of turning.

Table 2 depicts the results from the responsiveness test of safety limit switches. The result means that both the safety limit switches are functioning well and can support the main limit switches for a safe turning of eggs during the incubation period.

The automated egg incubator, with a capacity of 528 fertile eggs per batch, underwent various stages of incubation. Candling on the seventh day revealed 29 early-stage rotted eggs, resulting in a 95% fertility rate. By the twelfth day, with 19 more rotten eggs, the fertility rate dropped to 91%. On the nineteenth day, marking the hatching phase, eight eggs pipped, leading to a 1.52% increase in the hatch rate. Subsequent days saw a substantial increase, with a total of 418 chicks produced on the twenty-second day, achieving a hatch rate of 79.17%

To bolster the findings, researchers conducted a comparative analysis, involving interviews with a poultry farmer using manual incubators and practical testing with a poultry expert. The manual incubator, limited to 60 eggs, was contrasted with the automated one, emphasizing the latter's larger capacity of 528 eggs. Both were used in a 22-day incubation and hatching period, demonstrating the automated incubator's significant advantage for

Table 2. Safety Limit Switches Responsiveness Test for Egg Turning

Safety Limit Switch Responsiveness		
Trial	Limit Switch (Front)	Limit Switch (Back)
1	Passed	Passed
2	Passed	Passed
3	Passed	Passed

Table 3. Hatchability and Mortality Record

DATE	DAY	Eggs		Dead / Rots			PIPS Live / Dead	Chicks		PERCENTAGE	
		Fertile	Infertile	Early	Middle	Late		Cull	Good	Fertility	Hatch
INCUBATION PHASE											
03-25-23	0	528	0	0	0	0	NA	NA	NA	100%	0%
04-01-23	7	499	0	29	0	0	NA	NA	NA	95%	0%
04-06-23	12	480	0	0	19	0	NA	NA	NA	91.00%	0%
04-12-23	18	480	0	0	0	0	NA	NA	NA	91%	0%
HATCHING PHASE											
04-13-23	19	480	0	0	0	0	8/0	0	8	91%	1.52%
04-14-23	20	480	0	0	0	0	62/1	0	62	91%	13.26%
04-15-23	21	480	0	0	0	0	303/2	0	303	91%	70.65%
04-16-23	22	480	0	0	0	0	45/18	0	45	91%	79.17%

larger-scale breeding operations. The study's credibility was enhanced through expert opinion and practical testing, validating the superiority of the automated incubator.

According to the tables presented, the two incubation methods were compared to assess the differences in their control mechanisms and to determine the outcomes of each method. At the end of the 22-day incubation period, the manual incubation method yielded a total of 41 chicks, while the automated incubation method produced 418 chicks. The hatch rates were calculated as a percentage of the total eggs incubated, with the manual incubator achieving a hatch rate of 68.3% and the automated incubator achieving a hatch rate of 79.17%. These findings suggest that the automated egg incubator had a higher overall hatch rate and was more effective at producing healthy chicks compared to the manual egg incubation method.

Table 4. Automatic Incubation Table

AUTOMATIC INCUBATION					
DAY	Temperature (°C)	Humidity (%RH)	Frequency of Turning	No. of Hatch	Remarks
0	37.8	55-65	24	0	capacity: 528
1	37.8	55-65	24	0	
2	37.8	55-65	24	0	
3	37.8	55-65	24	0	
4	37.8	55-65	24	0	
5	37.8	60-70	24	0	
6	37.8	60-70	24	0	
7	37.8	60-70	24	0	Candling 29
8	37.8	60-70	24	0	
9	37.8	60-70	24	0	
10	37.6	60-70	24	0	
11	37.6	60-70	24	0	
12	37.6	60-70	24	0	Candling 19
13	37.4	60-70	24	0	
14	37.4	60-70	24	0	
15	37.4	60-70	24	0	
16	37.4	60-70	24	0	
17	37.4	60-70	24	0	
18	37.4	60-70	24	0	
19	37	65-75	x	8	Transfer
20	37	65-75	x	62	
21	37	65-75	x	303	
22	37	65-75	x	45	
Total No. of Hatch				418	

VI. Conclusions

After analyzing and discussing the findings and results, the researchers have arrived at the following conclusions:

1. The design and construction of the system device involved a total of seven stages of development that were carefully planned and executed. The process included conceptualization, material selection, procurement of equipment and materials, assembly of the system device's body, installation of all components, internal testing of each component, and implementation of necessary adjustments to meet the required specifications for the system device.
2. According to the standards set by ISO/IEC 25010, the device provided tests with the aspect's functional suitability, performance efficiency, compatibility, usability, reliability, and maintainability. The developed system device's level of acceptability is classified as only acceptable with an average weighted mean of 4.32.
3. The level of effectiveness of the machine was evaluated through a comparison between the manual incubator and the automatic incubator. The findings indicate that the automatic incubator, with a capacity of 528 eggs, has demonstrated higher effectiveness in comparison to the manual incubator, which can hold up to 60 eggs, due to a higher percentage of hatch rate. Specifically, the automated egg incubator was able to hatch 418 chicks, resulting in a hatch rate of 79.17%, whereas the manual incubator had a hatch rate of 68.3%.

VII. Recommendations

Based on the conclusions of the study, the researchers have determined recommendations for the modification and enhancement of the automated egg incubator.

1. First recommendation was to explore the use of a different type of controller for the Augmented Poultry Egg Hatchery system device that can effectively regulate the necessary parameters for successful incubation and hatching. Additionally, they suggest fabricating or welding the egg tray trolley parts to ensure stable positioning of the eggs during the incubation process.
2. Based on the evaluation of the developed system device using the ISO/IEC 25010 standard, it was recommended that further improvements and modifications be made on the initial design to achieve a higher level of acceptability. In order to improve the system device's overall performance, it is recommended to conduct additional research and testing to address the identified areas that need improvement as it can help improve the functionality, performance

efficiency, compatibility, usability, reliability, and maintainability, and eventually lead to a more successful and acceptable machine.

3. The researchers recommended to continue using and developing the automated egg incubator due to its higher effectiveness in terms of hatch rate. And the improvement to renewable power source was found to be essential. Further testing and research should be conducted to explore the full potential of the automated egg hatchery, and to identify any areas that needs improvement.

VIII. Acknowledgments

The researchers extend their heartfelt gratitude to all those who have supported and contributed to the completion of this research paper entitled, "Augmented Poultry Egg Hatchery." This research journey has been a challenging yet rewarding experience, and the researchers are deeply thankful for the following individuals and organizations:

Engineering Experts: The researchers extend sincerest appreciation to all experts that collaborated in giving insights for the design and development of the system device, whose guidance, expertise, and unwavering support have been invaluable throughout this research. It has enriched the researcher's academic growth and provided clarity in navigating the complexities of this study.

Family: To the researcher's inspiration, Yan family, Tonido-Reyes family, and Alipio family, their unwavering belief in the researchers' abilities and their enduring encouragement have been a constant source of motivation. Their sacrifices and understanding during this academic journey are deeply appreciated.

Research Participants/Beneficiaries: The researchers deeply extend gratitude to the poultry farmers and industry experts who generously shared their insights and experiences, making this research empirically grounded and relevant to real-world challenges.

The completion of this research would not have been possible without the support and contributions of each of the above mentioned. Their belief in the significance of this research has inspired the researchers to strive for excellence, share information to various institutions, academe, and individuals who are currently involved in the similar study.

References

- [1] Advantages of Fumigation and Bizzy Bee Services to You. (2017, July 21). Bizzy Bee Exterminators, Inc. Retrieved October 15, 2022, from <https://www.bizzybeeexterminators.com/blog/fumigation-advantages-service/>
- [2] Ajayi, et al. (2020), An Appraisal of Traditional Incubation and Hatching Methods of Indigenous Poultry Eggs in Kwara State, Nigeria. Scientific Papers Series Management, Economic Engineering in Agriculture and Rural Development Vol. 20
- [3] Amran, A. et al, (2019) Analysis of Light Bulb Temperature Control for Egg Incubator Design. International Journal of Integrated Engineering. Vol. 11 No. 4 p. 268-276, penerbit.uthm.edu.my/ojs/index.php/ijie
- [4] AskUSDA. (n.d.). Ask.usda.gov. Retrieved April 25, 2023, from <https://ask.usda.gov/s/article/Are-fertilized-eggs-more-nutritious#:~:text=There%20is%20no%20nutritional%20difference>
- [5] Azahar, et al. (September, 2020) Intelligent Egg Incubator. International Journal of Recent Technology and Applied Science, vol. 2, no. 2, pp. 91-102, DOI: 10.36079/lamintang.ijortas-0202.129
- [6] B, E. (2017, February 14). How Do Chickens Mate? Chicken Reproduction. Love is in the Coop: A Guide to Chicken Reproduction. The Scoop from the Coop. <https://www.scoopfromthecoop.com/love-is-in-the-coop-a-guide-to-chicken-reproduction/#:~:text=A%20rooster%20often%20employs%20a>
- [7] Bharti, P., Singh, A., & Singh, P. (2021a). Smart-UPS with a priority-based load management system. Journal of Physics: Conference Series, 2007(1), 012006. <https://doi.org/10.1088/1742-6596/2007/1/012006>
- [8] Brown E O, Ebora R V, Decena F L C 2018 The current state, challenges and plans for Philippine agriculture Philippine Council for Agriculture Aquatic and Natural Resources Research and Development (PCAARRD) Department of Science and Technology (DOST) Los Baños Laguna Philippines
- [9] Clements, M. (2022, July 18). 10 tips for cleaning, disinfecting broiler houses. WATTAgNet | WATTPoultry. Retrieved October 15, 2022, from <https://www.wattagnet.com/articles/26539-tips-for-cleaning-disinfecting-broiler-houses>
- [10] Communication & Engagement Office. (n.d.). First Avian Flu Outbreak in PH Infographic| Research Institute for Tropical Medicine. Retrieved April 25, 2023, from https://ritm.gov.ph/first-avian-flu-outbreak-in-ph-infographic/?fbclid=IwAR3aIjROmXbJK9ZS_9uTU4HHb0tPqlsnFfvTE1cUSOWfahYz8ZsqBQHczjw
- [11] Darre, M. (2021, September 8). Cleaning and Disinfecting Your Poultry House. Cornell Small Farms. Retrieved October 15, 2022, from <https://smallfarms.cornell.edu/2014/04/cleaningand-disinfecting-your-poultry-house/>
- [12] F. Kyeremeh and F. Peprah (2017). Design and Construction of an Arduino Microcontroller-based EGG Incubator Int. J. Comput. Appl., Vol. 168, no. 1, pp. 15–23, doi: 10.5120/ijca2017914261
- [13] Fumigation (deciding to fumigate) - Kentucky pesticide safety education. (n.d.). Retrieved October 15, 2022, from <https://www.uky.edu/Ag/Entomology/PSEP/fumdecision.html>
- [14] Garbus, S. E., Lyngs, P., Thyme, A. P., Christensen, J. P., & Sonne, C. (2018). Candling and field atlas of early egg development in Common Eiders *Somateria mollissima* in the central Baltic. *Acrocephalus*, 39(178-179), 85-90.
- [15] How often should I Clean my Chicken Coops? (2021, March 15). Cocoon. Retrieved October 15, 2022, from <https://www.chickencoopsandhouses.co.uk/blog/how-often-should-i-cleanmy-chicken-coops/>
- [16] Jabbar A, et al., (2020). Influence of fumigation strength on hatchery parameters and later life of chicks.

Improving the Workforce Skills and Enhancing the Industry's Competitiveness Through the Mold Technology Support Center

Agustin M. Fudolig^{*1}, Lina B. Afable^{*2}, Zalda R. Gayahan^{*3}, Reynaldo L. Dela Cruz^{*4}, Francis F. Dime^{*5}

Abstract

The manufacturing industry is one of the drivers of the industry sector, which is among the three major sectors of the country's economy. Die and mold is crucial in the mass production of plastic and metal parts required by the leading manufacturing industries. The Mold Technology Support Center-Grant in Aid (MTSC-GIA) project was implemented to support the commitments of the Philippine party, led by the DOST-Metals Industry Research and Center, to the MTSC Official Development Assistance (MTSC-ODA) grant from the Republic of Korea. The ODA grant is focused on developing the skills of the human resources needed by die and mold companies, encouraging the advancement of the competitiveness of the local manufacturing industry, and contributing to the industrial cooperation between Korea and the Philippines. Involved in the ODA are the donation, installation, and commissioning of equipment and software at the MTSC facility located at General Trias in Cavite, the training of Filipino trainers in Korea, and the dispatch of Korean experts to carry out MTSC training programs. The MTSC-GIA also intends to pursue these goals and develop the MTSC's sustainability plan. The GIA project has supported the development of eight new training programs patterned after the training received by DOST-MIRDC engineers and technicians at the Korean Mold Center in South Korea. Through this GIA project, MTSC offered 162 training programs that were attended by a total of 8,131 participants. The use of equipment for mold-related requirements is also one of the MTSC's service offerings to the industry.

Keywords: die and mold, Official Development Assistance, Mold Technology Support Center

I. Introduction

The manufacturing sector contributes to the gross domestic product (GDP) but has not reached its full potential. The Philippine government implemented the Manufacturing Resurgence Program (MRP) in 2014 to address the concern of the slow growth of the manufacturing industry. The MRP is an initiative of the Department of Trade and Industry (DTI) in coordination with the Department of Science and Technology (DOST) and other government agencies [1].

A closer look at the manufacturing industry reveals various important economic sectors that fuel its growth. Among these is the metals and engineering industries where the tool, die, and mold sector plays a crucial role in all downstream industries, as shown in Figure 1.

The die and mold industry holds a significant influence on the manufacturing industry, particularly those involved in the mass production of plastic and metal parts and components. It is an industry that uses general and specialized metal cutting technology to fabricate dies, molds, and tooling employed to convert raw material into a required shape. The common products of this sector include dies (simple, compound, and progressive), molds (for forging, plastics injection or blow molding, die casting,

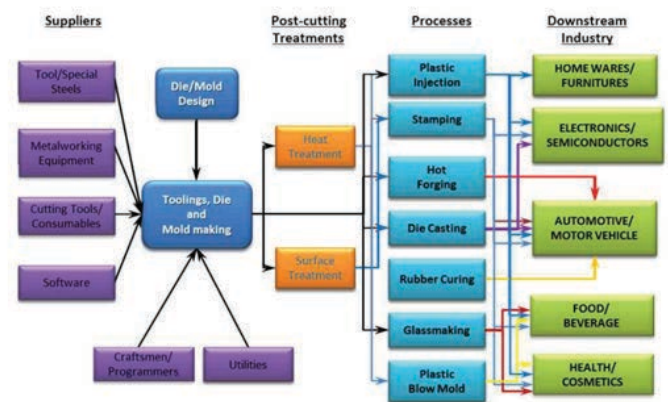


Fig. 1. Tool, die, and mold industry and its role in fueling the growth of various downstream industries [2]

glass blow molding), and tools, e.g. jigs and fixtures used for cutting and shaping different materials. Molds are shaping implements for glass, metal, rubber, and plastic components through processes such as die casting, blow molding, or sheet stamping.



^{*1} Deputy Executive Director for R&D Metals Industry Research and Development Center Bicutan, Taguig City Philippines



^{*2} Chief Science Research Specialist Metals Industry Research and Development Center Bicutan, Taguig City Philippines



^{*3} Supervising Science Research Specialist Metals Industry Research and Development Center Bicutan, Taguig City Philippines

The Competitiveness Roadmap for the Tool and Die Industry formulated in 2012, and submitted to the Board of Investment, identified and recommends manpower improvement and technology upgrading and modernization as strategies to address the concerns of the industry. So far, some programs have been implemented by DOST-MIRDC to address these: the establishment of the Die and Mold Solution Center (DMSC Project), the Die and Mold 3 Designers and Makers training program (D2M2 Project), and the engagement of local and foreign die and mold experts (DiMo Guru Project).

In 2015, the DOST-MIRDC conducted a survey among die and mold companies located in economic zones as a part of the pre-feasibility study in preparation for the implementation of the MTSC project. The survey done by MIRDC in cooperation with KOAMI brought forward the following statistics: 72.5 percent of the survey respondents required a continuous supply of trained employees; 64.7 percent required technology upgrades; and 60 percent expressed the need for assistance in terms of identifying existing and potential supply chain networks. The survey indicated the need for a pool of trained personnel in CAD/CAM, CNC machining and metalworking, and on die and mold design, assembly, and processing, as well as stressed on the need for experts to guide local talents in die and mold design and processing which is critical in the success for localization of die and mold supply to the industry. From the survey results, the feasibility of establishing a facility that will offer services to address the identified needs of the industry is highly justifiable.

In a separate and more recent study of the die and mold industry conducted by the DOST-MIRDC, it was found that the problems of the die and mold companies mostly fall into three broad issues: (1) unstable pool of human resources; (2) raw materials with regard to very long lead time between order and delivery, as well as high cost and inconsistent quality; and (3) frequent equipment downtime [3]. This survey of the die and mold industry highlighted the need for new die and mold designers and makers thereby necessitating continuous training in related courses.

Through the ODA, the following objectives will be met:

- (1) to develop the most needed human resources for the local die and mold companies;
- (2) to encourage the advancement of the Philippine manufacturing industry's competitiveness; and
- (3) to contribute to the industrial cooperation between the Republic of Korea and the Republic of the Philippines.

II. Materials and Methods

The implementation period of the ODA grant was from May 1, 2019, to December 31, 2022. Given the commitments of the Philippines in implementing the ODA, a Philippine Party was formed and each member, the PEZA, PDMA, Inc., BOI, and MIRDC, was a signatory in a Memorandum of Agreement (MOA). Among the stipulations in the MOA was for PEZA to allocate a lot and build the MTSC building to accommodate the donated equipment and provide technical services. MIRDC agreed to pay an annual rental fee of PhP5M for the next 10 years for PEZA to recover the cost of constructing the building and site development. Also, provided in the MOA is for MIRDC and PDMA, Inc., to enter into a co-management scheme to sustain MTSC operations. Figure 2 shows both the Korean and Philippine parties and how all organizations are linked in the MTSC-ODA.

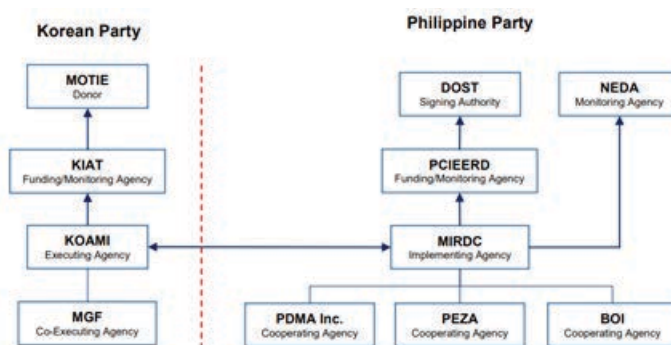


Fig. 2. Korean and Philippine parties collaborated to establish the MTSC.

Construction of the MTSC was bid out by the PEZA and construction work started on May 27, 2021.

Anticipating that additional project funding will be needed to accomplish all planned activities for the MTSC project, the team submitted a project proposal, with the same project title, to the DOST-Philippine Council for Industry, Energy, and Emerging Technology Research and Development (DOST-PCIEERD). This proposal was approved by the DOST EXECOM on April 23, 2020, and implementation commenced on August 1, 2020. The specific objectives of this approved MTSC-grant-in-aid project are as follows:

- 1) to develop needed human resources for the local die and mold companies;
- 2) to encourage the advancement of the Philippine manufacturing industry's competitiveness; and
- 3) to develop the sustainability plan of the MTSC.



*4 Supervising Science Research Specialist Metals Industry Research and Development Center Bicutan, Taguig City Philippines



*5 Supervising Science Research Specialist Metals Industry Research and Development Center Bicutan, Taguig City Philippines

The additional funding provided by the MTSC-GIA will help address the following: (1) the requirement of PHP 5M annual rental fee for the PEZA-built MTSC building in Gen. Trias, Cavite; (2) the requirement for contract of service personnel who will devote their time to the day to day needs of the project; (3) need for a project management team during and right after the duration of the ODA from Republic of Korea; (4) need for MOOE to conduct training and operate and maintain the machineries; and (5) requirements for logistical support in coming up with a sustainability plan for the established MTSC.

III. Results and Discussion

In the achievement of specific objective 1, to develop needed human resources for the local die and mold companies, the following tasks were successfully performed under the MTSC-GIA: agreement on the equipment/software to be procured; construction of the MTSC building, procurement of equipment, software, and tools for the MTSC; training of Filipino lecturers in Korea for 10 weeks; attendance to other training and meetings of MTSC project team in Korea; moving in and installation of machinery and manufacturing systems in the MTSC; promotion of MTSC services; and payment of rental to PEZA.

The MTSC building is part of the commitment of the Philippine party to the MTSC ODA project. The building was designed for functionality, and constructed with the easy and efficient installation of equipment and machinery under consideration. The PDMA commissioned a local architectural firm, Design Aid, Inc., for the architectural and engineering designs of the MTSC building. **Figure 3** presents side-by-side the design and the actual MTSC building located in General Trias, Cavite.

By the end of the construction, several building improvements such as those for the second floor, were charged to the MTSC-GIA project. The initial design was bare and required partitioning into different training and office rooms, as well as the installation of ceiling and electrical systems.

KOAMI purchased all the items in the list of equipment, software, tools, and furniture. KOAMI also handled all overseas delivery of equipment to the port of Manila. From the port of Manila to MIRDC, where the equipment were temporarily stored pending completion of the MTSC building, the cost of transport and delivery were charged to the MTSC-GIA project. The delivery came in eight batches: batch 1 - NX software; Batch 2 - workstation and monitor; Batch 3 - tooling and consumables; Batch 4 - cameras and other office furniture; Batch 5 - computer tables, chairs, and other furniture; Batch 6 - aircon, office furniture, generator set, conventional machines, 3D CMM; Batch 7 - CNC machining centers and accessories; and Batch 8 - injection molding machines and accessories. For Batches 6-8, delivery time fell under the congested season of trucking in December 2021 and the items were released only on January 22, 2022. Also, during the same

period, a surge in COVID-19 cases caused by the Omicron variant limited the activities at the Bureau of Customs (BOC) and delayed documentation procedures which resulted in prolonged delivery schedules and increased cost of demurrage, handling, and storage.

The MTSC GIA project spent a total of ₱13,984,635.23 for transport and delivery expenses which necessitated the reprogramming of project funds as well as requiring additional funds from DOST. This is 45.7% of the total MTSC-GIA budget and constitutes the biggest slice of the budget expenses of this project. This activity was completed during the Year 3 of the MTSC-GIA project. In the area of training, seven MIRDC staff and two PDMA representatives were sent to Korea from October 7, 2019, to December 13, 2019, for training as potential resource speakers and lecturers of the MTSC. The trainees were provided with the basics of mold design, processing, assembly, and plastic injection.

A second 10-week training was supposedly scheduled in 2020, but due to the COVID-19 pandemic, this was changed to a tour and orientation in South Korea where MTSC project members met equipment suppliers and had a chance to visit the suppliers' respective plants. The tour was conducted from September 18-25, 2022. Though the plane fare, food and accommodation and inland transportation were supplied by KOAMI, incidental expenses portion of the per diem were funded by the MTSC-GIA project and clothing allowance was funded by MIRDC. This activity was completed during the Year 3 of the MTSC-GIA project.

KOAMI handled the installation of the manufacturing systems for training and actual operations of the MTSC facility. These include the equipment and software for the operations of the MTSC as well as the installation of equipment and furniture intended for administrative use. Installation and commissioning were completed during year 3 of the MTSC-GIA project.

MTSC services such as webinars were promoted through teasers and invitation posters uploaded online. The MTSC also published the 2022 and 2023 versions of the catalog to further promote its services to target clients. Pushing further, the MIRDC and the MTSC team took advantage of the wide reach of the 2022 National Science and Technology Week (NSTW) to hold a forum about the MTSC services. Likewise, the MTSC was also promoted during the celebration of Metals and Engineering Week 2022, holding of several business-to-business meetings at the MTSC, and the technology demo where clients shared their experiences working with the MTSC. The MTSC opens its doors to industry players and members of the academe who want to see the facility. Also, the MTSC engages in consultancy and conducts visits to die and mold companies.

The accomplishments for specific objective 2, to encourage the advancement of the Philippine manufacturing industry's competitiveness, the MTSC team utilized an alternative venue to conduct training



Fig. 3. The design of the MTSC (L) and the actual MTSC building (R), whose construction was completed on May 20, 2022

while the MTSC facility was still being constructed; developed training curriculum; recruited training participants; and implemented training programs. Training was conducted at the DOST-MIRDC facilities before the MTSC building was constructed. The MTSC team developed a total of eight new training curriculums patterned after MIRDC-offered training programs and from the learnings gained from the training they attended at the Korea Mold Center. The new training programs are: Plastic Injection Mold Design, Plastic Injection Mold Assembly, Mold Assembly using NX, Mold Wizard Design Process, NX CAD Fundamental Course, Overview of Plastic Mold Making Process, Plastic Product Development, and Appreciation Course on Plastic Product Development. Training participants are recruited through posters and teasers uploaded on the official FB page of the DOST-MIRDC.

The training offerings of the MTSC were successful based on the continuous conduct of various training programs which are well-attended by participants that represent the academe and the industry. A total of 162 training programs were conducted, and a total of 8,131 participants attended the training sessions (Figure 4). Resource persons included both Filipino trainers and Korean experts.

Specific objective 3, which is about the development of the sustainability plan of the MTSC, is still being met

through the following action plans: identification of the training needs that suit the demands of the industry; conduct of dialogues with the industry; conduct of survey; drafting of the co-management scheme and actual operation and management period.

Sustainability of the MTSC

The accomplishments and the continuing milestones of the MTSC prove that this facility is serving its purpose: enhance the skills of the human resources for the enhancement of the productivity and competitiveness of the manufacturing industry through a more dependable and stable mold industry.

The operations and work instructions of the MTSC are made part of the MIRDC's Integrated Management System and Quality, Environmental, and Information Security System conforming to ISO 9001, ISO 14001, and ISO 27001.

Another factor that will make the MTSC sustainable is the effective implementation of the co-management scheme for its operations and management.

The co-management scheme of the MTSC signed by the DOST-MIRDC and the PDMA, Inc. is divided into two parts: (1) transition period, where all expenses of the MTSC will be handled by the MIRDC. Regular and contractual

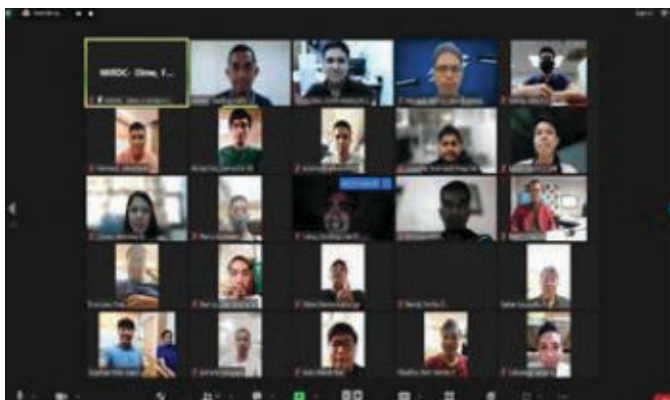


Fig. 4. The Introduction to Mold Design (webinar, May 11, 2021) and face-to-face (Nov. 8-12, 2021), is a sample of a training program offered by the MTSC.

personnel, as well as contract of service staff, as deployed to the MTSC by the MIRDC with GIA funding. During this period, PDMA, Inc. assumes a shadow role as it observes and learns how to operate and manage the facility; (2) actual operation and management, where expenses are supported by both PDMA and MIRDC – MIRDC handles the salaries of assigned personnel, payment of annual insurance fees of donated equipment, subcontracting of janitorial and security services, and the building rental. PDMA, Inc. is in charge of handling all other expenses.

IV. Conclusion

The die and mold industry in the Philippines requires intervention from the government particularly from MIRDC, which is mandated to assist the local metals, engineering, and allied industries. The ODA from the Republic of Korea on establishing the MTSC is timely in addressing the gaps in the local die and mold industry. In advancing the Philippine manufacturing industry's competitiveness, the MTSC offers its facilities for purposes of training industry personnel and for facility sharing schemes for industry to use. The MTSC also provides consultancy services to industries that make use of dies and molds. A sustainability plan has been agreed upon between MIRDC and PDMA, Inc. for the shared operation and management of the MTSC. PDMA Inc.'s management of the MTSC will allow the collection of revenues from MTSC services and flexibility in the use of revenue for the sustainability of operations.

The MIRDC, although already in a co-management scheme with the PDMA, will continue to make representations from the Department of Budget and Management for the allocation of funding support to the MTSC. Further, MIRDC will seek GIA funding support for its training programs for the industry.

With the successful track record of the MTSC, the MIRDC submitted another project proposal for the Philippine die and mold sector under the Technology Advice and Solutions from Korea (TASK). The objectives of this project are: to assist companies engaged in die and mold in resolving onsite technical difficulties and issues; to provide MTSC as a venue for the training of technical workforce; and to establish a network between Korean and Filipino companies to foster further industrial cooperation.

V. Acknowledgments

The DOST-MIRDC is grateful to the Republic of Korea, the ODA donor, for making the establishment of the MTSC possible. The MTSC team extends its gratitude to the DOST, PEZA, BOI, and PDMA, Inc. for the partnership. The team's deepest gratitude also goes to the MIRDC Governing Council, MIRDC management, and staff of all its MTSC partners. Above all else, the team is thankful to God for this opportunity to serve the industry and the country through the MTSC.

References

- [1] Department of Trade and Industry. Manufacturing Resurgence Program [Online]. Available: <https://industry.gov.ph/manufacturing-resurgence-program> [Accessed Oct. 20, 2023]
- [2] Department of Science and Technology-Metals Industry Research and Development Center. Competitiveness Roadmap of the Tool and Die Industry of the Philippines, 2012. [Unpublished]
- [3] Department of Science and Technology – Metals Industry Research and Development Center. The Philippine Die and Mold Industry Building Niches Amidst Global Challenges: A 2018 Study



M.E. INDUSTRIAL MACHINERY CO.

SUPPLIER OF QUALITY MACHINE TOOLS & ACCESSORIES



WHY M.E. INDUSTRIAL MACHINERY CO.?



- We have a long track record, technical expertise and application know-how.
- We are committed to supply quality machines at very competitive price.
- We deliver strong after sales service support.

- Lathe Machines (Conventional/CNC)
- CNC Vertical Machining Center
- CNC Wirecut
- Cylinder Reboring Machines
- Drilling & Milling Machines
- Electric Discharge Machine (EDM)
- Horizontal Bandsaw
- Vertical Bandsaw
- Hydraulic Power Hacksaw
- Surface Grinders
- Pipe Threading Machines
- Tapping Machines
- Gear Hobbing Machine
- Roller Bender
- Box & Pan Bender
- Busbar / CNC Busbar
- CNC Pipe & Plate Dual-Use Fiber Laser Cutting Machine
- CO2 Fiber Laser Cutting Machine
- Fiber Laser Cutting Machine
- Hydraulic Iron Worker
- Notcher
- Press Brakes (NC / CNC)
- Shearing Machines (NC / CNC)
- Lockformer
- Foot Shear
- Bordering Machines
- Section Bending Machines
- TDF Flange
- Water Jet Cutting Machine
- CNC Router
- Automatic PU Foam Sealing Machine
- Machine Tools Accessories



Automatic PU Foam Sealing Machine



At M.E. Industrial Machinery Co., we take pride in being a leading provider of metal fabrication machinery since 1968. Our long-standing reputation in the industry is a testament to our commitment to quality, innovation, and customer satisfaction. With over 50 years of experience, we have consistently delivered cutting-edge machinery that meets the evolving needs of the metal fabrication sector. Our extensive range of machinery includes state-of-the-art equipment for various applications, such as bending, cutting, welding, and shaping metal materials. Whether our customers operate small fabrication shops or large manufacturing facilities, we have the expertise and resources to provide tailored solutions to meet their specific requirements.



(632) 8716- 5355 / 8716- 5357
 Globe: (0977) 820-85-72
 Smart: (0908) 896-26-48
 meindustrial.inquiry@gmail.com
<https://www.facebook.com/meindustrialmachineryco1>
 Bldg. No. 11, MEIM, G. Araneta Ave, Quezon City, Metro Manila, 1113

Modification of a 1.5kW Shredder for ASA (Acrylonitrile Styrene Acrylate) 3D Printing Wastes

Godfreyson J. Nardo ^{*1}, Franz Joseph D. Libao ^{*2}, Von Jansen G. Comedia ^{*3}, Nicole Ann Portia U. De Luna ^{*4}, Glen D. Espeña ^{*5}

Abstract

Plastic recycling is considered as one of the key solutions to overcome environmental pollution. Shredders played an important role in plastic recycling as they turn the plastics into a reusable material. A conventional small-scale shredder used in recycling PET plastic wastes was acquired and modified to accommodate Acrylonitrile Styrene Acrylate (ASA) 3D printed wastes. The shredder could take thin plastic bottles up to 3mm and could produce a 10 kg per hour output. The motor of the shredder is 1.5 kW (2hp) and has a single shaft with 8 blades that shreds in one direction. To accommodate the harder ASA plastics, the torque was increased through the use of chain sprockets. Several sprocket ratio were chosen to study the effect on the shredding rate and size of the granules produced. The modified shredder could shred thicker (6mm) ASA plastics but is limited by the original mechanical system of the commercial shredder.

Keywords: plastic recycling, Plastic shredder, ASA/Acrylonitrile Styrene Acrylate Plastics, 3D printing waste

I. Introduction

3D printing is one of the fastest growing sectors [1]. The emergence on the use of 3D printers created significant amount of wastes that would add to the worldwide problem in plastic pollution. These wastes could become filaments, pellets, or granules that could be utilized again for recycling. In the era of 3D printing, turning wastes into a reusable resource is one of the keys to a circular economy [2].

It is estimated that 10% of 3D prints become wastes [3]. Thus, these wastes are significant in amount and would contribute to pollution if not handled properly. Usually, these wastes are comprised of base materials and supports that are removed in the final product. 3D printing uses different plastics like Acrylonitrile styrene acrylate (ASA), Acrylonitrile butadiene styrene (ABS), Polyethylene terephthalate (PET), Polypropylene (PP), etc. Recent technologies in 3D printing allow the printing of thicker, harder and more rigid materials to print larger structures [4]. ASA, which is tougher and more UV light-resistant than other plastics, enables the printing of larger outdoor structures. The demand for ASA material and the like is projected to increase and lead to much thicker, harder, and more rigid plastic waste. Hence, to reuse these plastic wastes, shredders need to handle more rigid materials to be recycled.

Some industrial shredders can produce flakes from more rigid plastics, but the production rate is high and inappropriate for small-scale applications. There are also shredders with low production rates but can only accommodate softer materials. Thus, to address the gap, it is necessary to develop a shredder for small-scale

applications that can produce flakes from thicker and harder plastic wastes.

This study will explore the possibility of modifying an existing plastic shredders that shred softer plastic materials like HDPE, PP, and PS to shred thicker and more rigid materials like ASA.

This study will serve as the basis for the design of a small capacity shredder that can produce granules from harder plastics.

Recycling of 3D Printing Wastes

Different methods are used in recycling 3D printing wastes. One of these methods is to shred the wastes into flakes, pellets or granules and turn these materials into other useful products. Shredded plastics are used as aggregates in road asphalt and concretes [5]. Another method is to use the flakes back in 3D printing by using an extruder and converting them as filament to be used again in 3D printers. In general, plastic flakes, pellets and granules have wide variety of usage in plastic recycling.

Utilization of ASA Plastic Materials

ASA or Acrylonitrile Styrene Acrylate is a type thermosplastic elastomer. It has good chemical resistance and high impact strength. ASA was originally developed as an alternative to ABS and is known as resistant to heat, weathering, chemical and UV radiation. Aside from these, ASA has resistance to discoloration and has better anti-aging performance compared to ABS [6],[7]. Due to this properties, ASA is suitable for outdoor application use. ASA are also used in several industrial applications such



^{*1} Sr. Science Research Specialist
Metals Industry Research and
Development Center
Bicutan, Taguig City
Philippines



^{*2} Sr. Science Research Specialist
Metals Industry Research and
Development Center
Bicutan, Taguig City
Philippines



^{*3} Science Research
Specialist II
Metals Industry Research
and Development Center
Bicutan, Taguig City
Philippines

as commercial sliding, outside furnitures and car exterior panels [8][9].

Plastic Shredder for 3D printing wastes

Shredder is an equipment that use mechanical advantage to physically reduce the size of input materials through shearing. Rotating blades are typically used to shear the materials.

While large industrial shredder can shred harder and thicker plastic wastes, their application is for high volume of plastic wastes and thus have a high production rate and power consumption. Meanwhile, there are small plastic shredders but they could only shred soft and thin plastics. Small scale plastic shredders are useful in laboratory use and additive manufacturing facilities.

3D Printers that can utilize granules

Conventional 3D printing process involves using filament as input material. Several 3D printers can print using flakes, granules, and pellets. Granules could be used in 3D printers and therefore shredded 3D printed wastes could be used again.

One example of 3D printing technologies that can utilize directly the recycled plastic flakes as feedstock is the Gigabot X. It uses fused granular fabrication (FGF), a type of 3D printing technology that do not need plastic filament as feedstock, instead it directly uses granules and recycled shredded plastics to print 3D materials. The Gigabot X is one example that uses FGF technology. It is capable of printing from recycled pellets, flakes, or regrind. The size of the input flakes must be 3 to 5 mm.

Another use of the plastic wastes of 3D printing is to convert it back to filament. 3devo is an example of a machine that utilizes shredded plastics and turns it back to filament.

The recycling of ABS for utilization in Fused Deposition Modelling (FDM) was investigated [10]. In this study 100% recycled ABS plastics were turned back into filament.

ASA materials are already widely used especially in 3D printing. Recycling of 3D printing wastes involves converting them to flakes, pellets or granules therefore the need for shredder that could shred harder and tougher plastics like ASA will be beneficial.

II. Materials and Methods

Blade Simulation

The blade used in the actual shredder equipment was modeled and subjected to Finite Element Analysis FEA

using Solidworks Software. This simulation is to confirm that the blade could withstand the forces due to the additional torque added because of the modification.

Blade simulation was done to ensure that the existing blades from the acquired plastic shredder can withstand the force and stresses of the ASA material. The deformation is less than 1mm. The stress is less than the yield strength of the mild steel. The factor of safety is 2.4. From these results, the existing blade could be used for ASA and will not be replaced in this study.

Preparation of Materials

The waste materials from 3D printing are prepared by grinding or sawing the large wastes into sizes of 0.5 in x 1 in.

Torque and Motor Speed

The torque was varied using three different sprocket ratios.

Test Procedures

Five trials was done for every thickness of test materials as shown in Table 1. The power consumption and amperage of the equipment was monitored using a power quality analyzer. Three passes per trial were done.

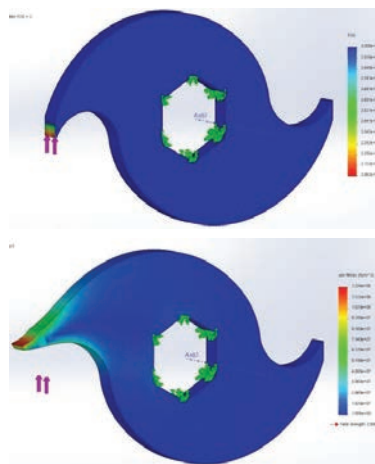


Fig. 1. Sample blade simulation

Table 1. Experiment design for the modified ASA plastic shredder

Test	Shredder	Test Material Thickness
1	Original Shredder	3 mm
2	Modified Sprocket Ratio 1:3	3 mm
3	Modified Sprocket Ratio 1:1	3 mm
4	Modified Sprocket Ratio 1:2	3 mm
5	Modified Sprocket Ratio 1:3	6 mm
6	Modified Sprocket Ratio 1:3	8 mm



*4 Science Research Specialist II
Metals Industry Research and
Development Center
Bicutan, Taguig City
Philippines



*5 S&T Fellow II
Metals Industry Research and
Development Center
Bicutan, Taguig City
Philippines

III. Results

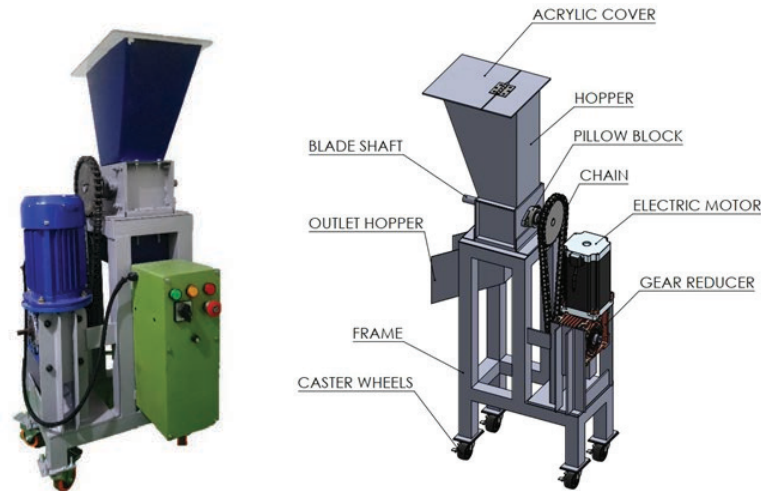


Fig. 2. Modified commercial plastic shredder

Table 2. Test results for the 3mm thickness ASA material for shredding

Test	Thickness (mm)	Shredding Rate (kg/hr)	1st Pass Average Amperage (A)	2nd Pass Average Amperage (A)	3rd Pass Average Amperage (A)	No. of observed over currents
1	3	3.6-5.3	3.87	3.19	3.47	1
2	3	2.1-2.9	3.35	2.99	2.84	0
3	3	1.4-2	3.57	2.94	3.2	1
4	3	1.8-2.4	3.26	3.16	3.02	3

Table 3. Test for Sprocket Ratio 1:3 (highest torque, lowest blade speed)

Test	Thickness (mm)	Shredding Rate (kg/hr)	1st Pass Average Amperage (A)	2nd Pass Average Amperage (A)	3rd Pass Average Amperage (A)	No. of observed over currents
1	6	2.8	3.98	3.10	2.93	3
2	8	N/A	6.15	N/A	N/A	1

IV. Discussion

The torque of the blade was increased due to the additional sprocket ratio. This modification also slowed down the blades to 20rpm, 30rpm, and 54rpm. As a result, the shredding rate also decreased. The sizes of the shredded materials were also relatively larger compared to the higher speed ratio sprockets. The blade could withstand the stresses during shearing of the 3mm to 8mm thick ASA materials and confirmed the result of the Finite Element Analysis (FEA).

There are instances that the electric motor's amperage was very high (value) and resulting in overcurrent and hence a fault in the inverter. This is a limitation due to the size of the electric motor. Several factors were identified such as the stacking of the test materials in a sideways

orientation which makes the effective thickness double the actual test material.

In general, the shredder could shred thicker than 3mm but the shredding rate would be decreased not only due to the slower blades but also to the slow input of test materials to make sure that stacking would not occur. The modified shredder releases output of fine shredder particles that can be tested for use in commercial 3D printer for ASA.

For a small-scale application, this shredder could be used to shred ASA materials and would produce 3-5mm granules that could be used for recycling such as 3D printing.

Shredding 8 mm test material resulted to the failure of mounting base of the modified shredder as shown in Figure x. The 8 mm test materials are large enough to block the shredder wheels against the shredding chamber, resulting to increase torque forces in the motor. The huge torque exerted by the shredder overcame the tensile strength of the mounting base, resulting to failure. The mounting base was repaired and reinforced to minimize the risk of another structural failure of the motor base mount.

V. Conclusions

The commercial shredder designed to shred less than 1mm thickness of PET plastic wastes could achieve a capacity of 10kg per hour could also be used for ASA plastics but with limitations. In this study, different thicknesses of ASA plastics were used. The rotational speed (rpm) of the shredder blade was also varied by changing the sprocket ratio. This change gives additional torque for shredding but decreases the shredding rate. For 3mm ASA plastics, the shredding rate is 2.1 to 2.9 kg per hour. All the specified sprocket ratios could shred the 3mm thickness ASA plastics but the 20 rpm was the only speed where a thickness of 6mm plastics could be shred. For 6mm ASA plastics, the shredding rate of 2.8 kg per hour could be achieved.

Motor amperage was also monitored during the testing. During the shredding of 6mm ASA there was an increase in amperage of the motor to an average of 3.98A which was still within the limits of the electric motor (rated at 5A).

The shredder blade could withstand the stresses of 8mm ASA but the mounting of the gear reducer failed. This mechanical system could be further improved by replacement of the gear reducer that could handle higher torque greater than 1,100 N·m. The chain link also failed but not due to the higher tensile stress from the blades but due to the twisting as a result from the failure of the mounting of the gear reducer.

The modified shredder could shred thicker (6mm) ASA plastics but is limited by the original mechanical system of the commercial shredder. It is therefore recommended to replace the gear reducer to handle the additional torque given by the chain sprocket. The mounting base of the shredder should also be reinforced. These would be enough to handle all the stresses from grinding waste ASA material.

VI. Acknowledgment

This paper is made possible a project funded by the Department of Science and Technology (DOST) titled "Study on the Suitability of Acrylonitrile Styrene Acrylate (ASA) as Material for a 3D-Printed Statue" and implemented by the Metals Industry Research and Development Center (MIRDC).

References

- [1] Mikula, K., Skrzypczak, D., Izydorczyk, G., Warchol, J., Moustakas, K., Chojnacka, K., & Witek-Krowiak, A. (2021). 3D Printing Filament as A Second Life of Waste Plastics - A Review. *Environmental Science and Pollution Research International*, 28(10), 12321-12333. <https://doi.org/10.1007/s11356-020-10657-8>
- [2] Raji, Nurudeen, Kuku, Rafiu, Ojo, Seun, & Hunvu, Sejero. (2020). Design Development and Performance Evaluation of Waste Plastic Shredder. *Journal of Production Engineering*, 23, 22-28. <https://doi.org/10.24867/JPE-2020-01-022>
- [3] Filamentive. (n.d.). The 3D Printing Waste Problem. Retrieved from <https://www.filamentive.com/the-3d-printing-waste-problem/>
- [4] Atadious, David, & Joel, Oluwayomi. (2018). Design and Construction of a Plastic Shredder Machine for Recycling and Management of Plastic Wastes. *International Journal of Scientific and Engineering Research*, 9.
- [5] Jin, D., Meyer, T. K., Chen, S., Boateng, K. A., Pearce, J. M., & You, Z. (2022). Evaluation of Lab Performance of Stamp Sand and Acrylonitrile Styrene Acrylate Waste Composites Without Asphalt as Road Surface Materials. *Construction and Building Materials*, 338. <https://doi.org/10.1016/j.conbuildmat.2022.127569>
- [6] Szamborski, G. (2007). Superior Balance of Weatherability and Impact Performance with Acrylic-Capped Vinyl Siding. *Journal of Vinyl and Additive Technology*, 13, 26-30. <https://doi.org/10.1002/vnl.20094>
- [7] Scheirs, J., & Priddy, D. (2003). *Modern Styrenic Polymers: Polystyrenes and Styrenic Copolymer*. John Wiley & Sons.
- [8] Fink, J. K. (2010). *Handbook of Engineering and Specialty Thermoplastics, Polyolefins and Styrenics*. Wiley. ISBN 9781118029282.
- [9] *Handbook of Plastics Joining: A Practical Guide*. (n.d.). Elsevier Science. ISBN 9780815517665.
- [10] Mohammed, M. I., Das, A., Gomez-Kervin, E., Wilson, D., & Gibson, I. (2017). EcoPrinting: Investigating the Use of 100% Recycled Acrylonitrile Butadiene Styrene (ABS) for Additive Manufacturing. In *Solid Freeform Fabrication 2017: Proceedings of the 28th Annual International Solid Freeform Fabrication Symposium – An Additive Manufacturing Conference* (p. Reviewed Paper).



METALS & ENGINEERING INNOVATION CENTER

"Transforming ideas into innovations"

METALS & ENGINEERING
INNOVATION
CENTER

REGION 3

SERVICES OFFERED:

- Equipment and Machine Design
- Fabrication and Prototyping
- Skills Training
- Technical Consultancy
- Use of facilities
 - Metalcasting equipment (NEUST only)
 - Shear cutting equipment
 - Sheet bending equipment
 - Sheet metal roller
 - TIG welding machines
 - Other equipment for M&E industry development

- Time Sharing - client provides their own machine operator
- Actual Time - MEIC provides the machine operator

CONTACT

US NOW

MEIC CAR

Ifugao State University,
Lagawe Campus
Engr. Dahlia Gay A. Bunolna
daggihao@yahoo.com

MEIC Region I

Don Mariano Marcos Memorial
State University,
Mid-La Union Campus
Dr. Victorio C. Palabay
vpalabay@dmmmsu.edu.ph

MEIC Region II

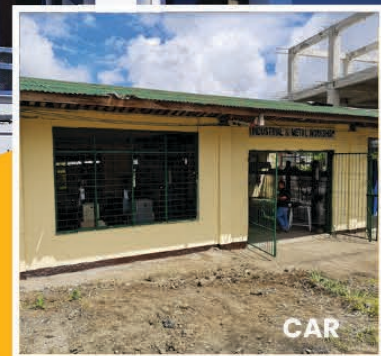
Cagayan State University,
Carig Campus
Dr. Arthur G. Ibañez
arthur_ibañez20@yahoo.com

MEIC Region III

Nueva Ecija University of Science
and Technology, Sumacab
Campus
Engr. Nathaniel S. Oliveros
Nathanielz25@yahoo.com

MEIC Region X

University of Science and
Technology of Southern
Philippines
Engr. Adonis G. Closas
adonis.closas@ustp.edu.ph
fablab@ustp.edu.ph



CAR



REGION I



REGION 2



REGION X



Metals and Engineering Innovation Center (MEIC) to rise in TEN regions across the country!

REGION IV-A
BATANGAS STATE UNIVERSITY
THE NATIONAL ENGINEERING
UNIVERSITY

REGION V
BICOL STATE COLLEGE OF APPLIED
SCIENCES AND TECHNOLOGY
(BISCAST)

REGION VIII
EASTERN VISAYAS STATE
UNIVERSITY (EVSU)

REGION IV-B
WESTERN PHILIPPINES
UNIVERSITY (WPU)

REGION VI
TECHNOLOGICAL UNIVERSITY
OF THE PHILIPPINES
(TUP Visayas)

REGION VII
NEGROS ORIENTAL STATE
UNIVERSITY (NORSU)

REGION XIII
SURIGAO DEL NORTE STATE
UNIVERSITY (SNSU)

REGION IX
ZAMBOANGA PENINSULA POLYTECHNIC
STATE UNIVERSITY (ZPPSU)

REGION XI
UNIVERSITY OF
SOUTHEASTERN
PHILIPPINES (USEP)

REGION XII
MINDANAO STATE UNIVERSITY
(MSU-Gensan)

Get ready as we transform a more innovative countryside!



**DEPARTMENT OF SCIENCE AND TECHNOLOGY
METALS INDUSTRY RESEARCH AND DEVELOPMENT CENTER**

MIRDC Compound, Gen. Santos Avenue, Bicutan, Taguig City, 1631 Metro Manila
P.O. Box 2449 Makati, 1229 Metro Manila, Philippines
Telephone Nos.: (632) 8837-0431 to 38 (connecting all departments)
Fax Nos.: (632) 8837-0613 and 8837-0479
Website: <http://www.mirdc.dost.gov.ph>
E-mail: mirdc@mirdc.dost.gov.ph